PRINCIPLES OF DOPPLER ECHOCARDIOGRAPHY AND THE DOPPLER EXAMINATION #1

Joseph A. Kisslo, MD
David B. Adams, RDCS

INTRODUCTION

Doppler echocardiography is a method for detecting the direction and velocity of moving blood within the heart. As will be seen in this program, the technique may be used for detection of cardiac valvular insufficiency and stenosis as well as a large number of other abnormal flows. The current interest in Doppler echocardiography has reached a remarkable level in just the past few years. Doppler methods extend the use of cardiac ultrasound into the evaluation of normal and abnormal flow states and provide quantitative data that are essential in the clinical decision making process concerning patients with heart disease.

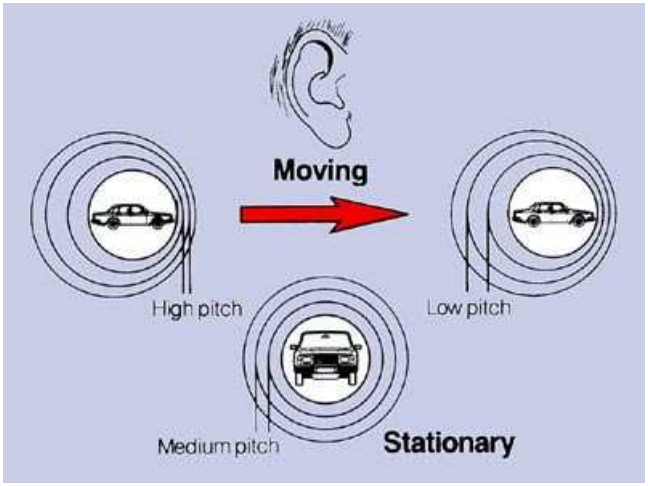

Figure 1.1: An example of the Doppler effect in every day life: the sound emitted from a stationary and moving automobile engine.

Understanding Doppler echocardiography begins with an understanding of the Doppler principle. All readers are familiar with the Doppler effect in every day life. For example, an observer stationed on a highway overpass readily notices that the pitch of the sound made from the engine of a passing automobile changes from high to low as the car approaches and then travels into the distance. The engine is emitting the same sound as it passes beneath, but the observer notices a change in pitch dependent upon the speed of the auto and its direction. **Figure 1.1** demonstrates the changes in the frequency from an approaching and departing sound source (the moving automobile) relative to a stationary sound source.

The first description of the physical principles used in Doppler echocardiography is attributed to Johann Christian Doppler, an Austrian mathematician and scientist who lived in the first half of the 19th century. Doppler's initial descriptions referred to changes in the wavelength of light as applied to astronomical events. In 1842, he presented a paper entitled "On the Coloured Light of Double Stars and Some Other Heavenly Bodies" where he postulated that certain properties of light emitted from stars depend upon the relative motion of the observer and the wave source. He suggested that the colored appearance of some stars was caused by their motion relative to the earth, the blue ones moving toward earth and the red ones moving away.

He drew an analogy of a ship moving to meet, or retreat from, incoming waves. The ship moving out to sea would meet the waves with more frequency than a ship moving toward the shoreline. Interestingly, Doppler never extrapolated his postulations to sound waves.

The Doppler principle is now used in many complex technologies. It is the fundamental principle upon which complex radar weather systems detect the severity of approaching storms and tracks its speed. It is also used by police to determine the speed of fast moving automobiles.

THE DOPPLER PRINCIPLE AND THE STUDY OF CARDIAC FLOWS

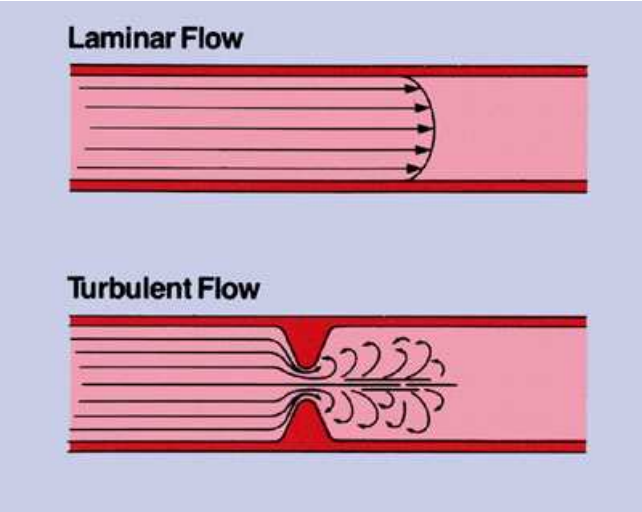

Figure 1.2: Diagrammatic representation of normal laminar flow in comparison with turbulent flow that results in whirls and eddies of many different velocities.

Blood Flow Patterns

Blood flow through the heart and great vessels has certain characteristics that can be measured using Doppler instruments designed for medical use. For the purpose of understanding flow patterns in the heart, it is important to recognize the difference between laminar flow and turbulent (or disturbed) flow. Laminar flow is flow that occurs along smooth parallel lines in a vessel so that all the red cells in an area are moving at approximately the same speed and in the same direction **(Fig. 1.2)**. Due to friction, flow is always slightly slower near the walls of a vessel. With the pulsations of the heart, the red cells generally accelerate and decelerate at approximately the same speed. Flow in most of the cardiovascular system, including the heart and great vessels, is normally laminar and rarely exceeds the maximum velocity of 1.5 m/sec.

In contrast, turbulent or disturbed flow is present when there is some obstruction that results in a disruption of the normal laminar pattern. This causes the orderly movement of red blood cells to become disorganized and produces various whirls and eddies of differing velocities and directions. Obstruction to flow usually also results in some increase in velocity. Thus, turbulent flow is characterized by disordered directions of flow in combination with many different red cell velocities. If the obstruction is significant, some of the red blood cells may be moving at higher velocities than normal and may reach speeds of 7 m/sec. Turbulent flow is usually an abnormal finding and is considered indicative of some underlying cardiovascular pathology.

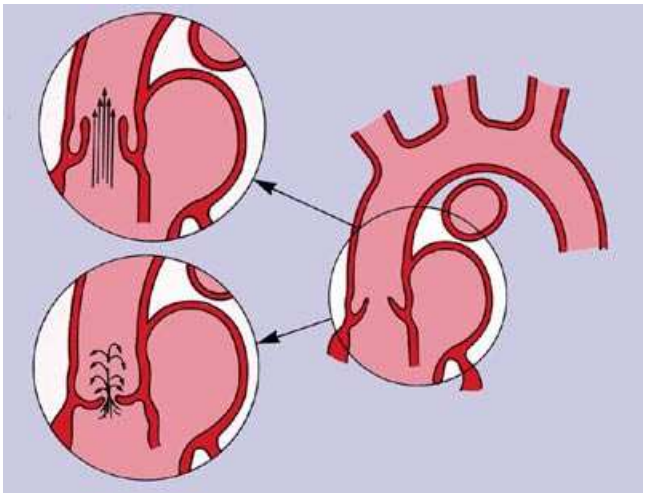

Figure 1.3: Examples of normal laminar flow through the aortic valve (top) and disturbed or turbulent flow resulting from aortic stenosis (bottom).

Abnormal flows are therefore generally characterized by turbulence and any increase in velocity. As an example, consider blood flow in the ascending aorta during systole. If the aorta and aortic valve are normal, then this flow is laminar. However, the presence of a valvular stenosis will induce a turbulent flow pattern. **Figure 1.3** shows that a narrowed aortic valve orifice interrupts the parallel lines of normal laminar flow and produces turbulent flow. The resulting jet of blood creates a short segment within the proximal aorta with complex flow and velocity characteristics.

The Frequency of Sound Waves

Conventional two-dimensional echocardiographic systems emit high frequency bursts of sound (ultrasound) into the tissues. In standard echocardiographic imaging a given pulse of ultrasound is transmitted into the body and then reflected back from the various tissues. Since the speed of sound in tissue is known (approximately 1540 m/sec), a standard ultrasound imaging system can wait for a given time for the transmitted pulse to travel to a target (time X) and then back (time 2X) and the given target will be received and recorded. In complex two-dimensional imaging systems this alternating process is repeated in a variety of directions thousands of times each second. The best ultrasound images are made when the target is perpendicular (or specular) to the sound waves.

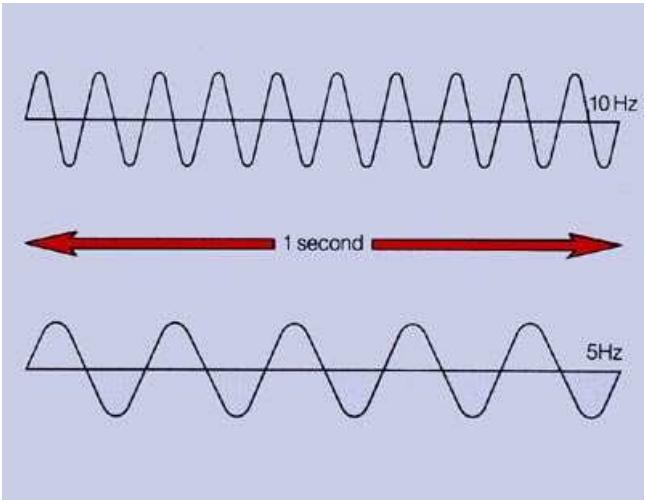

Figure 1.4: Sound is emitted in waves of measurable frequencies.

Frequency is a fundamental characteristic of any wave phenomenon, including sound, and refers to the number of waves that pass a given point in one second **(Fig. 1.4)**. It is usually described in units of cycles per second or Hertz (Hz). Thus, the top of the illustration in **Figure 1.4** shows an example of a waveform of 10 Hz while the one below is 5 Hz. Ultrasound is emitted in waveforms of a known frequency.

Doppler echocardiography, on the other hand, depends entirely on measurement of the *relative change* in the returned ultrasound frequency when compared to the transmitted frequency. Depending on the relative changes of the returning frequencies, Doppler echocardiographic systems measure these characteristics of disturbed flow: direction, velocity and turbulence. This enables examiners to differentiate between normal and abnormal flow patterns and, in some cases, to quantitate those characteristics that are helpful in determining the severity of abnormal flow states.

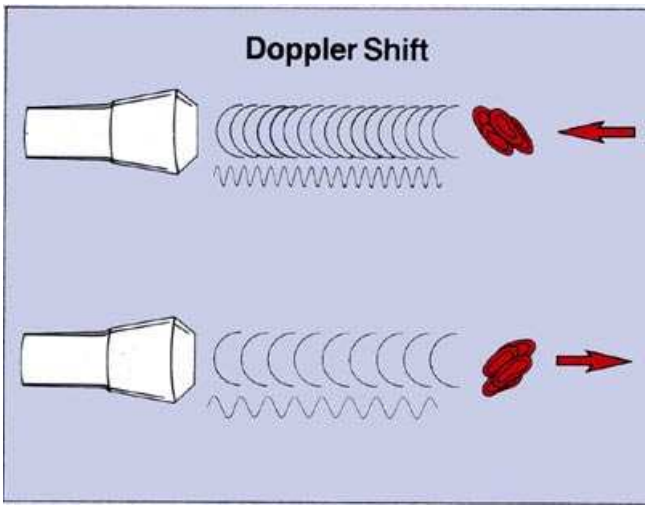

Figure 1.5: For any given transmitted ultrasound frequency, the returned frequency will be higher after encountering red blood cells moving toward the transducer and lower after encountering red cells moving away from the transducer.

Most readers understand frequencies in relationship to the pitch of audible sound. The relationship between pitch and frequency is simple: the pitch of any given sound is proportional to its frequency. As sound wave frequency increases, pitch gets higher; and as frequency decreases, pitch declines.

Doppler systems are totally dependent on the changes in the frequency of the transmitted ultrasound that result from the encounter of the wavefront with moving red blood cells. **Figure 1.5** shows a transducer on the left that is emitting a given frequency of ultrasound toward the right and into the tissues. The transmitted sound waves encounter a group of red cells moving toward the transducer and are reflected back at a frequency higher than that at

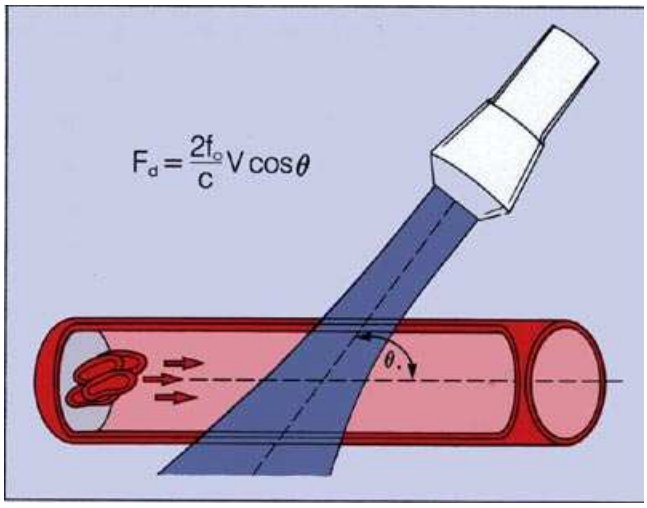

Figure 1.6 : The Doppler equation solved for frequency shift.

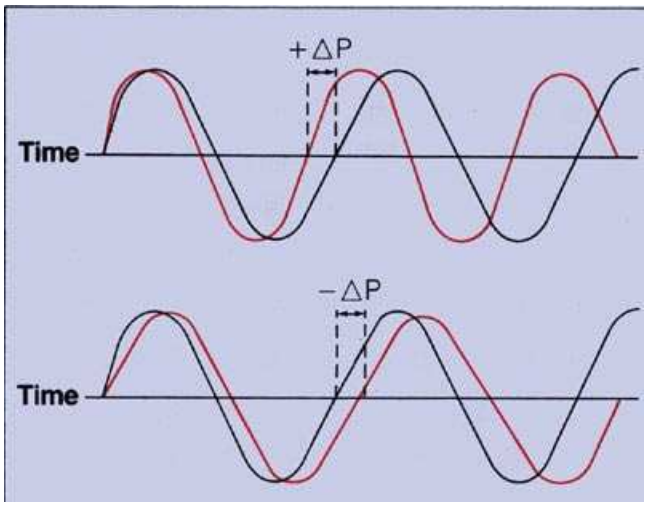

Figure 1:7: The phase shifts of returning frequencies are compared with transmitted frequency within the Doppler system. Positive shifts (top) result from blood moving away from, and negative shifts (bottom) result from blood moving toward, the transducer..

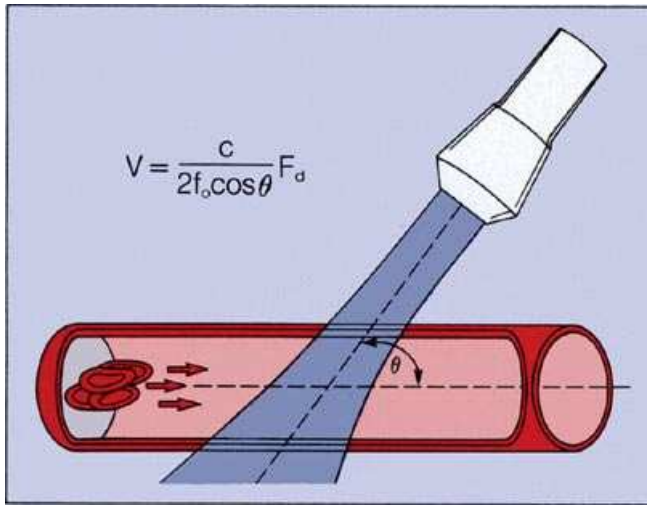

Figure 1.8: The Doppler equation rearranged for determination of velocity. It is velocity that is displayed by the Doppler instrument.

which they were sent producing a positive Doppler shift. The opposite effect occurs when a given frequency sent into the tissues encounters red cells moving away. The result is the return of a frequency lower than that transmitted, and the Doppler shift is negative.

The Doppler Equation

This Doppler effect in tissues maybe expressed as an equation as shown in **Figure 1.6**. Simply stated, the Doppler shift (Fd) of ultrasound will depend on both the transmitted frequency (fo) and the velocity (V) of the moving blood. This returned frequency is also called the "frequency shift" or "Doppler shift" and is highly dependent upon the angle (θ) between the beam of ultrasound transmitted from the transducer and the moving red blood cells. The velocity of sound in blood is constant (c) and is an important part of the Doppler equation.

The Direction and Velocity of Flow

The fact that makes frequency of the Doppler effect more than just an interesting curiosity is that it actually provides a method that is used to measure the direction and speed of moving red blood cells. Clinically we are most interested in measuring velocity since, as mentioned above, it is altered in disease states.

A Doppler system then compares the transmitted waveform with the received waveform for a change in frequency as shown in **Figure 1.7**. These are called "phase shifts" and they are automatically determined within the Doppler instrument. If there is a higher returning frequency (+AP) then the flow is called a "positive Doppler shift" and represented as moving toward the transducer. If there is a lower returning frequency (-AP) then the flow is called a "negative Doppler shift" and represented as moving away from the transducer. All components of the Doppler equation, except velocity, are readily measured by the Doppler instrument. The Doppler equation may be rearranged to solve for velocity of blood movement as shown in **Figure 1.8**. The angle θ (the angle the Doppler beam is incident to flow) may be measured or may be assumed to be parallel

depending upon orientation of the beam by the system operator.

The Doppler device can be regarded as a complex speedometer designed to detect red cell motion (i.e., blood flow) and measure its velocity. What is important to recognize is that:

FREQUENCY SHIFT → DOPPLER EQUATION → VELOCITY DATA

The Doppler Display

All Doppler systems have audio outputs and listening to this is very helpful during a Doppler examination. The changing velocities (frequencies) are converted into audible sounds and, after some processing, are emitted from speakers placed within the machine.

High pitched sounds result from large Doppler shifts and indicate the presence of high velocities, while low pitched sounds result from lesser Doppler shifts. Flow direction information (relative to the transducer) is provided by a stereophonic audio output in which flow toward the transducer comes out of one speaker and flow away from the transducer.

The audio output also allows the operator to easily differentiate laminar from turbulent flow. Laminar flow produces a smooth, pleasant tone because of the uniform velocities. Turbulent flow, because of the presence of many different velocities, results in a commonly high-pitched and whistling or harsh and raspy sound.

The audio output remains an indispensable guide to the machine operator for achieving proper orientation of the ultrasound beam, even when Doppler echocardiography is being used in conjunction with an ultrasound imaging technique. The trained ear can readily appreciate minor changes in spectral composition more readily than the eye, given the same information displayed graphically. The major limitation of audio Doppler outputs is the requirements for subjective interpretation and the lack of a permanent objective record. The audio output from a Doppler machine is not the same as that received by a stethoscope or a phonocardiogram. The sounds detected with a stethoscope are transmitted vibrations or pressure waves from the heart and great vessels that are believed to be the result of rapid accelerations and decelerations of blood. The Doppler audio output, in contrast, is an audible display of the Doppler frequency shift spectrum produced by red cells moving in the path of the ultrasound beam. It is a sound produced by the Doppler machine that does *not* occur in nature and, therefore, it does not originate in the heart. All newer generations of Doppler echocardiography equipment contain sophisticated sound frequency or velocity spectrum analyzers for hard copy recording. Most commercially available Doppler systems display a spectrum of the various velocities present at anytime and are, therefore, called "spectral velocity recordings.

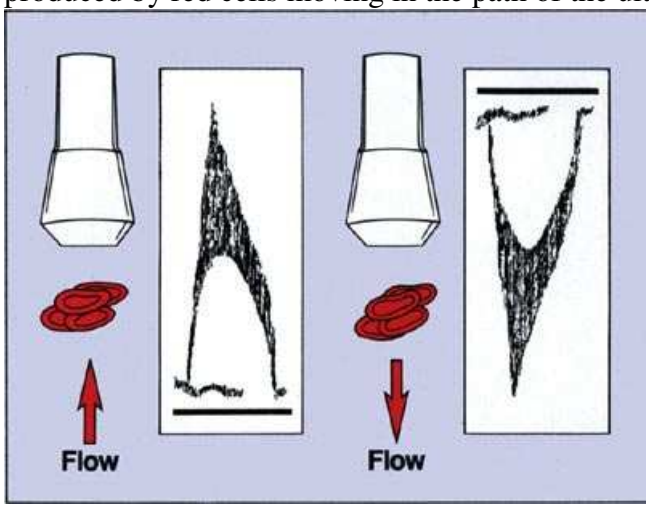

Figure 1.9: Schematic representation of the velocity output of flow. Flow toward the transducer is displayed above the baseline and flow away from the transducer is displayed below the baseline.

Flow velocity toward the transducer is displayed as a positive, or upward, shift in velocities while flow velocity away from the transducer is displayed as a negative, or downward shift in velocities **(Fig. 1.9)**. Time is on the horizontal axis.

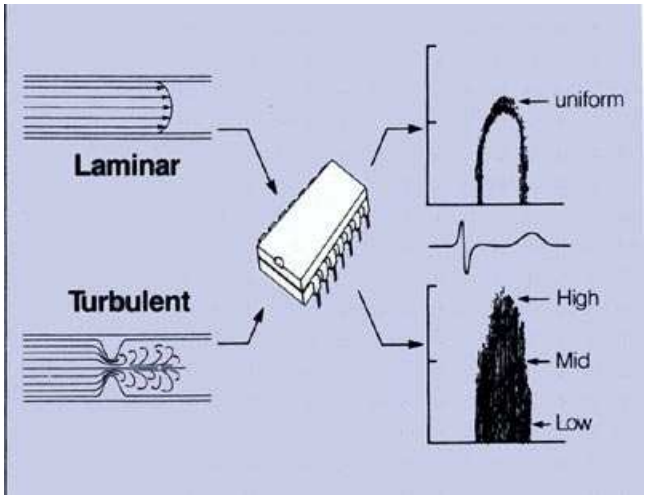

Figure 1.10: The various velocities detected by the Doppler instrument are processed by Fast Fourier Transform (FFT) and the resulting spectrum of velocities present is displayed. Laminar flows are uniform. Turbulent flows show spectral broadening.

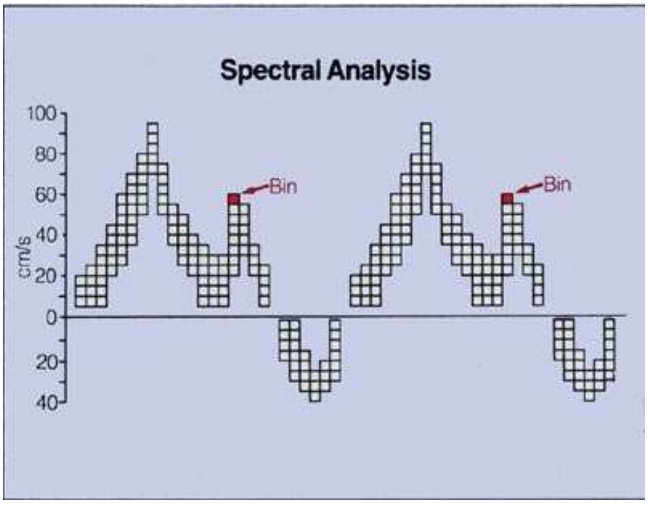

Figure 1.11 : The spectral analysis is created by placing the velocity data into bins that are displayed over time.

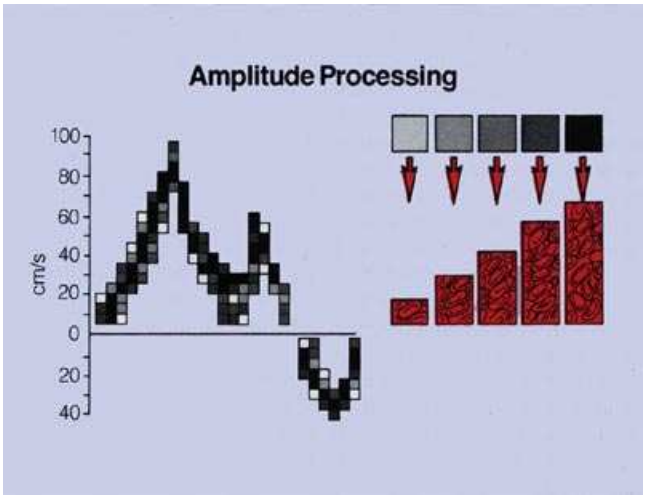

Figure 1.12: The brightness of the signal at any given bin relates to the relative number of red cells detected at that velocity. The term "amplitude" is applied to relative brightness.

The internal working of such systems are complex but the results are rather simple. When flow is laminar and all the red cells are accelerating and decelerating at approximately the same velocities, a neat envelope of these similar velocities is recorded over time **(Fig. 1.10)**. When flow is turbulent, however, there are many different velocities detected at any one time (a wide spectrum of velocities). Such turbulence, produced by an obstruction to flow, results in the spectral broadening (display of velocities that are low, mid and high) and an increase in peak velocity as seen in disease states.

This display of the spectrum of the various velocities encountered by the Doppler beam is accomplished by very sophisticated microcomputers that are able to decode the returning complex Doppler signal and process it into its various velocity components. There are two basic methods for accomplishing this. The most popular is Fast Fourier Transform (FFT) and the other is called Chirp-Z Transform. These are simply ways for deciphering, analyzing and presenting vast amounts of returning data.

A better understanding of the complex creation of a spectral velocity recording helps one in performing and interpreting Doppler studies. The spectral recording **(Fig. 1.11)** is really made up of a series of "bins" (vertical axis) that are recorded over time (horizontal axis). At any given point in time there is a differential speed of movement of red cells with more red blood cells moving at the velocity of the most intense bin than are moving at the other velocities which are represented by the less intense bins **(Fig. 1.12)**. The intensity of any bin refers to the "amplitude" or brightness. Thus, the velocity spectral analysis is really a complex plot of the various velocities over time.

Since this full spectral display is so highly processed there are a variety of other outputs that can be displayed and they are electronically derived from the spectral data **(Fig. 1.13)**. These include mean velocity and maximum velocity. A line drawn as an

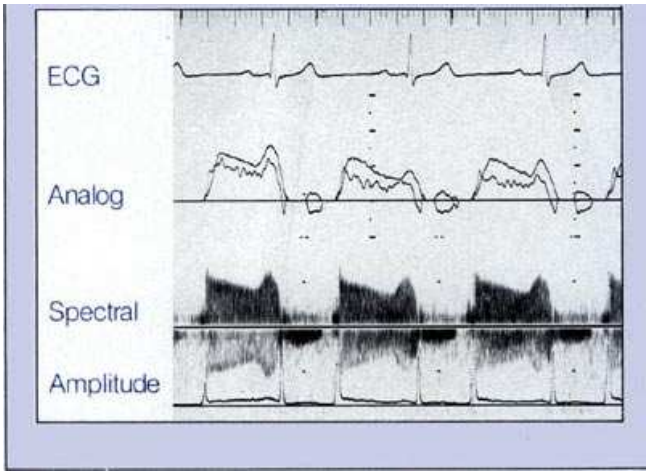

Figure 1.13: An example of the various Doppler displays from a patient with mitral stenosis with the transducer held at the apex. Flow in diastole is toward the transducer. The ECG, analog outputs (maximum and mean velocities), spectral display, and amplitude signals are shown.

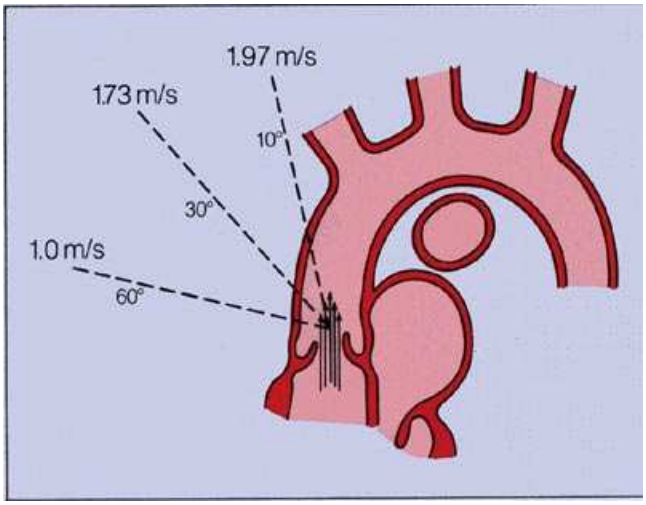

Figure 1.14: Schematic diagram showing the importance of being parallel to flow when detecting flow through the aortic valve. A jet of known velocity (2.0 m/s) emerges from the aortic valve in systole. Moving 60 degrees from parallel only allows a peak velocity of 1.0 m/s to be recorded. The most accurate

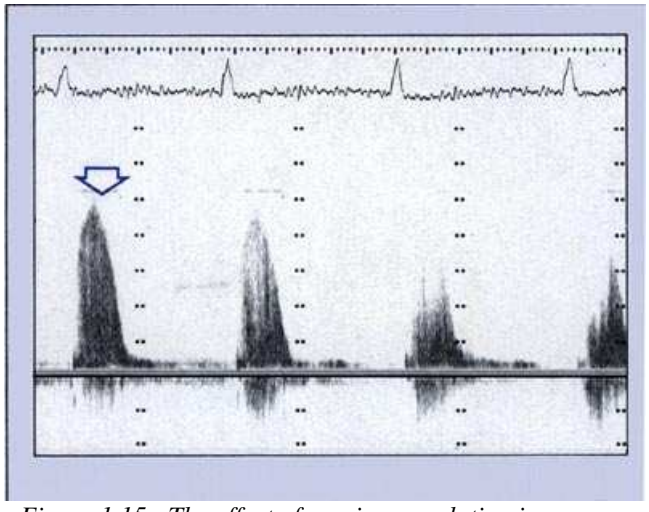

Figure 1.15: The effect of varying angulation in relation to a systolic jet in a patient with aortic stenosis taken from the suprasternal notch with flow toward the transducer. Note that the peak jet is nearly 5 m/s (open arrow). In subsequent beats the flow profile is lost.

envelope around the spectrum at the peak Doppler shift at any point during the cardiac cycle is the peak velocity profile. Mean Doppler shift can be estimated from a line drawn through the darkest part of the spectrum. The brightness, or "amplitude," may also be displayed. For standard clinical purposes the full spectrum is generally used.

The Effect of Angle

The Doppler equation also tells us that the angle the Doppler beam is relative to the lines of flow being evaluated is very important. This angle theta, (written as θ in the Doppler equation), is of crucial importance in the calculation of velocities from Doppler shift data in **Figure 1.14** where the effect of varying angle on the measurement of peak velocity of an aortic stenotic jet is shown.

When the ultrasound beam is directed parallel to blood flow, angle θ (cosine $0^o = 1$) and measured velocity on the recording will be true velocity. In contrast, with the ultrasound beam directed perpendicular to flow, angle θ = 90 degrees (cosine $90^o = 0$) and measured velocity will be zero. Therefore, the smaller the angle, the closer angle cosine θ is to 1.0 and the more reliable is the recorded Doppler velocity. A wider angle will result in a greater reduction in measured velocity compared to true velocity.

Thus, the more parallel to flow the Doppler ultrasound beam is directed the more faithfully the measured velocity will reflect true velocity. For practical purposes, angles of greater than 25^o between the ultrasound beam and the blood flow being studied will generally yield clinically unacceptable qualitative estimates of velocity.

A Doppler operator seeking the best quantitative estimates of flow must, therefore, always attempt to orient the beam parallel to flow. This concept is of fundamental importance in the clinical examination. The actual effect of changing angle on a systolic aortic stenotic jet toward a transducer in the suprasternal notch is shown in **Figure 1.15**. The first beat (open arrow) shows the only fully formed profile.

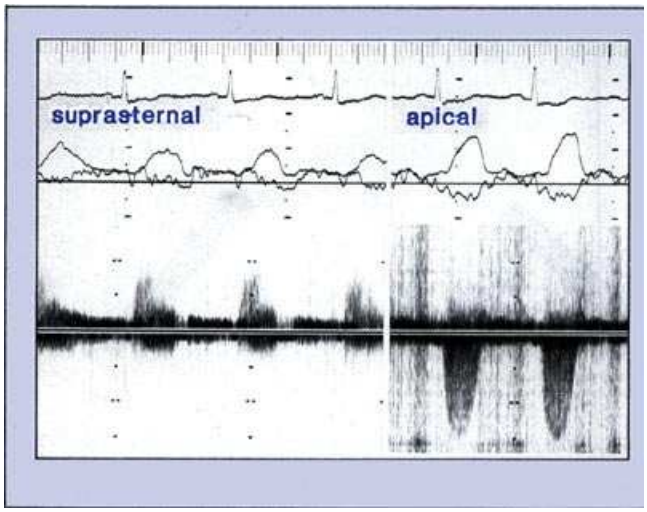

Figure 1.16: Suprasternal (left, with flow toward the transducer) and apical (right, with flow away from the transducer) jet of aortic stenosis. The best profile was taken from the apical position.

Such abnormal jets are often eccentric and their directions cannot always be predicted. A Doppler examiner must therefore interrogate the jet from a variety of angles. Note that the full jet is not seen from the suprasternal area in this patient but is detected from the apical approach. The great importance of this concept in the clinical examination for aortic stenosis is demonstrated in **Figure 1.16**. The need to be parallel to flow leads the Doppler examiner to depend on some windows for examination that may sacrifice the quality of the two-dimensional image. For example, the direction of the ultrasound beam through either the mitral or tricuspid orifices from the apical position offers an excellent Doppler window but one which may allow significant echocardiographic "drop-out" since the imaging beams are parallel to the endocardium.

Simultaneous Imaging and Doppler

Since both two-dimensional and Doppler echocardiography use ultrasound, it is logical to assume that both Doppler and imaging functions can be combined into one ultrasound instrument. It is important to realize that creation of the image takes time as does creation of the Doppler information. The imaging device is already working as quickly as it can to transmit, receive and then display the image data.

Therefore, time is the critical factor for any shared arrangement. These problems are solved by switching off the imaging mode (sometimes with the image held in memory) while the Doppler modes are in operation. This results in either an image or Doppler choice. In some systems a complex time sharing arrangement allows some Doppler to be carried on while the image of the heart is still moving. When this happens, there is always some sacrifice of the quality of the Doppler information and frequently also in the image information. Conventional Doppler and imaging simply do not work to their full capabilities in these interlaced modes.

PULSED AND CONTINUOUS WAVE DOPPLER

There are two main types of Doppler echocardiographic systems in common use today, continuous wave and pulsed wave. They differ in transducer design and operating features, signal processing procedures and in the types of information provided. Each has important advantages and disadvantages and, in our opinion, the current practice of Doppler echocardiography requires some capability for both forms.

Continuous Wave Doppler

Continuous wave (CW) Doppler is the older and electronically more simple of the two kinds. As the name implies, CW Doppler involves continuous generation of ultrasound waves coupled with continuous ultrasound reception. A two crystal transducer accomplishes this dual function with one

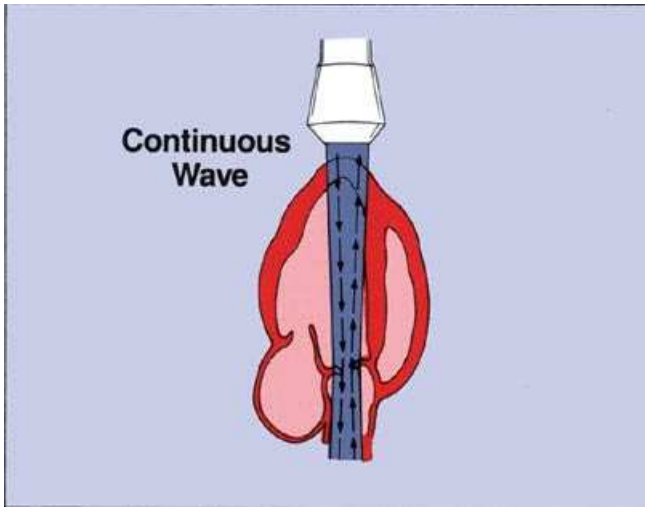

Figure 1.17: In CW Doppler, the transducer is constantly emitting and receiving ultrasound data.

crystal devoted to each function **(Fig. 1.17)**.

The main advantage of CW Doppler is its ability to measure high blood velocities accurately. Indeed, CW Doppler can accurately record the highest velocities in any valvular and congenital heart disease. Since velocities exceeding 1.5 m/sec are frequently seen in such disorders, accurate high velocity measurement is of particular importance for allowing the recognition of the full abnormal flow profile. It is also of considerable importance for the quantitative evaluation of abnormal flows, as will be seen later.

The main disadvantage of CW Doppler is its lack of selectivity or depth discrimination. Since CW Doppler is constantly transmitting and receiving from two different transducer heads (crystals) there is no provision for imaging or range gating to allow selective placing of a given Doppler sample volume in space. As a consequence, the output from a CW examination contains Doppler shift data from *every* red cell reflecting ultrasound back to the transducer along the course of the ultrasound beam.

Thus, true CW Doppler is functionally a stand-alone technique whether or not the capability is housed within a two-dimensional imaging transducer. The absence of anatomic information during CW examination may lead to interpretive difficulties, particularly if more than one heart chamber or blood vessel lies in the path of the ultrasound beam.

It is possible , however, to program a phased array system to perform both two-dimensional and CW Doppler functions almost simultaneously. The quasi-simultaneous CW-imaging uses a time sharing arrangement in which the transducer rapidly switches back and forth from one type of examination to the other. Because this switching is done at very high speeds, the operator gets the impression that both studies are being done continuously and in real-time. During the imaging period, no Doppler data is being collected, so an estimate is generated, usually from the preceding data. During the Doppler collection period, previously stored image data is displayed. This arrangement usually degrades the quality of both the image and Doppler data.

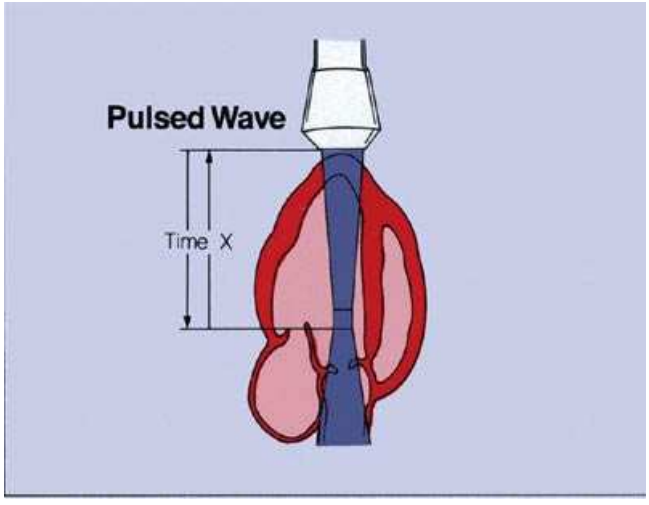

Figure 1.18: In PW Doppler, the transducer alternately transmits and received the ultrasound data to a sample volume. This is also known as range-gated Doppler.

Pulsed Wave Doppler

Pulsed wave (PW) Doppler systems use a transducer that alternates transmission and reception of ultrasound in a way similar to the M-mode transducer **(Fig. 1.18)**. One main advantage of pulsed Doppler is its ability to provide Doppler shift data selectively from a small segment along the ultrasound beam, referred to as the "sample volume". The location of the sample volume is operator controlled. An ultrasound pulse is transmitted into the tissues travels for a given time (time X) until it is reflected back by a moving red

cell. It then returns to the transducer over the same time interval but at a shifted frequency. The total transit time to and from the area is 2X. Since the speed of ultrasound in the tissues is constant, there is a simple relationship between roundtrip travel time and the location of the sample volume relative to the transducer face (i.e., distance to sample volume equals ultrasound speed divided by round trip travel time). This process is alternately repeated through many transmit-receive cycles each second.

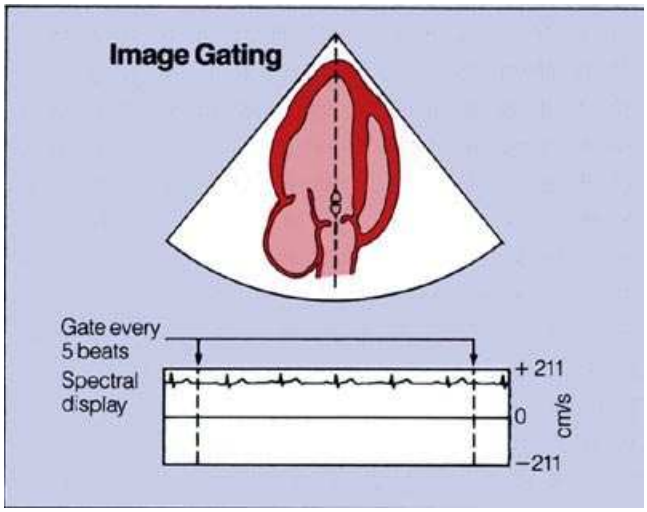

Figure 1.19: When the PW Doppler operates, it causes the two-dimensional image to be held in a frozen frame. The image is periodically updated and will usually appear as a blank on the spectral display (dashed lines).

This range gating is therefore dependent on a timing mechanism that only samples the returning Doppler shift data from a given region. It is calibrated so that as the operator chooses a particular location for the sample volume, the range gate circuit will permit only Doppler shift data from inside that area to be displayed as output. All other returning ultrasound information is essentially "ignored".

Another main advantage of PW Doppler is the fact that some imaging may be carried on alternately with the Doppler and thus the sample volume may be shown on the actual two-dimensional display for guidance. PW Doppler capability is possible in combination with imaging from a mechanical or phased array imaging system. It is also generally steerable through the two-dimensional field of view, although not all systems have this capability.

In reality, since the speed of sound in body tissues is constant, it is not possible to simultaneously carry on both imaging and Doppler functions at full capability in the same ultrasound system. In mechanical systems, the cursor and sample volume are positioned during real-time imaging, and the two-dimensional image is then frozen when the Doppler is activated. With most phased array imaging systems the Doppler is variably programmed to allow periodic update of a single frame two-dimensional image every few beats **(Fig. 1.19)**. In other phased arrays, two-dimensional frame rate and line density are significantly decreased to allow enough time for the PW Doppler to sample effectively. This latter arrangement gives the appearance of near simultaneity.

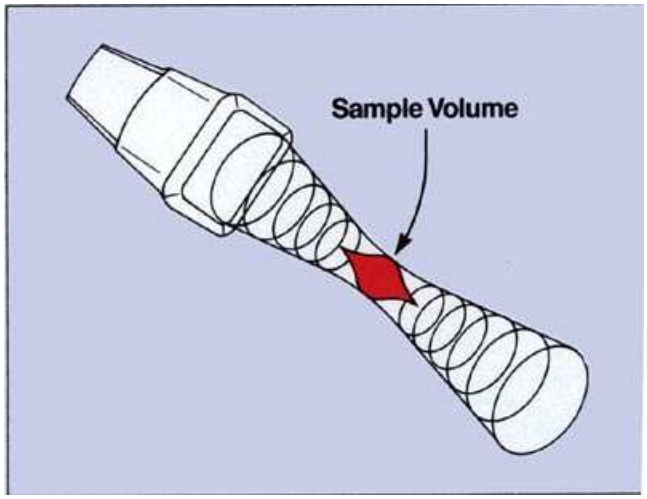

Figure 1.20: The sample volume of PW Doppler is actually a three-dimensional volume that changes in size at its location relative to the transducer is changed. When placed in the far field, it becomes very large.

The sample volume is really a three-dimensional, teardrop shaped portion of the ultrasound beam **(Fig. 1.20)**. Its volume varies with different Doppler machines, different size and frequency transducers and different depths into the tissue. Its width is determined by the width of the ultrasound beam at the selected depth. Its length is determined by the length of each transmitted ultrasound pulse.

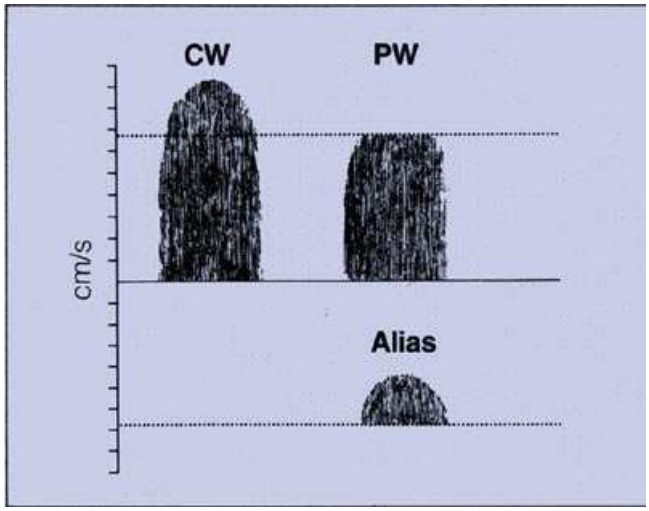

Figure 1.21: Schematic rendering of the full spectral display of a high velocity profile fully recorded by CW Doppler. The PW display is aliased, or cut off, and the top is placed at the bottom.

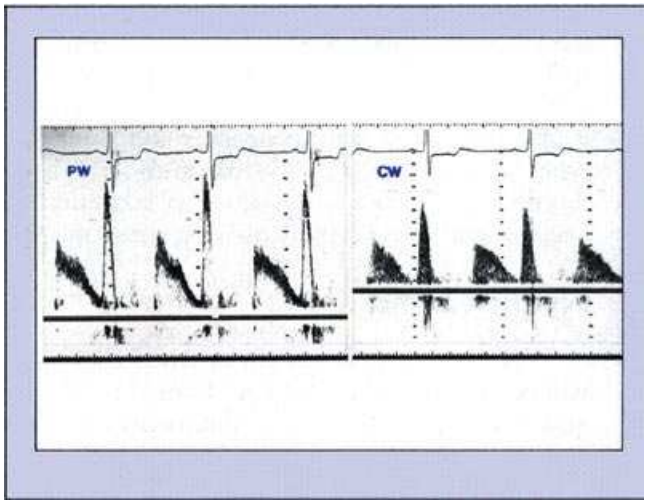

Figure 1. 22: Spectral displays of diastolic flow through the mitral orifice. The transducer is located at the apex and diastolic flow is toward the transducer (positive) Note the laminar appearance of the PW display. The CW does not usually display the same laminar flow pattern as it receives flow information from all portions of the ultrasound beam.

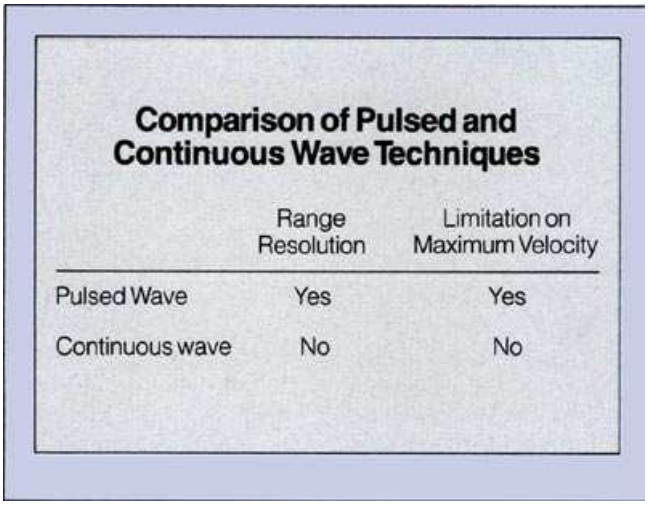

Comparison of Pulsed and Continuous Wave Techniques

	Range Resolution	Limitation on Maximum Velocity
Pulsed Wave	Yes	Yes
Continuous wave	No	No

Figure 1. 23: Table summarizing the advantages and disadvantages of pulsed and continuous wave Doppler echocardiography..

Therefore, the farther into the heart the sample volume is moved, the larger it effectively becomes. This happens because the ultrasound beam diverges as it gets farther away from the transducer.

The main disadvantage of PW Doppler is its inability to accurately measure high blood flow velocities, such as may be encountered in certain types of valvular and congenital heart disease. This limitation is technically known as "aliasing" and results in an inability of pulsed Doppler to faithfully record velocities above 1.5 to 2 m/sec when the sample volume is located at standard ranges in the heart **(Fig. 1.21)**. Aliasing is represented on the spectral trace as a cut-off of a given velocity with placement of the cut section in the opposite channel or reverse flow direction. Because aliasing is so common in disease states, it will be considered in more detail in the next section.

The spectral outputs from PW and CW appear differently **(Fig. 1.22)**. When there is no turbulence, PW will generally show a laminar (narrow band) spectral output. CW, on the other hand, rarely displays such a neat narrow band of flow velocities even with laminar flow because all the various velocities encountered by the ultrasound beams are detected by CW.

It can usually be said that when an operator wants to know where a specific area of abnormal flow is located that pulsed wave Doppler is indicated. When accurate measurement of elevated flow velocity is required, then CW Doppler should be used. The various differences between pulsed and continuous wave Doppler are summarized in **Figure 1.23**.

Aliasing

The aliasing phenomenon occurs when the abnormal velocity exceeds the rate at which the pulsed wave system can record it properly. PW Doppler spectral tracing in **Figure 1.24** from an individual with aortic insufficiency with the transducer positioned at the apex. In this situation, abnormal diastolic flow is detected toward the transducer and recorded in

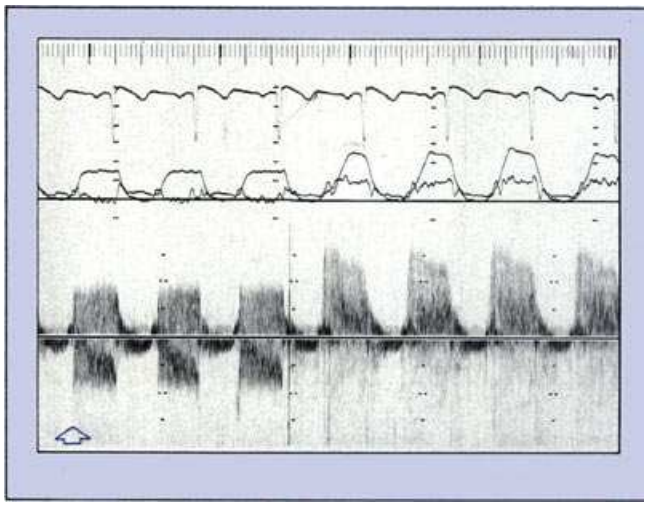

Figure 1. 24: Aliased spectral display of aortic insufficiency (left arrow) in PW mode detected from the ventricular apex. Abnormal flow is toward the transducer. After 3 beats, the system is switched to CW and the full profile is seen.

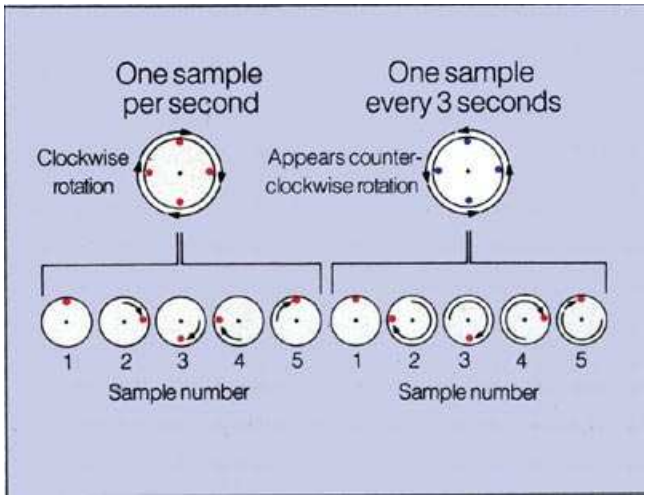

Figure 1. 25: Schematic depiction of the origin of the aliasing phenomenon using a turning wheel. When the Nyquist limit is exceeded, aliasing occurs. For details, see text.

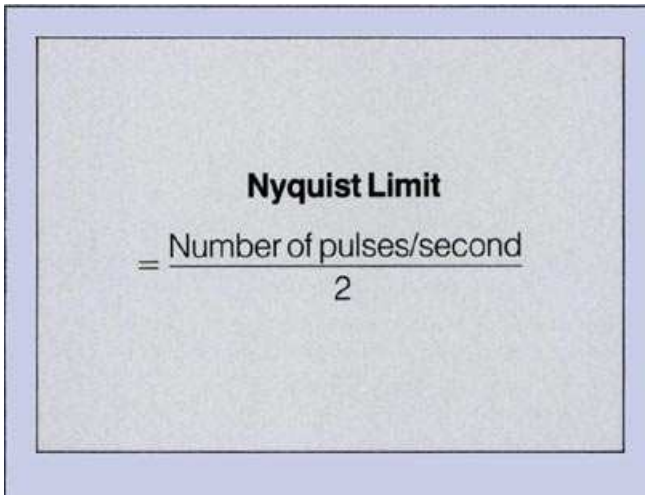

Figure 1. 26: The Nyquist limit is defined by the number of pulses/second divided by two.

a positive, or upwards direction. The system first detects a pulsed (and aliased) spectral profile. After the fourth beat, the system is switched into CW and the full profile is recognized. The aliased portion in the first three beats is cut off the top of the velocity spectrum and replaced at in the reverse channel, or below the baseline (open arrow).

The phenomenon of aliasing is best explained using a simple example **(Fig. 1.25)**. A mark is placed on a turning wheel and the wheel rotates in a clockwise fashion at a speed of one turn every four seconds. If the sample rate (or pulse repetition frequency) is one sample per second the mark is recorded at each progressive 90 degree position. The final recording would then show the proper clockwise direction of motion of the wheel **(Fig. 1.25 *left column*)**.

If the sample rate (or pulse repetition frequency) is slowed to only one sample every three seconds a strange phenomenon occurs **(Fig. 1.25 *right column*)**. Note that the mark is moving 180 degrees between sampling times and that while actually turning clockwise the recording makes the wheel appear to be moving in the opposite, or counter-clockwise, direction. This is also the reason why propellers and wagon wheels appear to go backwards in movies as the film frame rate is too slow to accurately keep up with these rapidly moving structures.

Nyquist Limit

The Nyquist limit defines when aliasing will occur using PW Doppler **(Fig. 1.26)**. The Nyquist limit specifies that measurements of frequency shifts (and, thus, velocity) will be appropriately displayed only if the pulse repetition frequency (PRF) is at least twice the maximum velocity (or Doppler shift frequency) encountered in the sample volume.

It is obviously desirable to use as high a PRF as possible for recording abnormally elevated velocity jets. The problem is that the maximum PRF is limited by the distance the sample volume is placed into the heart.

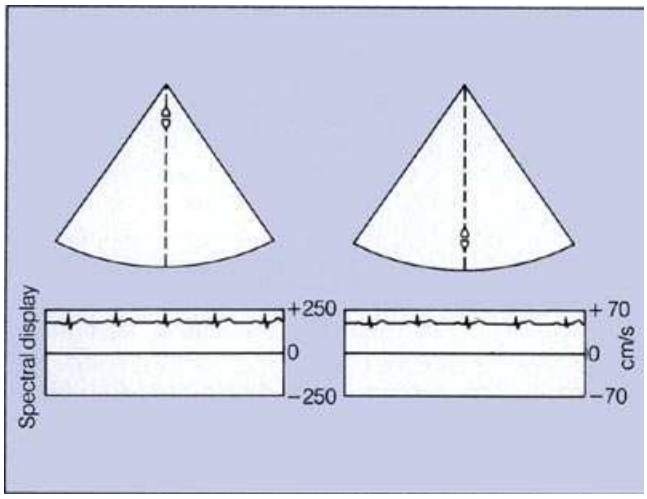

Figure 1. 27: The left panel shows the sample volume placed in the near field. Higher velocities may be recorded with a location near the transducer than when the sample volume is positioned at a farther range (right panel).

The closer the sample volume is located to the transducer the higher the maximum PRF that can be used. Conversely, the farther the sample volume is placed into the heart the lower the maximum PRF becomes. This occurs because the distance (and therefore pulse travel time) to and from the sample volume is much shorter in the near field and, therefore, pulse roundtrip transit time is much less when compared with greater distances. An example of the spectral velocity display with the sample volume located in the near field is shown in **Figure 1.27**. The maximum velocity that can be recorded without aliasing is 2.50 m/sec in either direction **(Fig. 1.27 *left panel arrow*)**. When the sample volume is positioned farther into the field the maximum possible velocity in either direction is reduced to .70m/sec **(Fig. 1.27, *right panel arrow*)**.

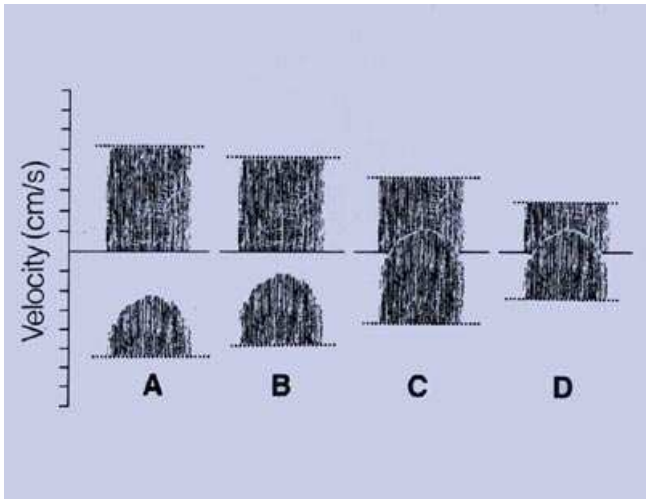

Figure 1. 28: Schematic drawing of the effect of a reduction in the Nyquist limit in PW echo when a high velocity jet is encountered in the near field (A) or successively deeper into the tissues (B, C, and D). Note the progressive and marked aliasing of the spectral signal the farther away the jet is encountered from the transducer.

Note that with the Doppler system used in the previous example, the scale of the spectral display automatically changes. In some systems, the scale is fixed and the size of the spectral tracing will alter. **Figure 1.28** demonstrates mild aliasing when a high velocity jet is in the near field (A). Progressively more severe aliasing with distortion of the full profile occurs if this same jet is encountered at progressively increasing distances from the transducer face (*B, C and D*). At point D the aliased profile is so distorted as to be unrecognizable.

In a practical sense, the Nyquist limit is a descriptive term which specifies the maximum velocity that can be recorded without aliasing. This limit is controlled by two factors: depth into the tissue and transducer frequency.

When dealing with valvular heart disease, most abnormal jets exceed 1.5 to 2.0 m/sec. Therefore, Doppler beginners should not expect to record easily the full flow profile of these abnormal jets using PW Doppler. In fact, most beginners should simply attempt to recognize the presence of aliasing. With experience, it will become easier to identify an aliased signal. The recognition of aliasing on the audio output is difficult

Control of Aliasing

It is also important to realize that the maximum recordable velocities in any jet relate to the frequency of the transducer used. A lower frequency transducer increases the ability of a PW

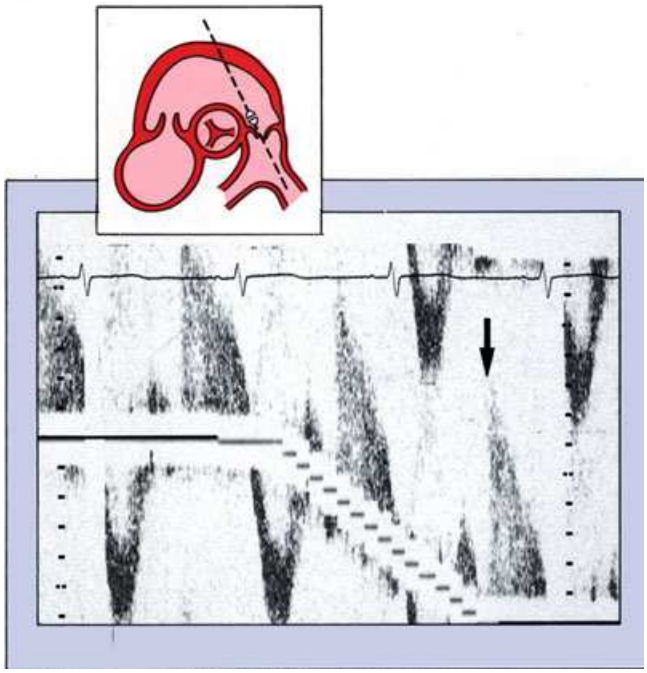

Figure 1. 29: Pulmonic insufficiency is detected by PW Doppler with the sample volume located in the right ventricular outflow tract. The baseline is lowered to reveal the full profile (arrow) of the regurgitant jet toward the transducer.

system to record high velocities at any given range. Thus, aliasing will be encountered at lower velocities with a 5 MHz transducer when compare to a 2.5 MHz transducer.

The main drawback of lowering the transducer frequency is a reduction in the signal to noise ratio of the resulting Doppler data (and thus the quality of the output). For this reason, most standard PW Doppler systems operate at approximately 2.5 MHz.

The second, and most practical, method to overcome aliasing is to take advantage of the range of velocity available in the opposite channel by moving the baseline (also known as "baseline shift"). In **Figure 1.29** almost the entire profile of a pulmonic insufficiency jet can be seen when the baseline is at the bottom of the display. In the left portion of this velocity spectrum, the top of the pulmonic insufficiency profile is poorly seen. As the baseline is moved downwards to the bottom of the display, the top of the spectral profile becomes obvious. This baseline control may be called "zero shift" or "zero off-set" on some systems. Note that use of the baseline shift control doubles the Nyquist limit at any given depth.

High PRF Doppler

It seems reasonable to expect that if the problem of aliasing is caused by an insufficiently high PRF, the way to reduce the problem is to find some method of increasing the PRF. Recently, some PW Doppler systems have been introduced which allow the operator to increase PRF above the Nyquist limit and thereby reducing aliasing. High PRF Doppler can use multiples of the PRF corresponding to the Nyquist limit at a given depth.

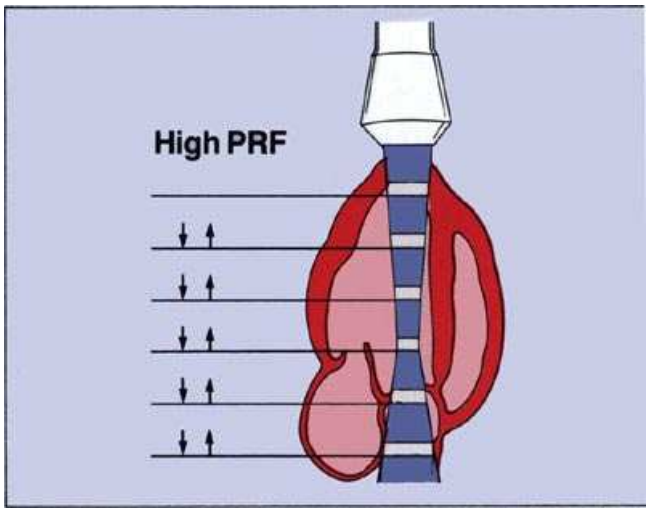

Figure 1. 30: High PRF systems do not wait for a single pulse to return to the transducer before pulsing again. Higher pulse repetition rates are achieved but some range ambiguity exists.

The basic principle of the so-called "high PRF" Doppler is illustrated in **Figure 1.30**. In this example a given high velocity is located near the mitral valve. If the pulse transit time to the jet and then back to the transducer is one second then the PRF is one pulse per second. Because the velocity being sampled exceeds the Nyquist limit, aliasing is seen in the spectral display. High PRF systems emit multiple pulses without waiting for the original one to be received. In this example multiple pulses are emitted and received each second. This results in an increase in PRF and a spectral display that is not aliased.

The problem with this approach is that some of the range selectivity used in precisely locating the sample volume is relinquished. As this pulsing sequence is carried on over and over, some data is returned to the transducer the points that are located by the increased PRF in space. If other turbulence were located at any one of these ranges the operator would not be able to tell where the high velocity jet of interest was located, as data from all these volumes are added together. This results in what is called "range ambiguity".

This method of increasing the PRF for the acquisition of high velocity data has been described as programming the machine to "think" that the high velocity jet is much closer to the transducer than it really is. In reality, the machine knows exactly what it is doing and the beginning operator is the one that is fooled.

When using the high PRF mode, it is best first to locate the high velocity jet or turbulence using standard single gate PW Doppler, and to ensure the absence of other areas of turbulence along the path of the ultrasound beam. The high PRF mode can then be used to record the unaliased Doppler signal.

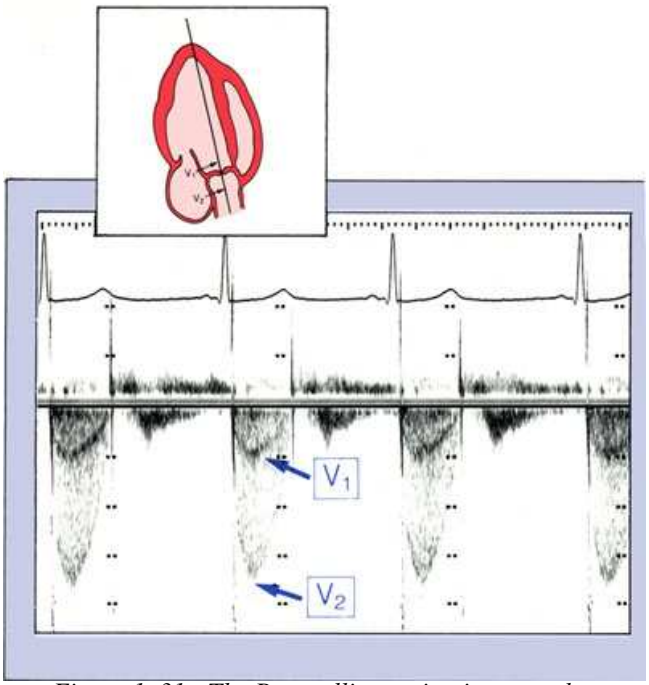

Figure 1. 31: The Bernoulli equation is a complex formula that may be reduced to its simplest expression

The Bernoulli Equation

There is clear justification for concern over accurate recording of very high velocity jets within the heart. As will be discussed in more detail later, the presence of an obstruction to flow, such as aortic stenosis, will result in a significant increase in velocity across the aortic valve in systole. In practice, these jets attain speeds of up to 7 m/sec.

The Bernoulli equation is a complex formula that relates the pressure drop (or gradient) across an obstruction to many factors, as is seen in **Figure 1.31**. For practical use in Doppler echocardiography this formula has been simplified to: $p_1-p_2=4V^2$

As we shall see later, Doppler recordings of velocity may, in certain situations, be used to estimate pressure gradients within the heart. When used for this purpose, it is important to keep in mind that the angle the Doppler beam is incident to any given jet may not be known since these examinations are frequently done blindly by CW. In these cases the operator always tries to orient a beam as parallel to flow as possible so that the full velocity recording is obtained (this assumes cosine θ =1).

Note that the full Bernoulli equation requires velocity data from below (V_1) and above (V_2) any given obstruction. Since V_1 is normally much smaller than V_2 **(Fig. 1.32)** it can usually be ignored in the calculation of a pressure gradient.

In the example cited, the peak velocity is approximately 3.5 m/sec and this would correspond to an aortic gradient of 48 mmHg by the simplified Bernoulli equation. Obviously, faithful recording of

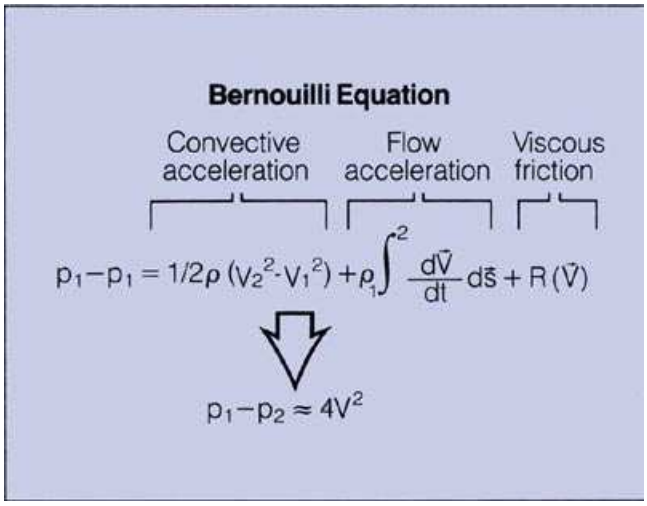

Figure 1. 32: An example of a CW spectral recording of aortic stenosis. There is a given velocity (V_1) on the ventricular side of the valve that is accelerated (V_2) as blood is ejected through the stenotic orifice. V_1 is usually ignored in the simplified Bernoulli equation.

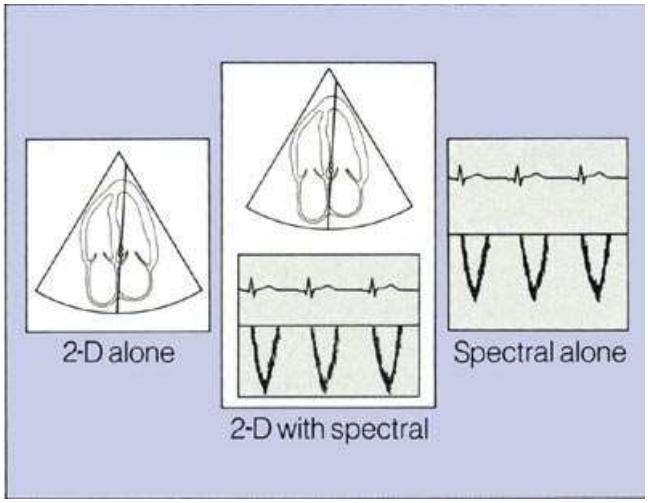

Figure 1. 33: Schematic representation summarizing the various displays available in the combined two-dimensional and Doppler system. Hard-copy spectral recordings are also available in systems with this capability.

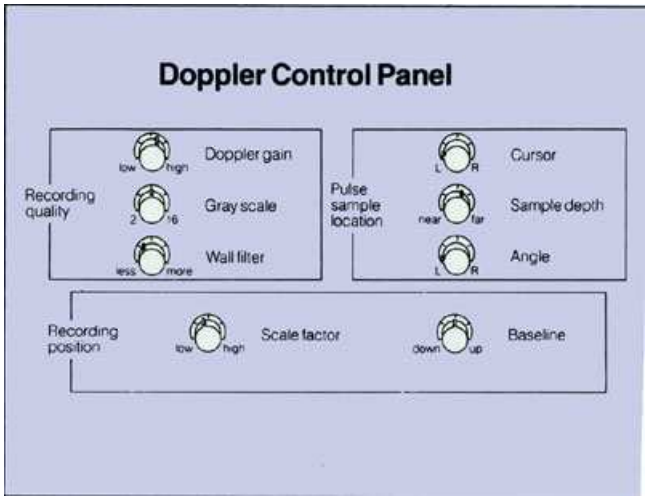

Figure 1. 34: Mock Doppler control panel showing the most common CW and PW Doppler controls. Almost every Doppler system with pulsed and continuous wave capabilities will contain these controls.

abnormal velocities has great importance, not only for clear identification and recognition of abnormal profiles but also for quantitative purposes.

System Display Capabilities

There are various displays available in Doppler echocardiographic systems **(Fig 1.33)**. The operator sees a normal two-dimensional echocardiographic image when not in the Doppler mode. When the PW Doppler is switched on the cursor and sample volume indicator appear along with a video picture of the spectral display, and the system goes into an automatic gating mode which, in this case, updates the two-dimensional image periodically. Notice the location of the sample volume in the apical four chamber view just below the aortic root. The spectral displays an obviously aliased flow pattern. The scale factors on the spectral display indicate the maximum velocity able to be detected before aliasing occurs.

A hard copy printout of the PW spectral tracing on the screen is also usually available on most machines from a graphic recorder. If a CW examination is then performed, the video screen on the system shows the CW mode spectral display since no imaging is possible in this mode. The full profile of the abnormal jet may then be recorded on the screen or by hard copy strip chart recorder. Of course, higher velocity profiles may be displayed using the CW approach.

THE USE OF THE DOPPLER CONTROLS

Understanding the Doppler controls is very important because improper adjustment of these controls can increase or decrease the quality of the Doppler recordings. A summary of the important controls for Doppler examination of the heart is given in **Figure 1.34**. The schematic drawing of the control

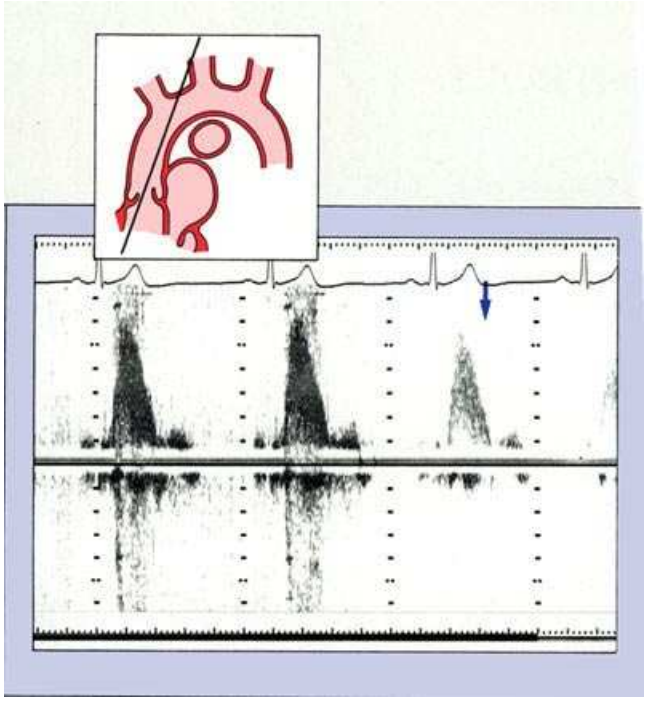

Figure 1. 35: Normal aortic CW spectral trace from the suprasternal window, showing spectral trace with proper gain settings (arrow). Tracings on the left have too much gain while the trace on the right has too little.

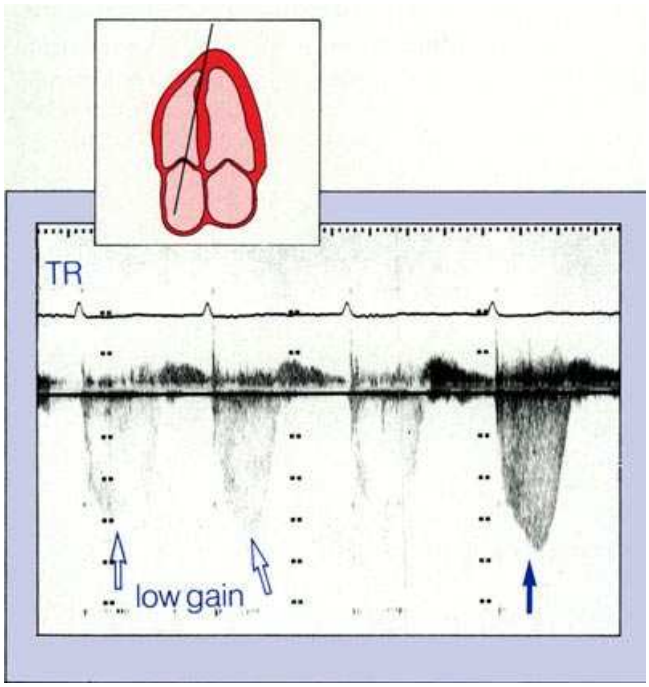

Figure 1. 36: CW spectral velocity trace of tricuspid insufficiency from a transducer located in the apical window. Note the low gain (open arrow) that fails to display the full spectral profile. Proper gain is on the right (closed arrow) and spectral broadening is observed.

panel is generic, and Doppler users should be able to find these controls on their system by the same or a similar name.

In this basic model, the eight controls are divided into three categories. First is the group of controls that influence the quality of the Doppler recording (Doppler gain, gray scale, and wall filter). This group is of importance in both CW and PW examinations. Second are the controls that change the appearance of the graphic display (scale factor and baseline position) and also apply to both CW and PW examinations. The third group are of use *only* for PW Doppler since they relate to the sample volume (cursor, sample depth and angle).

Doppler Gain

The most important Doppler control is the overall gain. Rotating between higher and lower settings will alter the strength of the Doppler signals from the audible output and will be perceived by the operator as a change in the volume of the sound. **Figure 1.35** shows the range in appearance of the velocity spectral recording for excessively high, correct and low gain settings.

As with any ultrasound system, it is prudent to use the lowest gain or power setting that allows the recording of adequate signals. More detailed examination of the recording in **Figure 1.35** shows a normal aortic spectral trace obtained from the suprasternal window. Systolic flow velocity toward the transducer is depicted as an upward profile and is laminar in appearance. The first two profiles show a gain setting that is too high. This results in excessive background noise that makes identification of the clear outline of systolic flow difficult and produces an overflow in the opposite channel represented below the baseline (this is called "mirroring" or "crosstalk"). The third profile **(Figure 1.35, *arrow*)** is set at an optimal gain setting and displays a clear systolic envelope of flow with minimum background noise, while the fourth profile demonstrates an incomplete spectrum due to an improperly low gain setting.

The practical use of correct gain setting is again shown in **Figure 1.36**. In this CW examination from the ventricular apex, tricuspid insufficiency is encountered as a systolic movement of the

velocity spectrum away from the transducer. In the complexes without adequate gain the full velocity profile is not well seen (**Figure 1.36, *open arrows***). It is not until the gain is increased to an adequate level that true spectral broadening and the true peak velocity are noted. A beginner should first detect some flow signal and then run through all of the possible gain settings to become familiar with the effect of too much or too little gain.

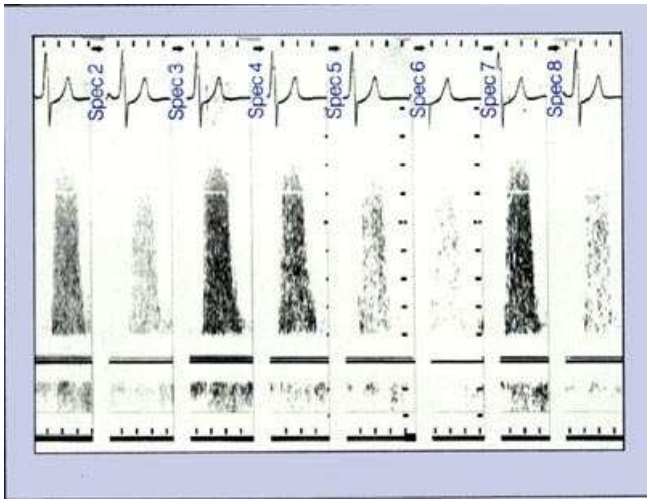

Figure 1. 37: CW spectral velocity recording of eight different gray scale settings. The eight beats are continuous as the gray scale setting changes.

Gray Scale

The gray scale control provides a means of altering the various ranges of gray (from white to black) on the spectral display and has no effect on the audio output of the Doppler system. Different Doppler instruments have from two to more than eight different ranges of gray scale display.

The use of this control at eight different gray scale settings is demonstrated in **Figure 1.37**. This recording was produced from the suprasternal notch and shows eight consecutive beats each with a different gray scale setting. Beginners should practice moving through all available gray scale settings of their Doppler instrument during the learning phase, as the effect of this control is frequently difficult to understand. Ideally, it is desirable to have as many shades of gray as possible in the display. Careful inspection of this tracing in **Figure 1.37** reveals that full range of spectral velocities are not present in the first, second, fifth, sixth or eighth profiles. Adequate gray scale is seen in the third, fourth and seventh profiles.

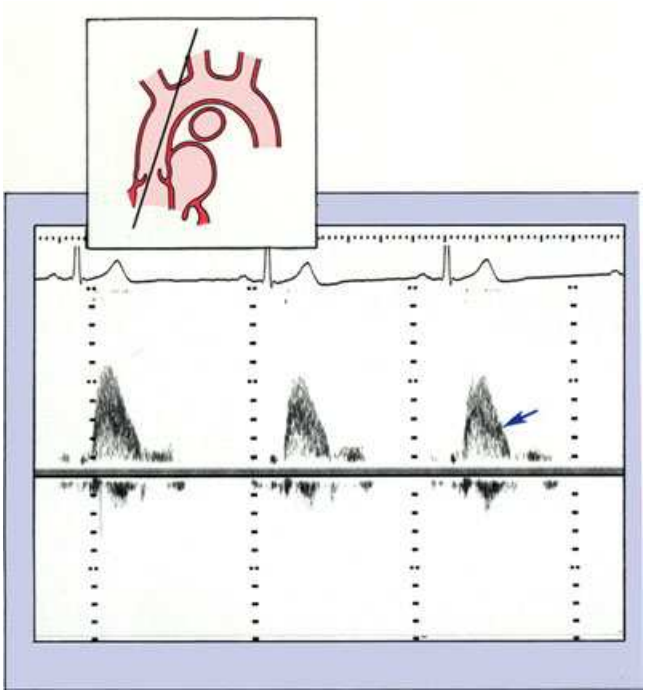

Figure 1. 38: Proper display of normal aortic flow from the suprasternal notch. Flow is laminar and toward the transducer.

Since the concentration of velocities within the spectral trace are displayed in varying intensities of gray, full operator understanding of this control is necessary. Lighter shades of gray indicate that there are fewer red cells moving at that velocity in comparison to darker shades of gray or black where many red cells are moving at that velocity.

The problem with leaving the gray scale control at the maximum setting is that a light level of gray is assigned to low amplitude background noise in the spectral trace. Thus, there must be a balanced adjustment between the gain control and the gray scale control so that the cleanest spectral trace with the most shades of gray is displayed. A spectral recording of normal aortic flow with properly set gain and gray scale is shown in **Figure 1.38**.

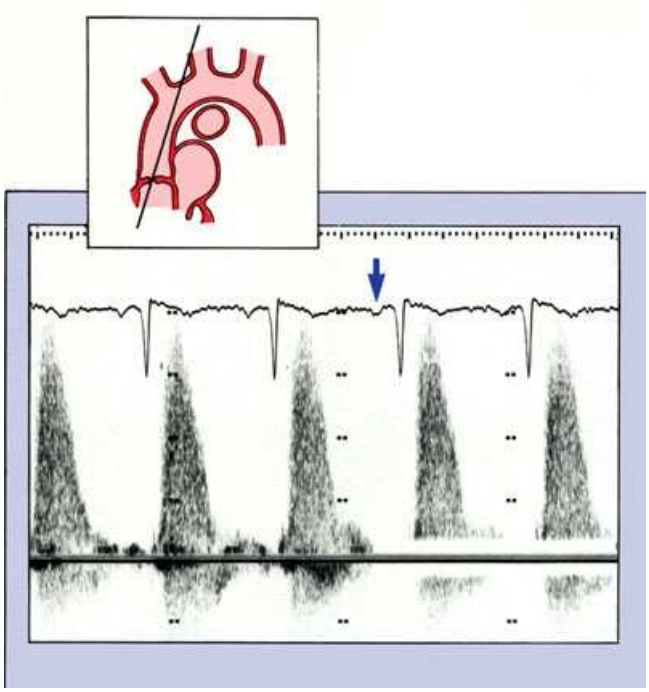

Figure 1. 39: CW spectral velocity recording from the suprasternal notch in a patient with aortic stenosis. Note that the baseline (or wall) filter is turned on (arrow) and the baseline is cleaned of low velocity noise.

Wall Filter

The low frequency (velocity) of heart motion is easily detected by all Doppler instruments and commonly interferes with clear recording of blood flow profiles. Movement of the heart walls produces easily heard, low pitched "clunking" sounds in the audio output that may obscure the higher frequency flow signals desired.

All Doppler systems have a variable wall filter control that sets the threshold below which low frequency signals are removed from the display. **Figure 1.39** shows improper wall filter settings in a spectral velocity of aortic systolic flow in a patient with aortic stenosis. The arrow points to where there is filtering of the lower frequencies that results in a cleaner baseline, free from low velocity interference. Since we are mainly interested in these high frequency flow signals, it is best to set the wall filter so that most, if not all, the lower frequency signals are attenuated.

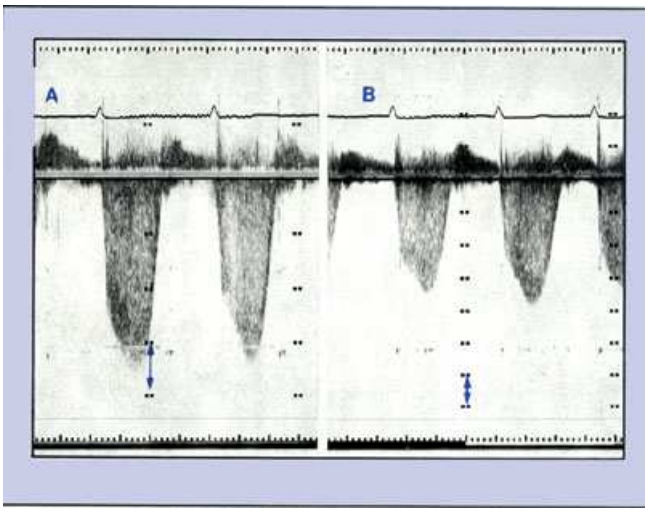

Figure 1. 40: CW spectral velocity recordings of mitral regurgitation from the apical window. The abnormal diastolic jet is away from the transducer. The scale factor is changed between A and B (note arrow).

Scale Factor

The scale factor control varies the range of velocity that can be displayed on the spectral recording. Altering this control has no effect on the audio output. **Figure 1.40** shows how increasing the scale factor (A vs B) increases the display range of a mitral regurgitation jet using CW Doppler. The velocity of the spectral trace has remained at between 3 and 4 m/sec even though the display size was decreased as well as the velocity calibration markers. The beginner should note that the actual velocity of the spectral trace does not change despite the differing appearances.

This control should be set so that the highest velocity spectral trace can be displayed without fear of cutting off a part of the peak velocity. For CW Doppler the operator is usually allowed to move through a full range of scale factors. When operating in pulsed mode, however, many instruments will automatically limit the range of scale factors possible, depending on the depth of the sample volume and the PRF. Scale velocity markers are usually expressed in meters or centimeters per second.

Baseline Control

The baseline control will vary the position of the velocity baseline (zero velocity) within the Doppler display. While altering this control has no effect on the audio output, it is very important for the graphic spectral display. Its use has been previously described in the section discussing aliasing. If an aliased signal is detected it is usually helpful to position the baseline in one of its extreme positions (top or bottom) in order to display as much of the abnormal velocity as possible. This takes advantage of the range of velocity available in the opposite channel.

Pulsed Cursor Position

The Doppler cursor placement is controlled by the cursor switch or paddle (on some machines a joystick or trackball). It is important to remember that the cursor control is operational in both PW and CW mode.

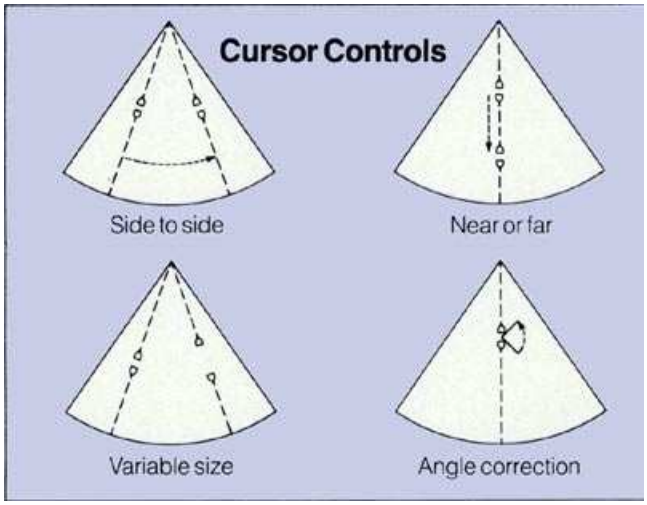

Figure 1. 41: Schematic diagram showing the various PW Doppler sample volume location controls.

This cursor allows movement of the Doppler beam to the left or right within the two-dimensional scan **(Fig. 1.41)**. In common use the movement of this control allows for positioning the pulsed sample volume from one heart chamber to another. Occasionally, this control is used for positioning the Doppler beam as parallel to flow as possible. As will be seen later, the most important use of cursor positioning is in the mapping technique for semi-quantifying regurgitant lesions.

Pulsed Sample Depth

In PW Doppler, the sample depth control selects the depth at which the sample volume gate is placed along the cursor line. As with all cursor and sample volume controls, sample depth has no effect in the CW mode.

Use of this sample depth control is important in properly positioning the sample volume properly for the detection of normal or abnormal flows, particularly in the mapping of various lesions. It should be remembered that deeper positioning of the sample volume into the heart results in an automatic decrease in the Nyquist limit. The farther into the tissues a sample volume is placed the lower will be the velocity at which aliasing will occur.

Other cursor controls include the size of the sample gate (large or small). Most users of pulsed Doppler will leave this gate in a mid-position for routine scanning and decrease or increase the size of the gate depending on the clinical situation.

Pulsed Angle Correction

Most pulsed Doppler systems have some kind of angle correction mechanism. By adjusting according to the direction of assumed flow, it changes the angle calculations in the Doppler equation resulting in different estimates of flow velocity. The use of this control does not actually change the direction of the Doppler beam and its use does not alter the quality of either the audio output or the spectral recording. It also assumes that the operator knows precisely where the jet is

directed. In actual practice it is better to realign the position of the transducer as parallel to perceived flow than to depend upon this angle correction.

There are no standardized methods for carrying out a Doppler examination such as exist for two-dimensional echocardiography. For conventional pulsed and continuous wave Doppler, a partially systematic approach is used by many examiners that begins after the imaging part of the examination is completed. Performing the two-dimensional examination first is very helpful in familiarizing the operator with the spatial positioning of the chambers and valves to be examined by Doppler.

Beam Orientation

It is critical that the operator remembers that the best Doppler information is obtained when the Doppler beam is oriented so that it lines up as parallel as possible to blood flow. This will ensure that the strongest Doppler signals are reflected back to the transducer and that maximum peak velocities are obtained. When using a combined two-dimensional and Doppler machine, the novice must bear in mind the fact that the best two-dimensional pictures usually will not be achieved from exactly the same window that yields the best Doppler tracings. In order to achieve the goal of a small intercept angle to blood flow (as required by the Doppler equation) the operator must try a wide variety of acoustic windows, some of which may not be used for standard M-mode or two-dimensional examinations.

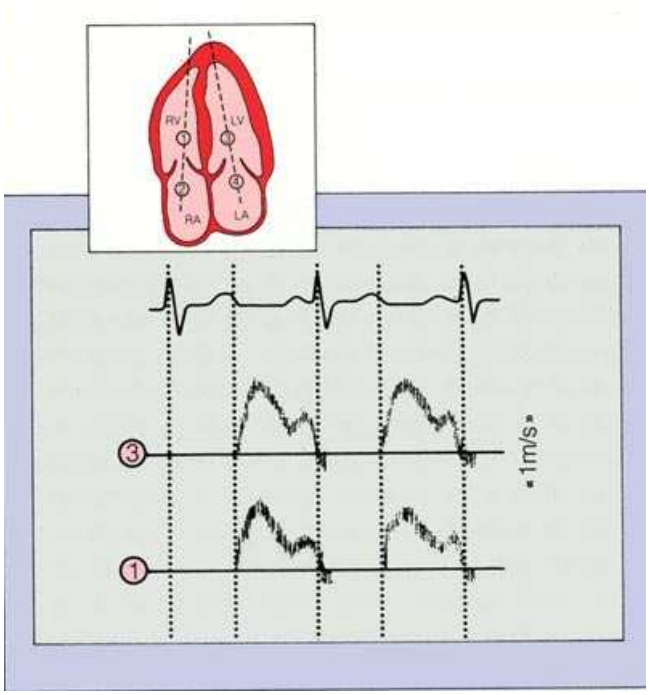

Figure 1. 42: Left panel shows a schematic representation of various starting positions for locating the sample volume of a PW Doppler system from the apical four-chamber view. Right panel shows a schematic spectral recording of normal mitral (site 3) and tricuspid (site 1) diastolic flow. Note that peak tricuspid velocity is normally lower than mitral.

Apical Window

For routine Doppler examination of patients with suspected valvular heart disease, it is usually best to begin by using the apical window. This allows selective orientation of the Doppler beam as parallel as possible to the direction of assumed flow through the mitral and tricuspid valves. It also allows the largest Doppler shift to be recorded and the strongest signals to be reflected back to the Doppler transducer.

The imaging mode of the system may be used to acquire an apical four-chamber view as seen schematically in **Figure 1.42**. The PW Doppler sample volume can then be positioned on the atrial or ventricular sides of the mitral or tricuspid valves. The *right panel* of **Figure 1.42** shows schematic representations of the normal spectral outputs through the mitral (*sample site 3*) and tricuspid valves (*sample site 1*).

In most normal individuals, whether the sample volume is on the atrial or ventricular sides of the mitral and tricuspid valves results in spectral flow outputs that are quite similar. In the presence of valvular disease, however, markedly different flow patterns are encountered depending upon sample volume position.

When in the apical four chamber view, slight superior angulation of the scan plane will allow the operator to encounter the left ventricular outflow tract. An operator can almost always obtain Doppler flow data from the ventricular side of the aortic valve. In some patients data may also be obtained from the aortic root side. A complete PW Doppler evaluation would continue with movement of the sample volume from place to place in the standard, and then intermediate points.

Normal Doppler Velocities

Flow	Children (m/s)	Adults (m/s)
Mitral diastolic	1.00 (0.7-1.4)	0.92 (0.6-1.4)
Tricuspid diastolic	0.62 (0.5-0.9)	0.58 (0.4-0.8)
Pulmonary systolic	0.84 (0.6-1.2)	0.72 (0.5-0.9)
Aortic systolic	1.52 (1.2-1.7)	1.40 (0.9-1.8)

Figure 1. 43: Table of normal peak forward velocities recorded across the various cardiac valves using PW Doppler Echocardiography.

Continued practice repositioning the PW cursor and sample volume in the various portions of the cardiac chambers accessible from the apical four chamber view will eventually provide the novice operator with an appreciation of the spatial locations and directions of normal and abnormal flows. The heart chambers are actually three dimensional structures and an abnormal flow jet may be directed anywhere within this three dimensions. An experienced operator will be able to track an abnormal jet even if it is directed out of a standard two-dimensional plane.

The apical window is also an excellent position for obtaining some initial experience with continuous wave Doppler. Placing the CW transducer directly over the apical impulse (located by palpation) and angling the beam somewhat leftward and posteriorly will usually result in a typical mitral flow profile. It is wise for the beginner to practice locating flow through the mitral valve as the flow profile resembles the appearance of the mitral valve on M-mode and is readily recognized. Marked medial redirection of the CW beam from the apex will result in a flow profile through the tricuspid valve. Because pressures are higher on the left side of the heart, velocities are generally higher on the left when compared to the right in normal and diseased states. Exceptions to this rule are encountered in severe pulmonary hypertension or stenosis.

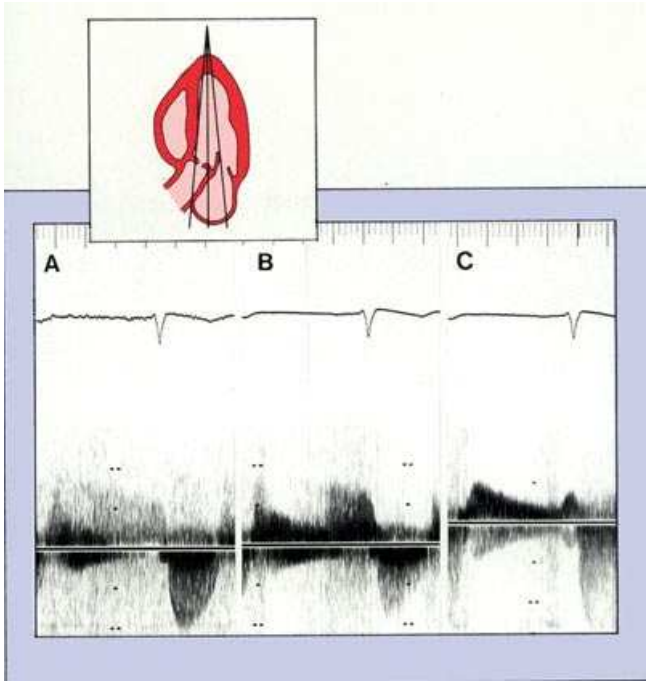

Figure 1. 44: CW velocity spectral recordings from three apical transducer beam angulations. Panel A shows aortic insufficiency and stenosis. In panel B, slight movement of the beam begins to mix the aortic insufficiency with diastolic flow through a mildly stenotic mitral valve. Panel C demonstrates pure mitral diastolic flow and mitral regurgitation.

The ranges of normal peak flow velocities are shown in **Figure 1.43**. Notice that the normal flows are slightly higher in children than adults and slightly higher on the left side of the heart in comparison to the right.

After some experience, an operator can become very skillful with minor manipulation of the CW transducer. The difference between the various waveforms obtained from the ventricular apex using a CW transducer is shown in **Figure 1.44**. At first, the beam is directed superiorly to encounter aortic insufficiency and stenosis **(Figure 1.44 *panel A*)**. The insufficiency is directed toward the

transducer and appears on the spectral display in diastole. The aortic stenosis flow moves away from the transducer in systole. The CW is then angled midway between ventricular outflow and inflow **(Figure 1.44 *panel B*)** and encounters a mixed diastolic profile with mitral inflow superimposed on the aortic insufficiency. Progressive angulation through the mitral valve demonstrates a pure mitral inflow in diastole with mitral insufficiency in systole **(Figure 1.44 *panel C*)**.

The problem of recording flow across mitral and aortic valve simultaneously **(Figure 1.44 *panel B*)** results partly from the fact that the ultrasound beam width is large enough to detect more than one jet. Failure to appreciate this may lead the unwary beginner to diagnose mitral stenosis, for example, when only aortic regurgitation is present.

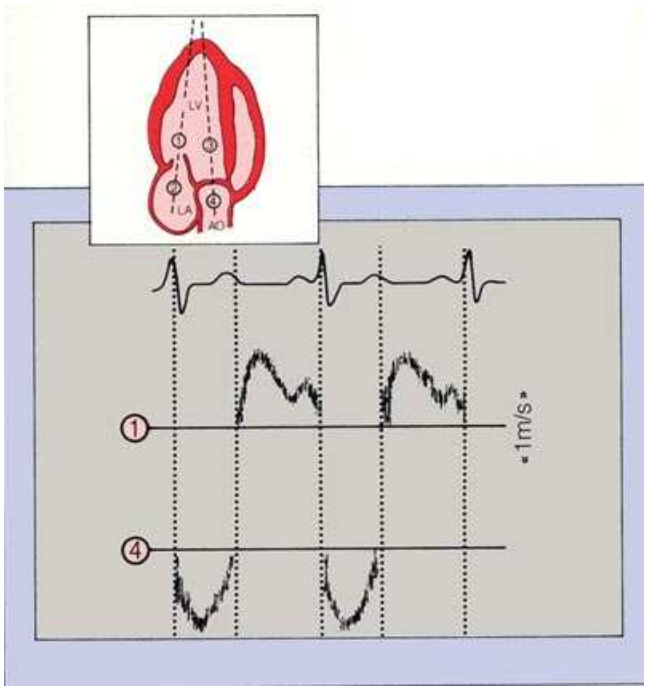

Figure 1. 45: Left panel shows a schematic diagram for location of pulsed Doppler sample volumes from the apical two-chamber view. Right panel shows schematic spectral velocity renditions of flows across the mitral and aortic valves.

The apical window also supplies an opportunity for examination of left sided flow with PW Doppler echocardiography by movement of the imaging plane to the apical two-chamber view **(Fig. 1.45)**. This view is obtained by rotating the two-dimensional transducer counterclockwise and 90 degrees from the apical four chamber view and is particularly suited for examination of both left ventricular inflow **(Fig. 1.45, sample sites 1 and 2)** and outflow **(sample sites 3 and 4)**. Flow velocity profiles through the mitral valve resemble those obtained in the apical four-chamber view and are directed toward the transducer in diastole. It is a little easier to position and hold the pulsed sample volume on the aortic side of the aortic valve using the two-chamber approach rather than the four-chamber with extreme superior angulation.

Suprasternal Window

The suprasternal window provides an opportunity for angulation of the Doppler beam parallel to flow in the ascending or descending aorta. Placement of the PW or CW transducer in the suprasternal notch allows easy access to systolic flow toward the transducer in the ascending aorta and systolic flow away from the transducer in the descending aorta. Positioning a large mechanical or phased array transducer in the suprasternal notch is frequently difficult and we have learned to depend upon CW for this window because the transducer is small and easily maneuvered.

In patients with aortic valve stenosis no such assumption as to direction of systolic aortic flow can be made. In this case, we are most interested in recording the highest peak systolic velocity present. As previously pointed out, the most faithful representation of flow will be obtained when the beam is parallel. The use of multiple positions for the recording of peak systolic aortic velocity is very important in aortic stenosis since this jet may be directed in a wide variety of orientations. When examining for aortic stenosis all available acoustic windows should be used.

Parasternal Windows

The right and left parasternal windows may also be utilized for Doppler echocardiography. Since abnormal jets may be directed anywhere in space, the right parasternal approach should be used in all patients with suspicion of aortic stenosis. This view is best obtained by rotating the patient into a right lateral decubitus position and placing the patient's right hand behind the head to open the intercostal spaces. Practice with the concomitant imaging will help in spatially orienting the beginner to the location of the ascending aorta.

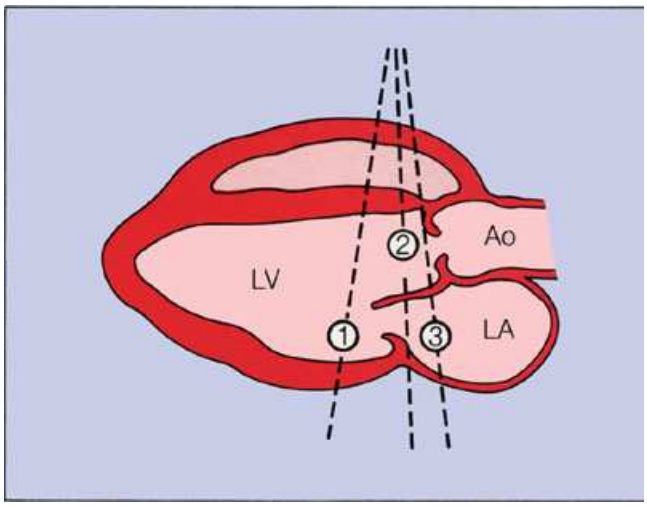

Figure 1. 46: Schematic diagram for sample site locations with PW Doppler from the parasternal long-axis view. Abnormal valvular flows from this view are usually perpendicular to the transducer and are poorly recorded.

The left parasternal window is usually not the best for routine recording of valvular flows through the left heart. As seen in **Figure 1.46**, where the left parasternal long-axis is represented, it is difficult to orient the Doppler beam parallel to flow through the aortic or mitral valves. While some flows may be detected, faithful representation of peak velocities is almost always unrewarding.

When using the left parasternal approach for interrogation of the aortic and mitral valves, it is frequently most profitable to use pulsed wave Doppler in order to provide some range information for interpreting the low amplitude signals. When experience is acquired, one may find this view helpful in specifically localizing turbulence and tracking the spatial orientation of any given jet. Occasionally, the direction of an abnormal jet such as aortic insufficiency will be posterior, making it easiest to record from the left parasternal window.

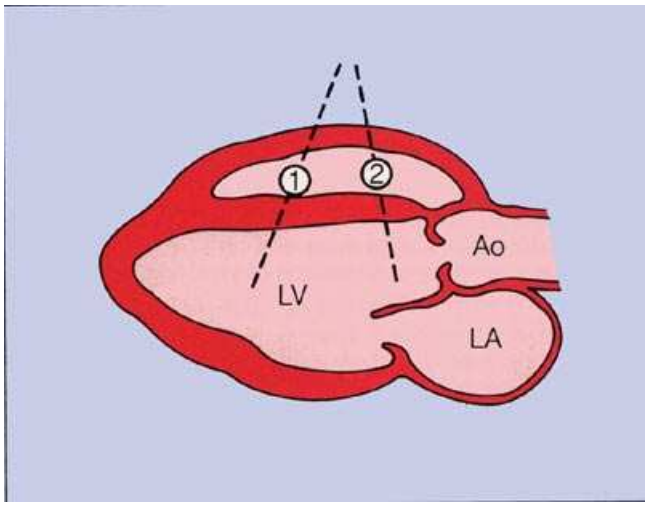

Figure 1. 47: The parasternal long-axis view, is, however good for sampling for the presence of a ventricular septal defect. If present, the abnormal flow is frequently aligned parallel rather than perpendicular to the Doppler beam.

The left parasternal window does have very important use for examining the interventricular septum for ventricular septal defects where flow through a ventricular defect is generally parallel to the interrogating Doppler beam from the left parasternal window **(Fig. 1.47)**. The technique of searching for a ventricular septal defect involves moving the sample cursor along the right ventricular side of the interventricular septum until abnormal flow is detected.

The left parasternal window is also ideal for detecting flow through the pulmonic and tricuspid valves. Using PW Doppler, it is best to start with a short axis view at the level of the aortic root **(Fig. 1.48)**. This shows that Doppler beams directed at the tricuspid or pulmonic valves are parallel to blood flow and will result in a strong Doppler signal. Sample volumes may be positioned on either side of these valves, and the flow profiles resemble the configuration of their left sided counterparts except that the velocities are a little lower.

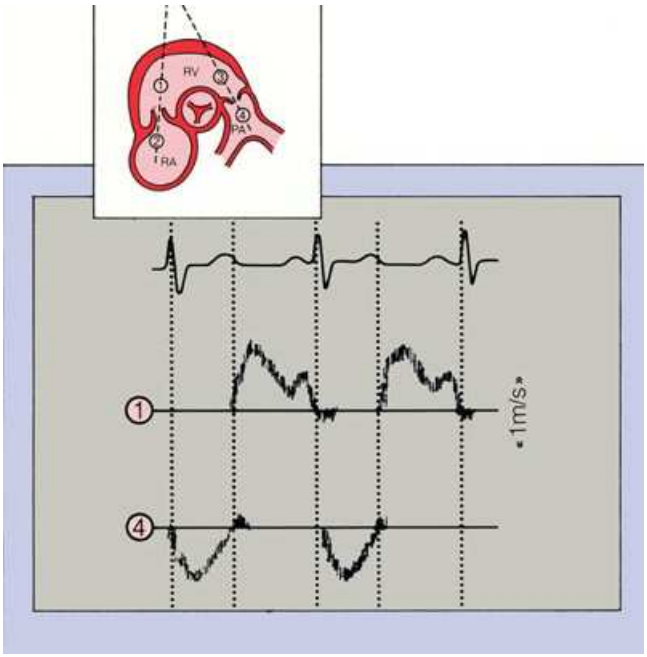

Figure 1. 48: Left panel shows a schematic diagram of possible pulsed Doppler sample sites in the left parasternal short-axis view. Right panel shows schematic renditions of normal tricuspid diastolic (site 1) and pulmonic systolic (site 4) flows.

In some patients the left parasternal view may be the only one where intelligible flow is detected through the pulmonic valve. Beginners will find the use of pulsed Doppler for detection of flow easiest. Note that normal systolic flow in the pulmonary artery is away from the transducer in this position. As the operator gains experience, he or she will also feel comfortable using continuous wave Doppler for recording the full spectral profile of abnormal jets. Skill in examining flow through the pulmonary valve is most useful in the study of congenital heart disease.

Other Windows

It is important note that all other available windows be used for interrogating flow through the heart. These include the lower left parasternal, subcostal and many intermediate windows. We have described a few windows in detail to provide a means for beginners to familiarize themselves with the easiest, and generally most productive, transducer positions and beam directions.

The Doppler Examination

Using this sequential window approach is not the only way to conduct a methodical Doppler examination but it has appeared to us to be very helpful to those with little, or no Doppler experience. When conducting a Doppler examination, the operator should remember that these studies may be very difficult to interpret for an individual not present during the actual examination. A poor quality echocardiographic image of cardiac structures may be identifiable by an experienced observer but a poor quality Doppler tracing may be impossible to identify and interpret.

For this reason we believe that sonographers and physicians interested in acquiring skills in Doppler echocardiography should conduct the examinations jointly during the learning period. We also highly recommend that each laboratory develop an annotation system so that sonographers may convey key orientation information to an interpreting physician not actually present during the examination. This may be accomplished on almost every commercial system by voice labeling (or commenting) on the audio track of the tape recording of the video or audio record. The information should concern the window used, probable beam orientation and suspected lesion encountered. We also suggest written annotation of similar information on the hard-copy paper output of the graphic recorder.

FIGURES:

Figure 1.20: The sample volume of PW Doppler is actually a three-dimensional volume that changes in size at its location relative to the transducer is changed. When placed in the far field, it becomes very large.

Figure 1.21: Schematic rendering of the full spectral display of a high velocity profile fully recorded by CW Doppler. The PW display is aliased, or cut off, and the top is placed at the bottom.

Figure 1. 22: Spectral displays of diastolic flow through the mitral orifice. The transducer is located at the apex and diastolic flow is toward the transducer (positive) Note the laminar appearance of the PW display. The CW does not usually display the same laminar flow pattern as it receives flow information from all portions of the ultrasound beam.

Figure 1. 23: Table summarizing the advantages and disadvantages of pulsed and continuous wave Doppler echocardiography.

Figure 1. 24: Aliased spectral display of aortic insufficiency (left arrow) in PW mode detected from the ventricular apex. Abnormal flow is toward the transducer. After 3 beats, the system is switched to CW and the full profile is seen.

Figure 1. 25: Schematic depiction of the origin of the aliasing phenomenon using a turning wheel. When the Nyquist limit is exceeded, aliasing occurs. For details, see text.

Figure 1. 26: The Nyquist limit is defined by the number of pulses/second divided by two.

Figure 1. 27: The left panel shows the sample volume placed in the near field. Higher velocities may be recorded with a location near the transducer than when the sample volume is positioned at a farther range (right panel).

Figure 1. 28: Schematic drawing of the effect of a reduction in the Nyquist limit in PW echo when a high velocity jet is encountered in the near field (A) or successively deeper into the tissues (B, C, and D). Note the progressive and marked aliasing of the spectral signal the farther away the jet is encountered from the transducer.

Figure 1. 29: Pulmonic insufficiency is detected by PW Doppler with the sample volume located in the right ventricular outflow tract. The baseline is lowered to reveal the full profile (arrow) of the regurgitant jet toward the transducer.

Figure 1. 30: High PRF systems do not wait for a single pulse to return to the transducer before pulsing again. Higher pulse repetition rates are achieved but some range ambiguity exists.

Figure 1. 31: The Bernoulli equation is a complex formula that may be reduced to its simplest expression.

Figure 1. 32: An example of a CW spectral recording of aortic stenosis. There is a given velocity (V_1) on the ventricular side of the valve that is accelerated (V_2) as blood is ejected through the stenotic orifice. V_1 is usually ignored in the simplified Bernoulli equation.

Figure 1. 33: Schematic representation summarizing the various displays available in the combined two-dimensional and Doppler system. Hard-copy spectral recordings are also available in systems with this capability.

Figure 1. 34: Mock Doppler control panel showing the most common CW and PW Doppler controls. Almost every Doppler system with pulsed and continuous wave capabilities will contain these controls.

Figure 1. 35: Normal aortic CW spectral trace from the suprasternal window, showing spectral trace with proper gain settings (arrow). Tracings on the left have too much gain while the trace on the right has too little.

Figure 1. 36: CW spectral velocity trace of tricuspid insufficiency from a transducer located in the apical window. Note the low gain (open arrow) that fails to display the full spectral profile. Proper gain is on the right (closed arrow) and spectral broadening is observed.

Figure 1. 37: CW spectral velocity recording of eight different gray scale settings. The eight beats are continuous as the gray scale setting changes.

Figure 1. 38: Proper display of normal aortic flow from the suprasternal notch. Flow is laminar and toward the transducer.

Figure 1. 39: CW spectral velocity recording from the suprasternal notch in a patient with aortic stenosis. Note that the baseline (or wall) filter is turned on (arrow) and the baseline is cleaned of low velocity noise.

Figure 1. 40: CW spectral velocity recordings of mitral regurgitation from the apical window. The abnormal diastolic jet is away from the transducer. The scale factor is changed between A and B (note arrow).

Figure 1. 41: Schematic diagram showing the various PW Doppler sample volume location controls.

Figure 1. 42: Left panel shows a schematic representation of various starting positions for locating the sample volume of a PW Doppler system from the apical four-chamber view. Right panel shows a schematic spectral recording of normal mitral (site 3) and tricuspid (site 1) diastolic flow. Note that peak tricuspid velocity is normally lower than mitral.

Figure 1. 43: Table of normal peak forward velocities recorded across the various cardiac valves using PW Doppler Echocardiography.

Figure 1. 44: CW velocity spectral recordings from three apical transducer beam angulations. Panel A shows aortic insufficiency and stenosis. In panel B, slight movement of the beam begins to mix the aortic insufficiency with diastolic flow through a mildly stenotic mitral valve. Panel C demonstrates pure mitral diastolic flow and mitral regurgitation.

Figure 1. 45: Left panel shows a schematic diagram for location of pulsed Doppler sample volumes from the apical two-chamber view. Right panel shows schematic spectral velocity renditions of flows across the mitral and aortic valves.

Figure 1. 46: Schematic diagram for sample site locations with PW Doppler from the parasternal long-axis view. Abnormal valvular flows from this view are usually perpendicular to the transducer and are poorly recorded.

Figure 1. 47: The parasternal long-axis view, is, however good for sampling for the presence of a ventricular septal defect. If present, the abnormal flow is frequently aligned parallel rather than perpendicular to the Doppler beam.

Figure 1. 48: Left panel shows a schematic diagram of possible pulsed Doppler sample sites in the left parasternal short-axis view. Right panel shows schematic renditions of normal tricuspid diastolic (site 1) and pulmonic systolic (site 4) flows.

DOPPLER EVALUATION OF VALVULAR REGURGITATION #2

Joseph A. Kisslo, MD
David B. Adams, RDCS

INTRODUCTION

Some of the earliest uses for Doppler echocardiography were in detection of valvular insufficiencies. The first Doppler echocardiography studies of valvular regurgitation were, however, focused outside the heart. As early as 1971, it was demonstrated that retrograde blood flow could be detected during diastole in the subclavian arteries of patients with aortic insufficiency. At about the same time, certain abnormalities were detected in the jugular veins of patients with tricuspid insufficiency. Since then, there have been many studies using direct evaluation of the heart valves for insufficiency, and it is now becoming generally accepted that Doppler is a fairly sensitive and specific method for the detection of valvular insufficiency.

DOPPLER CHANGES IN VALVULAR REGURGITATION

Characteristics of Regurgitant Jets

Valvular regurgitation is defined as the presence of backwards, or retrograde, flow across a given closed cardiac valve. It should be realized by beginners that the terms "regurgitation" and "insufficiency" are synonyms and may be used interchangeably.

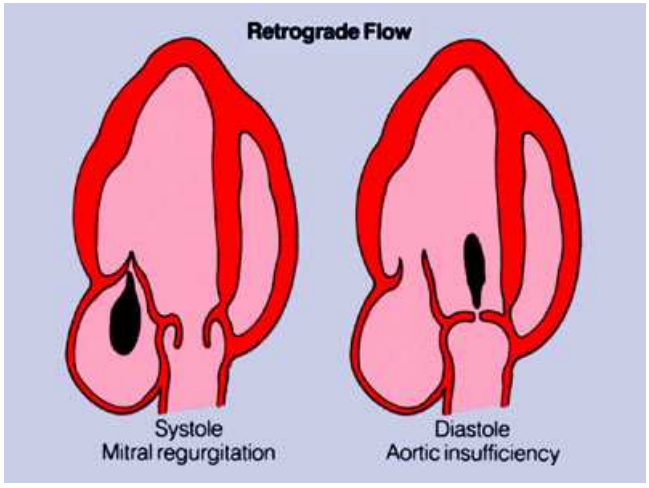

Figure 2.1 Valvular regurgitation is characterized by inappropriate retrograde flow during the cardiac cycle. The left panel demonstrates mitral regurgitation in systole, the right panel demonstrates inappropriate aortic insufficiency in diastole.

It is assumed that there is normally no flow backwards into the ventricles through the aortic or pulmonic valves in diastole. Similarly, there is no flow backwards into the atria across the mitral or tricuspid valves in systole. Thus, the first effect of regurgitation on blood flow through the heart is a change in direction. **Figure 2.1** demonstrates the abnormal direction of flow in the left heart for mitral and aortic regurgitation in systole and diastole respectively. Given the ability of Doppler echocardiography to detect the direction of blood flow, it is seems ideally suited for assessment of valvular insufficiencies.

The second effect of regurgitation on cardiac blood flow is the creation of turbulence. Most valvular regurgitation is associated with some abnormality of leaflet coaptation. Regurgitant jets originate from small, irregular openings. They may be directed quite eccentrically and they are almost always turbulent. Regurgitant jets are made

up of many different velocities and complex flow patterns. These features are represented on the Doppler recording as spectral broadening, which is the graphic equivalent of turbulent flow.

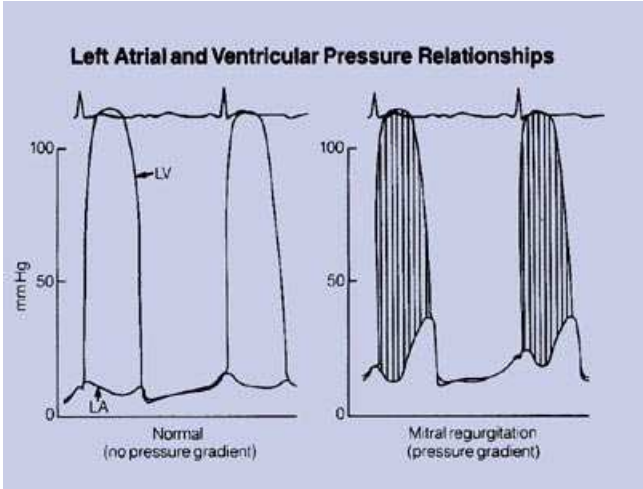

Figure 2.2 During systole, left ventricular pressure is greater than left atrial pressure (left panel). In the presence of mitral regurgitation, the flow communication between these chambers allows a high gradient to exist.

The third factor that characterizes the abnormal flow of a regurgitant jet is an increase in velocity, which is a result of a pressure gradient that exists across a regurgitant valve. For example, normal systolic pressure in the left ventricle is over 100 mmHg. At the same time, the pressure in the left atrium is very low and ranges from 2 to 12 mmHg. The left panel of **Figure 2.2** demonstrates these normal pressure relationships. Even though the pressure differences are great, no communication exists between the two chambers and no retrograde (or backwards) flow.

When mitral regurgitation is present, however, the abnormal communication between the left ventricle and left atrium in systole, and a pressure difference (or gradient) exists **(Fig. 2.2, *right panel*)**. When the pressures within both the left atrium and ventricle are within normal ranges a gradient of 85 mmHg or more exists and produces retrograde flow into the left atrium. This flow takes the form of a high velocity regurgitant jet, as predicted by the Bernoulli equation described in detail in Unit 1.

As mitral insufficiency becomes worse and leads to chronic elevation of left atrial pressure, the systolic gradient between the left ventricle and the left atrium is reduced. In these cases, left atrial pressure may rise to very high levels.

Velocity Pressure Relationships

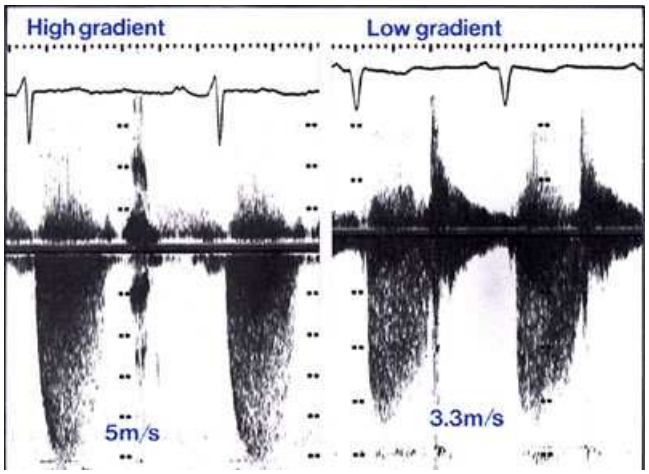

Figure 2.3 The gradient between the left ventricle and the left atrium in mitral insufficiency is reflected by the velocity of the Doppler spectral recording. A high gradient is seen in the left panel while a lower gradient is seen in the right panel. If systolic pressures are the same in both individuals, the recording on the right would suggest higher pressure within the left atrium.

Doppler echocardiographic findings are strongly influenced by the pressure gradients between chambers according to the Bernoulli equation. This relationship is simplified to:

$$p_2\text{-}p_1=4V^2$$

and is very important to understand for further appreciation of the wealth of information available in the Doppler velocity spectral display. The Doppler spectral recordings from mild and severe mitral regurgitation are shown in **Figure 2.3** to illustrate this point further. As describes above, small degrees of mitral regurgitation produce very high pressure differences between the left ventricle and the left atrium. Minor degrees of regurgitation will, therefore, result in very high velocity jets as a consequence of these great pressure differences. Severe mitral regurgitation results in relatively smaller differences between the two

chambers. These smaller pressure gradients result in relatively lower velocity jets. This, of course, assumes that the systolic pressures within the ventricles are similar in both situations.

Thus, the severity of valvular regurgitation is not reflected in an increase in the velocity of the regurgitant jet as detected by Doppler echocardiography. As will be demonstrated in more detail later, the inverse is usually the case. With greater degrees of regurgitation, pressures will rise in the chamber receiving the regurgitant volume leading to a general decrease in the velocity of the resultant Doppler spectral recording.

Another important implication of the increase in velocity in regurgitant jets is that almost all degrees of valvular regurgitation result in a velocity increase above 1.5 m/sec. The practical effect of these higher velocities on Doppler recordings is that aliasing is almost always produced in pulsed wave Doppler interrogations of valvular regurgitation. This is results in the fact that pulsed Doppler echocardiography may be used for detection of the location of the turbulence (or area of the jet) but not its peak velocity.

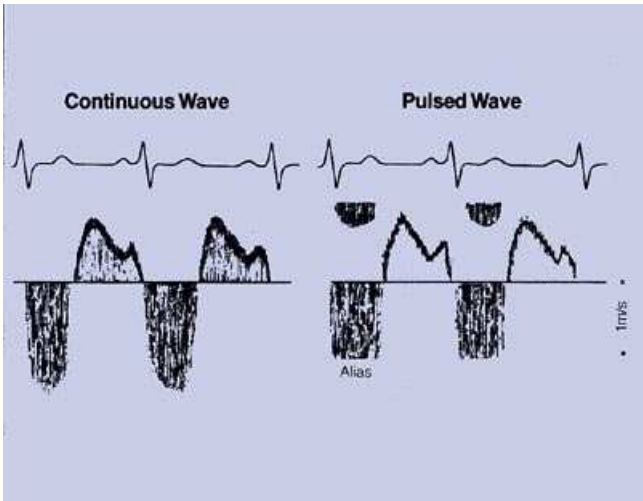

Figure 2.4 Schematic diagram of a mitral regurgitant jet recorded from the apex. Most regurgitant jets result in velocities that exceed 1.5 m/sec and require CW Doppler to record the full spectral velocity profile (left panel). PW Doppler recordings of mitral regurgitation are always aliased (right panel).

This is demonstrated in the idealized drawing of spectral recordings resulting from a mitral insufficiency jet shown in **Figure 2.4**. The left panel shows systolic turbulent flow moving away from a transducer positioned at the apex. The full profile is recorded by CW Doppler. When the same jet is interrogated by PW Doppler, aliasing occurs.

The Spatial Location of Abnormal Jets

Appreciation of the three main features of regurgitant jets described above (i.e., abnormal direction, turbulence, high velocity) is crucial to the success of the Doppler beginner. In addition, it is important to realize that a regurgitant jet may be directed anywhere within the spatial volume of the receiving chamber **(Fig. 2.5)**. The jet may also vary in size from small to large.

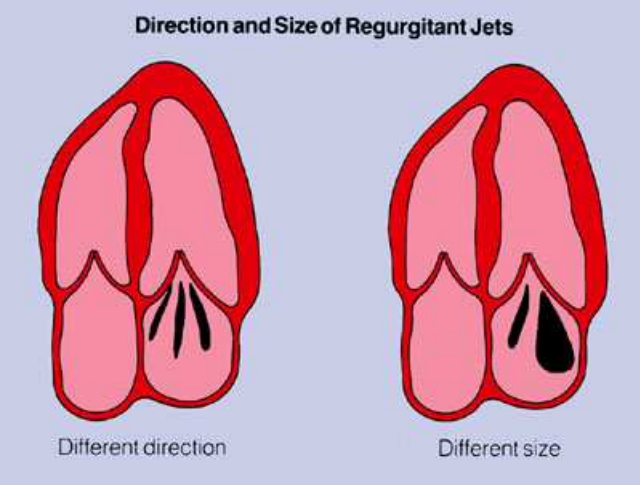

Figure 2.5 Left panel demonstrates that regurgitant jets may be directed in just about any direction; right panel shows that the area of the jets may also be widely different, from very small to very large. A complete PW Doppler examination requires tedious mapping throughout the image for detection of abnormal flow.

The spatial location and general size of a jet is best assessed using PW Doppler echocardiography, even though aliasing invariably occurs as a result of the high velocities encountered **(Fig. 2.6)**. This makes recognition of the complete abnormal flow profile of a regurgitant jet almost impossible by PW Doppler alone. In the pulsed spectral tracing of aortic insufficiency shown, the spectral recording is filled from top to bottom in diastole and recognition of the complete spectral profile is quite difficult. Thus, CW

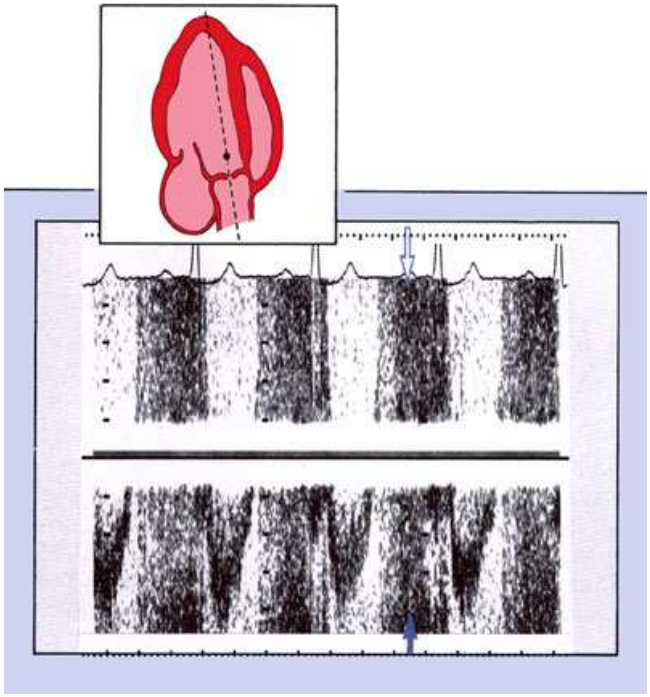

Figure 2.6 PW Doppler spectral recording of aortic insufficiency. Flow is toward the transducer and aliasing occurs (open arrow) with placement of the higher velocities at the bottom of the spectral tracing (closed arrow).

Doppler must be used to record the full contour of the abnormal regurgitant profile in this same patient **(Fig. 2.7)**. CW Doppler, in turn, has the disadvantage of lack of depth resolution, and is therefore not suitable for precisely localizing areas of turbulent flow in the heart.

VALIDATION OF DOPPLER FINDINGS

Limitations of Cineangiography

Almost all of the studies into the validation of Doppler detection of valvular regurgitation have been in comparison to cineangiography. Aside from physical examination, it is the only currently available clinical method for the detection of valvular regurgitation. Despite the present enthusiasm and interest concerning Doppler methodology, the beginner should understand the fundamental differences between these two approaches. It is unlikely that the results of Doppler and cineangiography will ever correlate exactly because the two methods are so fundamentally different in the presentation of data concerning valvular regurgitation. Cineangiography, of course, requires invasive cardiac catheterization and is based upon the dilution of injected radio-opaque contrast on the final X-ray image. However, this catheterization based method is not an ideal "gold standard". When small regurgitant jets are directed into enlarged chambers the resulting dilution of the angiographic contrast agent may render the regurgitation undetectable. Small degrees of regurgitation by angiography may also be highly dependent upon precise catheter location. Angiographic evaluation of right sided lesions is particularly difficult, since catheters must be placed across the valve being evaluated causing at least some degree of catheter induced insufficiency **(Fig. 2.8)**. Furthermore, the angiographic grading scheme for insufficiency used in most catheterization laboratories (0 to 4+) is based on subjective interpretation as contrast progressively opacifies a receiving chamber over several heart beats. There is general agreement that this method for estimation of severity is subject to considerable interpretive errors as a result.

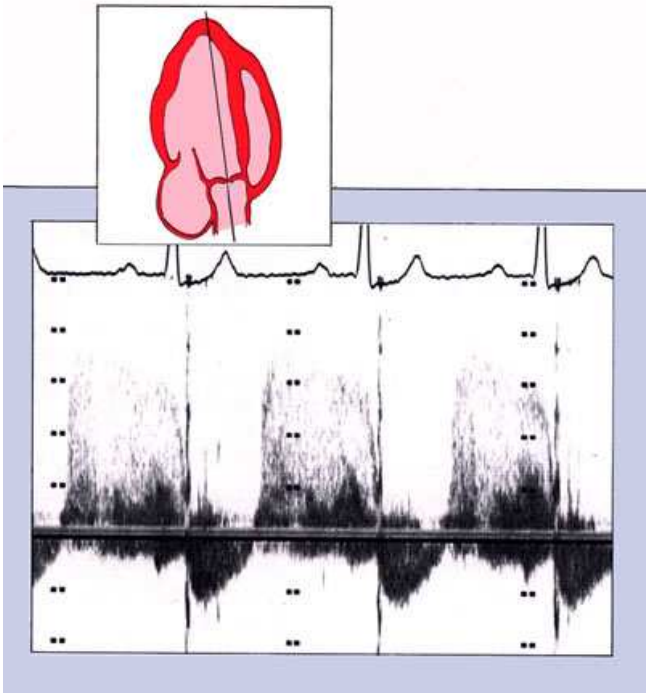

Figure 2.7 CW spectral velocity recording from the apex of the same patient as Figure 2.6. The full abnormal profile of aortic insufficiency is easily recorded toward the transducer (positive shift), (Scale marks – 1 m/sec).

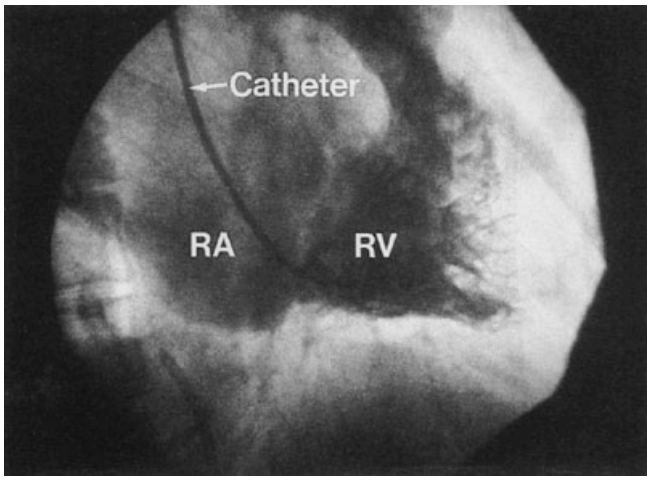

Figure 2.8 Right ventricular angiogram in slight right anterior oblique view. With a catheter across the tricuspid valve, some degree of tricuspid regurgitation almost always results.

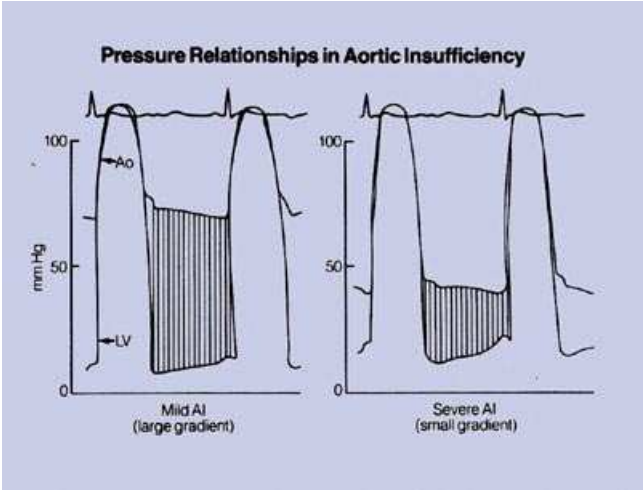

Figure 2.9 Idealized pressure relationships in aortic insufficiency. The left panel demonstrates the large gradient between aorta and left ventricle in mild aortic insufficiency. When aortic regurgitation is severe, central aortic pressure falls and ventricular diastolic pressure rises. This results in a small gradient and lower velocity by Doppler.

Limitations of Doppler Echocardiography

Doppler echocardiography also has its limitations. A beginner should always remember that Doppler detects the velocity and direction of moving blood. In situations where there is a small leak across a given valve there will be a large pressure gradient rendering high velocity of flow. This is illustrated in **(Fig. 2.9 *left panel*)** for trivial aortic insufficiency. Aortic insufficiency gradients occur in diastole. With large gradients **(Fig. 2.9*, right panel*)** the resultant high velocities might readily be detected. For very severe leaks, such as total absence of the aortic valve, little pressure differential would occur and result in very low velocities of flow. In this situation, the abnormal lesion might be missed. Indeed, we have encountered some cases where we have missed severe valvular regurgitation by Doppler that has been readily detected at catheterization by angiographic means.

In addition, the quality of Doppler signals is quite variable from patient to patient. Users of traditional ultrasound imaging methods are quite familiar with differences in the quality of images between patients. These differences may be accounted for by patient age, the presence of lung disease, chest wall configuration or other factors.

Doppler and Cineangiographic Comparisons

It is also important to remember that most Doppler-angiographic comparisons have involved relatively small numbers of catheterized patients and, in some cases, the criteria for patient selection have not been specifically stated. Almost all studies have involved patients with sufficiency disease of the valve to warrant catheterization, and the very favorable results reported might not apply to larger groups of patients with less advanced disease. Some studies have even included Doppler evaluations performed after the angiogram by operators who have been influenced by the angiographic results.

Given the limitations of these techniques, in our institution Doppler angiographic comparisons yield a sensitivity and specificity approach 100% when significant (2+ or greater) angiographic regurgitation is present. When there is little or no angiographic regurgitation (1+ or 0), the two techniques are somewhat less likely to agree.

As we shall see, Doppler may detect the presence of valvular regurgitation in patients without any evidence of a cardiac murmur. In fact, there are surprisingly high rates of detectable lesions such as tricuspid and pulmonic insufficiencies in normal patients. In our laboratory, tricuspid regurgitation is found in 38% of normal healthy young volunteers, while mitral regurgitation is found in 23%, pulmonic regurgitation in 8%, and aortic regurgitation in 8%. Most regurgitations in this series were judged as minor.

This seemingly high prevalence of valvular regurgitation may surprise clinicians experienced with cardiac auscultation. In each case, no murmurs were heard or recorded by phonocardiography. These findings serve to highlight two important points.

First, careful Doppler examinations may reveal trivial regurgitations that are not heard by common auscultatory techniques. Clinicians who use Doppler echocardiography generally accept that small degrees of valvular regurgitation may occur in otherwise normal individuals.

Second, auscultatory events are the audible result of valvular regurgitation. Doppler events are the electronic phase shift result of the same regurgitation. These are two fundamentally different ways of measuring the same event. The sound emitted from a Doppler instrument is not the same as that heard through a stethoscope and beginners should not expect the two to be the same.

As a consequence of all these factors, it must be recognized that exact correlations between methods will never exist. Experienced Doppler operators will detect regurgitant jets which cannot be documented by angiography and may also miss some small jets recognized by angiographic methods. It is clearly best for beginners to Doppler echocardiography to perform some Doppler-angiographic comparisons of their own in order to establish the level of reliability in their own laboratories. Similarly, clinical correlations of Doppler with auscultatory findings will rarely be identical.

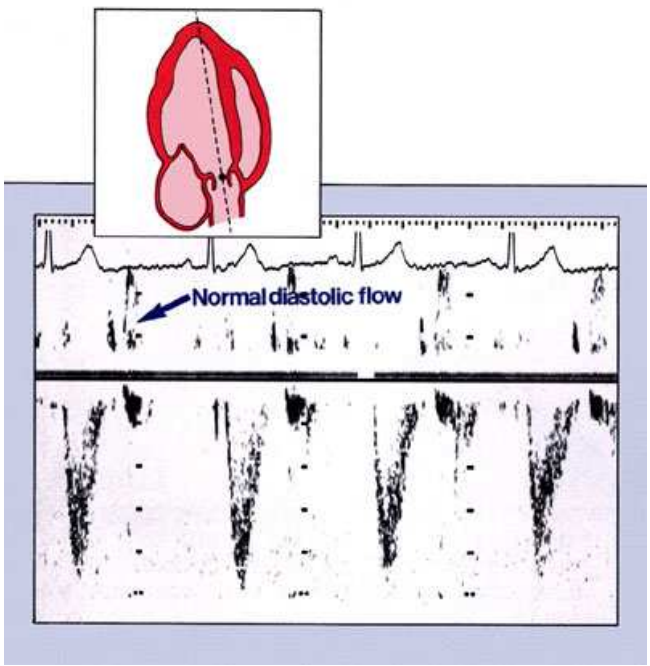

Figure 2.10 Normal spectral recording of left ventricular outflow using PW Doppler echocardiography. Systolic flow is away form the transducer and the velocity shift is negative. Some apparent "abnormalities" are usually recorded in diastole. (Scale marks=20cm/sec).

DOPPLER DETECTION OF VALVULAR REGURGITATION

Aortic Regurgitation

PW Doppler has been reported to have a sensitivity ranging between 86% and 100% for the detection of aortic regurgitation. PW Doppler examinations for this lesion are best begun using the apical two-or four-chamber two-dimensional views for operator guidance. **Figure 2.10** demonstrates a PW Doppler recording from just at the coaptation point of the aortic valve in a normal patient when the transducer was placed at the ventricular apex. Note that some low frequency diastolic sounds are normally encountered, which likely result from blood swirling through the mitral orifice and around the left ventricular outflow tract. The novice should not mistake these low velocity events for evidence of aortic insufficiency.

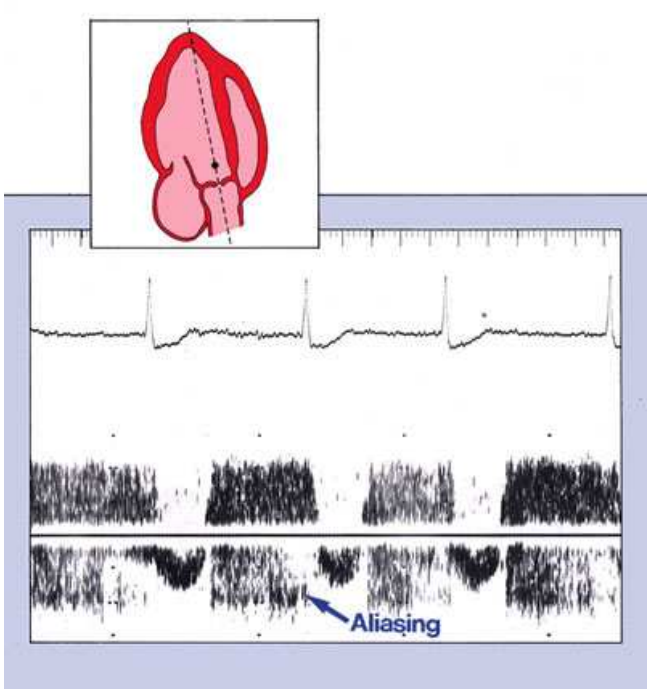

Figure 2.11 PW Doppler recording of aortic insufficiency with severe aliasing (Scale marks = 0.5 m/sec).

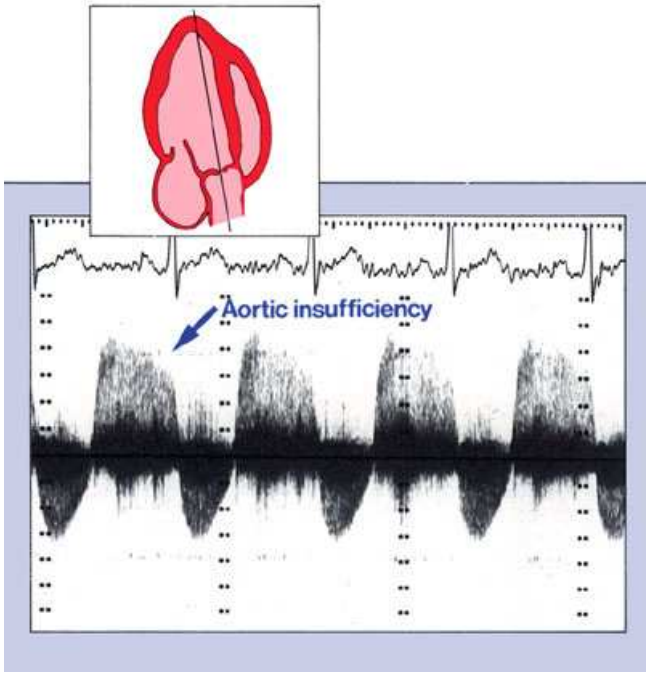

Figure 2.12 Aortic insufficiency as recorded from the ventricular apex using CW Doppler is represented as diastolic flow toward the transducer (Scale marks = 1 m/sec).

When regurgitation is present, careful searching just on the ventricular side of the aortic valve with PW Doppler reveals the high frequency sounds and diastolic spectral broadening typical of aortic insufficiency. This is shown in **Figure 2.11**, where almost all regurgitation jets are severely aliased and the top of the spectral trace appears cut off and placed at the bottom of the display. Note that the zero baseline of the spectral display has been moved to the bottom of the display, as described in Unit 1, in an attempt to eliminate the aliased diastolic signal and to provide as much display of the spectral profile as possible. Even with this maneuver, the top of the aliased signal is still missing.

Similarly, the best window for the evaluation of aortic insufficiency with CW Doppler is the apical window. Using this approach, aortic insufficiency appears as a holodiastolic, high frequency turbulent jet with spectral broadening and flow toward the transducer as noted in **Figure 2.12**. The resultant spectral shift is positive (i.e., above the baseline). Doppler spectral recordings of aortic insufficiency are invariably holodiastolic.

It is usually of interest to beginners to Doppler echocardiography who are familiar with auscultation, that the Doppler spectrum in aortic insufficiency has a holodiastolic duration and its duration does not vary with severity. This example serves to highlight the differences between the audible sounds generated by the Doppler shift device and those heard by auscultation. Using the latter approach, the typical murmur of aortic insufficiency is early diastolic and decrescendo. These differences emphasize the fact that the Doppler instrument is not an elaborate electronic stethoscope.

The operator should keep in mind some possible causes for false positive or false negative examinations when evaluating patients with suspected aortic insufficiency. One common reason for a false positive test is confusion with mitral valve diastolic inflow, particularly when mitral stenosis is present. **Figure 2.13** shows a CW recording taken from the apical window in a patient with aortic valve disease. Note the different timing of the aortic diastolic jet and the mitral inflow signal. The duration of diastole is longer in aortic insufficiency than mitral inflow.

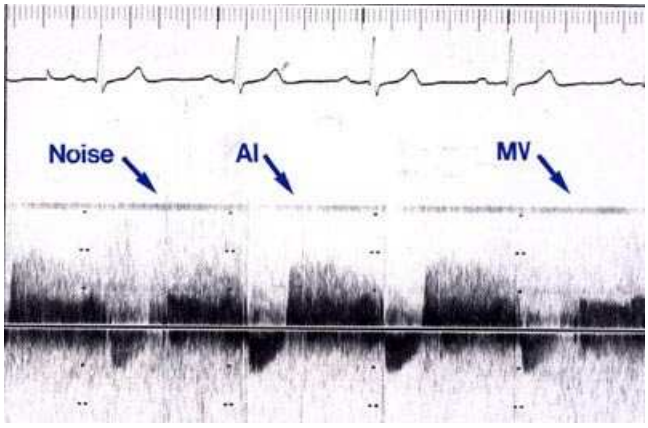

Figure 2.13 Changing CW spectral patterns encountered when mobbing the direction of the transducer (at the apex) from aortic outflow where aortic insufficiency (AI) is noted to mitral valve (MV) inflow. Note the mitral profile superimposed on the AI spectra. (Scale marks = 2 m/sec).

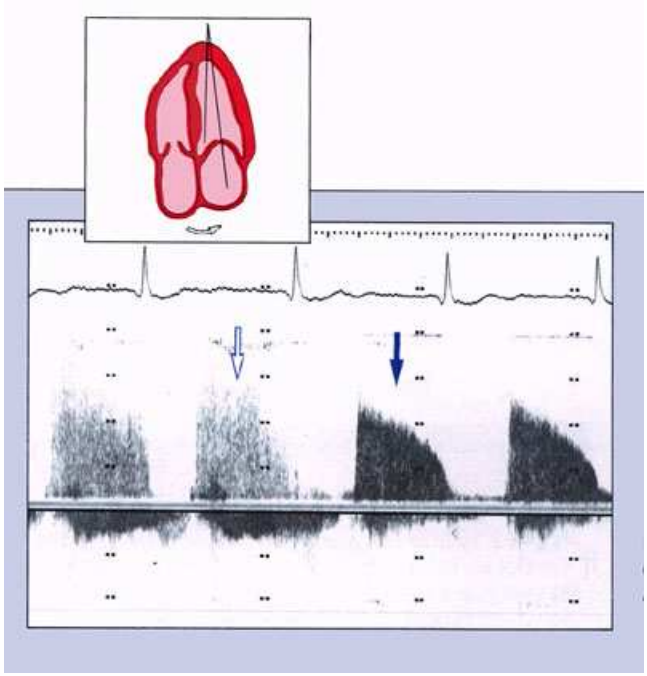

Figure 2.14 Similar spectral patterns of aortic insufficiency (open arrow) and mitral stenosis (closed arrow) occurring with slight movement of the Doppler beam. For details, see text. (Scale marks = 1 m/sec).

A maneuver performed from the apical window using a CW Doppler transducer is demonstrated in **Figure 2.14**. The first two beats were obtained with the beam angled toward the left ventricular outflow tract, and demonstrate aortic insufficiency. The beam is then angled toward the mitral orifice where the diastolic jet of mitral stenosis is encountered in the second two beats.

These jets are both diastolic events and are quite similar in contour. Note also that the spectral distribution of both abnormal jets is wide, but much less intense in aortic insufficiency when compared with mitral stenosis. Recognition of the different features of the spectral display in these two lesions, plus a thorough examination of the location of the suspected abnormal diastolic jet using the PW approach, should allow the operator to reliable separate aortic insufficiency from mitral stenosis in most cases.

It is also possible that a false positive recording of aortic insufficiency may result from inadvertent detection of coronary blood flow. Although coronary flow is mostly diastolic and the size of the Doppler beam is usually large at remote distances from the transducer, it seems unlikely that this is a very frequent cause of false positives in clinical practice.

It is worthwhile to keep in mind that detection of aortic regurgitation by Doppler with a negative cardiac catheterization may not necessarily constitute a false positive study. However, the amount of regurgitation in this situation is probably minimal. Rapid dilution of a small aortic regurgitant jet into the large left ventricular cavity probably accounts for the failure to appreciate this event by angiographic means.

The probable reason for a false negative diagnosis of aortic insufficiency is that the jet is small and not easily detected with either pulsed or continuous wave Doppler. Not only may the jet be small, it may move through the interrogating beam with the phases of the cardiac cycle. This makes it difficult to record a full profile because the jet is never positioned in the Doppler beam long enough to record the entire event, as seen in **Figure 2.15**.

Such an occurrence is the likely explanation for the PW Doppler spectral recording shown in **Figure 2.16**. Here, the full diastolic duration of the aortic insufficiency jet is poorly appreciated on some beats. The recording was obtained with the transducer held at the ventricular apex.

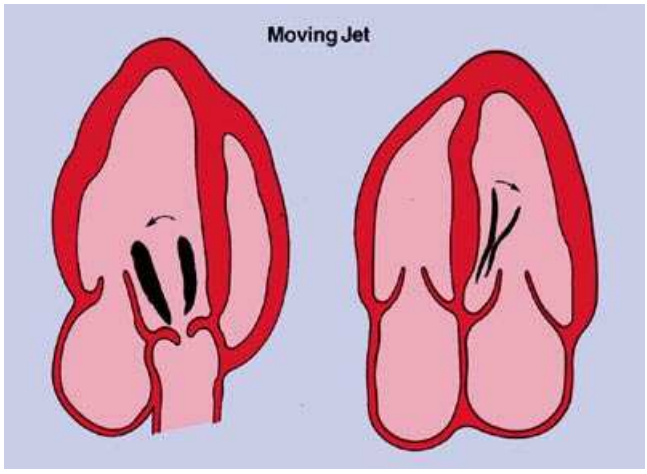

Figure 2.15 Regurgitation jets may move eccentrically during the cardiac cycle and cross the Doppler beam.

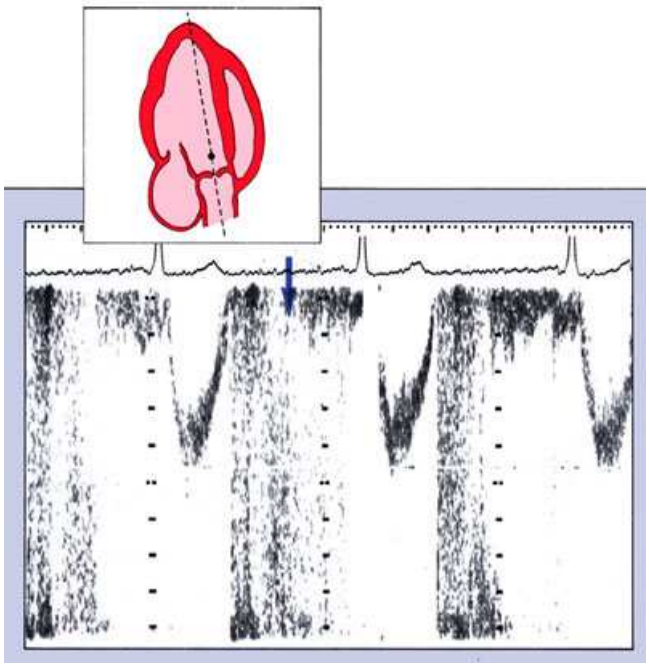

Figure 2.16 PW Doppler recording of changing patterns of an incompletely visualized aortic regurgitant jet that is encountered from slightly different angles from beat to beat (Range marks = 20 cm/sec).

This phenomenon also may occur due to the phases of the respiratory cycle. This is not because the volume of the jet is varying with respiration. Rather, the direction of the jet is probably changing slightly with respect to the direction of the interrogating Doppler beam as the heart moves up and down with the moving diaphragm. This phenomenon is demonstrated in **Figure 2.17** where the full profile of aortic insufficiency is seen from the ventricular apex using CW Doppler. Here the full profile of aortic insufficiency is recorded on some beats and not on others. When this occurs, and differences due to respiration are suspected, the operator should try many different transducer positions and angulations to record as much of the suspected abnormal profile as possible.

Some jets may be so small as to require interrogation from slightly different transducer positions to record the full profile. The spectral profiles in **Figure 2.18** are not the result of a continuous strip recording but are a five-panel composite demonstration of the diastolic appearance of aortic insufficiency from five slightly different apical positions in a patient with aortic insufficiency. The only way to overcome this problem is to be assured that every possible area has been adequately interrogated for aortic insufficiency during the Doppler examination.

Although the apical approach is the most profitable window for the detection of aortic insufficiency, it is worth keeping in mind that some jets are directed eccentrically and may be detectable only from some other window such as the left parasternal. Caution should be exercised, however, when using CW Doppler from parasternal windows. It might be possible to mistake pulmonic insufficiency, which can be recorded in many subjects, for aortic valve insufficiency. Fortunately, most aortic insufficiency encountered from the left parasternal approach is directed posteriorly toward the mitral valve and away from the transducer (a negative jet). This contrasts with pulmonic insufficiency, which is uniformly directed anteriorly into the right ventricle toward the transducer (a positive jet).

Some information as to left ventricular end-diastolic pressure may be gained in the setting of aortic insufficiency. Since the velocity of any jet relates to the pressure drop across the valve, there exists a pressure gradient between the aorta and left ventricle at end-diastole. This pressure gradient may be estimated by measuring the velocity of the aortic regurgitant jet at end-diastole using the simplified Bernoulli equation. Subtracting this pressure from diastolic blood pressure (as measured

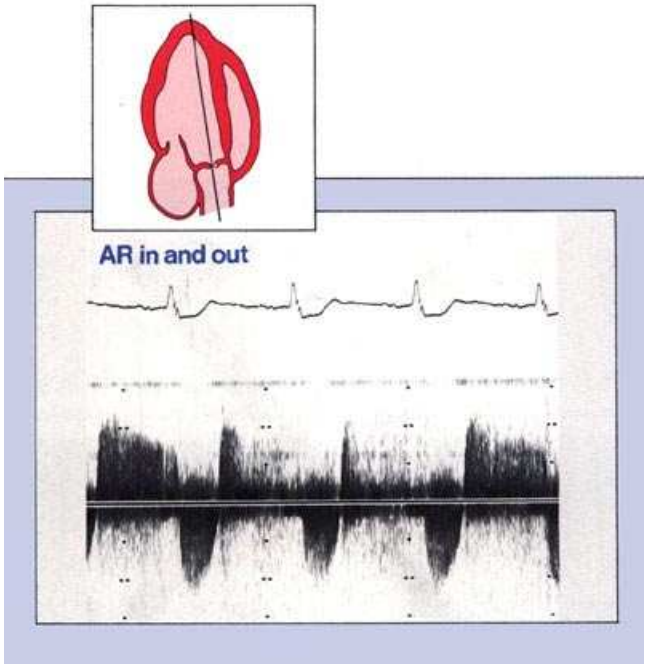

Figure 2.17 CW spectral recording of aortic regurgitation from apex where the regurgitant jet moves in and out of the beam. (Scale marks = 2 m/sec)

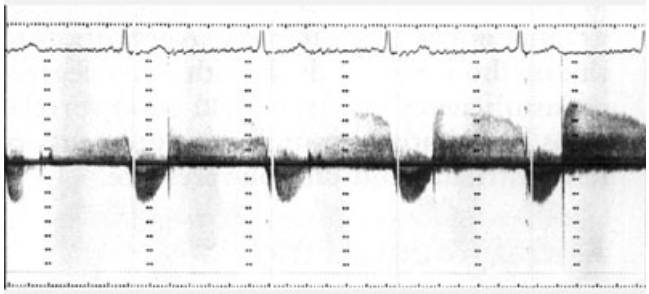

Figure 2.18 Five panels showing differing appearances of aortic regurgitation from five slightly different positions near the apex using CW Doppler. The best spectral profile is right. (Scale marks = 1 m/sec)

by cuff at the time of the Doppler examination) provides an estimate of left ventricle end-diastolic pressure.

A typical aortic regurgitant jet obtained by CW Doppler from the left ventricular apex is shown in **Figure 2.19**. In the example shown, the end-diastolic velocity is approximately 1.9 m/sec which corresponds to a pressure gradient estimate of 14mmHg. This patient had severe aortic insufficiency, and the measure diastolic blood pressure was 55mmHg by brachial arterial cuff measurement. This resulted in an end-diastolic pressure estimate of 41 mmHg. At catheterization, the actual measured pressure was 38 mmHg.

It should be noted, however, that this approach only shows satisfactory correlation in patients with severe (3+ to 4+) angiographic aortic insufficiency. Application of this method to individuals with lesser degrees of insufficiency does not yield good correlations with catheterization measurements of left ventricular end-diastolic pressure.

Mitral Regurgitation

A number of studies have shown that Doppler echocardiography is both very sensitive and very specific for the detection of mitral regurgitation when compared with cardiac catheterization. Using PW Doppler, most cases of mitral regurgitation can be detected with the transducer at the apex and the sample volume located in the left atrium just behind the mitral valve **(Fig. 2.20)**. Because of the high velocities of the regurgitant jet and the distance from the transducer to the jet, aliasing of the mitral regurgitant jet invariably occurs. As with all regurgitant lesions, location of the abnormal turbulence is done in pulsed Doppler mode and continuous wave Doppler is then used to record the full spectral profile.

The full spectral profile of mitral regurgitation obtained from the ventricular apex by CW Doppler commonly reaches peak velocities of between 3 and 6 m/sec, depending on the systolic pressure gradient between the two chambers. It is usually quite symmetric, as seen in **Figure 2.21**. The opening and closing motions of the mitral valve will sometimes result in sharp spikes on the spectral velocity recording because the rapidly moving valves will also render a Doppler signal. This phenomenon of valve opening and closing is seen in **Figure 2.22**.

Mitral regurgitation associated with endocarditis, ruptured chordae tendinae and/or partial leaflet flail, is frequently associated with loud clicking noises and high frequency spikes on the spectral recording. These are created by rapid movements of the diseased target through the field of view.

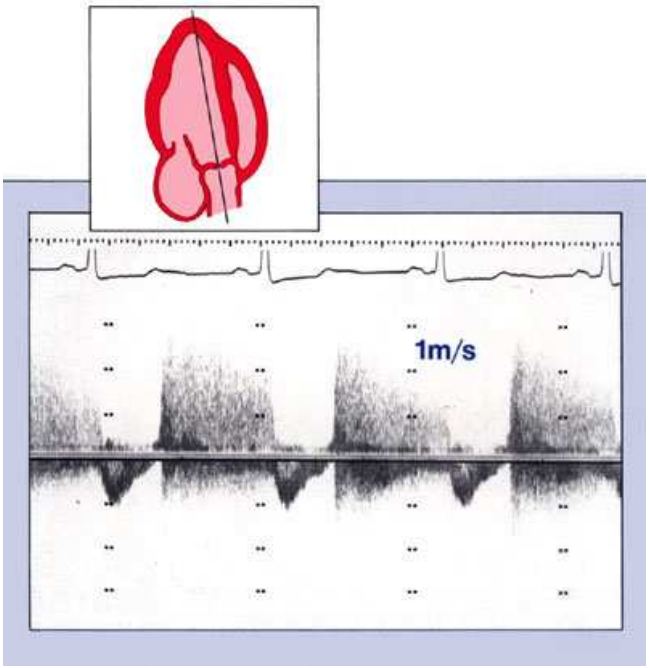

Figure 2.19 CW spectral recording of aortic insufficiency showing measurement of end-diastolic pressure gradient (Scale marks = 1 m/sec)

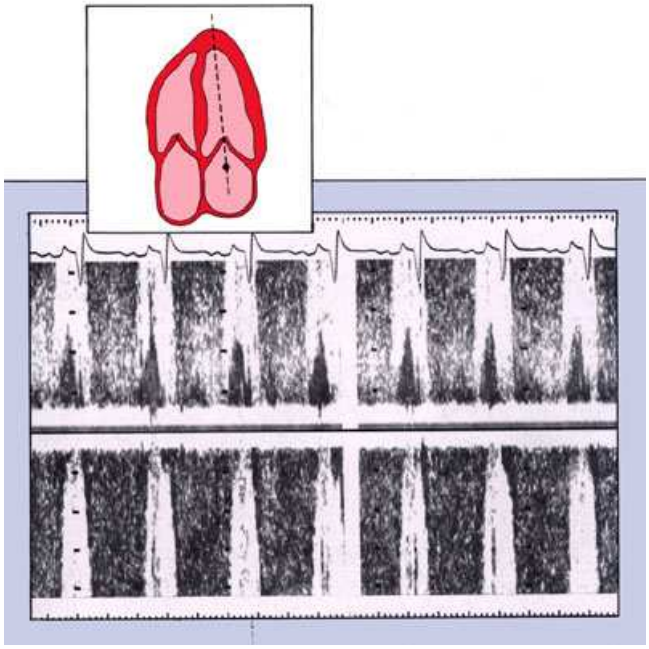

Figure 2. 20 PW Doppler spectral analysis of mitral insufficiency with the sample volume located in the left atrium. The high velocities encountered produce aliasing. (Scale marks = 20 cm/sec)

Thus, multiple high velocity spikes may be demonstrated on the spectral recording as seen in **Figure 2.23**. Occasionally, the systolic profile of mitral regurgitation peaks slightly early, as is seen in this patient with endocarditis when the regurgitation is severe and end-systolic pressures are high. These results occur because the gradient between left ventricle and left atrium is small.

Other factors may alter the usually symmetry of the mitral regurgitant spectral tracing. The *left panel* of **Figure 2.24** shows combined aortic insufficiency with aortic outflow tract obstruction. This tracing was obtained from an individual with hypertrophic cardiomyopathy and a resting outflow tract gradient. Note that the systolic peak velocity approaches almost 5 m/sec. Interrogation of the mitral valve **(Fig. 2.24, top panel)** shows a clear, late systolic profile typical of the late systolic mitral regurgitation seen in this disorder. This presumably occurs because the pressure within the left ventricle rises rapidly with the dynamic outflow obstruction and creates a very high gradient between left ventricle and atrium in mid-to-late systole.

False positive examinations for mitral regurgitation do occur. One common reason for false positive examinations is confusion of the aortic outflow signal with that of the mitral regurgitation. The similarity between the systolic flow profile away from the transducer in mitral regurgitation and aortic stenosis is shown in **Figure 2.25**. As previously mentioned, the longer duration of mitral systole may help to differentiate these two lesions. In addition, it is usual to see mitral diastolic flow in the same spectral recording with mitral insufficiency.

Even though the use of PW Doppler may help to locate the systolic turbulent jet in the left atrium rather than the aortic outflow tract, it is important to remember that the size of the sample volume becomes larger at remote distances from the transducer. For example, when the sample volume is positioned in the left atrium from an apical transducer location, the sample volume is almost always larger than it appears on the two-dimensional display (because of the diverging shape of the ultrasound beam). Therefore, it is best to use caution when a negative jet within the left atrium can be detected only in the vicinity of the aortic root, as it may represent aortic outflow **(Fig. 2.26)** rather than mitral regurgitation.

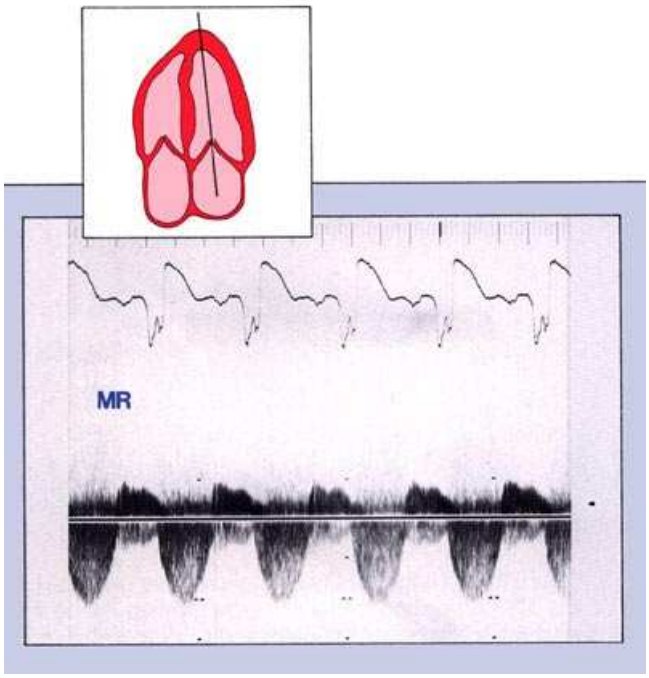

Figure 2. 21 CW recording of typical mitral regurgitation from the apex. The jet is away from the transducer in systole and is usually symmetric in shape. (Scale marks = 2 m/sec)

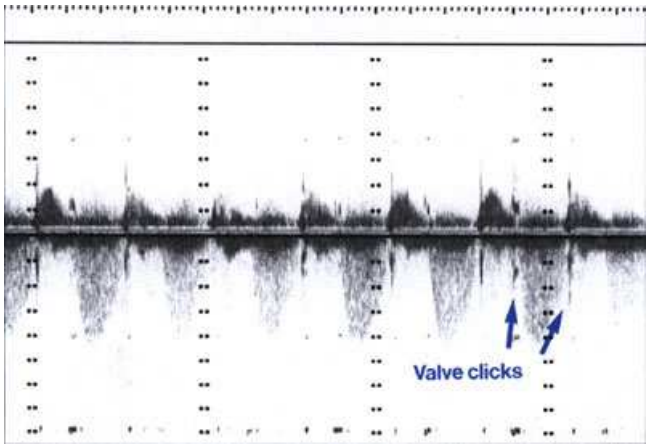

Figure 2.22 CW spectral recording of typical mitral regurgitation. Note valve closing and opening spikes or clicks. (Scale marks = 1m/sec)

It is also possible to confuse tricuspid with mitral regurgitation. This is more of a problem with CW than with PW echocardiography for a beginner, and the use of PW with concurrent imaging helps in recognizing this error. Another reason for false positives is the interpretation of a loud systolic closure sound of the mitral valve leaflets, commonly known as "valve slap", as partial recording of the early profile of a moving mitral regurgitation jet **(Fig. 2.27)**.

Detection of mitral regurgitation when it has not been found by angiography is uncommon, especially when an apical transducer position is used. It is, however, possible that a very small amount of regurgitation may be detected by Doppler and yet fail to be seen on left ventriculography, particularly if there is rapid dilution and poor opacification of the left ventricle with a contrast agent.

False negative evaluations for mitral regurgitation insufficiency also may occur and are probably most frequently due to a small jet that was missed on examination. A moving jet may also be encountered but is frequently difficult to differentiate from "valve slap" demonstrated in **Figure 2.27**.

Mitral insufficiency jets may also vary in appearance with arrhythmias. The CW spectral recording shown in **Figure 2.28** illustrates the altering profiles of mitral regurgitation encountered with premature ventricular contractions. As with all abnormal jets, mitral regurgitation can change its appearance with phases of the respiratory cycle as the orientation of the jet to the interrogating beam alters with the movement of the heart. **Figure 2.29** demonstrates the effect of these changing relationships on the mitral insufficiency recording. Mitral insufficiency may also be obscured by significant aortic stenotic lesions.

Mitral regurgitant jets, like others, are often eccentrically directed, and it is important to examine the left atrium from all available windows. Besides the apical window, the left parasternal region is very useful for this purpose.

Tricuspid Regurgitation

Tricuspid regurgitation is also best evaluation from the apical window. The left parasternal right ventricular inlet view and short axis at the aortic valve level are other useful positions. In tricuspid insufficiency, systolic turbulence is detected just behind the tricuspid valve leaflets. The contour of the flow profile is very similar to that of mitral regurgitation. AS with other regurgitant jets, CW

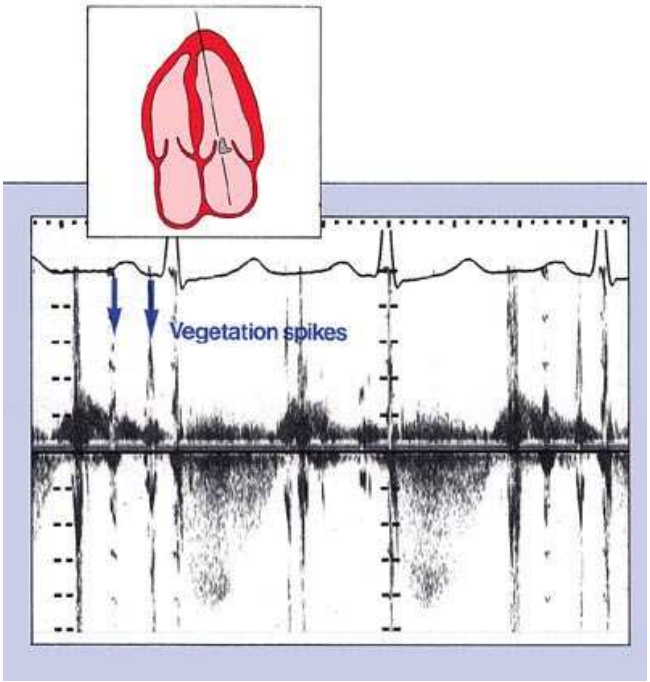

Figure 2.23 High velocity diastolic spikes (arrows) on the CW recording of mitral regurgitation made by vegetation movement. (Scale marks = 1m/sec)

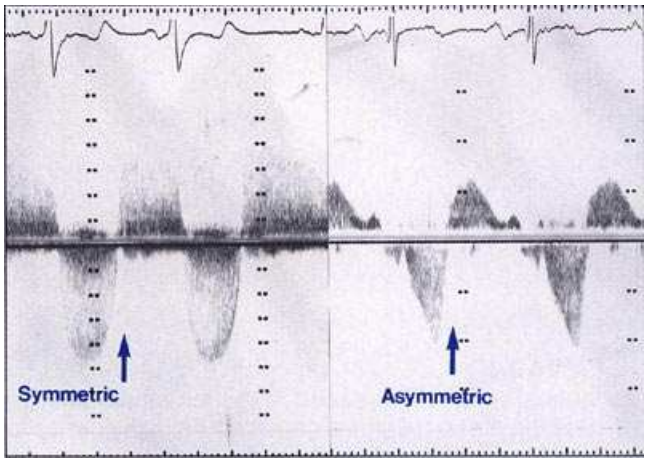

Figure 2.24 Left panel: typical recording of aortic insufficiency and obstruction. Note how the aortic outflow tract turbulence resembles the symmetric profile of mitral insufficiency (arrow) with continuous beam angles through

Doppler is usually needed to obtain an unaliased recording of the full spectrum as seen in **Figure 2.30**.

We frequently detect tricuspid regurgitation by Doppler in otherwise normal individuals and find that even beginners to Doppler instrumentation will readily record this entity in between 25% and 50% of their patients. Earlier studies found a similar, frequent systolic reversal of flow in normal individuals using contrast echocardiography of the inferior vena cava. Some investigators have indicated that a small degree of tricuspid regurgitation may be seen in as many as 96% of normal volunteers by Doppler. These findings were felt to be due to true valvular tricuspid regurgitation, and not to coronary sinus systolic flow.

These findings indicate that Doppler evidence for tricuspid regurgitation is common and presents an interpretive dilemma for echocardiographers. It is clear to us that the physical findings of tricuspid regurgitation are extraordinarily insensitive and are usually seen only when the regurgitation is severe. There is no widely accepted standard method for reporting this lesion. Currently, we prefer not to report tricuspid regurgitation if it is localized just behind the tricuspid leaflets; it is only reported if the regurgitant jet can be found, by PW Doppler, to extend at least halfway between valve leaflets and posterior wall of the right atrium.

Respiratory variations are frequently observed in tricuspid insufficiency Doppler spectra, as noted in **Figure 2.31**, and may be occasionally used to distinguish between mitral and tricuspid insufficiency when using the blind CW Doppler approach. They result from differential volume filling into the right atrium and ventricle during respiratory cycle. During inspiration, right ventricular filling is augmented due to a fall in intrathoracic pressure.

A tricuspid regurgitant jet may be used to estimate right ventricular systolic pressure (RVSP) in mmHg. This method, like all Doppler pressure estimates, is based on the modified Bernoulli equation ($dp=4V^2$) discussed in Unit 1. **Figure 2.32** shows the rationale for this calculation based upon idealized pressure tracings. When normal RVSPs are encountered and tricuspid regurgitation is present, only small pressure gradients occur and low velocity spectral recordings would be anticipated. When high RVSPs are encountered and tricuspid regurgitation is present, much higher systolic gradients exist between the right ventricle and right atrium in systole. Thus, much higher velocity spectral recordings would be anticipated.

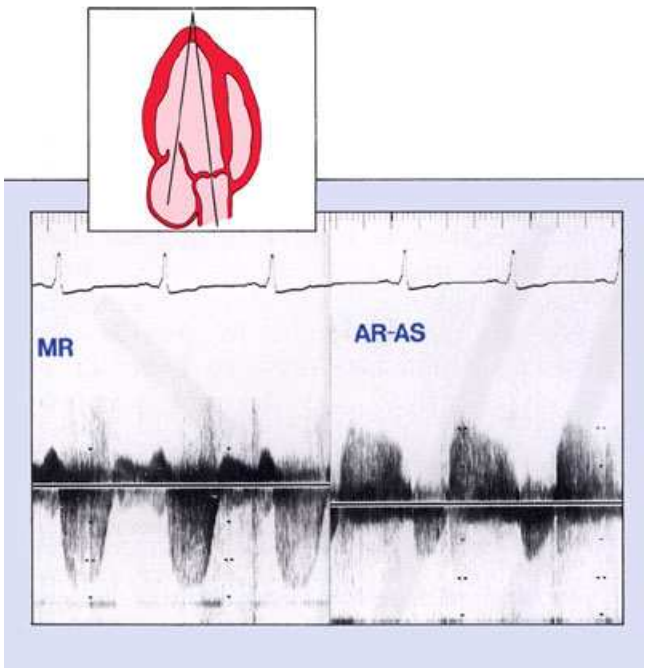

Figure 2. 25 With a transducer located at the apex, both mitral regurgitation (MR) and aortic stenosis (AS) appear as systolic movement in a negative direction. Note that mitral systole is longer in duration than aortic. Aortic regurgitation (AR) is also present. (Scale marks = 2m/sec) the mitral orifice. (Scale marks = 1m/sec)

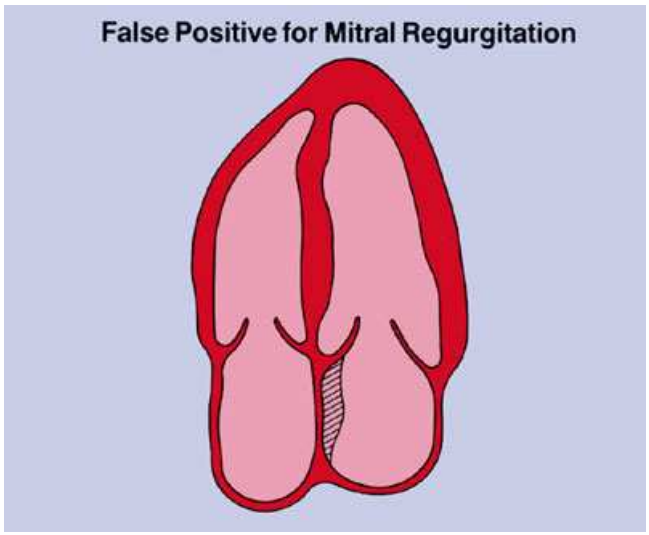

Figure 2. 26 A Doppler sample volume is large in the far field and, when placed in the left atrium in areas near the aortic root, may cause spurious evidence for mitral regurgitation.

It must be understood that the pressure within the right atrium exerts a significant effect on the peak systolic velocity of tricuspid regurgitation. **Figure 2.33** demonstrates this influence and shows the importance of estimating the pressure within the right atrium before attempting these calculations. For any given systolic pressure in the right ventricle, a low pressure in the right atrium would result in a higher gradient between atrium and ventricle and, therefore, a higher velocity than when a high right atrial pressure exists. In the latter case, the higher right atrial pressure reduces the gradient and, therefore, the resultant velocity of the tricuspid regurgitation jet.

The right atrial pressure may be estimated by examination of the patient's neck veins. Using this method, mean jugular venous pressure (JVP) in cmH_20 is first estimated by inspection of the jugular venous pulse with the patient at 45 degrees. Right atrial pressure (RAP) is estimated by adding 5 cm to the venous pressure measurement (to approximate the distance between the right atrium and the clavicle) and then converted to mmHg by dividing by 1.3. This is then added to the trans-tricuspid systolic gradient estimated from the peak tricuspid velocity. The formula is:

$$RVSP = (JVP+5/1.3)+(\text{peak systolic velocity}^2 x4)$$

The patient pictured in **Figure 2.30** has a peak systolic velocity of 2.4 m/sec that is equivalent to a peak trans-tricuspid systolic gradient of 23mmHg. Since the jugular venous pulse was estimated at 15 cm,, the right atrial pressure would be 20 cmH_20 (=15mmHg). Using the above equation, we would predict a right ventricular systolic pressure of 38mmHg.

Doppler catheterization correlations for measurement of RVSP have been reported as being very accurate, and practical application of these methods in our laboratory supports the reliability of this approach. When pulmonary stenosis does not exist, peak RVSP should reflect peak systolic pulmonary artery pressure.

Thus, many factors influence the peak velocity and appearance of the spectral tricuspid regurgitant jet. A demonstration of these differences is seen in **Figure 2.34** where one patient has a high velocity jet measuring 6 m/sec (left panel) and another has a systolic jet measuring 3 m/sec (right panel). If both patients had 5 cm of neck vein distension, the patient on the left would have a

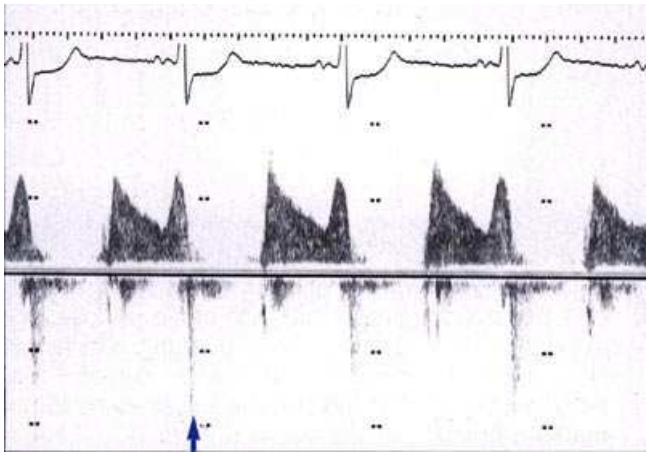

Figure 2. 27 CW spectral recording from patient with "valve slap" (arrow) that may be wrongly interpreted as incomplete recording of mitral regurgitation.

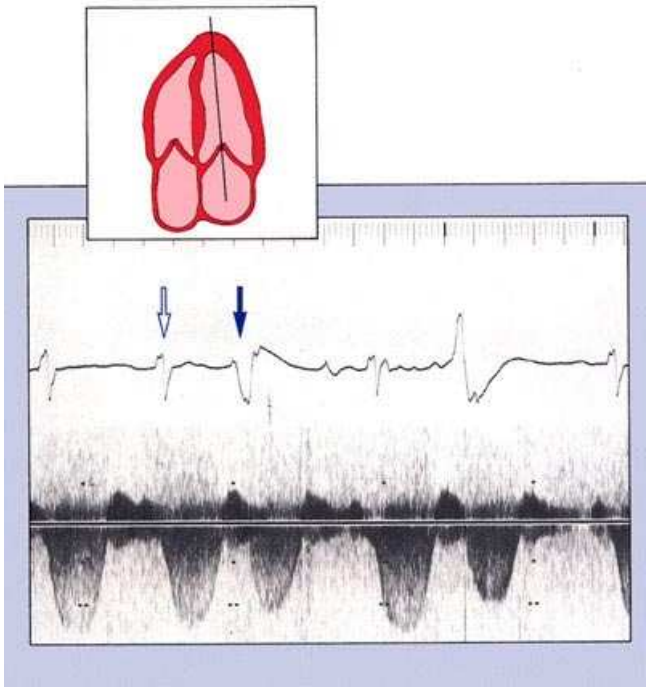

Figure 2. 28 Varying appearances of mitral insufficiency with arrhythmias. A smaller profile follows the PVC (closed arrow) than the normal beat (open arrow). (Scale marks = 2m/sec.

predicted peak RVSP of 152 mmHg and the one on the right would have a predicted peak RVSP of 44mmHg.

Arrhythmias will also profoundly affect the contour and peak velocities noted. A CW Doppler recording of tricuspid regurgitation from a patient with atrial fibrillation is seen in **Figure 2.35**. Note the differing velocities with the irregular rhythm.

As with the left-sided valves, there are reasons for the detection of false positive and false negative results that are similar to those previously discussed. One interesting cause of a false positive diagnosis is excessive upward angulation of the interrogating beam that thus intercepts aortic, rather than tricuspid flow **(Fig. 2.36)**. The left panel shows the assumed proper orientation of the CW beam while the center panel shows the actual superior angulation with the beam intercepting eh aortic root. The right panel shows the superior plane superimposed on the assumed plane when this error occurs. This is of particular importance in patients with aortic stenosis when higher velocity jets will be seen in the aorta.

Other reasons for a false positive diagnosis include confusion with mitral regurgitation or with valve slap as discussed previously. False negatives may occur due to small jets missed by inadequate examinations, moving jets, or intermittent jets due to the respiratory cycle.

Pulmonic Insufficiency

The diastolic pattern of pulmonic insufficiency greatly resembles that of aortic insufficiency as seen in **Figure 2.37**. This lesion is best detected from the left parasternal window with angulation of the beam toward the patient's left shoulder. As with tricuspid regurgitation, this abnormal pattern is found in a surprisingly high number of otherwise normal individuals. False positive results may occur from confusion with aortic insufficiency. Usually a careful PW Doppler examination will readily differentiate between these two entities. In addition, pulmonary insufficiency frequently has an end-diastolic movement that reflects atrial contraction. Some authors have suggested that flow in the left coronary artery (which crossed just below the right ventricular outflow tract) may also account for a false positive diagnosis. False negatives may occur as a result of small jets missed by an inadequate examination.

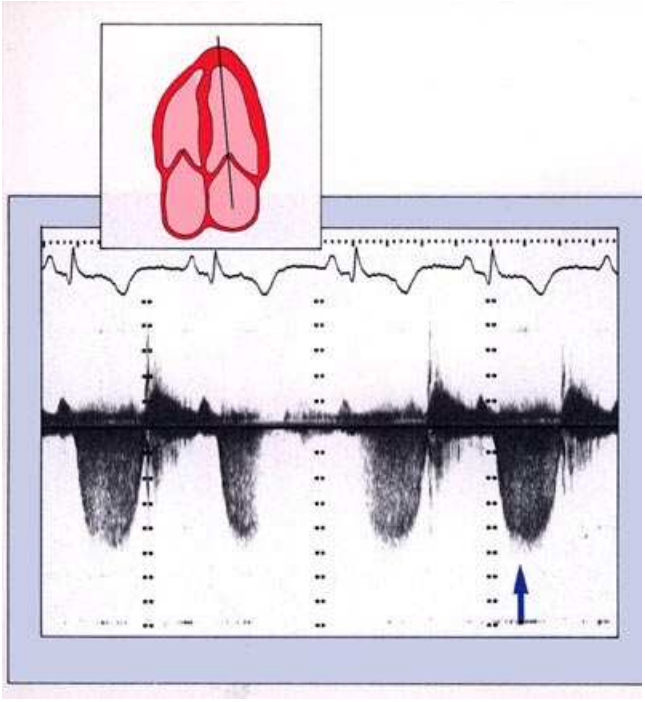

Figure 2.29 The jet of mitral regurgitation is incompletely recorded due to movement of the jet in and out of the beam. The best spectral profile is indicated (arrow). (Scale marks = 1m/sec)

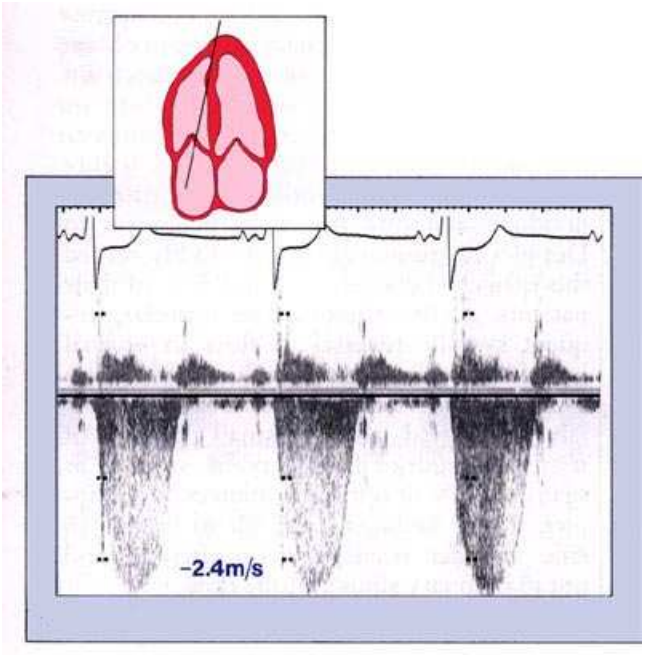

Figure 2. 30 Typical CW spectral recording of tricuspid regurgitation from the apex. The peak velocity in the jet measures 2.4m/sec. (Scale marks = 1 m/sec)

PROSTHETIC VALVE INSUFFICIENCY

Concept of Flow Masking

Understanding the role of Doppler for detection of abnormal flows through prosthetic valves begins with appreciation of the concept of flow masking. Once emitted from the transducer into the tissues, ultrasound is either reflected, attenuated (absorbed) or continues on to another tissue interface where the process is repeated. All prosthetic valves contain some degree of nonbiologic material which can be plastic, metal or cloth. Each of these materials may have highly reflective or attenuative properties that may not allow the ultrasound to penetrate and pass through the nonbiologic portion of the valve.

The nonbiologic material can interfere with the transmission of sound waves to such a degree that it may be impossible to detect some valvular regurgitation. Six commonly used heart valves are shown in Figure 2-A to demonstrate the varied appearance and materials used in fabrication of these devices: Starr-Edwards silastic ball, Starr-Edwards stellite ball, Bjork-Shiley, St. Jude's, Hall-Kastor, and a Carpentier-Edwards porcine bioprosthesis.

It is remarkable that all of the cardiac prosthetic valves cast a characteristic shadow, or mask, on the chamber behind them that obscured proper flow detection by Doppler. **Figure 2.38** shows idealized masks from two valves with the largest and smallest flow-masked areas.

The largest masked area emanates from behind the Starr-Edwards silastic ball, and the smallest is the Carpentier-Edwards porcine bioprosthesis where flow masking is limited only to the sewing ring of the prosthesis.

All valve sewing rings prevent proper transmission of ultrasound, and without the central occluding objects the area of masking would resemble that from the Carpentier-Edwards porcine valve. With the central occluding objects in place and seated in the close position, each of the valves depicted earlier has differential central transmission characteristics. The worst penetration is clearly

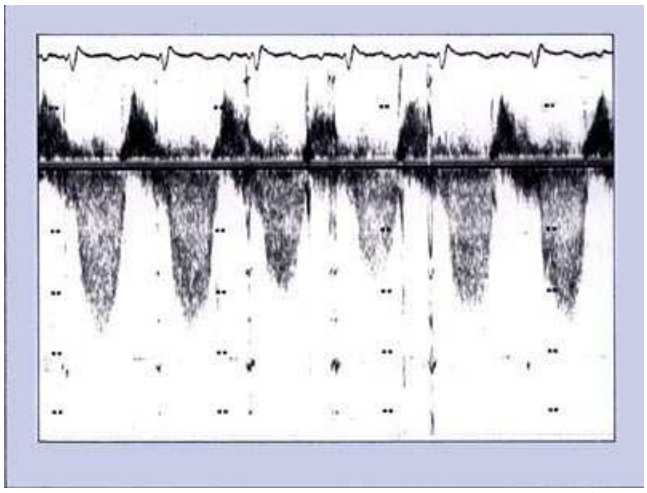

encountered with the two Starr-Edwards prostheses, each casting a large mask field behind. Very little ultrasound passes the Bjork-Shiley or the St. Jude's valves. Only slightly more penetrates the Hall-Kastor. Note that this valve's occluding disc has a hole in the center to allow the disc to interact with the central pivot arm. The Carpentier-Edwards bioprosthesis masks sound only around the valve sewing ring. The central portions of this valve assembly, made up of preserved biologic tissue, allow the sound to penetrate readily.

This differential penetration is illustrated in **Figure 2.39** where a CW Doppler system was used to attempt simulated flow behind these various valves placed on a stage. In a large water tank, a large flow phantom was positioned beneath the stage. Each valve was successively placed on the stage, before and after control (con) periods with no prosthesis in place. A strong signal was obtained from the flow during the control periods, which are shown on either end of the figure. Resultant spectral displays from all the valves are illustrated. Although system gain is held constant, there is a significant reduction in the flow signal resulting from the interposition of the prosthetic valves. Panel A demonstrates no flow detection through a Starr-Edwards valve with stellite poppit, panel C is through a Bjork-Shiley valve, panel D through a St. Jude's valve, panel E through a Hall-Kastor and panel F through a Carpentier-Edwards porcine valve.

igure 2. 31 Varying configuration of tricuspid ısufficiency with respiration. (Scale marks = 1m/sec)

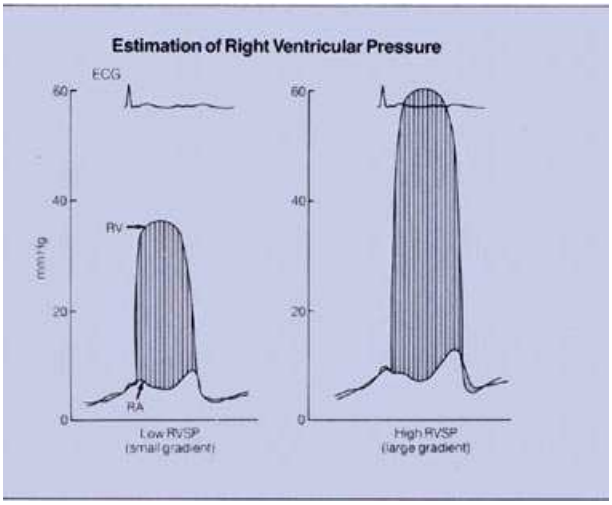

igure 2. 32 Idealized right atrial (RA) and right entricular (RV) pressure relationships in tricuspid ısufficiency. This demonstration is with similar right atrial ressures.

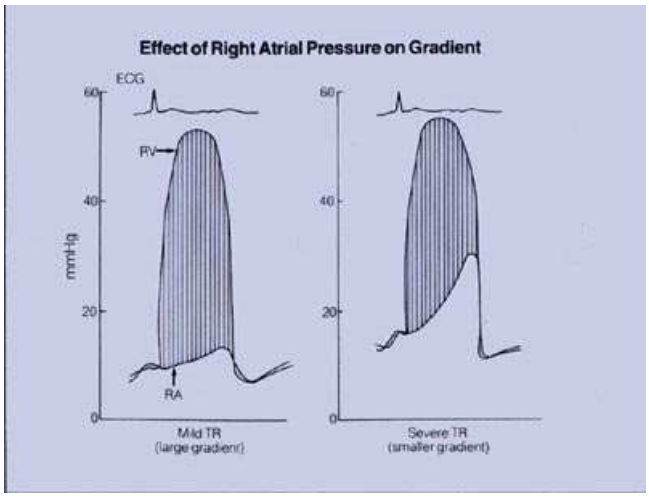

Clinical Implications

This concept has important clinical implications for the detection of prosthetic valvular regurgitation. These physical properties of prosthetic valves may significantly alter the ability of Doppler systems to detect abnormal flow even when present. Such masks also exist in vivo and evidence for their presence may be found in certain patients. Considerable clinical caution must, therefore, be exercised when encountering patients with prosthetic valves. It may be impossible to detect any flow on the opposite side of a prosthetic valve when the valve is interposed between the interrogating transducer and the area being examined.

igure 2. 33 The pressure within the right atrium also has n effect on the gradient between right atrium and ventricle. hus, right atrial pressures must be estimated from the ıgular veins for proper prediction of peak right ventricular

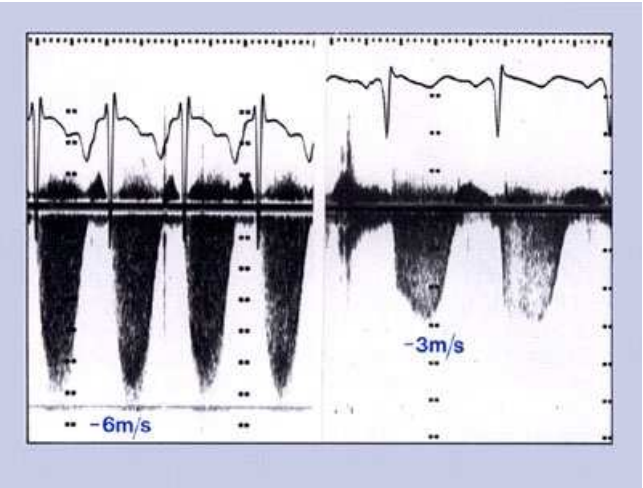

Figure 2. 34 Marked elevation in right ventricular systolic pressure will result in high velocity tricuspid regurgitant jets (left panel) in comparison to lower right ventricular systolic pressures (right panel).

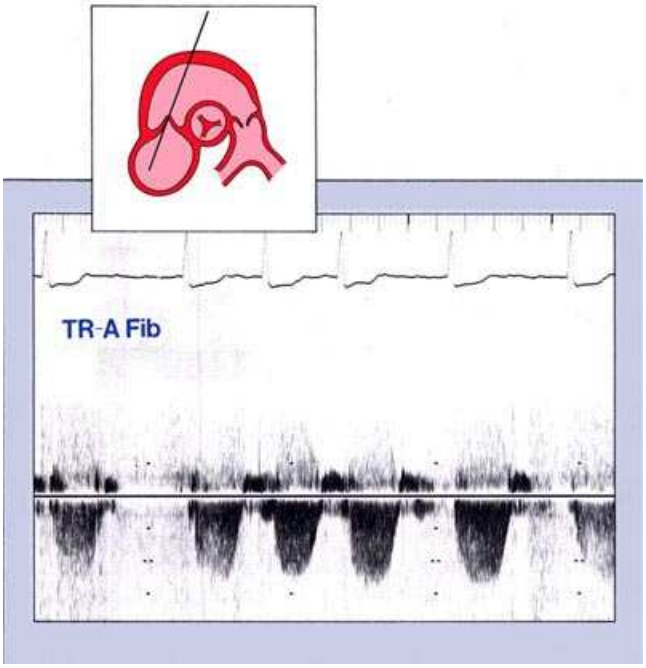

Figure 2. 35 Varying appearances of tricuspid regurgitation with atrial fibrillation. (Scale marks = 1 m/sec)

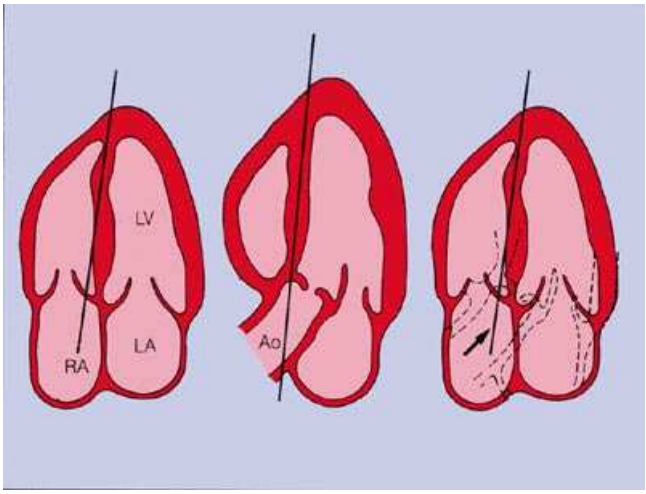

Figure 2. 36 Schematic diagram of CW beam direction for detection of tricuspid regurgitation (left). If angled a little too superiorly, the beam will actually intercept the aortic root (middle, right). Thus, aortic outflow may be a reason for false positive tricuspid regurgitation (arrow).

The best clinical example of this problem is when an operator is examining a patient with a prosthetic mitral valve for mitral regurgitation from the apical view **(Fig. 2.40, left panel)**. From this approach, almost the whole of the left atrium is masked by the prosthesis and the operator could incorrectly conclude that no mitral regurgitation existed. In this case, a very high parasternal view or a subcostal view of the left atrium must be selected for detection of the mitral insufficiency.

The problem is made worse **(Fig. 2.40, right panel)** in patients with both aortic and mitral prosthetic valves. The left atrium is inaccessible from the apical views due to the presence of the mitral prosthesis. Both prostheses obscure the left atrium from the parasternal views. In this setting, only the subcostal view is available for viewing the left atrium and, in our experience, this approach is rarely rewarding. Prosthetic aortic regurgitation may, of course, be detected from the apical view because the prosthesis is not between the transducer and the area of interest in the left ventricular outflow tract.

Because of these observations concerning the difficulty in detecting flow on the far side of a prosthetic valve, we always adjust our examination methods to interrogate these valves from all possible views, so that the prosthetic valve does not lie between the transducer and the chamber being examined. This requires considerable operator skill and is true for all Doppler methods. In many instances there is no view available in which the beam can be properly directed. Thus, we strongly suggest that operators of ultrasound equipment do all that is possible to detect flow properly. When none is detected on the far side of a prosthetic valve, it should not be assumed that none is present. We have seen cases of severe valvular regurgitation where the Doppler examination was rendered artifactually negative due to the masking effect. There are, however, some exceptions to this rule. In cases where the valve ball or disc is not allowed to seat correctly due to thrombus or vegetation,

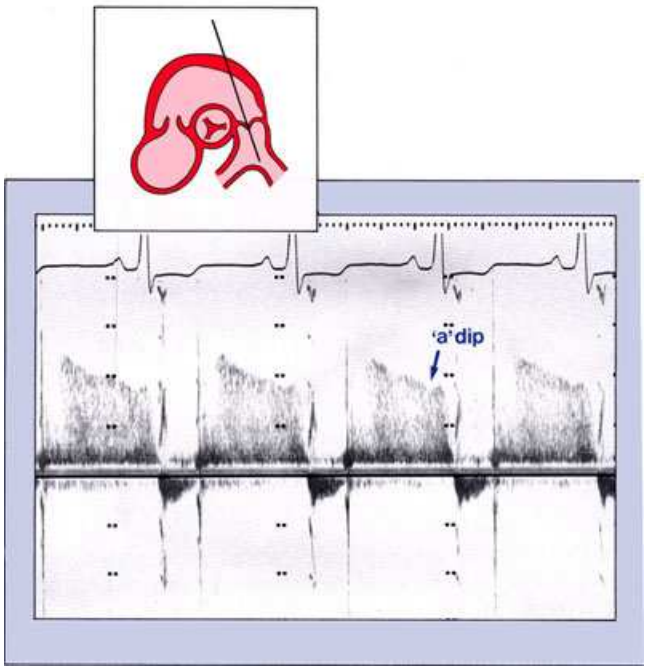

Figure 2. 37 Typical pulmonic insufficiency by CW Doppler. Pulmonic insufficiency may occasionally be differentiated from aortic by the presence of the "a" dip.

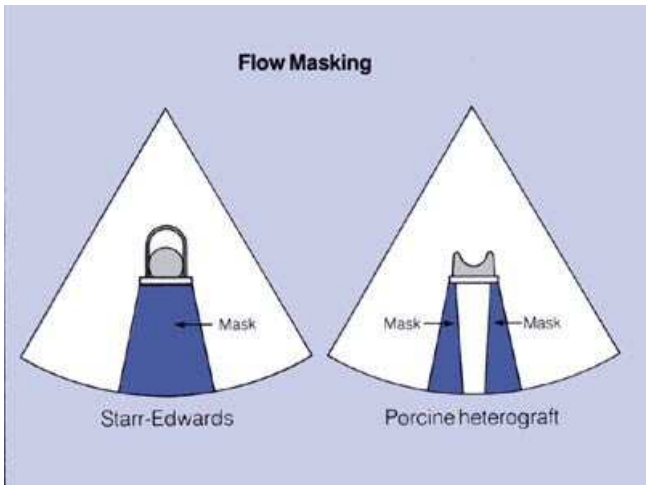

Figure 2. 38 A large flow mask is seen behind a Starr-Edwards prosthesis while only the area of flow making from a Carpentier-Edwards heterograft is seen behind the sewing i

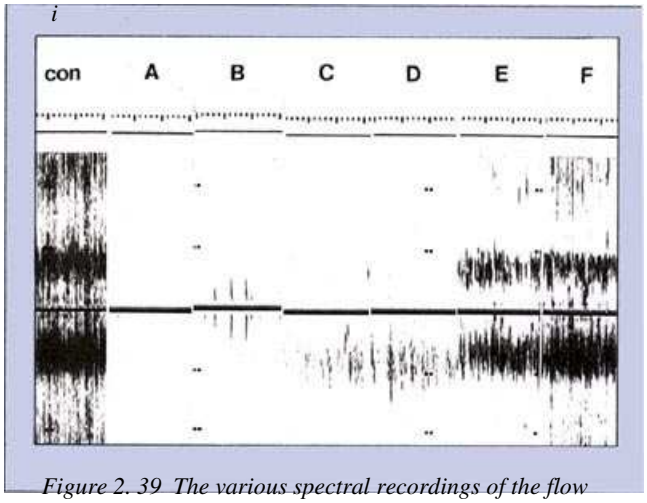

Figure 2. 39 The various spectral recordings of the flow behind prosthetic valves using CW Doppler echocardiography. The control period of flow detection when no valves were in place are shown at either end (con). The letters correspond to the valves shown in Figure 2-A,

some sound may be transmitted through the partially open area if it is correctly oriented to the sound beam.

SEVERITY OF VALVULAR INSUFFICIENCY

Quantifying Valvular Insufficiency

It can now be generally accepted that Doppler echocardiography is a reliable method for the detection of the presence of valvular regurgitation. Doppler assessment of the severity of valvular regurgitation has also been moderately successful in comparison with angiographic techniques. The invasive "gold standard" for quantifying valvular insufficiency is the volume of regurgitant blood flow calculated by subtracting the total cardiac output, calculated angiographically, from the forward output (calculated by some other method—usually by the Fick principle). The regurgitant volume divided by the total angiographic stroke volume (i.e., the sum total of blood ejected forwards and backwards out of the left ventricle with each systole) is referred to as the regurgitant fraction and the formula is:

Regurgitant fraction =
total output—forward output.

This approach requires considerable time and effort and is not in widespread use in most catheterization laboratories.

The other commonly used measure of severity is a subjective grading (usually 0-4+) based on a visual evaluation of the amount of regurgitation judged by progressive opacification of the receiving chamber as seen by contrast angiography. Both methods have limitations, and there is only an approximate correlation between them. Thus, it has been difficult to find a suitable "gold standard" for comparison with Doppler methods. Remember that the subjective angiographic criteria are based upon progressive opacification of a receiving chamber, usually over several heart beats. When Doppler methods are used, regurgitation is detected on a beat-to-beat basis

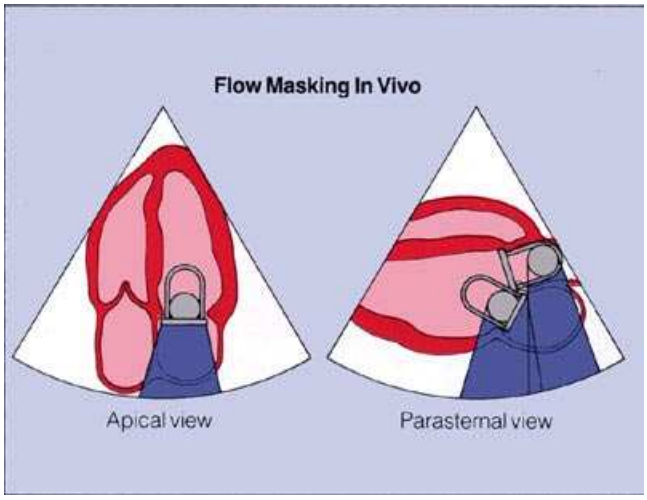

Figure 2. 40 Flow masking also occurs in vivo. The left panel demonstrates that most of the left atrium is obscured in the apical four-chamber view. When aortic and mitral valves are in place, almost all the left atrium is obscured from the parasternal approach (right panel).

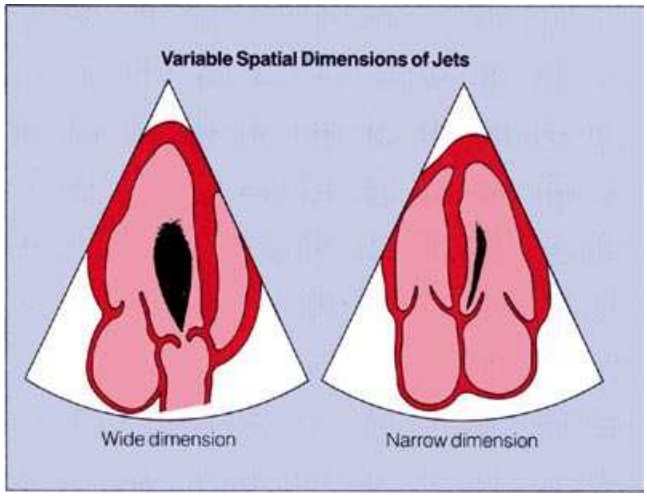

Figure 2. 41 Jets have variable spatial dimensions. On the left is an aortic insufficiency jet that is wide in the apical two-chamber view. The same jet may be quite narrow in the apical four-chamber view.

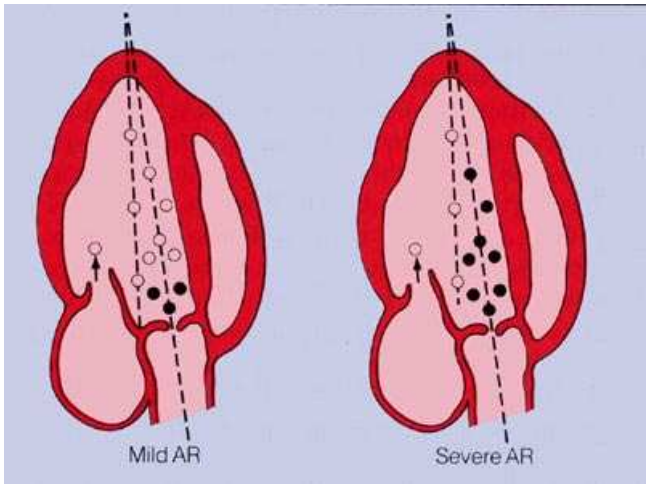

Figure 2. 42 Various sample sites for mapping the severity of aortic regurgitation (circles). Left panel shows positive detection of regurgitation just below the aortic valve (closed circles). Right panel shows broader distribution compatible with more severe disease. Sampling near the mitral orifice will invariable detect mitral inflow (arrows).

and differences between any comparisons should be expected.

Many approaches have been proposed to estimate the severity of valvular regurgitation using Doppler. One method relies on the use of PW Doppler to map the size and distribution of the regurgitant jet within a cardiac chamber and is the most common method used. Another is based upon the relationship of forward to reverse flow, while another has attempted to quantify the absolute flow through each valve orifice and then use these flow volumes to calculate the regurgitant fraction. The latter two methods are more complex and not easily performed by beginners to Doppler echocardiography. Another method based upon rate of descent of the velocity spectrum in diastole has been proposed for estimation of the severity of aortic insufficiency.

Pulsed Doppler Mapping Techniques

Even though mapping is the most straight-forward approach to the evaluation of severity of valvular regurgitation, it can be a difficult and time-consuming process. It is important to keep in mind the three-dimensional geometry of the camber being studied. Also, regurgitant jets may be directed anywhere within the camber and may also be of any three-dimensional configuration. One such possible spatial configuration of an aortic insufficiency jet in the apical four-chamber and apical two-chamber views is shown **in Figure 2.41**. Simply using a single standard two-dimensional view without angling the transducer in other planes in order to examine the whole chamber may result in significant under-or over estimation of severity.

The mapping technique can only be performed with PW Doppler echocardiography. It requires some experience with the Doppler technique as well as facility with two-dimensional imaging, since the sample volume has to be systematically located in various places, sampling for valvular regurgitation. The interrogating two-dimensional plane in the frozen or periodic updated image must be kept constant as each area is sampled until one view has been completely evaluated. Keep in mind

that the mapping technique only provides rough estimates of the severity of valvular insufficiency, and further comparisons with standards such as carefully validated angiographic volume measurements must still be made to assess the value of the technique.

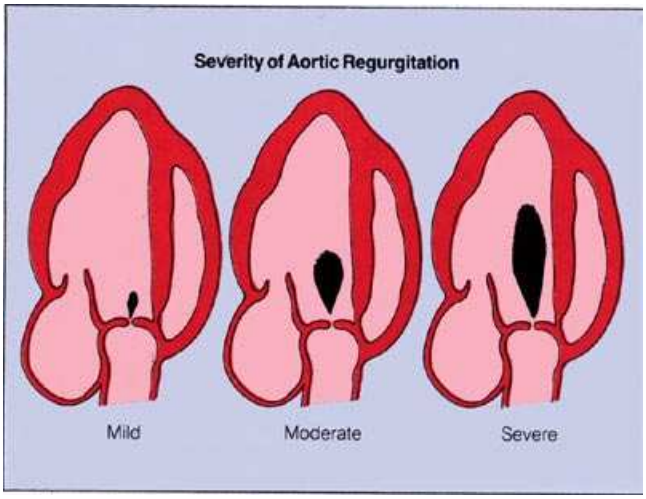

Figure 2. 43 Schematic diagram showing the relative areas of turbulence for mild, moderate, and severe aortic regurgitation.

In **Figure 2.42** there is an example of multiple areas sampled (circles) by the pulsed Doppler sample volume while in the apical two-chamber view. In the left panel, the PW Doppler detects aortic insufficiency only on the ventricular side of the aortic valve leaflets (closed circles) and this corresponds to mild aortic insufficiency. The right panel demonstrates the areas where aortic insufficiency was detected (closed circles) much deeper into the left ventricle and this corresponds to severe aortic insufficiency. Sampling directly in the mitral orifice (arrow) will almost always detect mitral diastolic flow that may be interpreted incorrectly as aortic insufficiency, particularly when there is associated mitral stenosis. Frequently these two abnormal jets blend together and coalesce into one jet directed toward the ventricular apex.

The general areas where turbulent flow would be found in mild, moderate and severe aortic regurgitation are shown in **Figure 2.43**. These are only approximate estimates of severity. The mapping technique assumes that the volume of a jet is proportional to the area of turbulence detected by PW Doppler. While this may be true for the most part, other factors are also likely to affect the area of the regurgitant jet. These are: the size and configuration of the regurgitant orifice, the pressure difference across the orifice, the size and configuration of the receiving chamber, and a host of other factors.

For mitral regurgitation the process is similar, and mapping of the left atrium may be done either from the parasternal long axis window or from an apical window. We generally prefer to begin with the apical window because mitral regurgitant jets are then usually parallel to the interrogating beam. Further spatial information about the size and direction of the regurgitant jet is then obtained using additional apical and parasternal views. **Figure 2.44** shows multiple placements of the pulsed Doppler sample volume (circles). In the left panel, regurgitation is detected only on the atrial side of the mitral leaflets, a finding consistent with mild mitral regurgitation (closed circles). The right panel shows abnormal flow detected over almost all the atrium and this corresponds to severe valvular regurgitation (closed circles). If higher velocity flows are detected only medially this may be due to aortic outflow because the sample volume is relatively large at this depth.

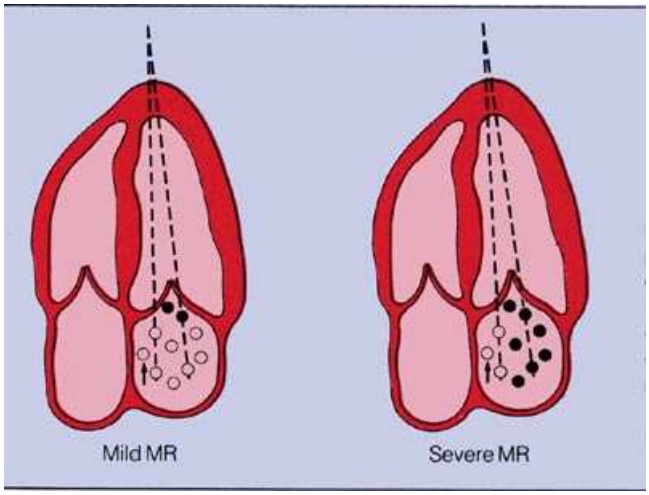

Figure 2. 44 Schematic diagrams showing many possible pulsed Doppler sample volume sites (circles). Left panel shows positive detection of mitral regurgitation just near the valve, consistent with mild disease (closed circles). Right panel shows wider distribution of positive sample sites compatible with more severe regurgitation. Sampling hear the aortic root (arrows) may bring interference from the

Interception of aortic outflow signals can present a particular problem in patients with aortic stenosis since this lesion, like mitral regurgitation, produces high velocity systolic flow away from the transducer. A schematic diagram of the general distribution of mild, moderate and severe mitral regurgitation is shown in **Figure 2.45**.

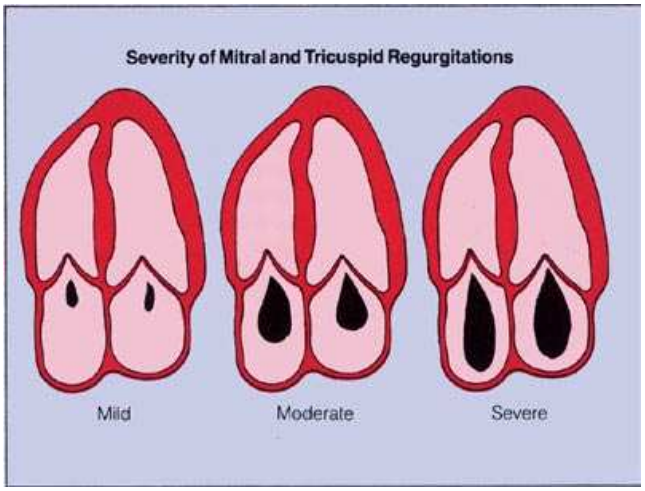

Figure 2. 45 Schematic diagram showing the relative areas of turbulence for mild, moderate, and severe mitral regurgitation.ascending aorta.

Similar methods are available for mapping tricuspid regurgitation which involve movement of the sample volume in various areas of the right atrium. A schematic representation of mild, moderate and severe tricuspid regurgitation is also shown in **Figure 2.45**. Mapping methods for estimation of the severity of pulmonic insufficiency are based on the same principles.

Other Doppler Methods

The other approaches to the estimation of severity of valvular regurgitation are more complex. The first attempts were indirect in assessing the amount of regurgitant flow in mitral regurgitation. Some investigators have used CW Doppler to study systolic velocity in the descending aorta. They divided the area under the velocity curve into two halves and compared the ratio of the two (first half of systole to the second half of systole) in normal subjects and mitral regurgitation patients. They found that in mitral regurgitation patients, more blood was ejected in the first half of systole. While these ratios showed a good correlation with the regurgitant fraction measured at cardiac catheterization, this approach is not in common use.

More recently, some investigators have explored the use of direct volume of flow measurement with Doppler (described in Unit 3) to calculate directly the regurgitant volume and regurgitant fraction. Again, these methods are very time-consuming and not in general use.

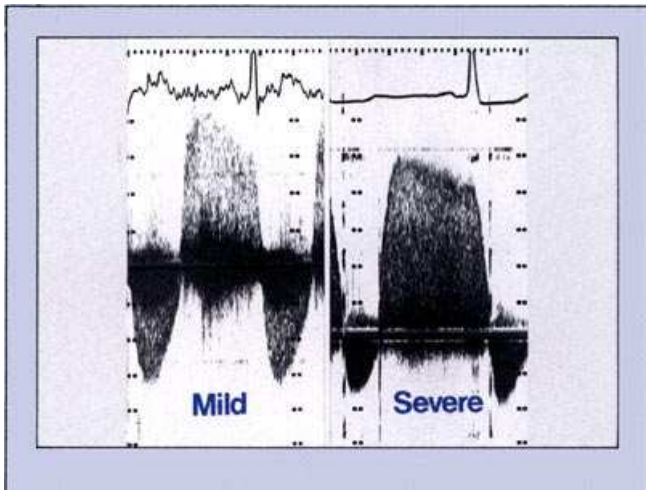

Figure 2. 46 The amplitude or intensity of a given signal is another method for judging the approximate severity of valvular regurgitation.

Direct inspection of the CW Doppler spectral recordings demonstrate some interesting relationships between flow and the Doppler spectral tracings. In Unit 1, we discussed the importance of amplitude (or intensity) of the spectral recording as a reflection of the number of red blood cells at that given velocity. Using this principle, the more intensive the spectral recording, the more severe the given amount of regurgitation that can be expected when compared with one of lesser intensity. The resultant spectra from a jet of mild aortic regurgitation compared with that of more severe regurgitation are demonstrated in **Figure 2.46**. Note that the more severe regurgitation results in greater amplitude (or intensity).

Obviously, this approach is highly subjective and is dependent upon gain and gray scale settings. Despite its subjectivity, experienced interpreters of Doppler data will use these criteria to separate

mild from more severe degrees of valvular regurgitation when observing examinations performed by experienced operators. Poorly formed, less intense profiles usually result from trivial regurgitations. Well-formed, highly intense jets usually result from more severe valvular regurgitation.

There have been attempts to directly quantify regurgitant flow in aortic insufficiency. One method involves obtaining a CW Doppler spectrum from the ascending aorta from the suprasternal notch. In this approach the area under the forward spectrum is compared with the area under the reverse spectrum and a ration of retrograde to forward flow is derived. This ratio has been compared with direct measurements made at operation using an electromagnetic flow meter as well as with regurgitant fractions measured at cardiac catheterization. While these results seemed favorable, they are not in common use. Many factors other than volume alone influence the area under the spectral velocity curves.

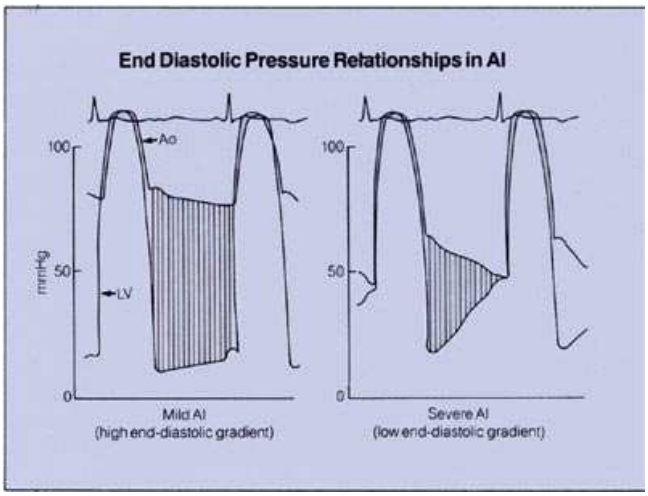

Figure 2. 47 Idealized pressure tracing in mild aortic insufficiency (left panel) and severe aortic insufficiency leaves a negligible end-diastolic gradient in comparison

There are several other methods for assessing aortic insufficiency that are based upon the rate of descent of the diastolic velocity. The theory behind these methods is demonstrated in **Figure 2.47** where idealized pressures from a patient with mild aortic insufficiency are compared with those from a patient with severe aortic insufficiency. When insufficiency is mild, left ventricular diastolic pressures are generally low and aortic diastolic pressure does not fall substantially. Significant diastolic pressure gradients are therefore maintained throughout this portion of the cardiac cycle and at end-diastole the resultant velocities are high. When insufficiency is severe, left ventricular diastolic pressures usually rise and aortic diastolic pressure may fall and approach that of the left ventricle. In this case, a large diastolic pressure gradient is not maintained throughout this portion of the cardiac cycle and end-diastolic velocities are low.

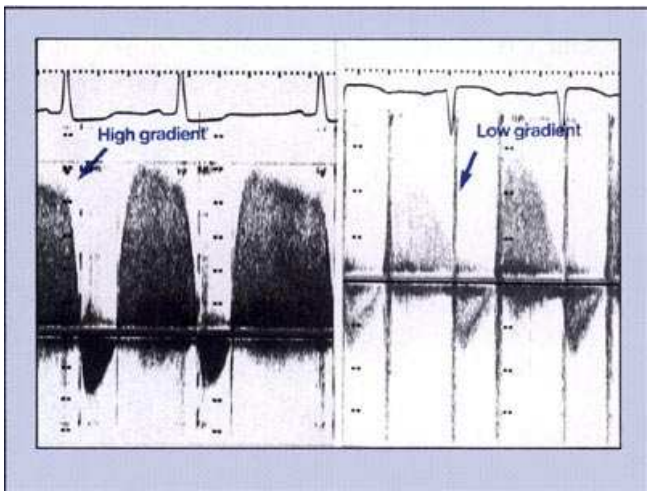

Figure 2. 48 CW Doppler spectral recording from two different patients, one with a high end-diastolic gradient and one with a very low end-diastolic gradient.

In **Figure 2.48**, a CW Doppler spectral recording from a patient with mild aortic insufficiency is compared with that from a patient with mild aortic insufficiency is compared with that from a patient with severe aortic insufficiency where there is little velocity at the end of diastole. These general observations have been extended into a variety of calculations of descend rates for more precision, with generally favorable results.

THE DOPPLER EXAMINATION FOR VALVULAR REGURGITATION

As seen from the many examples described in this Unit, there are several major points to keep in mind when examining patients for the presence of valvular insufficiency. These hints, which incorporate principles described in Unit 1, may increase the reliability of the Doppler data.

Hint 1: One practical point not previously emphasized is that the audible output may be more sensitive than the spectral display. Frequently, a given lesion is heard by audio but cannot be adequately recorded on the spectral hard copy. Interpretation in these cases is often difficult, and, in our experience, usually involves a compromise. Accepting audio evidence of a regurgitant lesion without hard copy confirmation increases the sensitivity of the procedure but will also result in an increased number of false-positive diagnoses. Currently, we require hard-copy confirmation before we will report definite evidence of valvular regurgitation.

Hint 2: It is important for the operator to take time to search for small regurgitant jets. When searching for insufficiency by PW Doppler with an instrument that has a variable sample volume size, the operator should not routinely begin the examination with a sample volume size that is as large as possible. While this may seem desirable for locating small jets, the operator must remember that this process will frequently result in a loss of system sensitivity.

Hint 3: The operator should expect regurgitant jets to exceed a velocity of 1.5 m/sec and result in aliasing when in PW mode. This is certainly true in most adults, since regurgitant lesions are located far enough away from the transducer to cause the Nyquist limit to be exceeded. Thus, in almost every instance, PW Doppler operators should expect aliasing of regurgitant lesions.

Hint 4: Doppler operators, particularly beginners, should be prepared to switch back and forth between pulsed and continuous wave modes. This will help locate areas of turbulence more precisely and will also make it easier to recognize the typical spectral profiles of these lesions. The end result will be an enhanced ability to separate one abnormal lesion from another.

Figure Legends

Figure 2.1 Valvular regurgitation is characterized by inappropriate retrograde flow during the cardiac cycle. The left panel demonstrates mitral regurgitation in systole, the right panel demonstrates inappropriate aortic insufficiency in diastole.

Figure 2.2 During systole, left ventricular pressure is greater than left atrial pressure (left panel). In the presence of mitral regurgitation, the flow communication between these chambers allows a high gradient to exist.

Figure 2.3 The gradient between the left ventricle and the left atrium in mitral insufficiency is reflected by the velocity of the Doppler spectral recording. A high gradient is seen in the left panel while a lower gradient is seen in the right panel. If systolic pressures are the same in both individuals, the recording on the right would suggest higher pressure within the left atrium.

Figure 2.4 Schematic diagram of a mitral regurgitant jet recorded from the apex. Most regurgitant jets result in velocities that exceed 1.5 m/sec and require CW Doppler to record the full spectral velocity profile (left panel). PW Doppler recordings of mitral regurgitation are always aliased (right panel).

Figure 2.5 Left panel demonstrates that regurgitant jets may be directed in just about any direction; right panel shows that the area of the jets may also be widely different, from very small to very large. A complete PW Doppler examination requires tedious mapping throughout the image for detection of abnormal flow.

Figure 2.6 PW Doppler spectral recording of aortic insufficiency. Flow is toward the transducer and aliasing occurs (open arrow) with placement of the higher velocities at the bottom of the spectral tracing (closed arrow).

Figure 2.7 CW spectral velocity recording from the apex of the same patient as Figure 2.6. The full abnormal profile of aortic insufficiency is easily recorded toward the transducer (positive shift), (Scale marks – 1 m/sec).

Figure 2.8 Right ventricular angiogram in slight right anterior oblique view. With a catheter across the tricuspid valve, some degree of tricuspid regurgitation almost always results.

Figure 2.9 Idealized pressure relationships in aortic insufficiency. The left panel demonstrates the large gradient between aorta and left ventricle in mild aortic insufficiency. When aortic regurgitation is severe, central aortic pressure falls and ventricular diastolic pressure rises. This results in a small gradient and lower velocity by Doppler.

Figure 2.10 Normal spectral recording of left ventricular outflow using PW Doppler echocardiography. Systolic flow is away form the transducer and the velocity shift is negative. Some apparent "abnormalities" are usually recorded in diastole. (Scale marks=20cm/sec).

Figure 2.11 PW Doppler recording of aortic insufficiency with severe aliasing (Scale marks = 0.5 m/sec).

Figure 2.12 Aortic insufficiency as recorded from the ventricular apex using CW Doppler is represented as diastolic flow toward the transducer (Scale marks = 1 m/sec).

Figure 2.13 Changing CW spectral patterns encountered when mobbing the direction of the transducer (at the apex) from aortic outflow where aortic insufficiency (AI) is noted to mitral valve (MV) inflow. Note the mitral profile superimposed on the AI spectra. (Scale marks = 2 m/sec).

Figure 2.14 Similar spectral patterns of aortic insufficiency (open arrow) and mitral stenosis (closed arrow) occurring with slight movement of the Doppler beam. For details, see text. (Scale marks = 1 m/sec).

Figure 2.15 Regurgitation jets may move eccentrically during the cardiac cycle and cross the Doppler beam.

Figure 2.16 PW Doppler recording of changing patterns of an incompletely visualized aortic regurgitant jet that is encountered from slightly different angles from beat to beat (Range marks = 20 cm/sec).

Figure 2.17 CW spectral recording of aortic regurgitation from apex where the regurgitant jet moves in and out of the beam. (Scale marks = 2 m/sec)

Figure 2.18 Five panels showing differing appearances of aortic regurgitation from five slightly different positions near the apex using CW Doppler. The best spectral profile is right. (Scale marks = 1 m/sec)

Figure 2.19 CW spectral recording of aortic insufficiency showing measurement of end-diastolic pressure gradient (Scale marks = 1 m/sec)

Figure 2. 20 PW Doppler spectral analysis of mitral insufficiency with the sample volume located in the left atrium. The high velocities encountered produce aliasing. (Scale marks = 20 cm/sec)

Figure 2. 21 CW recording of typical mitral regurgitation from the apex. The jet is away from the transducer in systole and is usually symmetric in shape. (Scale marks = 2 m/sec)

Figure 2.22 CW spectral recording of typical mitral regurgitation. Note valve closing and opening spikes or clicks. (Scale marks = 1m/sec)

Figure 2.23 High velocity diastolic spikes (arrows) on the CW recording of mitral regurgitation made by vegetation movement. (Scale marks = 1m/sec)

Figure 2.24 Left panel: typical recording of aortic insufficiency and obstruction. Note how the aortic outflow tract turbulence resembles the symmetric profile of mitral insufficiency (arrow) with continuous beam angles through the mitral orifice. (Scale marks = 1m/sec)

Figure 2. 25 With a transducer located at the apex, both mitral regurgitation (MR) and aortic stenosis (AS) appear as systolic movement in a negative direction. Note that mitral systole is longer in duration than aortic. Aortic regurgitation (AR) is also present. (Scale marks = 2m/sec)

Figure 2. 26 A Doppler sample volume is large in the far field and, when placed in the left atrium in areas near the aortic root, may cause spurious evidence for mitral regurgitation.

Figure 2. 27 CW spectral recording from patient with "valve slap" (arrow) that may be wrongly interpreted as incomplete recording of mitral regurgitation.

Figure 2. 28 Varying appearances of mitral insufficiency with arrhythmias. A smaller profile follows the PVC (closed arrow) than the normal beat (open arrow). (Scale marks = 2m/sec

Figure 2.29 The jet of mitral regurgitation is incompletely recorded due to movement of the jet in and out of the beam. The best spectral profile is indicated (arrow). (Scale marks = 1m/sec)

Figure 2. 30 Typical CW spectral recording of tricuspid regurgitation from the apex. The peak velocity in the jet measures 2.4m/sec. (Scale marks = 1 m/sec)

Figure 2. 31 Varying configuration of tricuspid insufficiency with respiration. (Scale marks = 1m/sec)

Figure 2. 32 Idealized right atrial (RA) and right ventricular (RV) pressure relationships in tricuspid insufficiency. This demonstration is with similar right atrial pressures.

Figure 2. 33 The pressure within the right atrium also has an effect on the gradient between right atrium and ventricle. Thus, right atrial pressures must be estimated from the jugular veins for proper prediction of peak right ventricular systolic pressure.

Figure 2. 34 Marked elevation in right ventricular systolic pressure will result in high velocity tricuspid regurgitant jets (left panel) in comparison to lower right ventricular systolic pressures (right panel).

Figure 2. 35 Varying appearances of tricuspid regurgitation with atrial fibrillation. (Scale marks = 1 m/sec)

Figure 2. 36 Schematic diagram of CW beam direction for detection of tricuspid regurgitation (left). If angled a little too superiorly, the beam will actually intercept the aortic root (middle, right). Thus, aortic outflow may be a reason for false positive tricuspid regurgitation (arrow).

Figure 2. 37 Typical pulmonic insufficiency by CW Doppler. Pulmonic insufficiency may occasionally be differentiated from aortic by the presence of the "a" dip.

Figure 2. 38 A large flow mask is seen behind a Starr-Edwards prosthesis while only the area of flow making from a Carpentier-Edwards heterograft is seen behind the sewing ring.

Figure 2-A Composite photographs of six different prosthetic heart valves. A-Starr Edwards silastic ball valve; B-Starr-Edwards stellite ball valve; C-Bjork-Shiley tilting disk valve in the open position; D-St.Jude's rotating disk valve in the open position; E-Hall-Kastor tilting disk valve in the open position; Figure 2.-Carpentier-Edwards porcine heterograft valve. For details, see text.

Figure 2. 39 The various spectral recordings of the flow behind prosthetic valves using CW Doppler echocardiography. The control period of flow detection when no valves were in place are shown at either end (con). The letters correspond to the valves shown in Figure 2-A, page 28.

Figure 2. 40 Flow masking also occurs in vivo. The left panel demonstrates that most of the left atrium is obscured in the apical four-chamber view. When aortic and mitral valves are in place, almost all the left atrium is obscured from the parasternal approach (right panel).

Figure 2. 41 Jets have variable spatial dimensions. On the left is an aortic insufficiency jet that is wide in the apical two-chamber view. The same jet may be quite narrow in the apical four-chamber view.

Figure 2. 42 Various sample sites for mapping the severity of aortic regurgitation (circles). Left panel shows positive detection of regurgitation just below the aortic valve (closed circles). Right panel shows broader distribution compatible with more severe disease. Sampling near the mitral orifice will invariable detect mitral inflow (arrows).

Figure 2. 43 Schematic diagram showing the relative areas of turbulence for mild, moderate, and severe aortic regurgitation.

Figure 2. 44 Schematic diagrams showing many possible pulsed Doppler sample volume sites (circles). Left panel shows positive detection of mitral regurgitation just near the valve, consistent with mild disease (closed circles). Right panel shows wider distribution of positive sample sites compatible with more severe regurgitation. Sampling hear the aortic root (arrows) may bring interference from the ascending aorta.

Figure 2. 45 Schematic diagram showing the relative areas of turbulence for mild, moderate, and severe mitral regurgitation.

Figure 2. 46 The amplitude or intensity of a given signal is another method for judging the approximate severity of valvular regurgitation.

Figure 2. 47 Idealized pressure tracing in mild aortic insufficiency (left panel) and severe aortic insufficiency leaves a negligible end-diastolic gradient in comparison with mild regurgitation.

Figure 2. 48 CW Doppler spectral recording from two different patients, one with a high end-diastolic gradient and one with a very low end-diastolic gradient.

DOPPLER EVALUATION OF VALVULAR STENOSIS #3

Joseph A. Kisslo, MD
David B. Adams, RDCS

INTRODUCTION

One reason for the rapid growth in the use of Doppler echocardiography is its utility in detecting and assessing the severity of valvular stenosis. Detection of the presence of stenotic valvular heart disease using Doppler echocardiography was originally described over ten years ago. It has subsequently been demonstrated that Doppler blood velocity data could be used to estimate the severity of a stenotic lesion.

FORWARD BLOOD FLOW PROFILES

Aortic Valve Flow Velocity Profiles

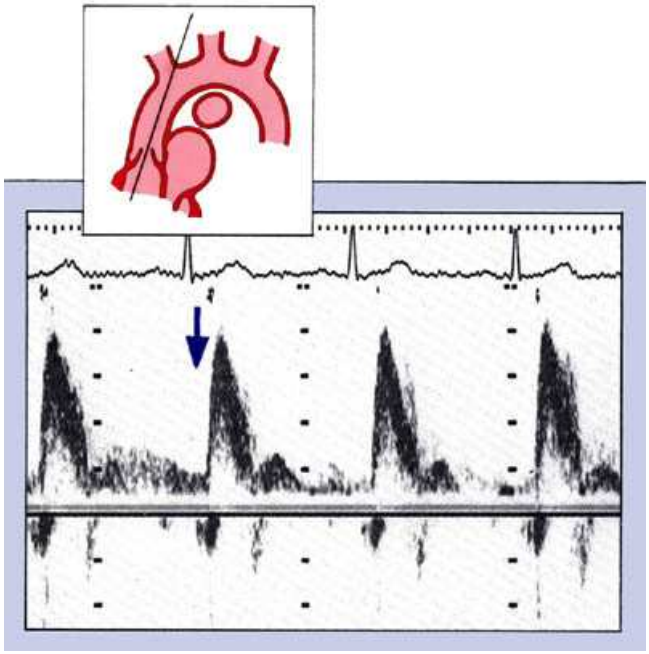

Figure 3. 1 CW Doppler recording of normal aortic systolic velocity taken from the suprasternal notch. Note that the onset of flow toward the transducer begins after the QRS complex of the electrocardiogram (arrow) and peaks in the first third of systole.

During systole, blood is ejected through the open aortic valve cusps. In normal individuals, the velocity rapidly rises to a peak somewhere in the first one-third of systole and then falls back to baseline during the remainder of this portion of the cardiac cycle. A normal flow velocity profile and its relationship to electrocardiographic events is shown in **Figure 3.1**. Note that the rise in velocity begins just after the QRS complex.

There are various indices, or measurements, that can be made from the spectral recording which help to characterize systolic functional characteristics. These are demonstrated in the idealized spectral velocity in **Figure 3.2**. These flow profiles are characterized by a peak velocity (in cm/s), the maximum velocity reached during systole. This measurement is easily obtained from the inspection of the spectral tracing. The time to reach peak velocity (or "time to peak") is another component of the systolic profile which helps to characterize systolic ejection and is measured in seconds. Left ventricular ejection time is the duration of the systolic flow velocity recording. These time durations are also easily measured directly from spectral recording.

The peak acceleration is a more complex measurement and usually requires the assistance of an automated, computerized device. It is found on the upstroke and is the maximum acceleration

expressed in centimeters per second. Likewise, measurement of the flow velocity integral usually requires computer assistance and is the area under the spectral flow velocity tracing.

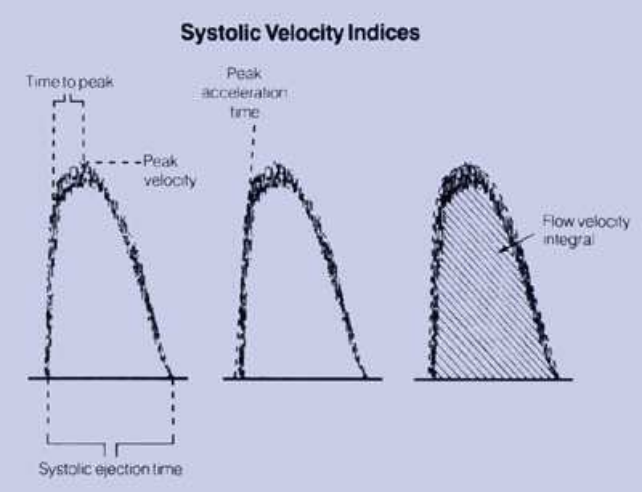

Figure 3. 2 Many systolic velocity indices may be calculated from the flow in the ascending aorta, as indicated in these idealized spectral recordings.

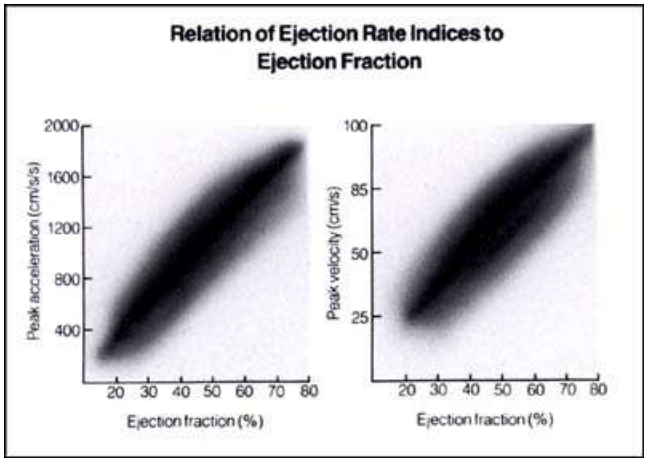

Figure 3. 3 The various ejection rate indices relate to left ventricular performance (ejection fraction).

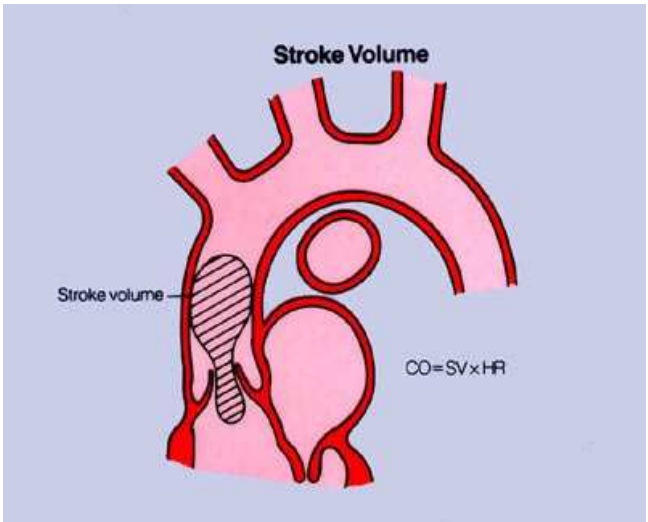

Figure 3. 4 Stroke volume is the volume of blood ejected from the left ventricle with each systole. Knowing stroke volume and heart rate provides a means for calculating cardiac output. Doppler may be used for calculating stroke volume. (CO =cardiac output; SV = stroke volume; HR=heart rate).

Ejection Rate Indices and Ventricular Function

Some of these indices relate directly to the systolic function of the left ventricle in patients with normal aortic valves. The better the left ventricular contraction the more rapid the acceleration, and the higher the peak velocity. Conversely, the poorer the left ventricular ejection (as seen in patients with low ejection fractions), the less rapid the acceleration of blood flow in the aorta and the lower the peak velocity. These approximate relationships are illustrated in the idealized graphs in **Figure 3.3**. Thus, rapid peak acceleration and high peak velocities characterize optimum ejection fractions.

Cardiac Output

Doppler echocardiography is useful for the determination of cardiac output; this is the volume of blood pumped by the left ventricle every minute and is expressed in liters per minute. The volume of blood ejected every systolic beat is called the stroke volume **(Fig. 3.4)** and is the basis for calculation of cardiac output according to the following equation:

Cardiac output = stroke volume x heart rate

Doppler calculation of cardiac output is based on the assumption that the aorta is a cylinder during every systolic beat. This cylindrical flow volume may be determined if its area and its length are known. The area is determined from the two-dimensional echocardiographic image while the length is derived from the Doppler spectral recording **(Fig. 3.5)**.

These relationships between area and flow velocity are shown schematically in **Figure 3.6**. Given identical volume of flow through a large cylinder **(Fig. 3.6, left panel)** and small cylinder **(right panel)**, the velocities recorded by Doppler will vary considerably. The same volume through the larger cylinder will render

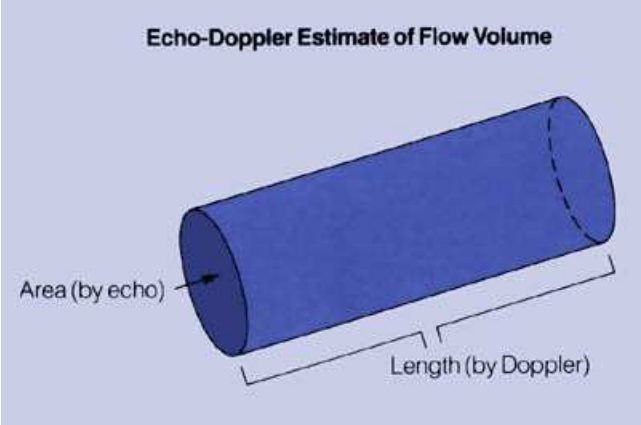

Figure 3. 5 Echo-Doppler estimates of flow volume are based upon a knowledge of the area of flow (from echocardiogram) and the length (from Doppler). It is assumed that the aorta is a cylinder.

a lower peak velocity (and small flow velocity integral) in comparison with the flow recorded through the smaller orifice. The flow velocity integral reflects the average velocity of the red cells during systole. Because the red cells are moving faster through the smaller cylinder, they travel farther. Thus, the Doppler recording of velocity relates to distance traveled.

Conceptually, derivation of cardiac output begins with the recognition that the volume of blood ejected every time the heart beats is first limited by the area of the aortic root (the area of the cylinder). While there remains some argument as to the precise point where this area is best determined from the two-dimensional echocardiographic image, most Doppler users measure the narrowest diameter in systole at the bases of the aortic valve cusps. This is most reliably accomplished using the parasternal long-axis view. Dividing the diameter in half then results in the radius of the open aortic valve. This area is assumed to be a circle and is determined by the standard plane geometric equation: area = r^2.

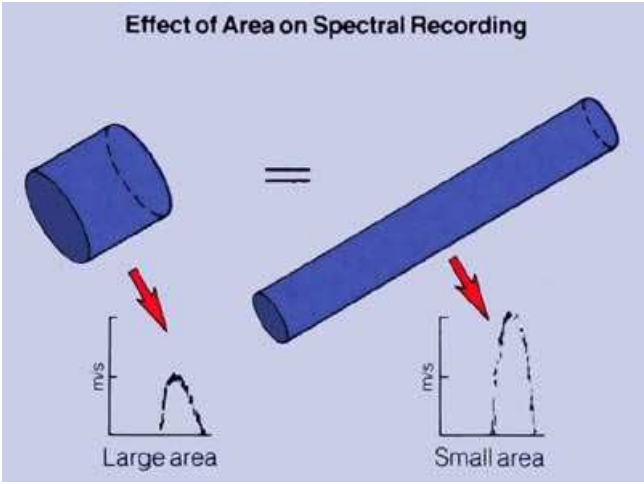

Figure 3. 6 When stroke volumes are equal and areas remarkably different, the resultant velocities of flow may be quite different. The velocity for large areas would be less than for small areas.

Secondly, the distance the ejected blood travels may be calculated from the Doppler spectral recording. Since this is a measure of velocity over time, the flow velocity integral will result in the average velocity during systole.

As a result of knowing the average velocity, his may be normalized for one second and is an index of how far the blood has traveled. The method for calculation of cardiac output is demonstrated in **Figure 3.7**.

It is important to recognize that for proper calculation of cardiac output using this approach the beam must be as parallel to flow as possible. Alterations of a few degrees from parallel will result in lower Doppler velocity recordings and underestimation of cardiac output. Therefore, aortic outflow is best obtained from the apical or suprasternal approaches where the beam is nearly parallel to normal flow.

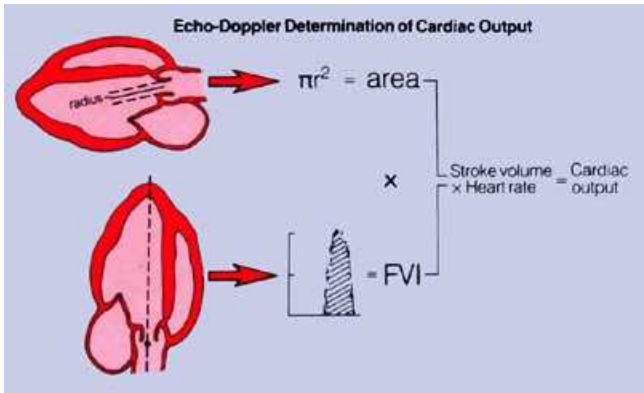

Figure 3. 7 Illustration of all the steps required for the calculation of cardiac output by Doppler.

It is also important to remember that the Doppler estimate of cardiac output is based on the square of the measured radius of the aorta. Any error in this measurement will be multiplied and may profoundly affect the resulting calculation.

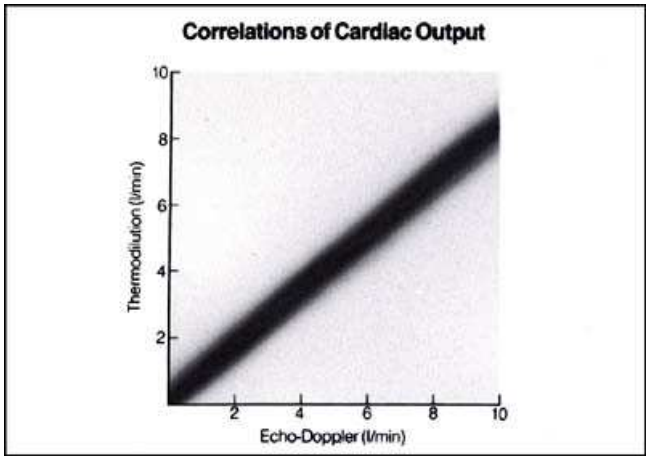

Figure 3. 8 Idealized representation of echo-Doppler calculations of cardiac output compared with that determined by thermodilution.

Doppler estimates of cardiac output compare quite favorably with those obtained by other methods. Comparisons have been made with cardiac output estimated by the Fick principle at catheterization, with thermodiultion, as well as with a host of other approaches. In general, these studies show very good correlations, being within $\pm$10% of the other method **(Fig. 3.8)**. Cardiac output may also be determined from flow and diameter measurements through any of the other cardiac valves.

Estimation of Pulmonary Arterial Pressures

Many methods have been proposed for the estimation of pulmonary arterial pressures. *Unit 2* discusses the method based on the presence of tricuspid regurgitation. Other methods are based on the time to peak velocity of the pulmonary arterial flow velocity recording. These methods only work when there is no evidence for pulmonary stenosis.

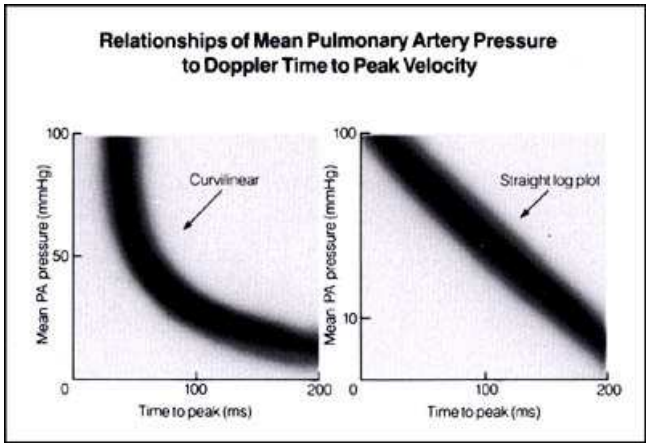

Figure 3. 9 Idealized comparisons of mean pulmonary artery (PA) pressure to time-to-peak velocity (left) and the logarithm of mean pulmonary artery pressure to peak velocity (right).

Methods for estimating pulmonary arterial pressures are based on alterations in the capacity of the pulmonary vasculature to accept forward systolic flow. In normal individuals without pulmonary hypertension, the pulmonary vasculature is a very low resistance circuit and has a great capacity to accept the sudden increase in volume. The vessels are quite distensible and as blood is ejected from the right ventricle the time to peak velocity and acceleration time are accordingly relatively slow.

In pulmonary hypertension, however, resistance rises as blood vessels thicken and become less distensible. This results in a diminished capacity to accept the forward systolic flow out of the right ventricle. The sudden rush of blood into the main pulmonary artery in this setting results in a more rapid time to peak velocity as well as a more rapid acceleration time.

These relationships are illustrated in **Figure 3.9**, where idealized plots of mean pulmonary artery pressure and time to peak velocity are shown. Note that these relationships are curvilinear, making estimates of very high, or very low mean pulmonary pressures difficult. To overcome this problem, several investigators have pointed out that plotting time to peak velocity against the logarithm of the mean pulmonary artery pressures makes the correlations much better.

The clinical application of this approach for estimation of mean pulmonary arterial pressure remains controversial and many methods have been proposed. Our purpose is to present the general concept of these relationships and the reader should consult current literature for more

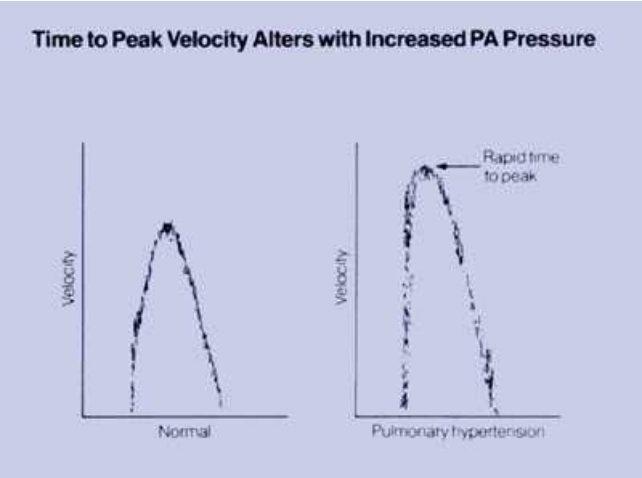

Figure 3. 10 Idealized spectral recordings demonstrating that time-to-peak velocity is very rapid in patients with pulmonary hypertension.

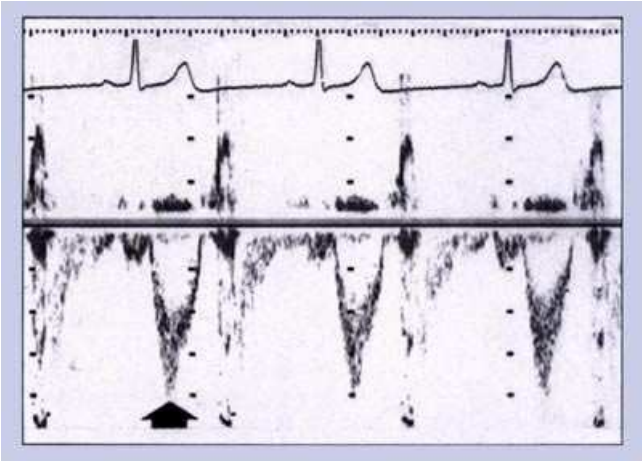

Figure 3. 11 PW Doppler spectral recording of aortic blood flow (arrow) taken from the apical window. Note the laminar appearance of normal flow. (Scale marks = 20 cm/s)

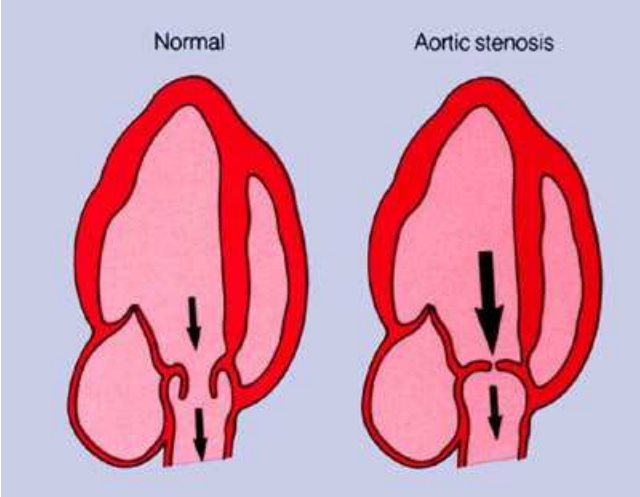

Figure 3. 12 Left panel – Without aortic valve obstruction, systolic pressures are almost the same in the ventricle and the aorta. Right panel – When significant aortic valve obstruction is present, left ventricular pressure rises much higher than aortic, and a systolic pressure gradient is present. The size of the arrows represents the magnitude of the pressures.

detailed descriptions of the continuing evolution of this principle. Many factors must be taken into account, an important one being heart rate. Adult patients with pulmonary hypertension may have normal heart rates of 60-70 beats/min, and infants and children >140 beats/min; this may significantly shorten measurements of time to peak velocity or acceleration times, and affect the reliability of these estimates of pressure.

What is most important is that time to peak velocity is significantly shortened in patients with pulmonary hypertension. **Figure 3.10** demonstrates both normal and rapid time to peak velocities in two idealized spectral recordings.

ESTIMATION OF THE SEVERITY OF VALVULAR STENOSIS

Effect of Stenosis on Blood Flow

The driving force for blood to move across any cardiac valve is the presence of a slight pressure difference normally found between the chambers (or chamber and great vessel) on either side of the valve. For example, systolic pressure builds within the left ventricle until it reaches a point where it exceeds the pressure in the aorta. The aortic valve is suddenly thrown open and blood is ejected into the aorta. In normal individuals, there is a very slight (1-2 mmHg) pressure difference between the left ventricle and aorta that helps drive the blood across the aortic valve.

Normal aortic valve blood flow is laminar **(Fig. 3.11)** and most of the red cells in the aortic root during systole are moving at approximately the same speed. Graphically, this translates into a narrow band of dark grey on the pulsed wave (PW) Doppler spectral recording **(Fig. 3 11, arrow)**. Normal peak systolic velocity of blood flow across the aortic valve rarely exceeds 1.5 m/s.

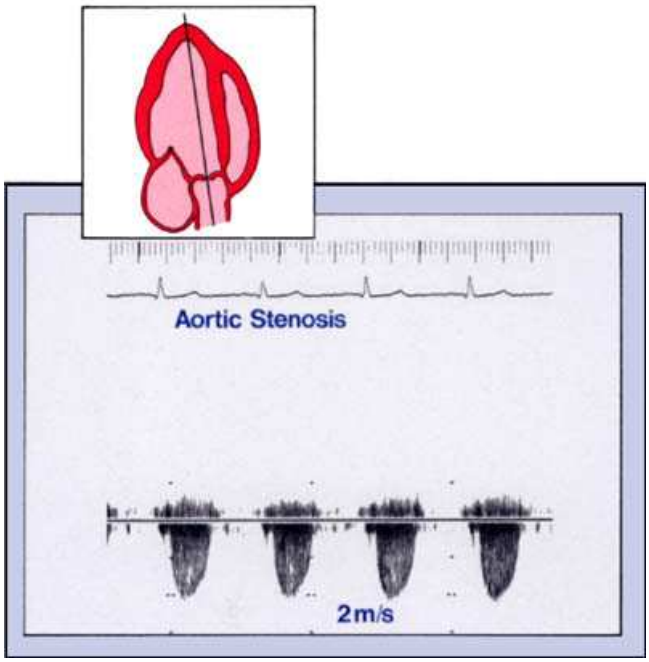

Figure 3. 13 CW spectral recording from the apex in a patient with aortic stenosis. The velocity spectrum is broadened and systolic velocity is increased to 4 m/s. (Scale marks = 2 m/s)

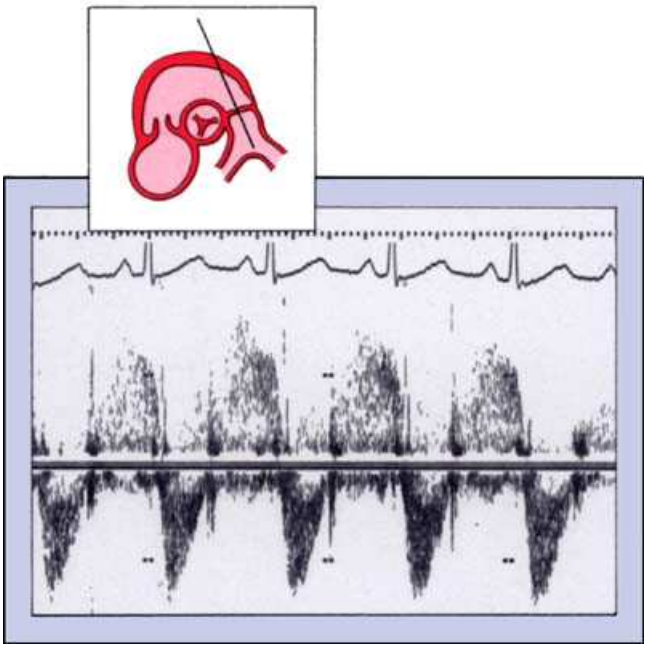

Figure 3. 14 CW Doppler spectral velocity recording of mild pulmonic stenosis and insufficiency. The abnormal diastolic flow toward the transducer of pulmonic insufficiency is easily recognized. (Scale marks = 1m/s)

When the aortic valve is diseased, the leaflets become thickened and progressively lose their mobility. Eventually, the valve itself becomes narrowed to the point where it begins to obstruct flow, and aortic stenosis is created. In the presence of aortic stenosis, systolic pressure in the ventricle must rise high enough to force the blood across the obstruction into the aorta. Thus, a pressure drop, or pressure gradient, is generated **(Fig. 3.12)**. Severe degrees of aortic stenosis may result in aortic valve gradients that exceed 100 mmHg in systole. As discussed in *Unit 1*, the presence of such an obstruction results in both turbulent flow and increased velocity, two characteristics readily detected by Doppler echocardiography. Because of the large gradient, the pressures within the left ventricle rise significantly and left ventricular hypertrophy results.

Doppler detection and evaluation of the presence or absence of aortic stenosis is based on recording turbulence and increased flow velocity in the ascending aorta. In **Figure 3.13** these characteristics are shown in a continuous wave (CW) spectral velocity recording of aortic systolic flow obtained from the apical window. Turbulent flow is represented by broadening of the velocity spectrum. There is also an increase in peak aortic velocity to 4 m/s. The Doppler audio in this case had a harsh, higher pitched quality during systole that was easily distinguished from the sound of laminar flow.

Similarly, the presence of these characteristics in the pulmonary artery during systole would indicate the presence of obstruction to right ventricular ejection. **Figure 3.14** demonstrates a CW Doppler spectral recording from the left parasternal window in a patient with mild pulmonic stenosis and insufficiency. Turbulent diastolic and systolic flows are noted with a slight increase in the peak systolic velocity to 1.4 m/s (normal <1 m/s).

The PW Doppler examination shown in **Figure 3.15** is from the same patient as **Figure 3.1** and demonstrates the ability of PW to localize the level of the obstruction. With the cursor positioned on the ventricular side of the pulmonic valve **(Fig. 3.15, A)**, the turbulent diastolic spectral recording of pulmonic insufficiency is noted, while systolic flow is undisturbed (laminar) with a peak systolic velocity of about 1 m/s. When the sample volume is positioned distal to the diseased pulmonic valve **(Fig. 3.15, B)** the systolic flow becomes

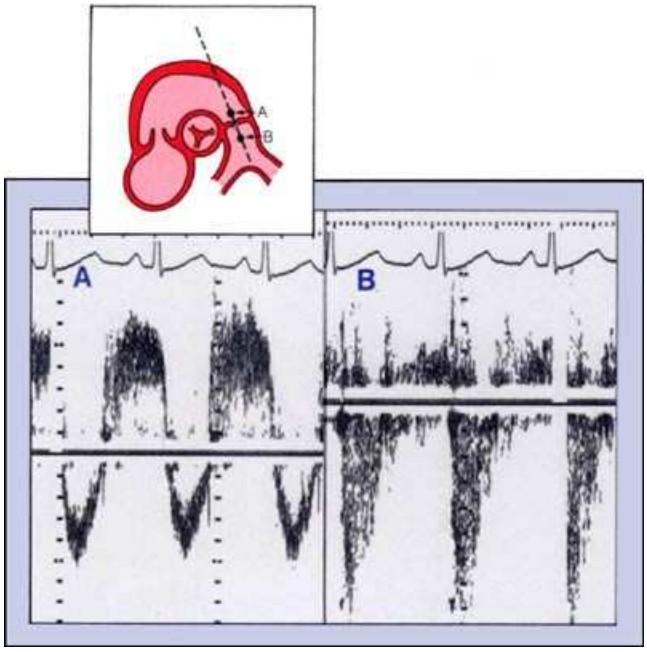

Figure 3. 15 PW Doppler spectral recording from the same patient as Figure 3.24. At position A, pulmonic insufficiency is noted. At position B, on the distal side of the valve, the systolic velocity is elevated. (Scale marks = 20cm/s)

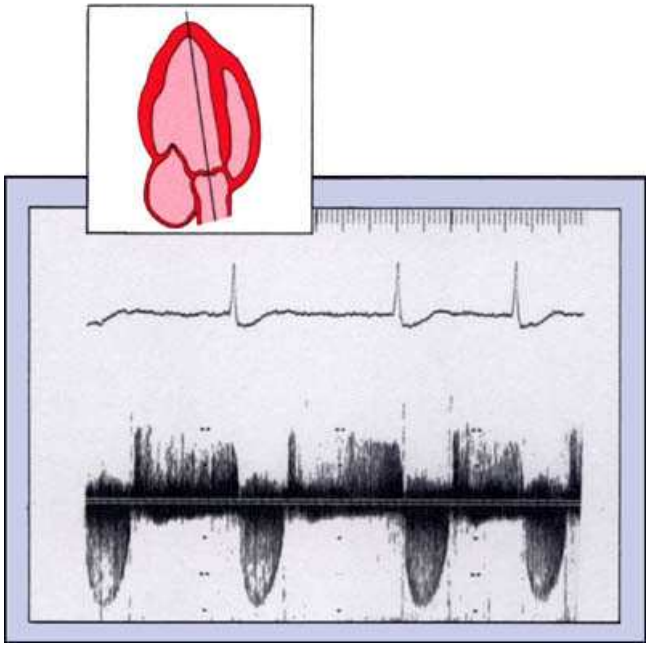

Figure 3. 16 Typical CW spectral velocity tracing from the apex in a patient with aortic stenosis and insufficiency. Peak systolic velocity is elevated to almost 6 m/s and peaking is delayed. (Scale marks = 2 m/s)

turbulent and the peak systolic velocity is elevated. The spectral recording of pulmonic insufficiency is lost because the sample volume is located distal to this lesion.

While PW Doppler is very useful for the localization of such obstructive lesions, it has limited value in establishing the severity of obstruction because most significant valvular obstructions result in velocities above 1.5 m/s. As emphasized previously, velocities above 1.5 m/s will usually cause aliasing of the PW recording. This prevents the faithful recording of peak velocities necessary for the calculation of valve gradients.

Estimation of the Severity of Stenosis

Use of Doppler ultrasound to estimated the severity of a valve stenosis is based principally on the fact that such obstructions result in an increase in the velocity of flow. In clinically significant mitral stenosis, the diastolic velocity of mitral flow usually exceeds 1.7 m/s. Systolic velocity of aortic flow in clinically significant aortic stenosis may reach 5-6 m/s **(Fig. 3.16)**. Thus, CW Doppler is required for the detection of these increased velocities and for recording the full spectral profiles.

We have already noted that there is a relationship between the pressure increase (or gradient) across a valve and the velocity of blood flow across the valve. For any given pressure gradient there is a corresponding increase in velocity, as predicted by the simplified Bernoulli equation:

$$p_1\text{-}p_2 = 4V^2$$

where p_1 = pressure distal to obstruction p_2 = peak velocity of blood flow across the obstruction.

As the stenosis becomes more severe, the valve orifice area will become smaller, and the velocity of flow across the orifice will increase as a function of the increased pressure gradient. Thus, by measuring the peak velocity in a systolic aortic jet with Doppler echocardiography, it is possible to estimate the pressure gradient that produced it using the above simple algebraic expression. The peak aortic velocity of the spectral recording in **Figure 3.16** is approximately 5.8 m/s. Using the previous formula

$$p_1\text{-}p = 4(5.8)^2$$

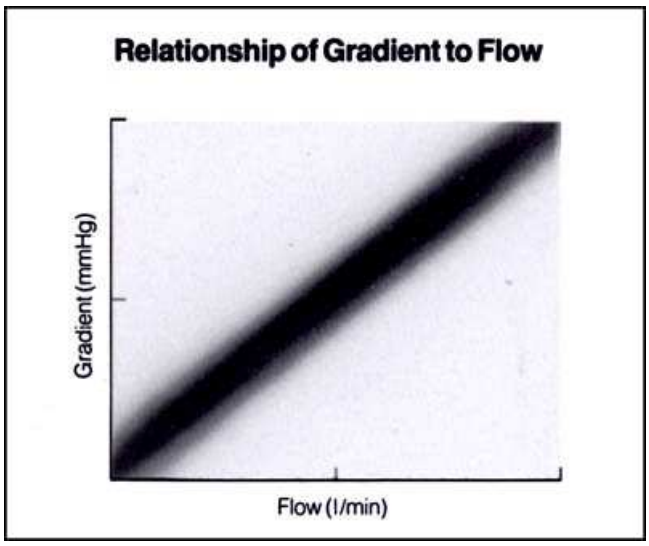

Figure 3. 17 Idealized relationship between pressure gradient and flow. As flow increases, the gradient will also rise even though the valve area is fixed

the pressure gradient is therefore 135 mmHg.

There are, however, three major technical requirements that must be satisfied if Doppler is to be used for this purpose. First, an adequate "window" into the chest for ultrasound propagation and reception must be found so that well formed Doppler profiles can be recorded. Second, as emphasized in *Units 1* and *2*, for the velocity measurement to be accurate, this window must allow orientation of the ultrasound beam so that it is as parallel as possible to flow through the valve. Third, the high velocities present in the disturbed jet often exceed the Nyquist limit of PW Doppler, so that CW or high pulse repetition frequency Doppler must be used.

Expressing the Severity of Stenosis

It should be recognized that knowledge of the gradient across a stenotic valve does not provide all the information necessary to assess the severity of obstruction. The gradient will vary with flow across the stenotic valve orifice and will increase in high flow situations and decrease in low flow situations. Thus, a patient with a fixed valve area will have a higher gradient during exercise when cardiac output is increased, than at rest when cardiac output is lower. **Figure 3.17** shows the idealized relationship of valve gradient to flow. As flow across a valve rises, as with rapid tachycardia, the gradients will vary.

Valve orifice size is generally considered not to vary with the amount of flow across the valve and is, therefore, a preferred expression of the severity of a given stenosis. The following discussion will begin with estimates of gradients across stenotic valves and then review some of the simplified methods for estimating valve orifice area.

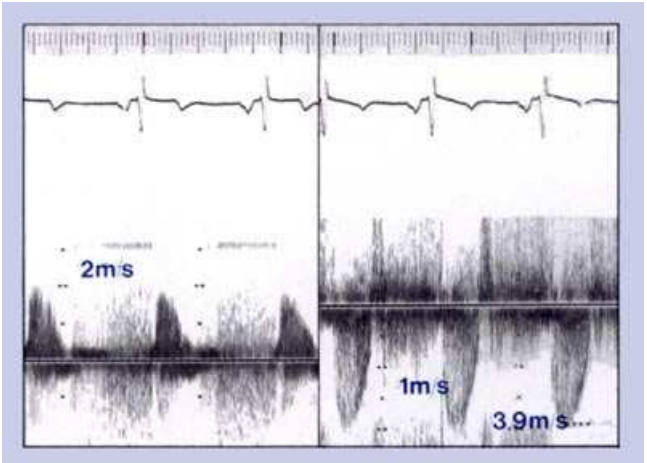

Figure 3. 18 CW Doppler spectral recording of aortic outflow from the suprasternal notch with flow toward the transducer (left) and apex with flow away form the transducer (right). The spectral recording from the apex is better formed than the one from the suprasternal notch.

Finding the Stenotic Jet

The most common windows utilized for recording peak aortic systolic velocity are the apical, suprasternal, and right parasternal. While stenotic jets, like regurgitant jets, are often directed eccentrically, it is usually possible to find a fully formed aortic systolic profile from one of these windows. A comprehensive Doppler examination for aortic stenosis requires that the ascending aorta be examined from all possible windows in order to align the beam parallel to the jet. **Figure 3.18** shows a CW examination of a patient with aortic stenosis from the suprasternal notch **(left panel)** and the apex **(right panel)**. The spectral tracing from the apical window is

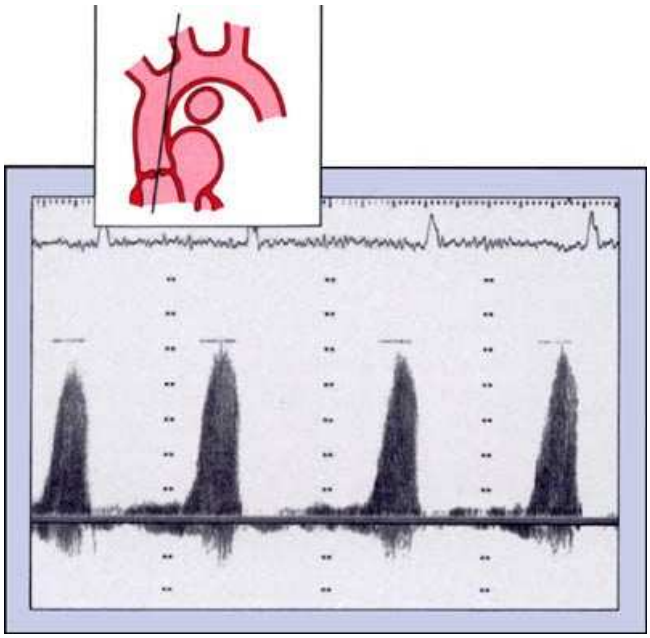

Figure 3. 19 Typical aortic systolic velocity recording from the suprasternal notch in a patient with aortic stenosis. Note that the peak velocity is almost 5 m/s. As gradient increases, so does the peak systolic velocity. (Scale marks = 1m/s)

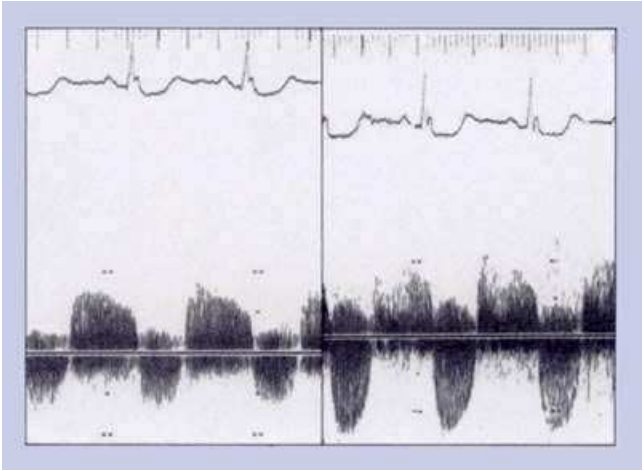

Figure 3. 20 Operator skill is important in obtaining an adequate systolic aortic jet profile in aortic stenosis. This figure shows a recording made by a less experienced operator (left panel) compared with one from a more experienced operator (right panel).

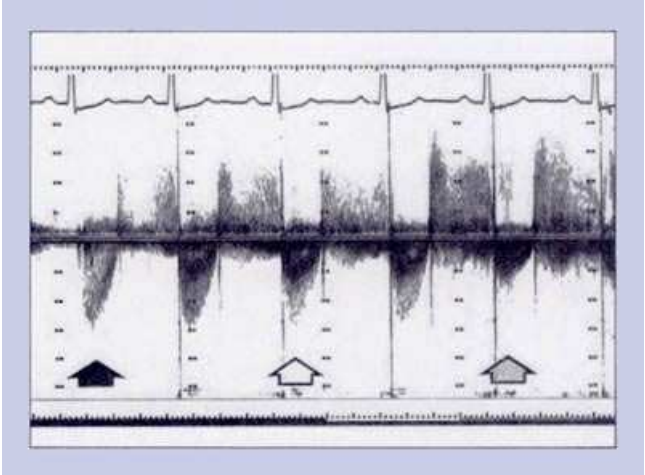

Figure 3. 21 The systolic jet of aortic stenosis and diastolic jet of aortic insufficiency often cannot be recorded at the same time. As the transducer beam is angled from the stenotic jet (closed arrow) to intercept the aortic insufficiency, the left ventricular outflow tact velocity is encountered (stippled arrow). Both outflow tract velocities are superimposed during the beam sweep (open arrow). (Scale marks = 1 m/s)

superior as judged by the presence of a fully formed profile with a discrete ascent, peak, and descent. While we have found the apical window to be most productive, we always examine the aorta from every possible view. Occasionally, the suprasternal window will be perfectly aligned to flow and will present the typical spectral profile of aortic stenosis. This is demonstrated in a patient with severe aortic stenosis in **Figure 3.19**. In this condition, there is marked spectral broadening, delayed systolic peaking, and a marked increase in velocity. In this patient, the peak systolic velocity is almost 5 m/s (100mmHg).

Considerable operator skill is required to obtain adequate spectral tracings for measurement of peak velocity. It is our experience that the Doppler examination for aortic stenosis will add an average of 15-30 minutes to the two-dimensional and routine Doppler echocardiographic examination, even with the experienced operator.

In **Figure 3.20 (left panel)** there is a recording from the apical window obtained by an operator with only modest experience. Both aortic stenosis and aortic insufficiency are recorded, but the systolic flow away form the transducer fails to show a fully formed profile. The spectral recording in **Figure 3.20 (right panel)** was performed by a more experienced individual, and the fully formed systolic profile is seen. Had a measurement been made on the upper panel, peak systolic velocity would have been approximately 2.8 m/s, while the true velocity shown on the panel below is 5 m/s. Use of the inadequate tracing would have severely underestimated the valve gradient.

Most experienced Doppler operators can obtain aortic systolic velocity profiles adequate for measurement of peak velocity in about 95% of patients. **Figure 3.21** demonstrates combined aortic stenosis and insufficiency by CW Doppler from the apex of the left ventricle.

Note that at the left, the full profile of the aortic stenotic jet is encountered. With minimum transducer angulation, the aortic insufficiency

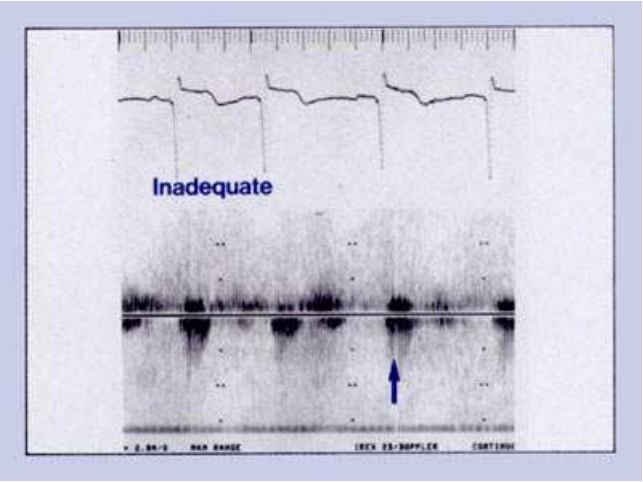

Figure 3. 22 Inadequate recordings of aortic systolic velocity do occur and should not be used for estimation of gradient. Note that the profile is poorly formed on the upstroke, peak (arrow), and down stroke. (Scale marks = 2 m/s)

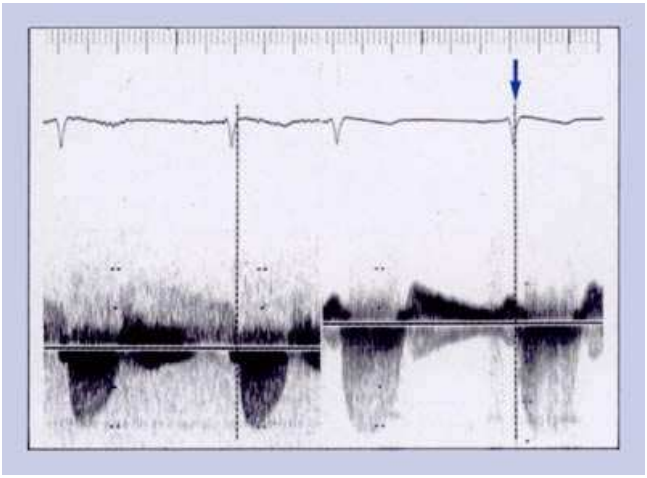

Figure 3. 23 Aortic stenosis (left) should not be mistaken for mitral insufficiency (right). Mitral systole begins before aortic (arrow) and is longer in duration. (Scale marks = 2m/s)

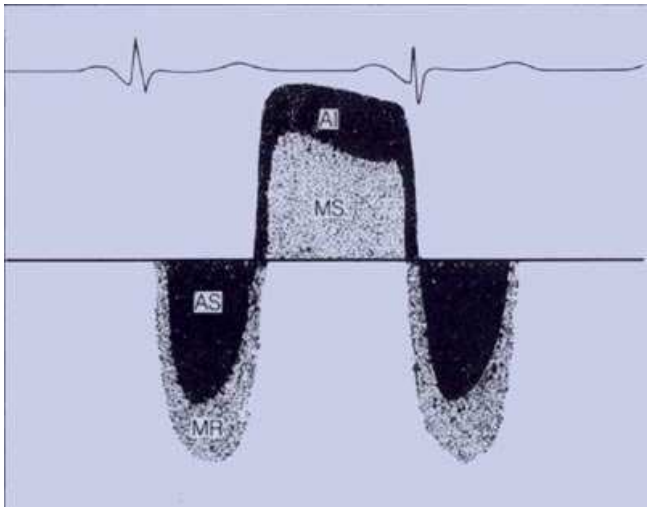

Figure 3. 24 Relationship between abnormal systolic and diastolic flows through the left heart valves. For details, see text.

profile is readily encountered. At the far right, the systolic flow away from the transducer is lower in velocity and represents the velocity in the left ventricular outflow tract before the obstruction. The lower velocity proximal to the stenotic valve should not be confused with aortic stenosis.

Occasionally, only incompletely formed profiles are recorded. These should be considered inadequate and never used for estimation of gradient. An incompletely formed profile from an older patient is shown in **Figure 3.22**.

Another potential source for error is mistakenly interpreting the profile of mitral insufficiency for that of aortic stenosis. When recorded from the apical window, both occur in systole and are displayed as downward spectral velocity shifts. This is seen in the spectral tracings shown in **Figure 3.23**. These may be differentiated by remembering that the onset of ventricular systole and mitral regurgitation **(3.23 arrow)** occurs prior to aortic valve opening. In addition, mitral regurgitation is longer in duration.

At first, it may appear that the spectral profiles of aortic stenosis resemble mitral insufficiency and those of aortic insufficiency resemble mitral stenosis. These disease profiles may be differentiated by a knowledge of the various timing relationships of left-sided valvular opening and closing. **Figure 3.24** shows the relationships between these various abnormal spectral velocities. The duration of mitral insufficiency is generally longer than that of aortic stenosis, partly because the time from mitral valve closing to opening is longer than for aortic valve opening to closing. Similarly, the duration of aortic insufficiency is longer than mitral stenosis because the time from aortic valve closing to opening is longer than for mitral valve opening to closing. Similar relationships are true of the pulmonic and tricuspid valve on the right side of the heart. Those experienced in phonocardiography will realize the advantage of using this technique to assist in the identification of the various valve profiles.

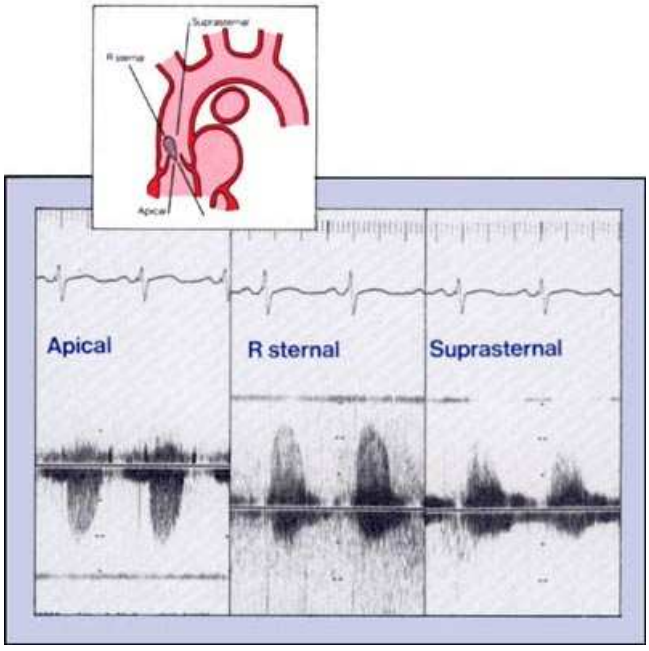

Figure 3. 25 Left panel shows an aortic stenotic jet in relation to possible viewing directions using CW Doppler. Right panel shows spectral velocity tracings from each respective window. The best recording is from the right sternal window. (Calibration marks = 2m/s)

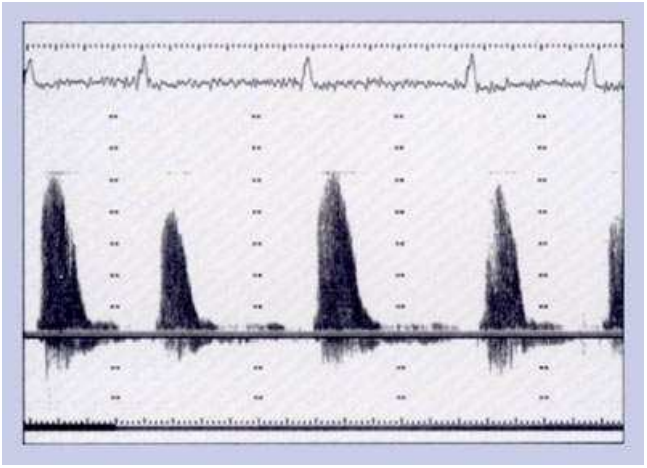

Figure 3. 26 CW spectral velocity recording from the suprasternal window into the ascending aorta from a patient with severe stenosis. Note the varying peak velocities with varying R-R interval of the ECG. (Calibration marks = 1 m/s).

In patients with aortic valve disease and stenosis, a careful examination must be performed from all possible views as the abnormal jet may be directed anywhere in the aorta. In these cases, we are most interested in recording the highest peak systolic velocity present. As previously pointed out, the most faithful representation of flow will be obtained when the beam is parallel. The use of multiple positions for the recording of peak systolic aortic velocity is very important in aortic stenosis since this jet may be directed in a wide variety of orientations. This is especially true in older patients with acquired aortic stenosis. **Figure 3.25** demonstrates one such direction of flow and its relationship to various transducer positions for CW Doppler recording. In this case, peak flow was best recorded by CW Doppler from the right parasternal approach, rather than from the suprasternal notch. The velocity profile from the apex seems adequate but is slightly lower than the right sternal recording. The recording from the suprasternal notch is grossly inadequate and lacks a fully formed profile. When examining for aortic stenosis, all available acoustic windows should be utilized.

There will be times when the changing appearance of the spectral trace is not the result of an improper beam direction or misadjustment of system controls. **Figure 3.26** shows a CW recording from the suprasternal notch with the beam directed toward the ascending aorta. The differing appearances of the velocity profiles are a result of an irregular heart rate which leads to beat-to-beat changes in stroke volume and, consequently, aortic gradient. Stenotic jets, like regurgitant jets, readily change their configuration with cardiac rhythms.

Aortic Valve Gradient at Catheterization

Estimation of transvalvular aortic gradients in patients with aortic stenosis using Doppler has been in common use for some time. There is an abundance of papers in the literature discussing the relative merits and limitations of this approach. All are based upon correlations with pressure measurements obtained at catheterization.

In **Figure 3.27** three possible methods are shown for calculating pressure gradients across the aortic valve at catheterization. All depend upon the recording of pressure from the left ventricle and aorta, or some peripheral artery. If a peripheral artery is used, it takes time for the systolic pulse to

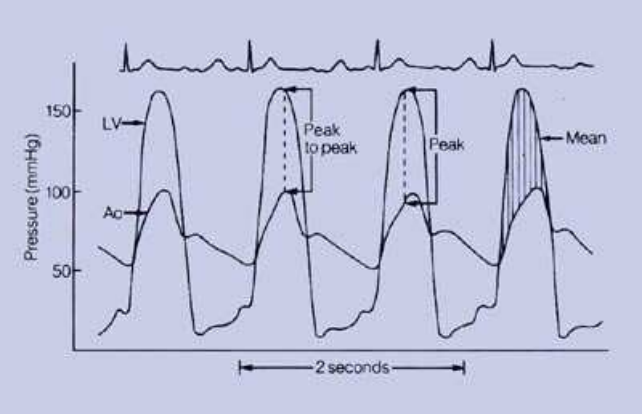

Figure 3. 27 Schematic representation of simultaneous left ventricular (LV) and aortic (Ao) pressure recordings obtained at catheterization with representation of different gradient measurement methods.

be conducted into the aorta and there is usually a short delay in the upstroke of the aortic pulse when compared with that of the ventricle. This requires the individual measuring these pressures to trace the aortic pulse and move it slightly backwards in time to adjust for the time delay. A peak to peak gradient is measured from the peak of the left ventricular pressure recording to the peak of the aortic. Peak gradient is measured as the largest difference between the two and occurs somewhere on the ascending pressure tracings. Mean gradient is estimated by summing the gradients measured at sequential time intervals during systole and dividing by the number of measurements made.

Appreciation of these various invasive methods for calculation of the aortic valve gradient is very important for a critical interpretation of the Doppler literature on aortic stenosis. Almost all catheterization laboratories report peak to peak and mean gradients since both are readily performed. Accurate measurement of peak gradient, however, is more difficult and requires precise alignment of ventricular and aortic pressures in time, and careful searching for the peak, or largest, instantaneous gradient.

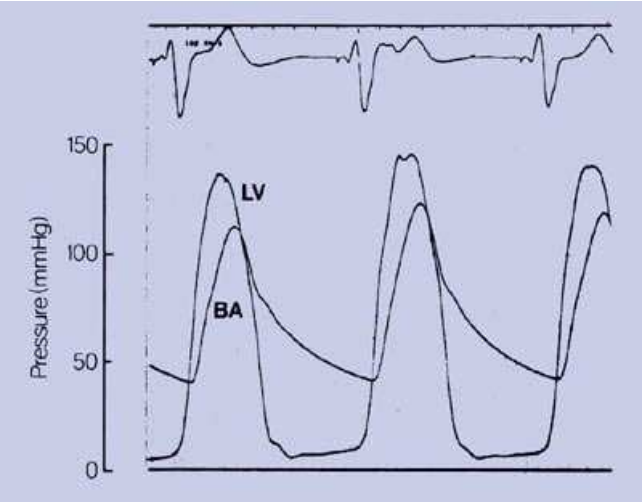

Figure 3. 28 Pressure recordings from the left ventricle (LV) and brachial artery (BA) from a patient with aortic stenosis. Note the delay in the upstroke of the brachial arterial pressure tracing and the delay in onset of the brachial pressure tracing when compared with that from the ventricle.

Actual left ventricular and brachial arterial pressure tracings from a patient with aortic stenosis are shown in **Figure 3.28**. Note that the rate of rise of the left ventricular pressure is much more rapid than that of the brachial artery. Note also that there is a time delay in the onset of rise of the brachial artery. Note also that there is a time delay in the onset of rise of the brachial arterial pulse. This results because of the time required for the bolus of ejected blood to transit the aortic valve and aorta to the brachial artery. For proper measurement of peak gradient the brachial pulse must be "set back" to correspond to the rise of the left ventricular pressure tracing.

With the fluid-filled catheters commonly used, rapid changes in pressure, such as occur with ventricular ejection, occasionally create overshoot artifacts on the pressure recording. Peak gradients are often not reported from catheterization data, in part because of these artifacts and timing delays which can create large measurement errors.

Doppler Estimation of Gradient in Aortic Stenosis

It is most important to remember that the peak gradient is usually higher than the peak-to-peak or mean gradients. The spectral recordings resulting from Doppler interrogations of aortic stenosis reflect the highest gradients within the jet. This is frequently referred to as "peak instantaneous gradient". Doppler estimates of the aortic peak gradient calculated using the simplified Bernoullis

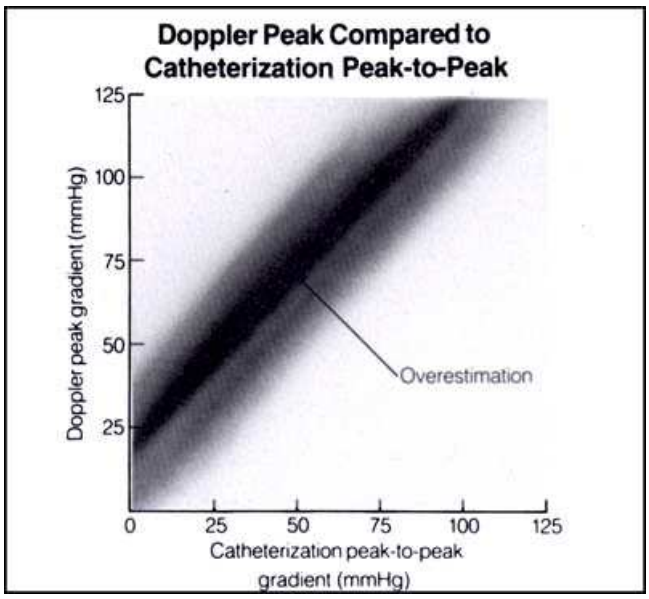

Figure 3. 29 Idealized relationship between Doppler peak gradient and catheterization peak-to-peak gradient. Comparisons show that there is overestimation of catheterization peak-to-peak gradient.

formula generally overestimate severity when compared with catheterization peak-to-peak gradients. Accordingly, Doppler estimates of severity would be expected to correlate best with the peak gradient at catheterization.

In an attempt to evaluate the use of Doppler echocardiography in clinical practice, we studied sixty consecutive patients who were referred to the catheterization laboratory with clinical findings suggestive of possible aortic stenosis (aortic systolic murmur and peripheral pulse deficit). All patients underwent cardiac catheterization at a time remote from the Doppler study (usually after 24 hours). The Doppler examination and interpretation was performed without knowledge of the results of catheterization. Our patients were older than many of the groups reported from other centers (mean age 63 years), as one might anticipate in routine clinical practice, and 45% had a 2+ or greater aortic insufficiency.

As can be seen in **Figure 3.29**, Doppler over-estimation of catheterization peak-to-peak gradient in our series was sometimes quite significant. Indeed, overestimations are evident over the entire spectrum of gradient values and vary in magnitude between 1 and 53mmHg. In our view, this finding suggests that the clinician must be very careful in using catheterization laboratory criteria for estimating the severity of an aortic gradient with Doppler peak aortic gradient valves.

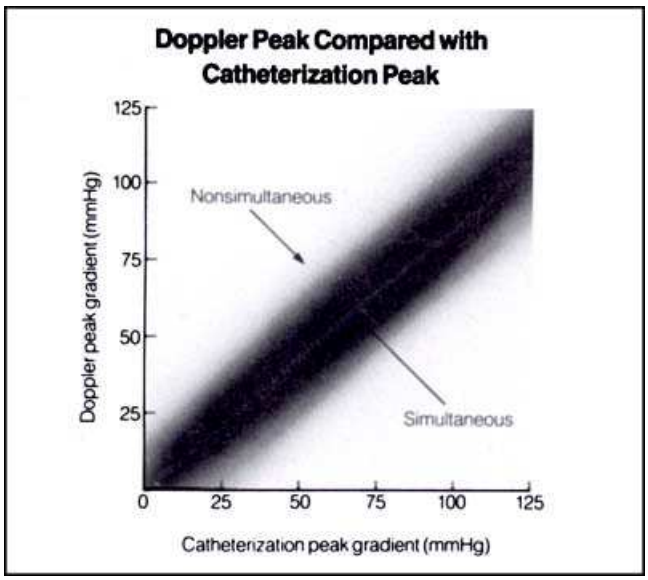

Figure 3. 30 Idealized relationship between Doppler peak gradient and catheterization peak gradient. Since Doppler reflects peak catheterization gradient, the comparisons are more favorable.

Doppler and catheterization estimates are more comparable when both laboratories report the peak aortic valve gradient **(Fig. 3.30)**. The scatter of our data is obviously great because the studies were not performed simultaneously with catheterization. Altered hemodynamic states with different volumes of blood flow across the aortic valve could easily account for the differences between catheterization and Doppler gradients in nonsimultaneous studies. When Doppler data are collected simultaneously with catheterization, using micromanometer-tipped catheters, the correlations are much better.

In routine clinical practice, Doppler estimates of the severity of aortic stenosis are likely to be made at least 24 hours before catheterization. These Doppler measurements may find a role in selecting patients for invasive study. Eventually, they may be used to refer some patients to surgery without prior catheterization.

It is encouraging that even though comparative data were collected at different times in our study, peak gradients correlated favorably. In our experience, if heart rates vary more than 20 beats/min between the two studies, agreement between them will be reduced (due to differences in blood flow across the valve). Therefore, heart rate serves as one convenient index for assessing the similarity between hemodynamic states, when Doppler and catheterization comparison studies are performed at remote times.

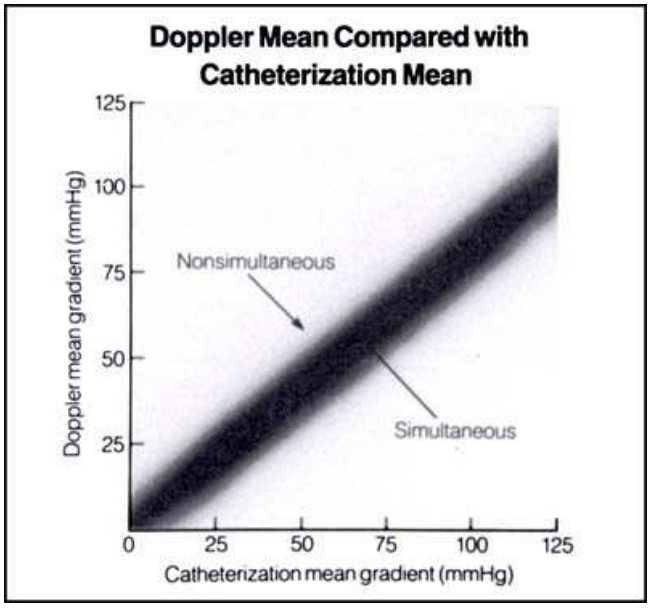

Figure 3. 31 Idealized relationship between Doppler mean gradient and catheterization mean gradient. Mean gradient comparisons are favorable because they average data over time.

There are some limitations inherent in using Doppler peak aortic gradient estimates. Few catheterization laboratories report peak gradient data, and a suitable frame of reference to judge severity of stenosis (as exists for peak-to-peak gradients) is not available. Clinicians have commonly used peak-to-peak gradients in excess of 50mmHg to identify severe aortic stenosis. There is no corresponding figure for peak gradients in current use.

The comparison of mean Doppler gradient with mean catheterization gradient also shows good overall agreement **(Fig. 3.31)**. Mean gradients may be less sensitive to individual measurement errors since they reflect an average of multiple measurements. The calculation of mean Doppler gradient also has the advantage that such gradients are available from most catheterization laboratories and are familiar to most clinicians. When Doppler and catheterization measurements are collected simultaneously, the correlations are even better because of these factors.

Understanding the details of these various gradient comparisons is important for the beginner to Doppler echocardiography. We have seen a conflict of opinion develop between the echocardiography and catheterization laboratories when there is not a mutual understanding of the capabilities and limitations of both techniques. Despite these cautions, we do believe that Doppler comparison with catheterization data acquired with pressure transducer-tipped catheters are most satisfactory when obtained simultaneously.

Other Aspects of Aortic Stenosis

We occasionally encountered patients with a small gradient predicted by Doppler but with no gradient at catheterization. In most instances, heart rates were nearly identical at the time of Doppler and catheterization, making it unlikely that differences in hemodynamic status were responsible for the discrepancies. However, it is noteworthy that all of these patients had high cardiac outputs and, in most, significant aortic regurgitation was present. It is possible that the use of the simplified Bernoulli equation in such patients may be at least partly responsible for the overestimates. The full Bernoulli equation takes into account blood velocity on both sides of the valve, whereas the simplified form only uses peak velocity after the flow crosses the valve.

In **Figure 3.32** the velocity of flow on the ventricular side of the valve (V_1) is simultaneous with flow in the aortic side (V_2) using CW Doppler from the apical approach. Patients with hyperdynamic circulatory states, such as those with aortic regurgitation, may have a significant velocity component below the aortic valve. We have also encountered a few patients with very

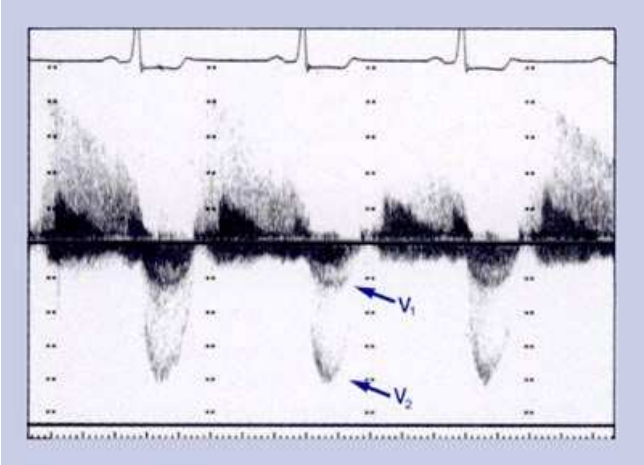

Figure 3. 32 Velocity below the valve (V_1) is not recorded as often as velocity on the aortic side (V_2). V_1 is ignored in the simplified Bernoulli equation. (Scale marks = 1m/s)

severe systemic hypertension (with high peripheral resistance) and high cardiac outputs where Doppler peak systolic velocities approached 5 m/s. In each, no gradient was found at catheterization.

Failure to take these experiences into account may lead the Doppler operator to attribute the elevated aortic velocity to an obstruction of the outflow tract, even in patients with pure aortic regurgitation or other reasons for the increased systolic velocities. In our series, the effect of aortic insufficiency was most evident when there was a minimal or no aortic valve gradient. It seemed to be less important in patients with combined stenosis and insufficiency.

Several observations may be helpful in recognizing such overestimated gradients. In patients with increased systolic velocities due to aortic insufficiency, early peaking of the aortic velocity profile suggests an insignificant gradient. In addition, patients whose aortic valve cusps open to the periphery of the root, on echocardiography will rarely, if ever, have significant aortic gradients at catheterization. Indeed, full mobility of the aortic valve cusps frequently indicates caution against assuming that an increased velocity is due to aortic stenosis. It may be best to use PW Doppler echocardiography with the sample volume located just before the aortic valve orifice to verify that V_1 is within the range of normal. If high velocities are encountered at this level, caution should be exercised and if V_1 is high it must be taken into account.

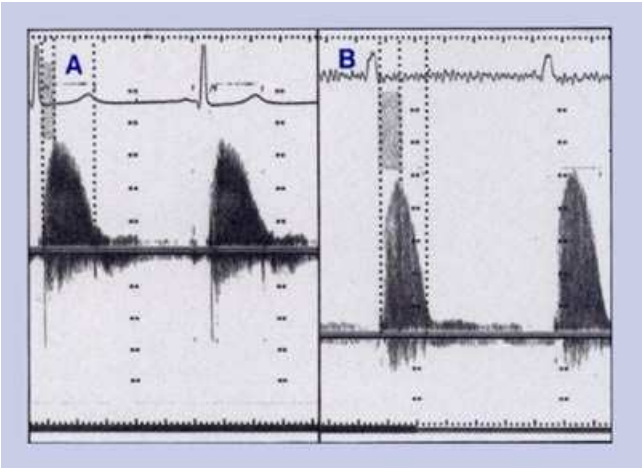

Figure 3. 33 The severity of aortic stenosis may also be judged by the relative proportion of total systolic time taken to reach peak velocity (stippled areas). Both time to peak and peak velocity are lower in panel A than in panel B. ((Scale marks = 1m/s)

Other Estimates of Severity of Aortic Stenosis

Alternative methods are available for estimating the severity of aortic stenosis. One method uses the time to peak velocity in systole and examples are illustrated in **Figure 3.33**. **Panel A** shows a patient with less severe stenosis and a shorter relative time to peak than the patient in the **panel B**. A value of 0.50 or greater has been found to correlate with moderate-to-severe obstruction. The method is most accurate when clear evidence of aortic valve opening and closing is seen on the Doppler recording. If these are not evident, a phonocardiogram or Doppler signal amplitude tracing must be used to indicate the boundaries of the systolic ejection period.

One of the most promising methods makes use of the principle of the continuity of flow and may be used to estimate aortic valve area. The principle is simple: forward volume flow on the ventricular side of the valve is the same as forward flow on the aortic side. Whether or not an obstruction is present, these two flows are always equal

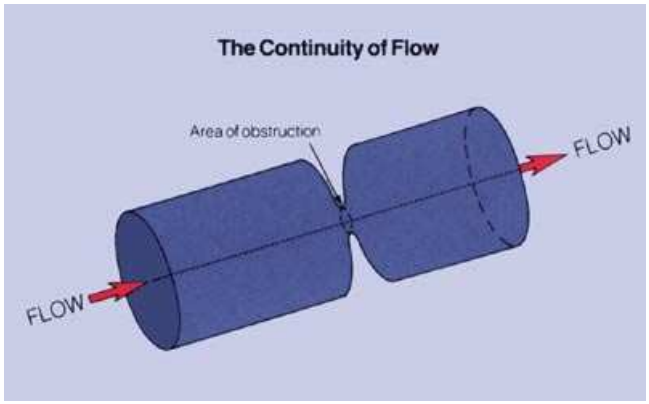

Figure 3. 34 Continuity of forward flow. Flow that enters a cylinder is equal to the flow passing through an obstruction and exiting from the distal side.

(Fig. 3.34). Flow must first pass through a larger area (with low velocity) before entering the obstruction where the velocity will increase. Thus, there must always be a continuity of flow.

During the previous discussion of cardiac output calculation, it was shown that volume flow could be estimated from knowing the area of the aortic valve orifice and the flow velocity integral that crosses it in systole. This knowledge sets up the simple algebraic equation, shown in **Figure 3.35**, in which we want to find the aortic valve area (A_2).

In aortic stenosis, systolic flow first passes through the left ventricular outflow tract at one velocity (V_1) and then is rapidly accelerated to a higher velocity (V_2) through the narrowed area of the stenotic orifice. Both V_1 using PW Doppler in the left ventricular outflow tract) and V_2 (using CW Doppler) can be determined. Both are usually obtained from the apical window.

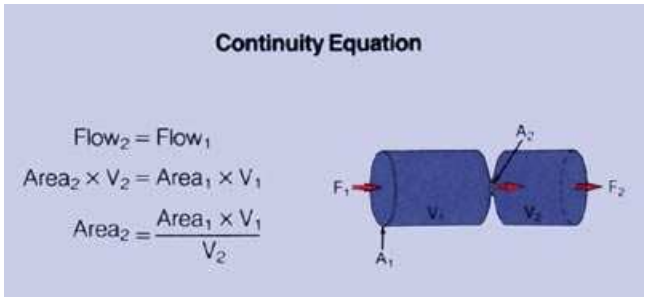

Figure 3. 35 The continuity of flow equation. For details, see text.

The area of the outflow tract (A_1) may also be measured and requires the use of two dimensional echocardiography. This is best performed by measuring the radius at the base of the aortic cusps in the parasternal long axis, in a similar way as for calculation of cardiac output. Using the algebraic relationships given in **Figure 3.35**, the equation may then be solved for the area of the obstructed aortic valve (A_2).

Using this equation, it is not even necessary to perform the complex calculation of the flow velocity integrals for V_1 and V_2. The spectral recordings of each may be likened to triangles with bases that are equal in size but heights that are different. Their time durations (bases of the triangles) are nearly identical if the patient is in sinus rhythm. Therefore, the flow velocity integrals of both are nearly proportional to their height (or peak velocities). These concepts are brought together in diagrammatic form in **Figure 3.36**.

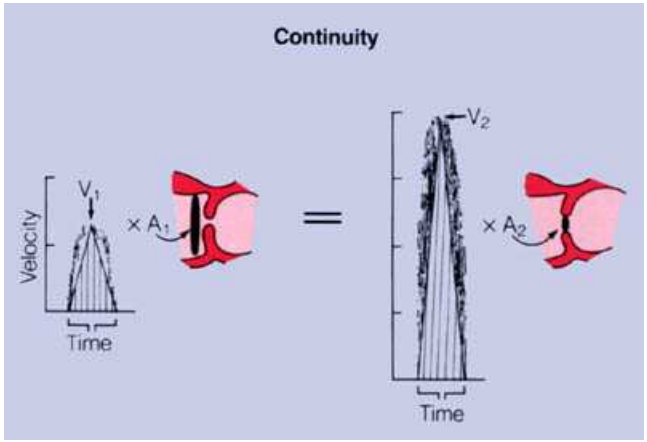

Figure 3. 36 The continuity of flow relating the Doppler-determined velocity and area below the stenotic aortic valve (V_1 and A_1) to the Doppler-determined velocity and area at the stenotic site (V_2 and A_2). For details, see text.

The Clinical Role for Doppler in Aortic Stenosis

Determining the severity of aortic stenosis by physical examination can be difficult, particularly in older patients. One useful clinical role for Doppler echocardiography would be to serve as a supplement to the history and physical examination in patients where the physical examination is confusing. In our experience it has been valuable in identifying

patients with significant aortic stenosis, particularly in the elderly. A perfectly normal Doppler examination, when aortic stenosis is clinically suspected, has been of extreme help in avoiding unnecessary cardiac catheterization in these individuals.

However, it is important for the beginner to appreciate that difficult patients do occur and considerable experience is required to perform these procedures properly. When recordings of poor quality are seen, they should be disregarded since they will generally underestimate the severity of the gradient. Even when good traces are obtained, it is possible to record falsely high gradients by Doppler, especially in the setting of aortic insufficiency. We have found that it takes most beginners a year of experience of examining reasonable numbers of patients to obtain reliable results.

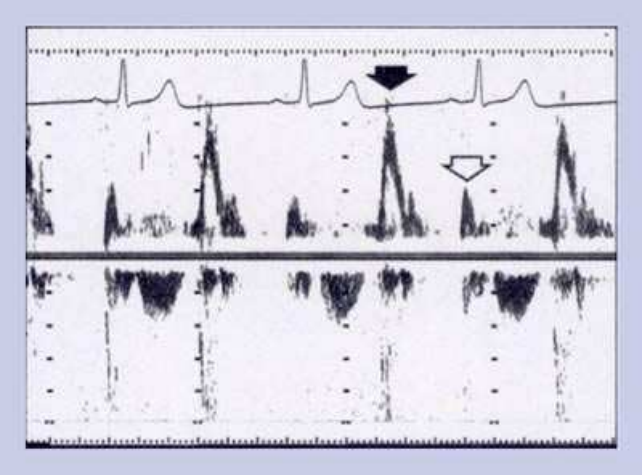

Figure 3. 37 PW Doppler spectral recording from the mitral orifice taken from the apical window. Early diastolic flow is high (closed arrow), followed by a rapid descent and then peaks again after atrial contraction (open arrow) (Scale marks = 20cm/s)

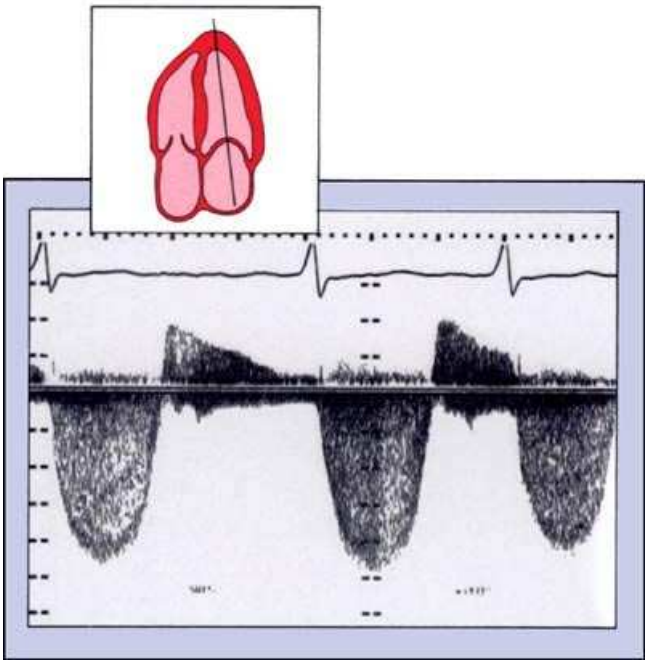

Figure 3. 38 Typical CW spectral velocity recording from a patient with mitral stenosis and insufficiency. From the apex, the diastolic flow of mitral stenosis is toward the transducer. There is a rise in velocity in early diastole followed by a slow diastolic descent.

Mitral Gradient in Mitral Stenosis

The best window for examination of mitral valve diastolic flow is invariably apical. With the transducer at the cardiac apex, the ultrasound beam should be directed posteriorly and slightly laterally to intercept mitral valve flow. In normal individuals, PW Doppler is adequate for recording mitral valve diastolic flow. Mitral flow is typically laminar and biphasic **(Fig. 3.37)**, peaking in early diastole (closed arrow) and rising again with atrial contraction in late diastole (open arrow).

The examination for mitral stenosis is usually much easier and more straightforward than that for aortic stenosis. The typical CW spectral recording of mitral stenosis demonstrates spectral broadening in diastole, with peak flow in early diastole and a progressive but slowed diastole descent **(Fig. 3.38)**.

The secondary increase in diastolic velocity due to atrial contraction is absent in patients with atrial fibrillation.

A mitral valve gradient is calculated using the modified Bernoulli equation, discussed previously. The spectral recording in **Figure 3.39** shows a peak diastolic velocity of 2 m/s that is equivalent to a 16mmHg peak transmittal pressure gradient. As with aortic stenosis, the transmitral pressure gradient may be reported in several ways. Catheterization laboratories usually report the mean gradient. In order to compute a comparable mean gradient for Doppler data, multiple instantaneous peak gradients must be measured during diastole (such as 40-100 ms intervals) and the values averaged. At least 10 well

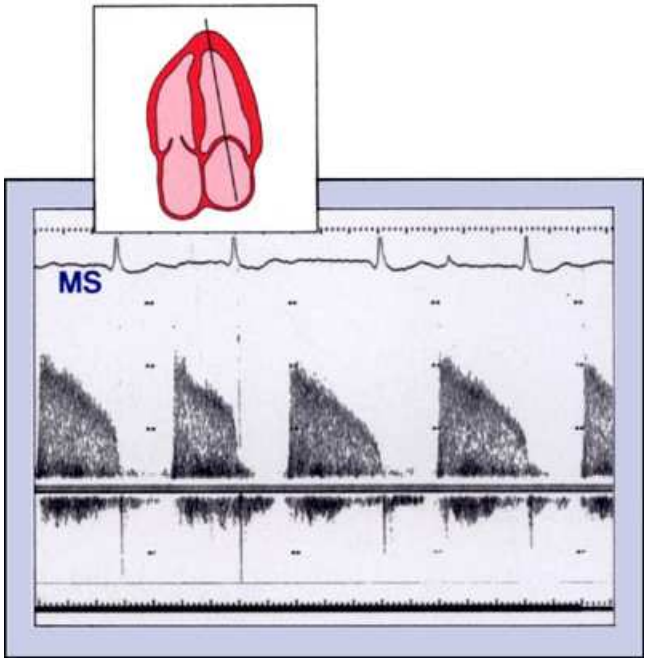

Figure 3. 39 Typical diastolic pattern of mitral stenosis using CW Doppler. Note early diastolic velocity rises to 2 m/s. Mitral valve pressure gradients may be estimated using this technique. For details, see text. (Scale marks = 1m/s)

formed Doppler profiles should be averaged in this manner if the patient is in atrial fibrillation.

Results published to data have shown excellent agreement between CW Doppler estimates of the mitral valve pressure gradient, using the simplified Bernoulli equation, and simultaneous estimates derived from cardiac catheterization data. However, when the two studies are performed on separate days, the agreement between the two is reduced. This apparent discrepancy derives, in part, from the labile nature of the mitral pressure gradient. The value of this parameter at any particular instant is determined not only by the extent of mitral valve obstruction present but also by the flow across the valve (i.e., cardiac output) and the length of the diastolic filling period, which in turn is determined by the heart rate. Therefore, if the heart rate during catheterization differs from the rate during the Doppler study, the pressure gradients estimated by these two techniques would be expected to differ. In this situation, the higher gradient would be recorded in the study performed at the faster heart rate.

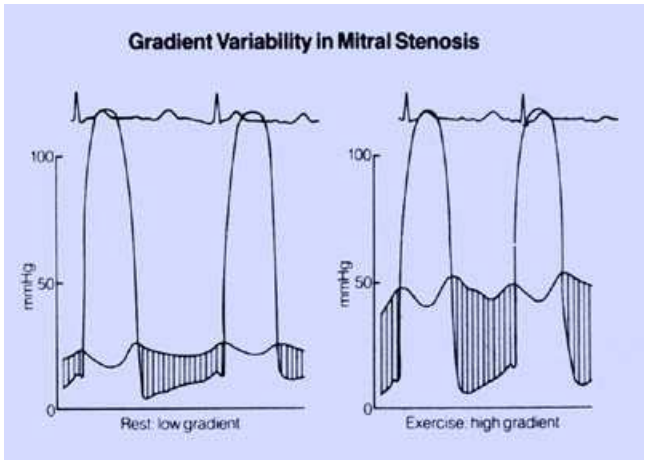

Figure 3. 40 Idealized pressure gradients in mitral stenosis demonstrating that at rest the gradient may be low (left panel) but rises significantly with exercise (right panel).

These relationships are pointed out in the idealized pressure recordings shown in **Figure 3.40**. The diastolic gradient is relatively low at rest **(left panel)** and rises significantly with exercise as heart rate and cardiac output rise **(right panel)**.

Mitral Valve Area Estimates

The sensitivity of the mitral pressure gradient to changes in heart rate and cardiac output clearly makes it an incomplete description of the severity of mitral stenosis. As stated previously, valve area is generally considered not to vary with changes in cardiac output and is the preferred method for expressing the severity of mitral stenosis.

Mitral valve area may be calculated at catheterization using pressure gradient and flow information by the Gorlin equation. It may also be directly planimetered in diastole using the two-dimensional, echocardiographic image of the mitral valve orifice obtained in the short-axis view. In our laboratory, catheterization-derived mitral valve area correlates well with that measured by a two-dimensional echocardiography. We find both two-dimensional echocardiography and Doppler to be useful for noninvasive assessment of the severity of mitral valve obstruction.

A method has been described for estimating mitral valve area from Doppler measurements. The approach is based on the measurement of a parameter called the atrioventricular (AV) pressure half-time. This quantity was originally proposed as an alternative to the Gorlin formula for

estimating the severity of mitral stenosis from catheterization pressure data. It is defined as the time interval in milliseconds (ms) required for the diastolic pressure gradient across the mitral valve to fall to half of its initial value.

The original studies of atrioventricular pressure half-time carried out in the catheterization laboratory showed it to correlate well with effective mitral valve area and to be relatively insensitive to changes in heart rate or cardiac output. Doppler pressure half-time calculations reflect the rate of diastolic descent of the spectral velocity recording.

In normal subjects, pressure half-time values range between 20 and 60 ms. In patients with mitral stenosis, there is a marked delay and a strong correlation between the pressure half-time estimated from Doppler data and the mitral valve area calculated from catheterization data using the Gorlin formula. Pressure half-time is relatively insensitive to the effects of exercise, atrial fibrillation or coexisting mitral regurgitation. Patients with mitral stenosis had values from 100 to 400 m/s, with the higher values seen in subjects with smaller valve areas. Pressure half-times greater than 220 ms correlate well with a valve area less than 1.0 cm^2. Patients with isolated mitral regurgitation have values $\leq$80 ms.

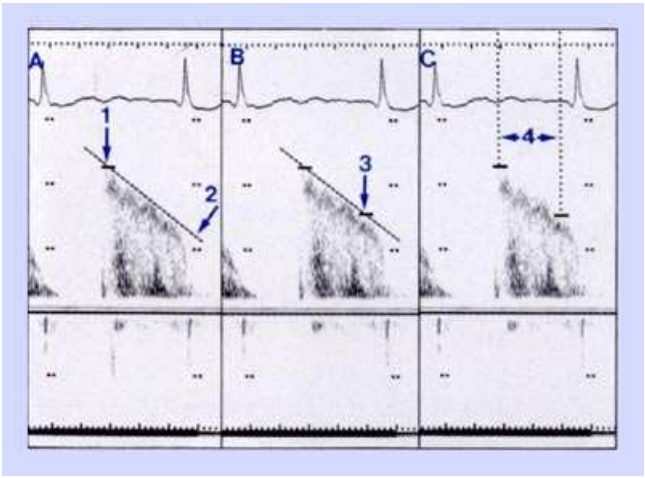

Figure 3. 41 Method for calculation of pressure half-time by Doppler. For details, see text. (Scale marks = 1m/s)

The pressure half-time is the time for the diastolic pressure gradient in mitral stenosis to fall to half of its original value. **Figure 3.41** illustrates how the pressure half-time is measured. The starting point is the time of peak velocity (point 1), which in this case is 2.2 m/s. This corresponds to a peak pressure gradient of 19mmHg by the simplified Bernoulli equation. A line along the diastolic descent of the mitral valve velocity spectrum is drawn (step 2). A point is then found along this line where the pressure has dropped to half of its initial value (point 3) This point is rapidly determined by dividing the initial velocity by 1.4 (square root of 2); that is, 2.2/1.4=1.6 m/s. Thus, when velocity falls to 1.6m/s the pressure is at half of its initial (point 1) value. The pressure half-time is simply the time interval between point 1 and point 3, in this case 400 milliseconds (interval 4).

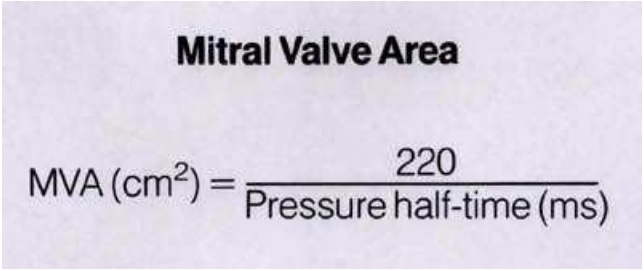

Figure 3. 42 Formula for estimation of mitral valve area in cm^2 using the pressure half-time. The number 220 is an empiric constant.

Beginners sometimes have difficulty relating the spectral velocity tracings to pressure changes on which this method is based. Most of this confusion is based on the relationship between pressure gradients and velocity. It is important to remember that the spectral recordings display velocity information. Derivations of pressure are based upon the modified Bernoulli equation where the gradient equals $4V^2$. Thus, the time taken for the gradient to fall to half the original is always shorter than the time taken for the velocity to decrease to half.

Subsequently, it was found that the pressure half-time could be used to estimate mitral valve area from an empirical formula shown in **Figure 3.42**. In the case of the patient in **Figure 3.41**, the

predicted valve area would be 0.6cm^2. There have been several published correlations of this method for estimating mitral valve area with that derived by the Gorlin equation catheterization, with generally favorable results. The effect of heart rate and other factors that might influence the reliability of these calculations has not, however, been adequately addressed. We find that estimation of valve area by the pressure half-time method is always best confirmed by direct planimetry of the stenotic mitral valve orifice method on the two-dimensional echocardiogram. When the results are disparate, the reliability of estimates by both methods should be questioned.

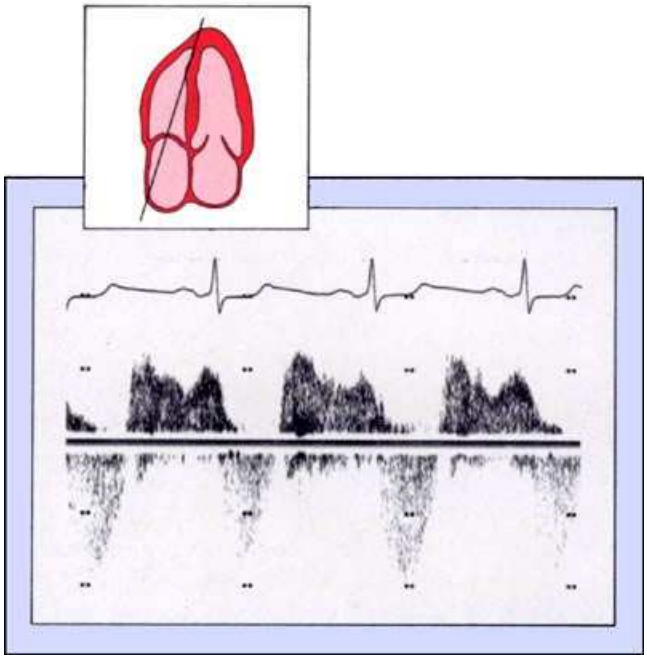

Figure 3. 43 CW Doppler recording of tricuspid stenosis. Note the similarity in appearance to mitral stenosis.

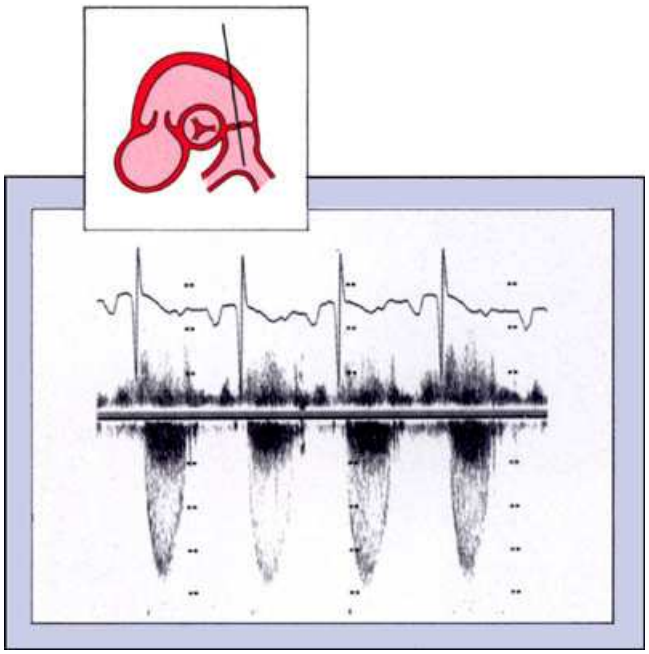

Figure 3. 44 CW Doppler spectral recording from a child with pulmonic stenosis. Note that velocity approaches 4m/s, indicating a significant obstruction across the pulmonic valve. (Scale marks = 1m/s)

Tricuspid Stenosis

Evaluation of tricuspid stenosis with Doppler poses problems similar to mitral stenosis but, since it is a rarer disease, the accumulated experience is less extensive. The presence of tricuspid stenosis is readily determined with either pulsed or continuous wave Doppler by detecting turbulence and increased velocities emerging from the tricuspid orifice into the right ventricle during diastole **(Fig. 3.43)**. Since the pressure gradient across a stenotic tricuspid valve is fairly low, even with severe obstruction, peak Doppler velocities will be correspondingly reduced from those seen in severe mitral stenosis. Experience with both catheterization-derive and Doppler-derived estimates of tricuspid valve areas is limited. Consequently, assessment of the severity of tricuspid obstruction in the noninvasive laboratory consists of a two-dimensional, echocardiographic evaluation followed by Doppler measurement of the transvalvular mean pressure gradient.

Pulmonic Stenosis

Like all the other cardiac valves, stenosis of the pulmonic valve results in marked turbulence and an increase in velocity. A CW Doppler recording of pulmonic stenosis is shown in **Figure 3.44**. The peak velocity is nearly 4 m/s, indicating that a 64mmHg gradient is present. Gradients estimated by Doppler have favorable comparisons with those obtained at catheterization. In high right-sided flow states, such as those seen in patients with large left-to-right shunts, there may be a mild elevation in peak pulmonary arterial flows. This presumably results from the increased volume being ejected through the normal pulmonic valve orifice. In these cases it is sometimes

difficult to determine the presence of mild pulmonic stenosis.

OTHER OBSTRUCTIVE LESIONS AND GRADIENTS

Coarctation of the Aorta

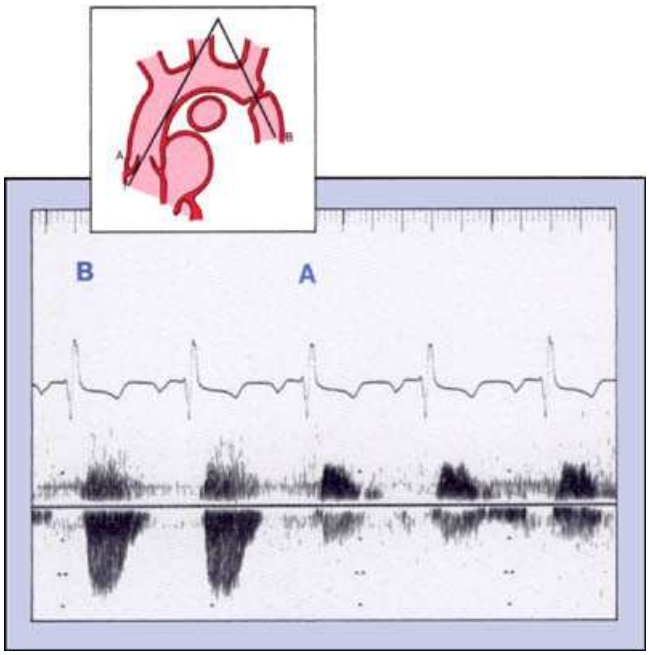

Figure 3. 45 Schematic representation (left) showing direction of the CW beam from the suprasternal window into the ascending aorta (A) and descending aorta (B) in a patient with coarctation of the aorta. The resulting spectral velocity recording is shown on the right. (Scale marks = 1m/s)

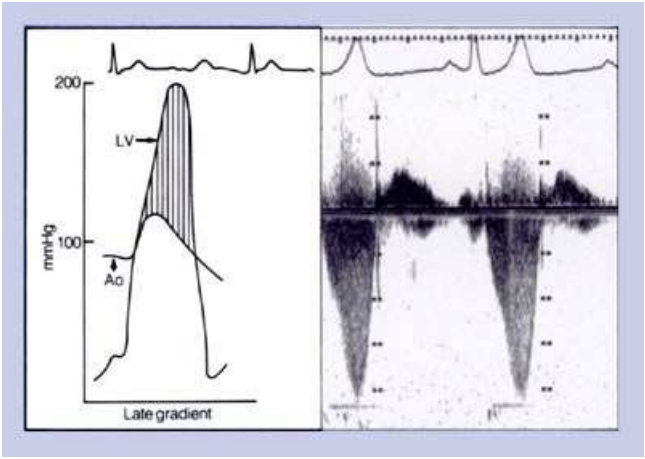

Figure 3. 46 In hypertrophic obstructive cardiomyopathy, the largest gradient occurs in mid-to-late systole (left panel). This usually shows a late peaking velocity across the left ventricular outflow tract (right panel). (Scale marks = 1m/s)

These basic principles may be applied to almost any situation where pressure-gradient information is desired. Coarctation of the aorta may be readily identified with the transducer in the suprasternal notch and the Doppler beam angled slightly anteriorly and to the patient's right side. Systolic flow from the ascending aorta is encountered moving toward the transducer using this window **(Fig. 3.45)**. With angulation of the beam slightly posteriorly, the higher velocity jet through the coarctation in the descending aorta is then encountered moving away from the transducer. Doppler echocardiography has been shown to be a reliable method for determining the presence of this disorder.

Hypertrophic Obstructive Cardiomyopathy

The area of obstruction in hypertrophic obstructive cardiomyopathy (also called idiopathic hypertrophic subaortic stenosis) is thought to occur where the anterior mitral valve leaflet opposes the interventricular septum. This is a dynamic, rather than fixed, obstruction that usually becomes more severe as systole progresses.

In **Figure 3.46** idealized aortic and left ventricular pressure tracings indicate that the peak gradient usually occurs in mid to late systole as a consequence of the changing relationships between the tip of the mitral leaflet and the septum. On the right is a typical CW spectral recording from a patient with this disorder. Note the late peaking of the jet as a result of the altered pressure dynamics.

Continued clinical practice indicates that patients with this disorder may have some of the highest velocities encountered by Doppler echocardiography. The peak velocity illustrated in

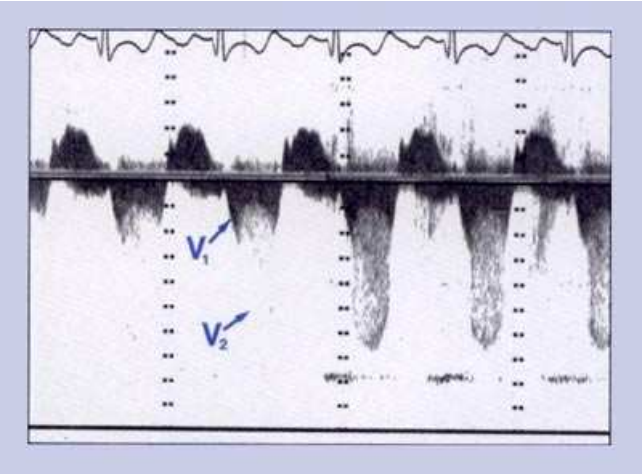

Figure 3. 47 CW Doppler spectral recording from the apex across the area of obstruction from a patient with hypertrophic obstructive cardiomyopathy. Note the mid-systolic decreases in V_1. Many varied patterns to V_1 may be seen in this disorder.

Figure 3.47 is nearly 7 m/s.

There are many other interesting phenomena that occur in patients with obstructive cardiomyopathy. Careful CW examination will frequently reveal multiple patterns of V_1 in relationship to V_2. One such unusual pattern is seen in **Figure 3.47** where V_1 appears to fall during mid-systole, then rise again in late systole. These unusual patterns have not yet been fully correlated to the hemodynamic events in these patients, but differentiate CW spectral recordings of dynamic outflow obstruction from that due to fixed obstruction at the valvular level.

Ventricular Septal Defect

Ventricular septal defects are usually best interrogated using the parasternal long-axis approach. In this view, the abnormal flows between ventricles are normally parallel to the beam, and reasonably faithful velocities are recorded.

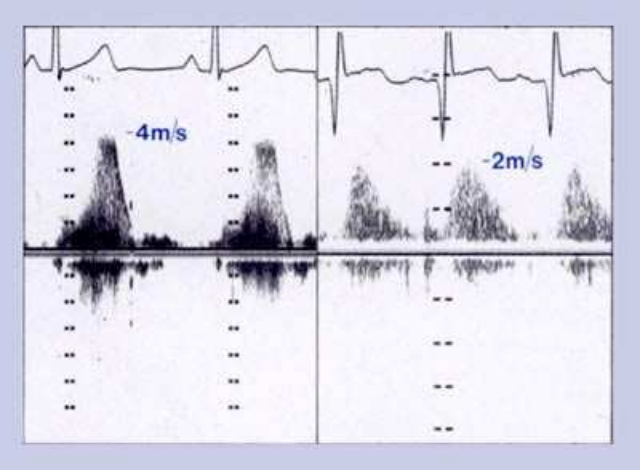

Figure 3. 48 CW spectral recordings from two different patients with ventricular septal defects. If both patients had similar systemic systolic pressures, the low gradient in the patient on the right would indicate nearly systemic right ventricular pressures. For details, see text. (Scale marks = 1m/s)

Doppler serves as a method for estimating right ventricular systolic pressures when ventricular septal defects are encountered. **Figure 3.48** shows CW spectral recordings from two different patients with ventricular septal defects taken from the left parasternal approach. The peak velocity in the child in the left panel is slightly higher than 4 m/s, indicating a 64mmHg gradient between left and right ventricles. The peak velocity in the infant in the right panel is 2 m/s, indicating a gradient of only 16 mmHg.

Since aortic (and, therefore, left ventricular) systolic pressure can be measured by a blood pressure cuff, the difference between the cuff pressure and the gradient measured by Doppler results in the estimated right ventricular systolic pressure. Given the fact that both patients in **Figure 3.48** had systemic systolic pressures of 110mmHg by cuff, the patient on the left had an estimated right ventricular systolic pressure of 46mmHg while the patient on the right had an estimated right ventricular systolic pressure of 94mmHg.

PW Doppler echocardiography has been used for the calculation of pulmonary-to-systemic shunt ratios in patients with intracardiac shunting. The approach is based upon the principles described earlier in the section on calculation of cardiac output. In brief, output through the pulmonary valve is related to output through the aortic valve.

DOPPLER EXAMINATIONS FOR VALVULAR STENOSIS

As seen from the many examples described in this Unit, considerable operator skill is necessary to acquire the critical quantitative data necessary by Doppler for the assessment of valvular stenosis. Points to keep in mind when carrying out an examination include:

Hint 1: An operator should never be satisfied by interrogating an abnormal jet by only one view. Stenotic jets may move in any direction. This is particularly true of aortic stenosis and apical, right parasternal, and suprasternal approaches must be used before an operator can be assured that the highest peak jet possible has been recorded.

Hint 2: Reliable quantitative assessments require that high quality spectral recordings are available for analysis. Measurement of peak velocities from poorly formed Doppler profiles may lead to serious underestimations of transvalvular gradients. When it is impossible to acquire a fully formed profile, it is best not to attempt quantitative assessment. Beginners are sometimes tempted to make some measurement with the expression that a gradient is "at least" a certain amount. In our experience, this only leads to confusion in later decision-making processes.

Hint 3: Much of the utility of Doppler for the assessment of valvular stenosis is based on the use of CW methods. Since this is frequently performed with a stand-alone transducer, there is no image available for anatomic reference. An operator must use frequent voice annotations on the video recording to assist in later interpretation and reference. We recommend voice notation of the valve being interrogated and the angulations being used as the beam is directed spatially. This frequently helps in eliminating confusion between the various abnormal flows that might be encountered during a Doppler examination.

Hint 4: When interpreting Doppler information for assessment of the severity of valvular stenosis all available information must be taken into account to avoid excessive dependence on any one quantitative index. For example, a patient with severe aortic stenosis, a dilated left ventricle and low cardiac output may only have a 3 m/s aortic stenotic jet since flow across the aortic valve is low. Without an estimate of aortic valve area, this would lead to the incorrect assumption that minimal aortic stenosis is present.

Figure Legends

Figure 3. 1 CW Doppler recording of normal aortic systolic velocity taken from the suprasternal notch. Note that the onset of flow toward the transducer begins after the QRS complex of the electrocardiogram (arrow) and peaks in the first third of systole.

Figure 3. 2 Many systolic velocity indices may be calculated from the flow in the ascending aorta, as indicated in these idealized spectral recordings.

Figure 3. 3 The various ejection rate indices relate to left ventricular performance (ejection fraction).

Figure 3. 4 Stroke volume is the volume of blood ejected from the left ventricle with each systole. Knowing stroke volume and heart rate provides a means for calculating cardiac output. Doppler may be used for calculating stroke volume. (CO =cardiac output; SV = stroke volume; HR=heart rate).

Figure 3. 5 Echo-Doppler estimates of flow volume are based upon a knowledge of the area of flow (from echocardiogram) and the length (from Doppler). It is assumed that the aorta is a cylinder.

Figure 3. 6 When stroke volumes are equal and areas remarkably different, the resultant velocities of flow may be quite different. The velocity for large areas would be less than for small areas.

Figure 3. 7 Illustration of all the steps required for the calculation of cardiac output by Doppler.

Figure 3. 8 Idealized representation of echo-Doppler calculations of cardiac output compared with that determined by thermodilution.

Figure 3. 9 Idealized comparisons of mean pulmonary artery (PA) pressure to time-to-peak velocity (left) and the logarithm of mean pulmonary artery pressure to peak velocity (right).

Figure 3. 10 Idealized spectral recordings demonstrating that time-to-peak velocity is very rapid in patients with pulmonary hypertension.

Figure 3. 11 PW Doppler spectral recording of aortic blood flow (arrow) taken from the apical window. Note the laminar appearance of normal flow. (Scale marks = 20 cm/s)

Figure 3. 12 Left panel – Without aortic valve obstruction, systolic pressures are almost the same in the ventricle and the aorta. Right panel – When significant aortic valve obstruction is present, left ventricular pressure rises much higher than aortic, and a systolic pressure gradient is present. The size of the arrows represents the magnitude of the pressures.

Figure 3. 13 CW spectral recording from the apex in a patient with aortic stenosis. The velocity spectrum is broadened and systolic velocity is increased to 4 m/s. (Scale marks = 2 m/s)

Figure 3. 14 CW Doppler spectral velocity recording of mild pulmonic stenosis and insufficiency. The abnormal diastolic flow toward the transducer of pulmonic insufficiency is easily recognized. (Scale marks = 1m/s)

Figure 3. 15 PW Doppler spectral recording from the same patient as Figure 3.24. At position A, pulmonic insufficiency is noted. At position B, on the distal side of the valve, the systolic velocity is elevated. (Scale marks = 20cm/s)

Figure 3. 16 Typical CW spectral velocity tracing from the apex in a patient with aortic stenosis and insufficiency. Peak systolic velocity is elevated to almost 6 m/s and peaking is delayed. (Scale marks = 2 m/s)

Figure 3. 17 Idealized relationship between pressure gradient and flow. As flow increases, the gradient will also rise even though the valve area is fixed.

Figure 3. 18 CW Doppler spectral recording of aortic outflow from the suprasternal notch with flow toward the transducer (left) and apex with flow away form the transducer (right). The spectral recording from the apex is better formed than the one from the suprasternal notch.

Figure 3. 19 Typical aortic systolic velocity recording from the suprasternal notch in a patient with aortic stenosis. Note that the peak velocity is almost 5 m/s. As gradient increases, so does the peak systolic velocity. (Scale marks = 1m/s)

Figure 3. 20 Operator skill is important in obtaining an adequate systolic aortic jet profile in aortic stenosis. This figure shows a recording made by a less experienced operator (left panel) compared with one from a more experienced operator (right panel).

Figure 3. 21 The systolic jet of aortic stenosis and diastolic jet of aortic insufficiency often cannot be recorded at the same time. As the transducer beam is angled from the stenotic jet (closed arrow) to intercept the aortic insufficiency, the left ventricular outflow tact velocity is encountered (stippled arrow). Both outflow tract velocities are superimposed during the beam sweep (open arrow). (Scale marks = 1 m/s)

Figure 3. 22 Inadequate recordings of aortic systolic velocity do occur and should not be used for estimation of gradient. Note that the profile is poorly formed on the upstroke, peak (arrow), and down stroke. (Scale marks = 2 m/s)

Figure 3. 23 Aortic stenosis (left) should not be mistaken for mitral insufficiency (right). Mitral systole begins before aortic (arrow) and is longer in duration. (Scale marks = 2m/s)

Figure 3. 24 Relationship between abnormal systolic and diastolic flows through the left heart valves. For details, see text.

Figure 3. 25 Left panel shows an aortic stenotic jet in relation to possible viewing directions using CW Doppler. Right panel shows spectral velocity tracings from each respective window. The best recording is from the right sternal window. (Calibration marks = 2m/s)

Figure 3. 26 CW spectral velocity recording from the suprasternal window into the ascending aorta from a patient with severe stenosis. Note the varying peak velocities with varying R-R interval of the ECG. (Calibration marks = 1 m/s).

Figure 3. 27 Schematic representation of simultaneous left ventricular (LV) and aortic (Ao) pressure recordings obtained at catheterization with representation of different gradient measurement methods.

Figure 3. 28 Pressure recordings from the left ventricle (LV) and brachial artery (BA) from a patient with aortic stenosis. Note the delay in the upstroke of the brachial arterial pressure tracing and the delay in onset of the brachial pressure tracing when compared with that from the ventricle.

Figure 3. 29 Idealized relationship between Doppler peak gradient and catheterization peak-to-peak gradient. Comparisons show that there is overestimation of catheterization peak-to-peak gradient.

Figure 3. 30 Idealized relationship between Doppler peak gradient and catheterization peak gradient. Since Doppler reflects peak catheterization gradient, the comparisons are more favorable.

Figure 3. 31 Idealized relationship between Doppler mean gradient and catheterization mean gradient. Mean gradient comparisons are favorable because they average data over time.

Figure 3. 32 Velocity below the valve (V_1) is not recorded as often as velocity on the aortic side (V_2). V_1 is ignored in the simplified Bernoulli equation. (Scale marks = 1m/s)

Figure 3. 33 The severity of aortic stenosis may also be judged by the relative proportion of total systolic time taken to reach peak velocity (stippled areas). Both time to peak and peak velocity are lower in panel A than in panel B. ((Scale marks = 1m/s)

Figure 3. 34 Continuity of forward flow. Flow that enters a cylinder is equal to the flow passing through an obstruction and exiting from the distal side.

Figure 3. 35 The continuity of flow equation. For details, see text.

Figure 3. 36 The continuity of flow relating the Doppler-determined velocity and area below the stenotic aortic valve (V_1 and A_1) to the Doppler-determined velocity and area at the stenotic site (V_2 and A_2). For details, see text.

Figure 3. 37 PW Doppler spectral recording from the mitral orifice taken from the apical window. Early diastolic flow is high (closed arrow), followed by a rapid descent and then peaks again after atrial contraction (open arrow) (Scale marks = 20cm/s)

Figure 3. 38 Typical CW spectral velocity recording from a patient with mitral stenosis and insufficiency. From the apex, the diastolic flow of mitral stenosis is toward the transducer. There is a rise in velocity in early diastole followed by a slow diastolic descent.

Figure 3. 39 Typical diastolic pattern of mitral stenosis using CW Doppler. Note early diastolic velocity rises to 2 m/s. Mitral valve pressure gradients may be estimated using this technique. For details, see text. (Scale marks = 1m/s)

Figure 3. 40 Idealized pressure gradients in mitral stenosis demonstrating that at rest the gradient may be low (left panel) but rises significantly with exercise (right panel).

Figure 3. 41 Method for calculation of pressure half-time by Doppler. For details, see text. (Scale marks = 1m/s)

Figure 3. 42 Formula for estimation of mitral valve area in cm^2 using the pressure half-time. The number 220 is an empiric constant.

Figure 3. 43 CW Doppler recording of tricuspid stenosis. Note the similarity in appearance to mitral stenosis.

Figure 3. 44 CW Doppler spectral recording from a child with pulmonic stenosis. Note that velocity approaches 4m/s, indicating a significant obstruction across the pulmonic valve. (Scale marks = 1m/s)

Figure 3. 45 Schematic representation (left) showing direction of the CW beam from the suprasternal window into the ascending aorta (A) and descending aorta (B) in a patient with coarctation of the aorta. The resulting spectral velocity recording is shown on the right. (Scale marks = 1m/s)

Figure 3. 46 In hypertrophic obstructive cardiomyopathy, the largest gradient occurs in mid-to-late systole (left panel). This usually shows a late peaking velocity across the left ventricular outflow tract (right panel). (Scale marks = 1m/s)

Figure 3. 47 CW Doppler spectral recording from the apex across the area of obstruction from a patient with hypertrophic obstructive cardiomyopathy. Note the mid-systolic decreases in V_1. Many varied patterns to V_1 may be seen in this disorder.

Figure 3. 48 CW spectral recordings from two different patients with ventricular septal defects. If both patients had similar systemic systolic pressures, the low gradient in the patient on the right would indicate nearly systemic right ventricular pressures. For details, see text. (Scale marks = 1m/s)

Doppler Color Flow Imaging #4

Joseph A. Kisslo, MD
David B. Adams, RDCS

INTRODUCTION

Doppler color flow imaging is a method for noninvasively imaging blood flow through the heart by displaying flow data on the two-dimensional echocardiographic image. This capability has generated great excitement about the use of the technique for identifying valvular, congenital, and other forms of heart disease, as the color flow image imparts spatial information to the Doppler data. To inexperienced Doppler users, the color flow display makes the Doppler data more readily understandable because of the avoidance of complex spectral velocity displays.

Figure 4. 1 Systolic parasternal long-axis color flow image of mitral regurgitation. The mitral regurgitation jet comprises a mosaic of varying colors. A variance map is used. Note the direction of flow indicated by the color bar on the right (Abbreviations, page 39).

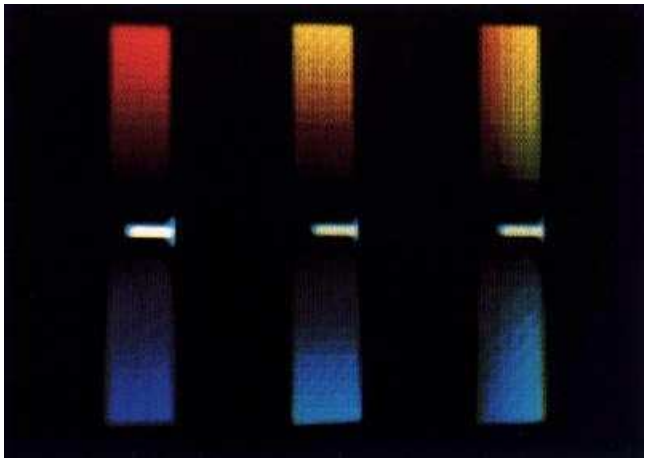

Figure 4. 2 Three color bars from a color flow system. When there is no flow, black is displayed (center) in the standard bar (left), flow toward the transducer at the top is in red, flow away in blue. Progressively faster velocities are displayed in brighter shades of red or blue. The center bar is in an enhanced map, and the right bar in a variance map (explained later in the text).

COLOR FLOW IMAGING IN CLINICAL PRACTICE

Doppler Color Flow Imaging

In **Figure 4.1** there is a mitral regurgitant jet into the left atrium in systole and the regurgitant blood flow is displayed on the two-dimensional echocardiographic image. In color flow imaging, the colors red and blue represent direction of a given jet; the various hues from dull to bright represent the differing velocities. When turbulence is present, a mosaic of many colors results. A two-dimensional display of flow is, therefore, produced with ready identification of size, direction, and velocity.

The Meaning of Color

The colors displayed on the flow map image contain useful information. By convention, Doppler color flow systems assign a given color to the direction of flow; red is flow toward, and blue is flow away from the transducer. Three typical color bars from a color flow imaging device are shown in **Figure 4.2** and give an initial frame of

reference to the meaning of colors. Such color reference bars always appear on the screen of Doppler flow imaging devices. The center of the standard color bar on the left is black (white center reference mark) and represents zero flow.

In addition to simple direction, velocity information is also displayed. Progressively increasing velocities are encoded in varying hues of either red or blue. The more dull the hue, the slower the velocity. The brighter the hue, the faster the relative velocity.

In the color bar shown in the center of **Figure 4.2**, the colors have been "enhanced" so that the hues of red are increased from very dull red to bright yellow and the hues of blue are increased from very dull blue to a bright pale blue. The enhanced map helps a beginner to understand the relationship between velocity and color. The bar at the right demonstrates variance.

As will be seen later, color is also used to display turbulent flow and allows an operator to discriminate between normal and abnormal flow states.

The Angiographic Concept

One way of conceptualizing Doppler color flow methods is to recognize its similarity to angiography. It provides a noninvasive "angiogram" of blood flow, where the contrast medium is the moving red blood cells and the detector of this contrast is ultrasound. The complex Doppler ultrasound processing circuitry allows for the detection of movement of these red cells in various directions – forward and backward through the heart. Doppler color flow information, however, is obtained and displayed in a cross-sectional image, making the spatial details of flow and anatomy readily recognizable. In effect, Doppler color flow looks inside the cineangiographic silhouette.

Unlike angiography, Doppler color flow does not depend on dye dilution accumulated over several heartbeats. Rather it displays an abnormal flow jet for each cardiac cycle. This results in the ability to display the differing sizes of regurgitant jets depending on severity. The larger the volume of the regurgitant jet, the larger the size represented on the display.

CREATION OF THE COLOR IMAGE

The Importance of Time

Time is the key factor to keep in mind. A conventional two-dimensional ultrasound imaging system is already working as hard as it can. Pulses must be transmitted along a given line, reflected from the heart valves and walls, then received. The process is repeated, line by line, through the entire sector arc that comprises several hundred lines. This completes one frame of information, usually in one-thirtieth of a second. In order to have the image appear as though it is continuously moving, the entire image must be updated 30 times in a second (30 frames/second). This results in relatively long waiting periods for the transmit-receive sequence to be completed. It also means that considerable amounts of information need to be quickly processed and presented in the image.

A problem, therefore, results. If all this time is taken to simply create the image, where is there time to sample rapidly with the Doppler, left and right, in all portions of the image field? From earlier units in this series, we have already learned that high quality imaging and high quality pulsed Doppler cannot really be conducted simultaneously.

Anatomic and Flow Information Together

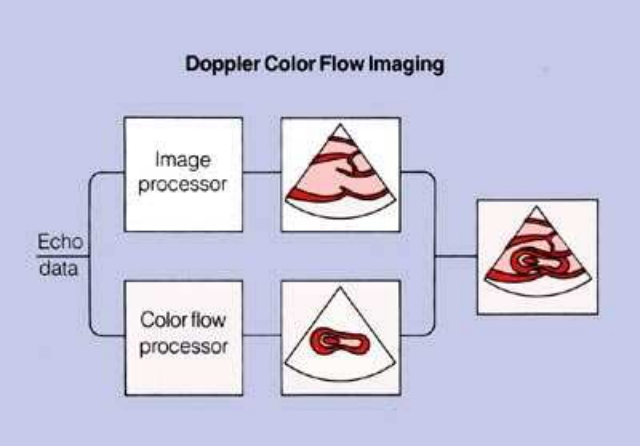

Figure 4. 3 In a color flow-imaging device, the returning echo data are processed through two channels that ultimately combine the image with the color flow data in the final display.

Expressed in its most simplistic terms, color flow systems add a separate processor that creates the color flow image based on the returning data and then integrates it with the two-dimensional anatomic image **(Fig. 4.3)**. Both the anatomic and the color flow data are then displayed in the final image.

The returning ultrasound data from any conventional scanner also contains frequency shift information that results from the encounter of the transmitted pulse with moving structures and blood. Until the advent of color flow imaging, this frequency shift data was simply ignored.

The key to color flow mapping is that the returning data may also be processed for the frequency shifts (or red blood cell velocities). Thus, color flow imaging systems take advantage of data that are available in every ultrasound image of the heart.

While this is a simplistic explanation, it is not true in most color flow systems. In reality, the lines of color flow data are alternated with lines of anatomic scan data. The anatomic data are acquired and received by conventional means and the color flow data are acquired, received, and processed separately.

Multigate Doppler

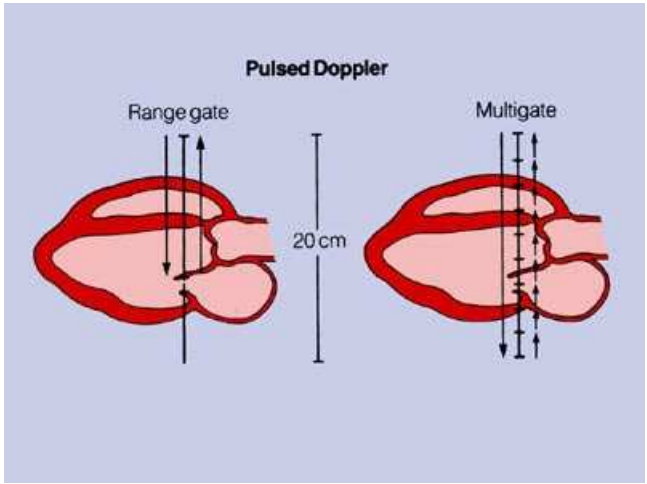

Figure 4. 4 Color flow Doppler systems use PW Doppler principles in a multigate, rather than range-gate format. For details, see text.

Doppler color flow instruments are all currently based upon pulsed wave (PW) Doppler methods. Conventional PW techniques are range gated **(Fig. 4.4, left)**. The Doppler sample volume is determined in range by the time it takes for the ultrasound pulse to travel to the area of interest and then back. If the same method was employed in color flow, it would simply take too long to sample over the entire image and there would be serious compromises made in frame rate.

Instead, all color flow systems are "multigated". In the illustration in **Figure 4.4 (right)** a simple ten-gate system is illustrated and compared with the conventional PW approach. Here, a burst of ultrasound is sent into the tissue along a given line and then the system rapidly receives at ten incremental times. This results in the reception of

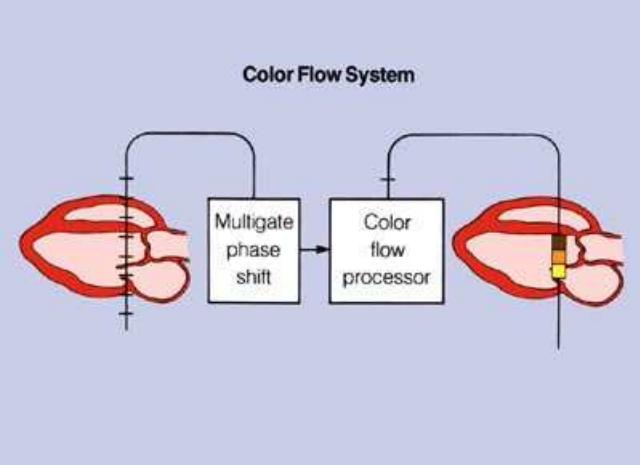

Figure 4. 5 Color flow imaging systems collect the phase shift information at each of the multiple gates and then process the information with color presented in the final display.

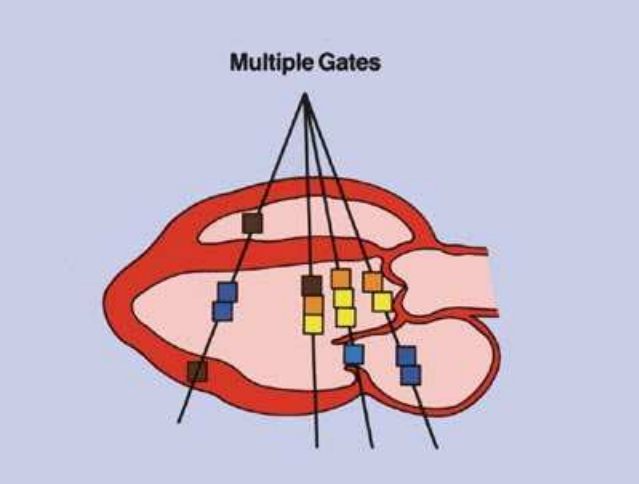

Figure 4. 6 Hundreds of gates are present along each line throughout the color flow image. In gates where there is target information, no color is displayed (open gate at lower left),

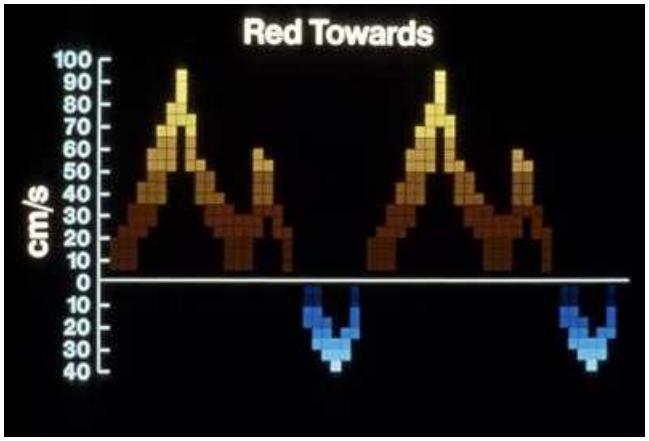

Figure 4. 7 If color was mapped on a conventional spectral recording, only one color could be placed in each bin. Progressively increasing velocities towards the transducer would be displayed in brighter hues of red while flow away would be displayed in blue.

Doppler data from the near flow areas first, while the pulse is still continuing into the tissue. Obviously, reception of the flow data in the far field occurs later.

This multigating takes advantage of Doppler information all along the line that is "ignored" in the conventional range-gated approach. In reality, each line has many gates that number in the hundreds. **Figure 4.5** demonstrates a simple ten-gate system where the amplitude and phase shifts are detected for each gate and presented to the color flow processor for final display of the color in each gate.

It is best to think of the color flow map image as comprising little gates throughout the field of view, each gate containing some composite of the Doppler information. A typical image can consist of as many as 256 lines depending upon sector size and depth of range. **Figure 4.6** demonstrates that multiple gates of color flow information are displayed throughout the entire image along each ultrasound line.

More About Color

All Doppler flow imaging systems encode the directions of flow into two primary colors: red and blue. Any number of color assignments could be made, but red and blue are chosen because they are primary colors of light (together with green).

If such encoding were done on a conventional spectral Doppler display, the result would look very much like **Figure 4.7**. There is also relative flow velocity information in the color hues; the brighter the color the higher the velocity detected. Thus, high velocities away from the transducer will appear as lighter shades of blue, and higher velocities toward the transducer will be represented by lighter shades of red, or even yellow. Low velocity flow will be represented by darker shades of these colors. Absence of flow is always represented by black.

Choosing a Velocity for Display

Even in laminar flow, many different velocities (and therefore colors) may be detected at any instant in time. In the two-dimensional color display, only one color can be displayed in each gate at any time. The problem is even worse when turbulent flows are detected where there may be a wide range of velocities at any instant. At each spatial location, or gate, only one color can be displayed for any selected map. What color should be chosen?

Detection of Mean Velocity

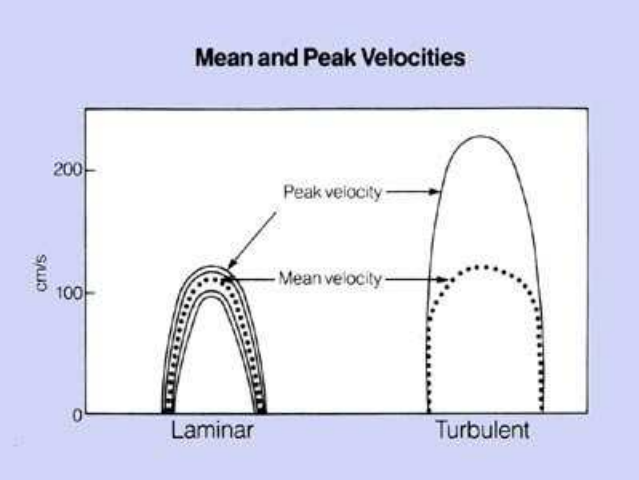

Figure 4. 8 Schematic representation of spectral recording showing the differences between peak and mean velocities. In the case of normal laminar flow, peak and mean velocities may be very close. For turbulent flow, there may be a significant difference between peak and mean velocity.

The color presented at each gate is determined by the mean velocity. Mean velocity is the average of all the different velocities detected at any moment in time. For normal laminar flow, mean and peak velocities are very close **(Fig. 4.8)**. In turbulent flow, when there are many different velocities, mean velocity may be only half of the peak velocity.

Thus, for a color flow map system to correctly assign a color into a given gate, it must be able to detect both the direction of flow and the mean velocity in the area sampled. Since everything happens very quickly, it is best to think of color flow map systems as estimating, rather than precisely calculating, the mean velocity at any gate.

About Pulses, Packets and Trains

The calculation of mean velocity presents an intriguing problem. If you were asked to determine the mean (average) height of a hundred people line up before you, you would want to measure each individual, then divide by the number of people measured and arrive at the true mean height. Such a procedure would take considerable time, equipment and personnel.

If such facilities were not available, you might want to measure just one person at random and hope that your number reflected the entire population. But if you were given another brief period to measure another person, you would arrive at a better estimate because you could take the height from the first sample and add it to the second sample, then divide by two. Given a third, fourth, and perhaps fifth sample period, you would progressively arrive at a better estimate of mean height in the population. This is an imperfect way to estimate mean height: under the limitation of time and equipment it is, however, the only way.

The problem is similar for the color flow Doppler device. Since there are very narrow time constraints for the system to do all of its estimations of mean velocity at any gate and then process the results for presentation, a method is needed to obtain the best estimates possible and then move on. Naturally, compromises must be made along the way.

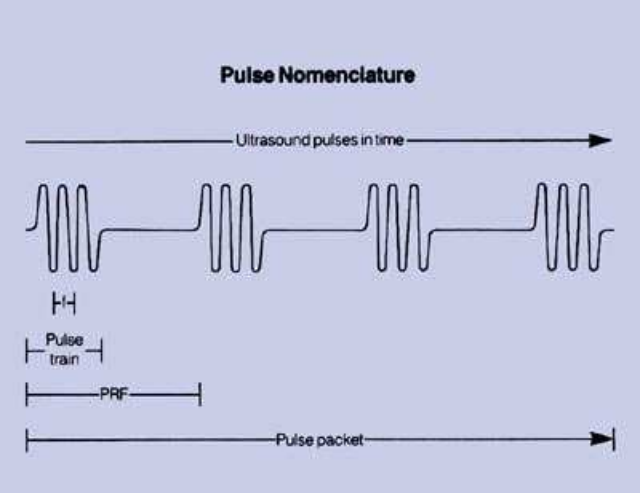

Figure 4. 9 Pulse nomenclature used in the development of color flow images. The number of pulse trains determines the size of the pulse packet. The larger the packet, the better the estimation of mean low velocity.

Color flow systems use an elaborate sequence of pulses to arrive at these estimates; all are shown in **Figure 4.9**. The ultrasound transducer transmits sound waves at a given frequency (f) and the frequency is fixed by the transducer being used (2.5, 3.5, or 5.0 MHz). Bursts of pulses are known as the "pulse train". The time between successive pulse trains determines the pulse repetition frequency (PRF). A number of pulse trains are also emitted at a given angle and this is called the "packet size". In color flow mapping, the principle of packet size is particularly important as it determines the length of time required for sampling to occur before the system moves on to the next beam line.

Conventional two-dimensional anatomic imaging uses only a single pulse train to acquire the necessary anatomic information. Conventional PW Doppler typically uses 128 pulse trains to obtain detailed velocity spectra from a single point in space. Since the sample volume is held in one place, there is plenty of time to perform the detailed spectral analysis. Because color flow mapping attempts to estimate velocity at multiple points in space, far fewer pulse trains can be employed. Time will not permit such detailed sampling with simultaneous construction of a two-dimensional flow image.

Color flow requires the most samples possible in the shortest period of time because so much Doppler information needs to be acquired. What results are small packet lengths, usually of at least three pulse trains per line (or a packet size 3), and up to sixteen pulse trains (or a packet size 16). Obviously, large packet sizes give the best estimates of flow but require the longest time.

Clinical Implications of Packet Size

The requirement for multiple pulse trains per line means that a greater period of time is required to sample along each beam direction than in conventional two-dimensional imaging. Therefore, some reduction in frame rate, line density, depth, or sector angle in comparison with routine two-dimensional imaging is necessary. When a machine is turned into the color flow mode, an operator will immediately notice compromises made in these factors.

Sector angle and depth range can be chosen. In some systems, packet size can also be selected. Once these factors are determined, frame rate and line density are automatically adjusted according to the specifications of the particular system (although in some systems line density can also be selected by the operator). In general, better quality flow data will be obtained with a higher packet size since this allows more sampling along each beam direction. Choosing a higher packet size, however, necessitates either a smaller line density or a lower frame rate and will affect the quality of the image in other ways that will be discussed later. In systems where the operator can control packet size, it is best to start with an individual manufacturer's recommended settings.

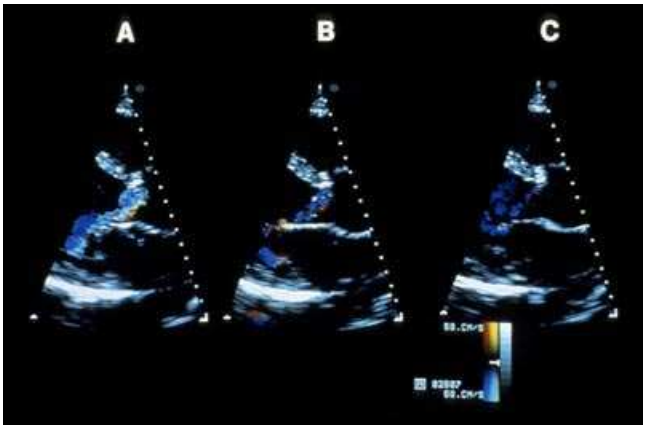

Figure 4. 10 Parasternal long-axis views of an aortic regurgitant jet showing the effect of packet size changes. Panel A was acquired with large packet size, panel B with medium packet size, and panel C with small packet size. Large packet sizes have the best estimates of mean flow but come at the expense of frame rate. Spatial filtering is used with variance maps.

The effects of higher and lower pulse packet sizes are seen in **Figure 4.10**. Better detection of aortic regurgitant flow is achieved using the larger pulse packet size **(panel A)** than when medium **(panel B)** or small **(panel C)** packet sizes are used.

Velocity and Color Assignments

The next step is to understand something of how these systems process the returning waveforms and assign a given color. The analysis of returning Doppler signals from each sector line is complex.

A pulse packet is sent and received along a given line. The frequency shift (or Doppler shift) between successive transmitted and returned packets is usually processed with a circuit called the "quadrature detector". This device employs common electronic circuits to allow determination of the frequency shift.

Simply explained, the quadrature detector supplies a measurement to be used later for the color flow processor in assigning the velocity, and thus the color, at any gate. The main function of the quadrature detector is to make this phase shift measurement for each pulse train, then convert it from analog to digital form (which simply means the data from a continuous sine wave form is assigned a given number to allow further high-speed processing). This digital measurement is then sent to the color flow processor for assignment of velocity and then color.

To obtain the best estimates of flow possible, the signals must first be cleaned as the frequency shifts are cluttered by system noise and signals that arise from heart valves and other cardiac structures. Returning data from one pulse train is held in the processor memory to be used for eliminating system noise from all the other pulse trains in the packet. Data from the second pulse train then returns and is compared with the first, leaving a single, clean signal. The third pulse train then returns and is cleaned in a similar fashion. To get a single phase shift, the two clean signals (second and third) are then compared. Thus, to get a single measurement of phase shift a minimum of three pulse trains are required. This filtering, or cleaning process, utilizes "clutter reject filters" or "comb filters".

Frequency shifts are determined from multiple sample volumes along the line, using the multigate approach previously described. Depending on the system employed, data from 250-500 points (or gates) along the beam line can be processed. Reflected ultrasound is simply analyzed at multiple times (corresponding to multiple gates) as a pulse train makes its way to, and back from, a given depth.

In the color flow processor, analysis of the filtered data from the quadrature detector is finally performed. This analysis cannot be accomplished by fast Fourier transform methods as is used in conventional PW Doppler, since only a few pulse trains are available in color flow imaging devices. Color flow systems must acquire data from thousands of gates throughout the entire field of view. They do not have the luxury of spending enough time in one place to deliver and receive such a high number of pulse trains. Thus, an alternative means of analysis, based on less data, is required to construct a two-dimensional flow map.

These data are analyzed in color flow mapping by utilizing one of two mathematical approaches. The methods are known as "autocorrelation" and "instantaneous frequency estimation". Some systems use a combination of the two methods, which we have termed a "hybrid". These methods are very difficult to understand and have minimal impact on the conduct of an examination. Simply stated, all make a frequency shift estimate for each gate along a given beam line.

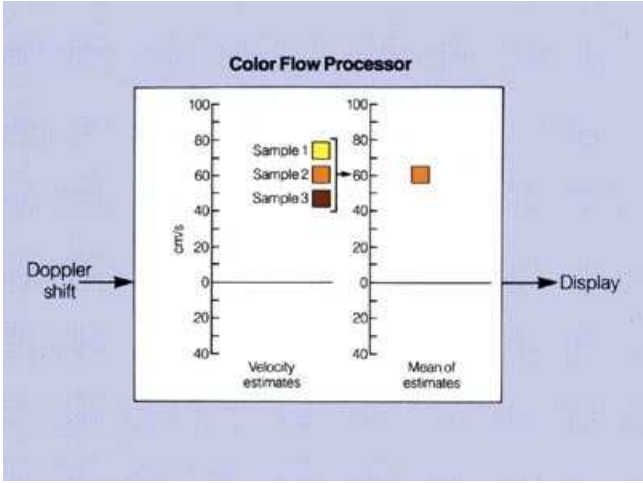

Figure 4. 11 A simple diagram showing the operation of a color flow processor where data from three pulse trains are used to estimate velocity, and one mean estimate is finally displayed in the gate.

The frequency shift information from each sample gate, obtained from successive pulse trains along the same beam line, is stored. The phase shift information is then assigned a velocity and color in the color flow processing section of the system for each packet (or series of pulse trains). This process if simply demonstrated in **Figure 4.11**, in a system using three phase shift estimates that result from a pulse packet size of 5. Mean velocity data, returning from a given pulse train, are simply called a sample. The mean of the frequency shift estimates obtained from the multiple pulse trains for each gate is then determined, and displayed as one color in each gate at any point in time.

The Price of Compromise

As noted above, the more pulse trains in a given line (higher packet size), the better will be the mean estimate of flow for each gate. Too small a packet size will likely result in unreliable flow data. As also explained previously, the minimal usable packet size is three. Too large a packet size will result in too much time being devoted to each line, and frame rate or line density or sector angle will be sacrificed. Most systems have a normal packet size of between six and eight.

The time taken for various flow map systems to create this two-dimensional image of flow is variable. To move quickly, and thus maintain rapid frame rates, color flow operation requires fewer samples to be collected and processed and the resultant displayed velocity estimates are made less reliable. Conventional, two-dimensional imaging has frame rates of 30 per second that preserve the smooth movement of the valves and walls. The time compromises in color flow imaging severely reduce the frame rate. The rate may, in fact, drop as low as four or six frames per second. This can create a situation that makes analysis of data quite difficult when flow is rapid, when rapidly moving anatomic targets are involved, or when heart rates are high as seen in neonates.

By sacrificing completeness of velocity information at each point, it is possible to determine only mean velocity, but at many points. As the ultrasound line sweeps through the sector arc, mean velocity is determined throughout the field of view. All of this velocity information is then converted to color and finally combined with the anatomic image. This leads to the display of a cineangiogram-like picture of intracardiac blood flow.

Line Averaging

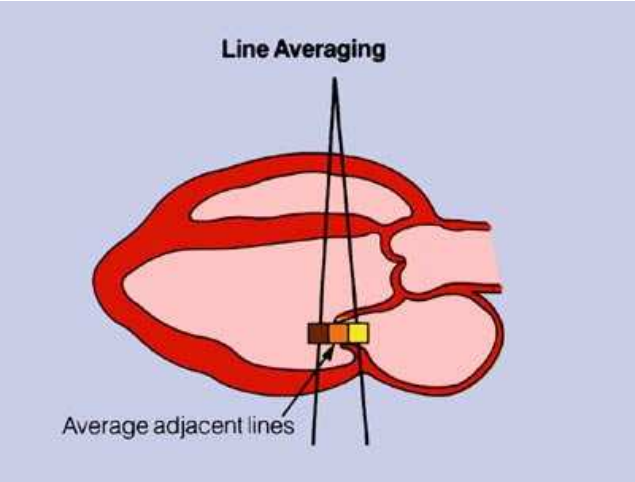

Figure 4. 12 At the far ranges gates are separated due to divergence of the radial scan lines. Data from adjacent gates are averaged to smooth the image.

As the ultrasound lines diverge into the far field of the image, they become increasingly separated. At some point in space they are so far apart that the resultant image would appear broken. To overcome this problem, data from a gate on the line are averaged with data on the adjacent line **(Fig. 4.12)**. This process is repeated for each frame of color data throughout the field of view. The resultant averaging smoothes the appearance of colors in the final display and is called "interline interpolation". This type of processing is also applied to the two-dimensional anatomic data as well.

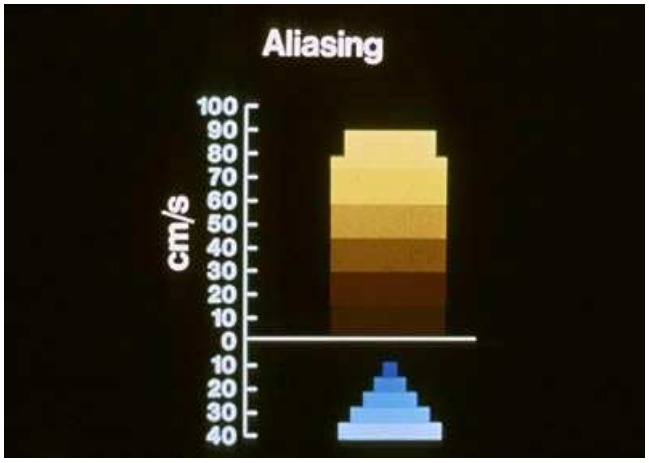

Figure 4. 13 If the color flow data were displayed in a spectral format, aliased flow towards the transducer would be cut off at the top and the aliased flow into the opposite channel would be reversed in color.

Aliasing in Color Flow

As with conventional PW Doppler, aliasing occurs when using color flow methods. The reasons for this are identical to those described in Unit 1. Like conventional PW Doppler, both depth and transducer ultrasonic frequency will determine the actual velocities at which aliasing occurs. Less aliasing would be encountered when using lower frequency transducers than with those of higher frequency.

The implications for this in clinical scanning are significant. The highest resolution ultrasound scanning is carried out with higher frequency transducer systems, yet these frequencies have the greatest problem with aliasing. In small children, with rapid flow rates, aliasing may present tremendous interpretive difficulties differentiating between normal (but aliased) flow and abnormal (but aliased) flow.

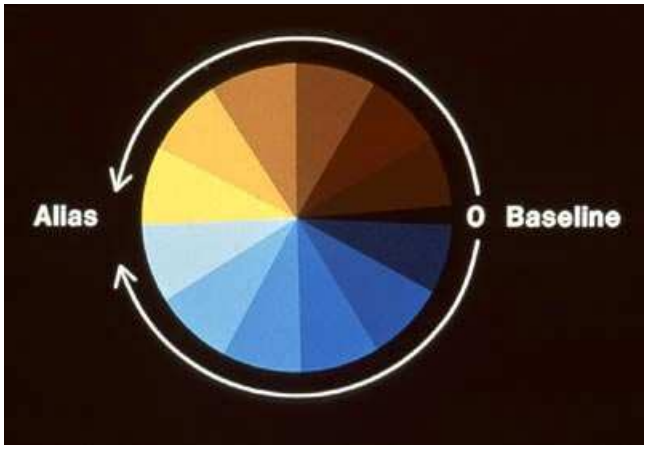

Figure 4. 14 Using a color wheel, baseline, or zero, flow is displayed in black. High mean velocity data are aliased between brighter hues of red and blue and may be easily recognized in the final display.

The color correlates of aliasing are shown in **Figure 4.13** with colors depicted on a spectral-type recording. In the "red-toward" mapping schema this would be displayed as a reversal of flow to the opposite direction and therefore as blue.

It is best to think of aliasing as a color wheel with zero flow at the right and represented as black. Such a color wheel with zero flow is shown in **Figure 4.14 (right)**. In the enhanced rendition of colors, the hues of red and blue are accentuated into very bright colors. This is used to aid the

beginner in understanding how aliasing appears in the color display. In either direction, as the mean velocities rise, increasingly brighter colors are encountered until the aliasing point is reached at which there is a reversal of color into the opposite directional channel. Note that at the aliasing point the brightest hues of red and blue are adjacent. This fact aids the eye in the recognition of aliasing in the final display. Some aliasing may be present in the Doppler color flow images of normal flows, but it is usually minimal.

The aliasing point for color flow systems is also dependent upon the maximum range of the field of view selected. As explained in Unit 1, conventional PW Doppler systems will have variable aliasing points depending on the location of the sample volume in the field. For color flow imaging, the same principle applies but its effect in the final image is a little different than with conventional systems. In color systems, the maximum pulse repetition frequency is set by the maximum overall depth selected. This influences each gate in the entire image field and is independent of whether the gate is near or far from the transducer. More aliasing will be seen throughout the image when scanning at deep range settings than at shallow range settings.

Using standard 2.5MHz transducers, aliasing is frequently associated with the higher velocities and turbulent flow that are found in disease states.

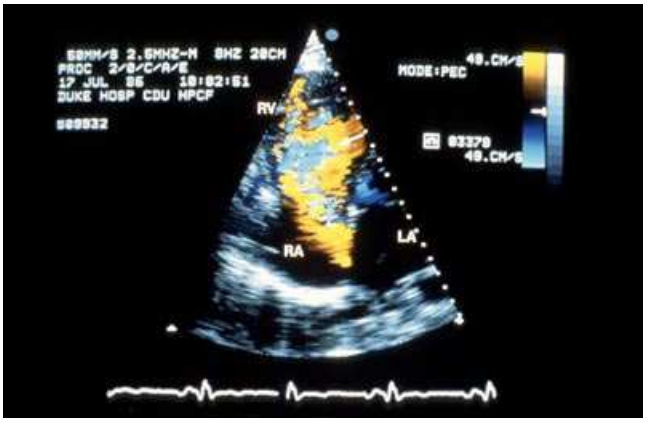

Figure 4. 15 Modified apical four-chamber view of flow through an atrial septal defect and into the tricuspid orifice in diastole. The bright yellow flow aliases into bright blue within the central core of the flow jet (arrow). This is an enhanced map.

On the color display, as the signal is aliased from one color to the next, it appears as a mosaic of the very bright hues at the aliasing point. In **Figure 4.15** there is a large mosaic encountered in a jet from an atrial septal defect as it moves through the right atrium and tricuspid valve into the right ventricle in diastole. The red flow towards the transducer aliases into bright shades of blue. Note that the brightest of the red and blue are adjacent to one another, indicating the aliasing point. The dullest of the colors are also adjacent to one another, indicating the zero flow point.

While aliasing is a major problem for conventional PW Doppler echocardiography, it is less so for color flow. Because the aliasing is displayed in two dimensions as a mosaic, it frequently allows the operator to readily recognize areas of turbulence associated with disease states. Aliasing is therefore, frequently used to advantage in the color flow map since it may dramatically highlight the presence of abnormal high velocities.

Variance

In some of these difficult states, detection and display of variance is helpful in differentiating the complex flows. In laminar flow, mean velocity is very close to peak velocity. As seen in *Unit 1*, the velocity spectrum is narrow. In turbulent flow, the velocity spectrum is broadened with many different velocities being presented at any one time.

Color flow systems can, however, present only one color at any one gate. In an attempt to present turbulence in the color image, methods have been developed to detect this spectral broadening ("variance detection"). Variance expresses the degree to which velocities within a

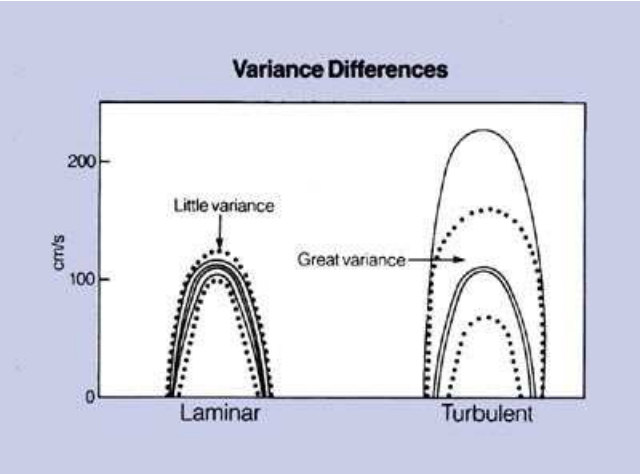

Figure 4. 16 In laminar flow there is little variation (variance) of velocities on either side of the mean velocity. In turbulent flow, when many different velocities are present, there is great variance.

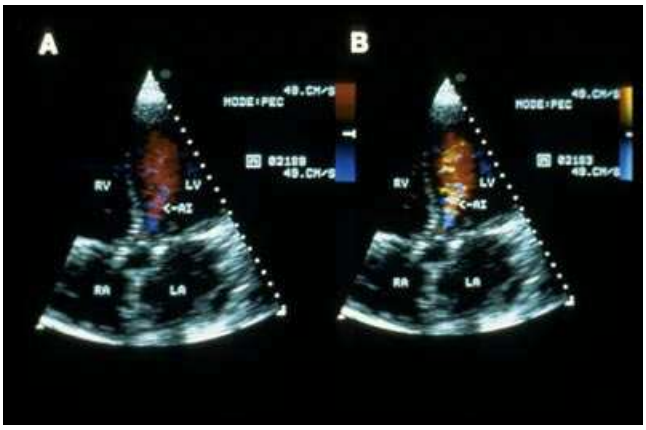

Figure 4. 17 Apical four-chamber diastolic view of aortic insufficiency demonstrating two different maps. The image is identical except for the map changes. Panel A shows a conventional red/blue map. Panel B shows a velocity/variance map where the regurgitant jet is readily identified.

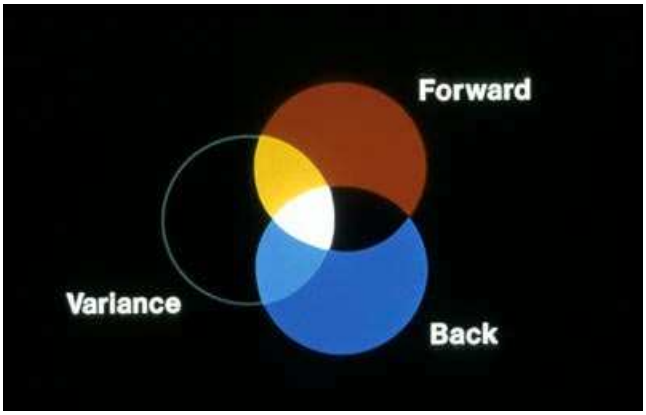

Figure 4. 18 When variance is detected, hues of green may be added to the red and blue flows, resulting in shades of yellow, white, and blue-green (cyan).

given sample volume differ from the mean velocity within that sample **(Fig. 4.16)**. The more the velocities differ within a sample volume, the greater will be the variance. In this example of laminar flow, there is very little variance (difference) in velocity about the calculated mean. Since turbulent flow is characterized by flow at multiple different speeds in many different directions, the variance in a region of turbulent flow is high. Variance estimation circuits within the color flow imaging system detect variance around the mean and, when present beyond a given point, incorporate it into the display.

A better understanding of how variance is displayed can be achieved by studying the colors of the aortic regurgitation jet seen from the apical window in **Figure 4.17**. The accompanying color bars to the right of each image help to identify which maps are being used. In **Figure 4.17 (panel A)**, a standard color velocity display of direction (red or blue) and relative velocity (varying brightness of each color) makes identification of the aortic regurgitation difficult. In most systems, shades of green are added when greater variance in blood velocity is present (when turbulence is greater). This results in the incorporation of green into the display as show in **Figure 4.17 (panel B)**. Here, the variance is seen overlaid on the identical image in the left panel and renders the aortic regurgitation jet recognizable.

The method chosen for the display of variance is demonstrated by the intersecting circles of color in **Figure 4.18** (also see **Fig. 3.21**). Green is the third primary color of light. Since red and blue are already in the display, green is simply added on top of each of these colors. Forward flow with turbulence would result in yellow. Backward flow with turbulence results in cyan (blue-green). Pure green is rarely present in the display. If multi-directional turbulence could be encountered at the same time, the result of all three colors would be white. If multidirectional flow without turbulence could be encountered, combinations of red and blue (without green) would result in magneta.

These intersecting color wheels have been presented to enhance your understanding of the rules that govern the final color display. In reality, the red and blue circles do not intersect, as color flow systems can assign only one color to a gate. Since the color is finally assigned to a mean velocity estimate, it is either in the red or blue direction. There is no true white or magenta in the final display. It is important to recognize that a variance display in green can only be used with the standard red-blue map as baseline. Adding green to red and blue results in the various colors of yellow and cyan. Since these colors are already used in the enhanced map, the addition of green would have no visible effect. Thus, yellow in an enhanced map only reflects velocity information. Yellow in a variance map reflects turbulence. When turbulence is present, the range of mean velocities is broadened, and variance is detected. The result in the display is a "mosaic" of reds, blues, yellows, and cyan in the turbulent area.

Mechanical and Phased Array Scanners

For some time, it was thought that mechanical scanning systems could not be used to perform color flow analysis due to marked frequency artifacts introduced by the moving scan heads. While this may be true, some systems currently under development minimize this problem and may produce acceptable color flow images from mechanical scanning systems. Currently, since phased array systems have no such problem, they are the most common type of color flow system in use.

USE OF THE COLOR FLOW CONTROLS

From system to system, the color flow controls may be simple and readily recognized, or excessively complex, intimidating, and sometimes buried in many pages of software. Essential controls are very few.

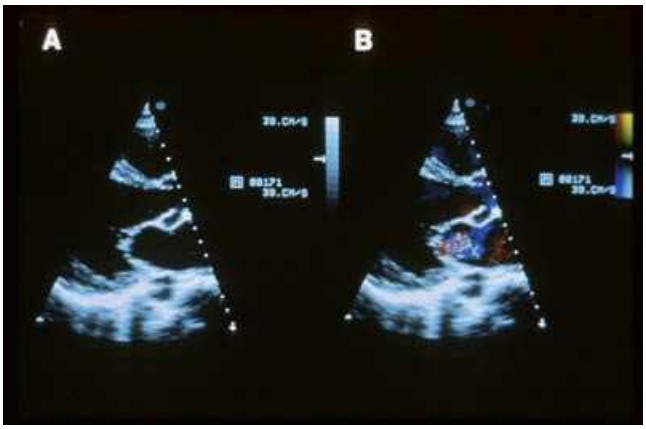

Figure 4. 19 Parasternal long-axis view of two-dimensional echocardiogram (panel A). The color is switched on (panel B) revealing the mitral regurgitant jet. A variance map is used.

The Doppler Color Flow Examination

The color flow examination is most easily accomplished during the two-dimensional examination when there is suspicion that any abnormal flow state exists, such as valvular regurgitation or communication between the cardiac chambers. The color flow may be readily switched on and off using the *color on* control while the operator proceeds with the two-dimensional examination as the various routine, or other pertinent views, are obtained. In **Figure 4.19** the same parasternal long axis image is shown without **(panel A)** and then with the color flow superimposed **(panel B)**. Conducting a separate color flow examination after the normal two-dimensional examination is unnecessarily time-consuming.

Gain

The next most important control is the *color gain*. Optimal adjustment of the gain setting is essential, as too much gain will result in excessive noise in the image and detract from image quality and interpretability. In most systems, excess gain is readily recognized by the appearance of background noise and distortion in the continuity of flow. Like conventional Doppler, this obscures the flow data. Too low a gain setting will diminish the sensitivity of the system in detecting small flow disturbances. It will further make large flow disturbances appear artificially smaller as the spatial representation of the limits of an abnormal flow jet are entirely dependent upon gain. **Figure 4.20 (panel A)** demonstrates a mitral regurgitant jet with too little gain; the area appears small. Slight increase in the gain reveals the full extend of the regurgitant jet **(Fig 4.20 panel B)** that fills virtually all of the left atrium. In our experience, it is quite difficult to make small jets abnormally large by the use of excess gain. It is however, easy to make large jets appear very small by the lack of proper gain settings.

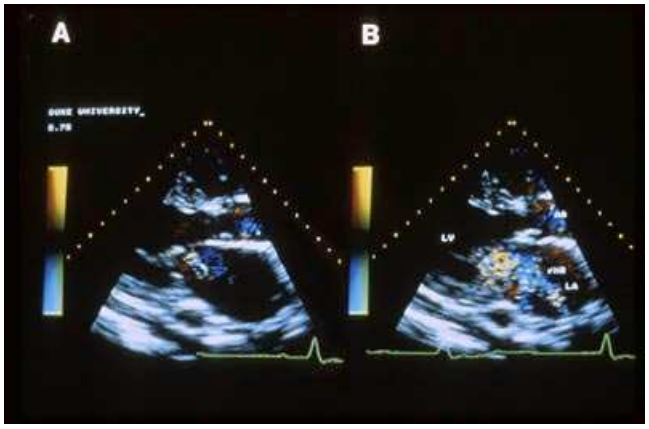

Figure 4. 20 Parasternal long-axis images of mitral insufficiency demonstrating the effect of color gain on the area of a regurgitant jet.

Other Controls

Most color systems will not map flow where there is anatomic target data on the display. It is very important, therefore, not to have excessive *image gain* on the two-dimensional display before switching to color flow, because excessive gain on the anatomic image may obscure flow on the color display.

Sector size and location may also be selected. Large sectors, however, reduce frame rates as previously discussed. Of the several choices available, the two most commonly used are the color image, within a wedge of the full sector arc and color within the entirety as a small sector arc. Increasing *depth* range will also decrease PRF, resulting in increased aliasing at lower velocities. Decreasing depth range will consequently decrease aliasing.

Some systems have various *color processing settings* that allow a choice of the way in which color is used to display flow information. Color processing controls may be generically grouped into four categories that provide choices of direction and turbulence/enhance displays: wall filters, spatial filters, color reject, and packet size. All have an effect on the final display.

Wall filter processing controls may be changed in some systems. Baseline filter controls variably eliminate low velocity flow information that results from the movement of the heart walls and valves. Without the use of these controls, considerable artifact results in the image from the moving anatomic structures. This is referred to as “ghosting” and appears in the display as dull hues of red or blue depending on the direction of movement of the given structure. Most newer systems have preset wall filter controls that considerably reduce the ghosting artifact.

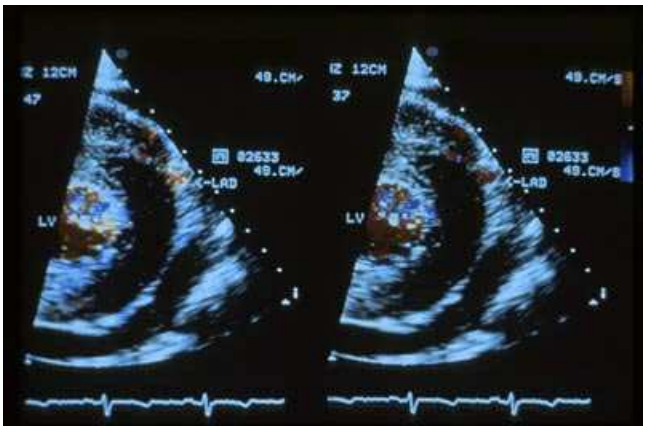

Figure 4. 21 Parasternal short-axis view showing the left anterior descending coronary artery. The flow within the vessel is obscured by the surround tissue artifact in the panel A. The panel B shows good separation between flow and vessel wall.

Some of these controls may be used to discriminate between flow and target data more precisely. **Figure 4.21 (panel A)** demonstrates one setting where flow in the left anterior descending coronary artery is obscured by the surrounding tissue artifact. In **panel B** an alternative setting is used that renders flow in this coronary artery separate from the vessel wall.

Spatial filtering is complex; most systems have some spatial filter built in and preset. Spatial filtering results in a smoother color image but comes at the cost of eliminating bright and dull hues from the display. *Packet size* may also be changed in some systems, and this effect has been previously shown.

Other Combinations

Most color flow systems also have a color flow M-mode presentation. This allows for the freezing of the two-dimensional image and the presentation of line-selectable M-mode with the color superimposed. M-mode is sometimes very helpful for displaying information where critical timing of flow events is desired. Other combinations of controls such as the use of combined color flow and conventional pulsed or continuous wave Doppler will be discussed later.

COLOR FLOW IMAGING OF VALVULAR REGURGITATION

Perhaps the most useful application of color flow imaging is in the detection of valvular regurgitation. Many of the patients examined in echocardiography laboratories dealing primarily with adult populations undergo Doppler examination for the presence and relative severity of valvular insufficiency. Color flow techniques avoid time-consuming PW Doppler examination mapping techniques and thus reduce patient examinations and interpretation times.

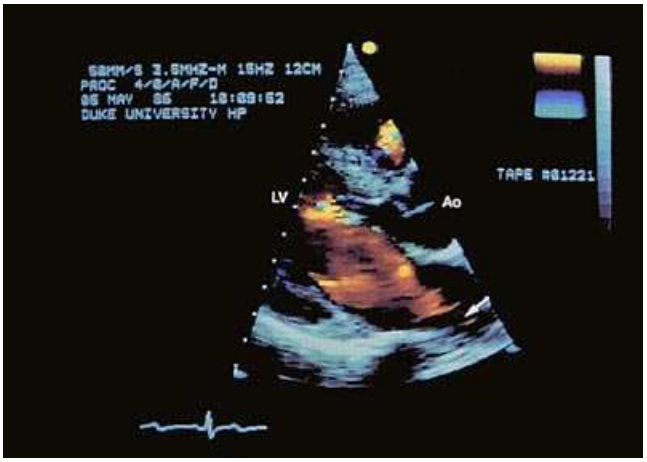

Figure 4. 22 Left parasternal long-axis view of blood emerging from a pulmonary vein (arrow) and filling the mitral valve orifice. An enhanced map was used.

Normal flows through the heart are easily detected, but to a beginner may simply appear as confusing flashes of color. Normal flows rarely alias and serve as a background for recognition of the aliasing that occurs with abnormal flows, such as valvular regurgitation.

Mitral Regurgitation

Normal diastolic flow through the mitral valve is very low velocity and rarely exceeds 1.5 m/s. Aliasing is, therefore, seldom seen during diastole when using a 2.5 MHz transducer. **Figure 4.22** demonstrates normal diastolic flow emerging from a

Figure 4. 23 Parasternal long-axis view of mitral regurgitation directed toward the posterior left atrial wall. A turbulence map was used.

superior pulmonary vein and then entering the left ventricle through the open mitral valve leaflets.

During systole, the left atrium is usually free from color. In **Figure 4.23** mild mitral regurgitation is seen to be directed along the posterior mitral leaflet toward the posterior left atrial wall. Aliasing is present due to the increased velocity and turbulence through the closed valve orifice, and appears as a bright mosaic of colors.

Mitral regurgitation can usually be detected using any view, even the parasternal long axis when the jet is perpendicular to the ultrasound beam. This is possible because most abnormal flows within the heart are turbulent. Many eddy currents exist in literally hundreds of directions simultaneously. Thus, while the main vector of the regurgitant jet may be generally perpendicular to the interrogating beam, some of the eddies within the main jet are oriented parallel to the beam. In most cases, these signals are sufficiently strong to be detected by the color flow imaging device. Thus, some spatial representation of flow will be seen by color flow methods.

Figure 4. 24 Left parasternal long-axis view showing a more severe degree of mitral regurgitation than seen in the previous figure. A variance map was used.

Quantifying the severity of valvular regurgitation is based approximately on the size and configuration of the regurgitant jet. Very small jets, localized just to the proximal side of the regurgitant valve, usually signify trivial valvular insufficiency. Large jets that fill the receiving chamber usually indicate significant valvular insufficiency **(Fig. 4.1)**.

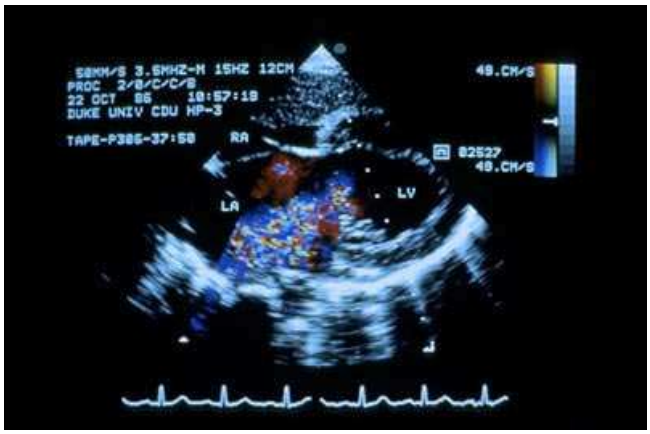

Figure 4. 25 Subcostal view of severe mitral regurgitation. A variance map was used; spatial filters are off.

Moderate mitral regurgitation is shown in **Figure 4.24**. Again, the hallmark is the systolic appearance of a posteriorly directed jet comprising aliased colors and turbulence. Regurgitant jets may go in any direction and have virtually any appearance. **Figure 4.25** demonstrates mitral regurgitation seen from the subcostal view in a 5-year-old boy where the jet is more diffuse and occupies almost all of an enlarged left atrium. In this case, severe mitral regurgitation is present.

It is imperative to remember that many factors influence the size, configuration, and appearance of regurgitant lesions. Among them are the volume of the jet, pressure difference between the regurgitant and receiving chamber, size of the regurgitant orifice, configuration of the regurgitant orifice and the size of the receiving chamber. Other factors such

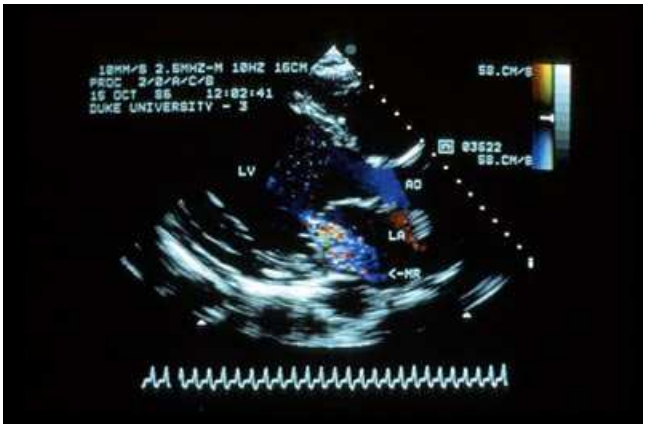

Figure 4. 26 Parasternal long-axis views of a mitral regurgitant jet in a patient with a diffuse cardiomyopathy. A variance map was used.

as the timing of regurgitation, loading conditions, heart rate, and rhythm may also be of importance. As mentioned above, the orientation of the jet to the beam is also a factor. Considerable work remains in verifying the significance of these and other influences.

Mitral regurgitation may be found by color flow imaging in any clinical state associated with this lesion, and may result from prolapse, rheumatic, infectious or other etiologies. Continued use of color flow imaging has revealed the frequent association of mitral regurgitation **(Fig. 4.26)** in patients with diffuse cardiomyopathies of virtually any origin. In our laboratory, we have encountered mitral regurgitation in 100% of patients with this disorder when the left ventricle measures 6 cm or greater in diastole. In each case, the mitral regurgitation was quantified at 2+ or greater (out of a scale of 4). Of further interest is the fact that there is a surprisingly high prevalence of regurgitation of the other heart valves. In patients with dilated cardiomyopathy, there is 2+ or greater regurgitation of the tricuspid valve in 91%, the aortic valve in 23%, and the pulmonic valve in 58%. In these patients, forward flow is usually of very low velocity and results in dull hues of color.

Due to the considerable savings of time, we now use only the color flow approach in routine cases for detection of all valvular insufficiencies. This is not done, however, without attending to all the factors that may affect the reliability of our estimation of severity.

Operator skill is important. The use of too little gain will make regurgitant lesions appear unduly small, and can be a prime source of underestimation. Proper transducer angulation into the regurgitant lesion is also important. For small and eccentrically direct jets, extra time is required to be sure of proper identification. Hastily conducted studies limited only to traditional views may not reveal these types of abnormalities.

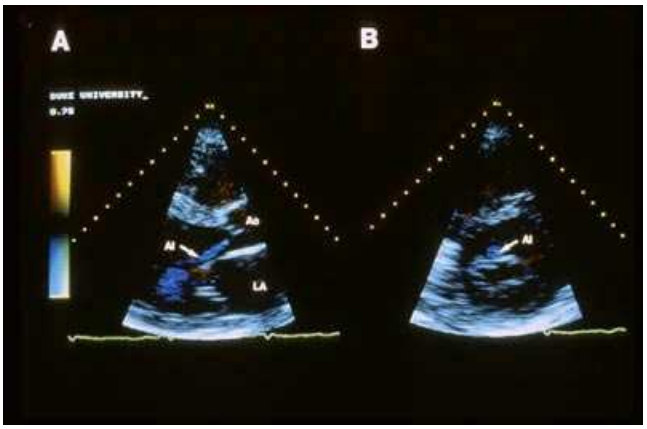

Figure 4. 27 Panel A shows a left parasternal long-axis view of a patient with a very narrow jet of aortic insufficiency. Panel B shows the limits of the jet in short axis.

Aortic Insufficiency

Almost all of the previous comments also apply to the detection and approximate quantification of aortic insufficiency. Aortic regurgitant jets may be small and narrow. When they are, location and mapping by convention PW techniques may be very time-consuming. Color flow approaches can readily identify these abnormalities, as seen in **Figure 4.27**. This narrow jet occupied only a very small portion of the area of the outflow tract when viewed in short axis **(Fig. 4.27, panel B)**.

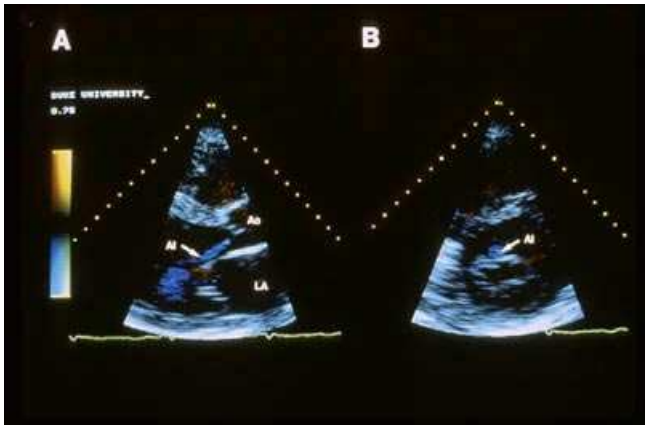

Figure 4. 28 Left parasternal long-axis view of aortic insufficiency filling the entirety of the left ventricular outflow tract in diastole. A variance map was used.

Figure 4. 29 Parasternal long-axis view of a narrow aortic regurgitant jet directed at the anterior mitral valve leaflet. This jet seems to bounce off the leaflet toward the left.

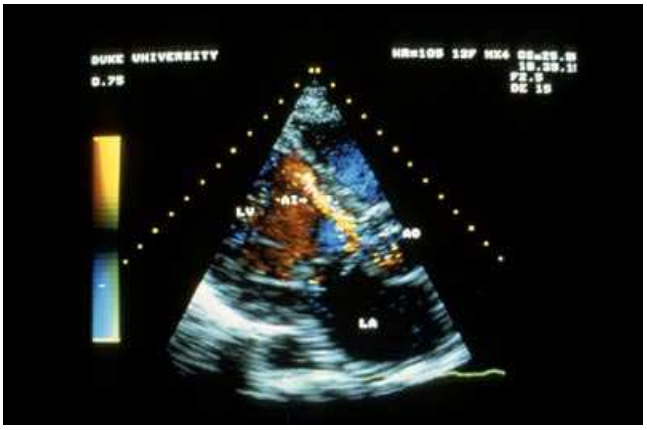

Figure 4. 30 Parasternal long-axis view of severe aortic insufficiency following the posterior portion of the interventricular septum. A variance map was used. This is the same patient as shown in the next figure.

More typically, a strong turbulent signal is detected and aliasing occurs. **Figure 4.28** demonstrates the resultant mosaic across the entire left ventricular outflow tract in diastole resulting from aortic insufficiency.

The various directions of flow produced by aortic insufficiency also reveal useful information other than presence or severity alone. In **Figure 4.29** an aortic regurgitant jet is directed toward the anterior mitral valve leaflet, then reflected off to the left in a patient with a low-pitched diastolic rumbling murmur suggestive of mitral stenosis. No aortic insufficiency murmur was audible. No mitral stenosis was present by conventional echocardiography or by Doppler. Even though the degree of aortic insufficiency was small, the direction of the jet readily explained the origin of the murmur, as it was likely that the regurgitant jet set the mitral valve into rapid vibrations. This is the classical description of the origin of the Austin-Flint mitral rumble.

Use of the color M-mode is frequently helpful for timing of cardiac events. In **Figure 4.30** there is a parasternal long-axis view from a 30-year-old patient who had had mild fevers and two positive blood cultures several months prior to admission with a large and markedly turbulent aortic insufficiency jet direct toward the apex of the left ventricle along the posterior aspect of the interventricular septum. With the M-mode beam directed through the mitral valve, premature closure of the mitral valve apparatus was noted to occur well before the QRS complex, probably as a result of the significant hemodynamic load of the aortic insufficiency **(Fig. 4.31)**. The left ventricular diastolic pressure was high enough to close the mitral valve before the onset of systole. Of note is the fact that most of the mitral regurgitation was seen before mechanical systole began; following the QRS complex, little mitral regurgitation was noted.

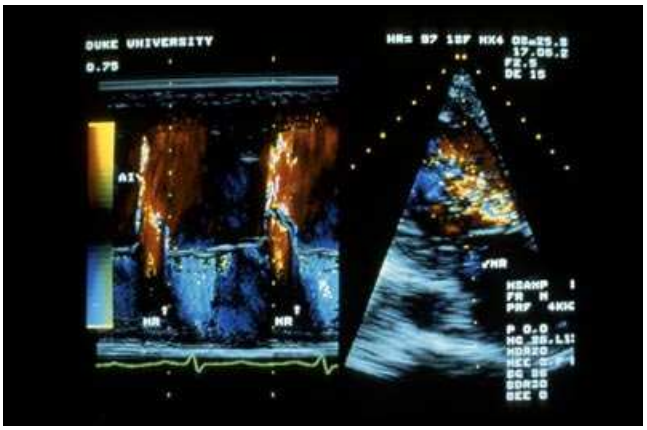

Figure 4. 31 The severe aortic regurgitation is seen on the right. The simultaneous M-mode color recording (left) shows premature closure of the mitral valve apparatus and the onset of mitral regurgitation in mid-to-late diastole. A variance map was used.

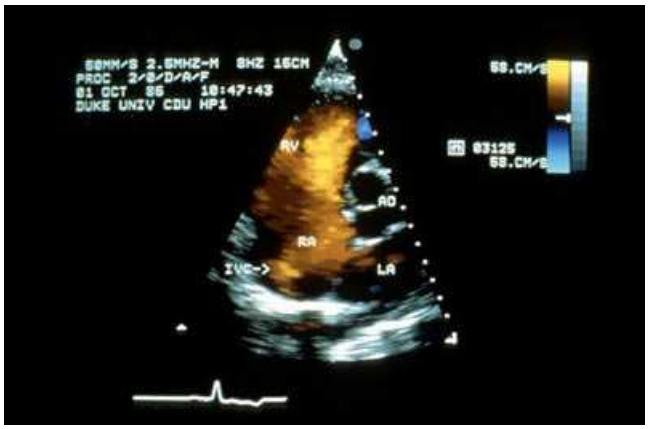

Figure 4. 32 Left parasternal short-axis view of the aortic root and right atrium. Low velocity flow can be seen to emerge from the inferior vena cava and move through the right atrium and tricuspid valve into the right ventricle. An enhanced map was used.

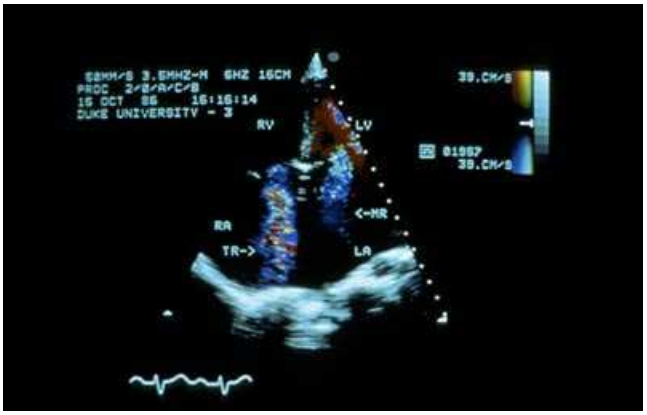

Figure 4. 33 Apical four-chamber view of both tricuspid and mitral regurgitations. The tricuspid regurgitant jet is directed toward the interatrial septum. A variance map was used; spatial filters are off.

Tricuspid Regurgitation

In **Figure 4.32** is shown the typical low-velocity appearance of blood flow emerging from the inferior vena cava and moving into the right ventricle through the open tricuspid valve. Note that flow in the right ventricle curling toward the outflow tract at the upper right exhibits a color change corresponding to the direction.

Regurgitation of the tricuspid valve, like all the other cardiac valves, is best detected during the two-dimensional echocardiographic examination. The most common views where such insufficiency is found are the apical four-chamber, short-axis parasternal at the level of the aortic root, subcostal, and right ventricular inlet views.

As with the other valves, tricuspid regurgitant jets may be found in any size, spatial configuration, and direction. **Figure 4.33** demonstrates a long and narrow jet of tricuspid regurgitation that nearly reaches the posterior wall of the right atrium, directed toward the interatrial septum. Tricuspid regurgitation is frequently found, even in normal patients. In these cases, the area of the regurgitation is usually small.

The effects of tricuspid insufficiency may also be seen in the inferior vena cava as shown in **Figure 4.34**. Here a burst of red is visible in systole as the flow is typically reversed in direction backwards into the hepatic veins.

Pulmonic Insufficiency

As blood emerges from the right ventricular outflow tract into the proximal pulmonary artery in systole, velocities are increased and aliasing frequently occurs. Very early systolic flow into the main pulmonary artery is shown in **Figure 4.35 (panel A)**. **Panel B** demonstrates the marked aliasing that occurs an instant later in systole, which is typical of normal right ventricular outlflow. Note also that the flow can typically be detected to the bifurcation of the main pulmonary artery and

Figure 4. 34 Long-axis view of the inferior vena cava during systole where tricuspid regurgitant flow is shown in red. Note the regurgitant flow into the hepatic vein. A variance map was used; spatial filters are on.

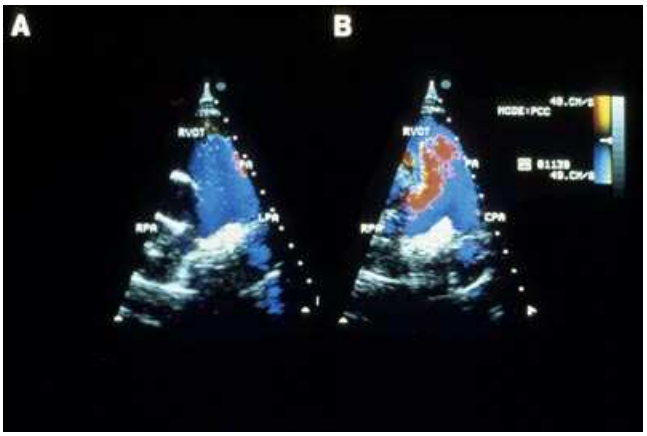

Figure 4. 35 Parasternal short-axis views of the aortic root showing the pulmonary outflow tract. Panel A shows flow in very early systole as it fills the proximal pulmonary artery to the bifurcation. Panel B shows flow an instant later when marked aliasing normally occurs. Variance maps were used.

Figure 4. 36 A flame-like appearance of pulmonic insufficiency is seen in the left parasternal short-axis view. A turbulence map was used.

occasionally into the right and left pulmonary arteries.

Color flow detection of pulmonary insufficiency is typically manifest in the left parasternal short-axis view where the flame-like regurgitant jet is seen in diastole **(Fig. 4.36)**. An operator may need to angle the beam to open the right ventricular outflow tract more fully to detect and appropriately record small degrees of this disorder.

COLOR FLOW IMAGING OF VALVULAR STENOSIS

Doppler color flow imaging methods allow for identification of the presence of certain valvular stenotic jets. There are, however, no specific characteristics in the color display of stenotic flows that assist in quantifying the severity of valvular obstruction at the present time. Spatial location of the direction of a jet is possible and this may be used to direct a conventional CW Doppler beam at an optimum angle to flow for precise measurement of peak velocity data.

Mitral Stenosis

Mitral stenotic jets are characterized by a bright burst of color from the mitral valve orifice in very early diastole. An instant later, a central core of aliasing is frequently seen that persists throughout the remainder of diastole. This appearance has often been referred to as the "flame-like" pattern of mitral stenosis and is present in many, but not all, patients with mitral stenosis.

The apical views are clearly the best for recording this characteristic appearance, as the interrogating beam is nearly parallel to flow and the best mean velocity estimates are possible.

A typical mitral stenotic jet from the apical two-chamber view is shown in **Figure 4.37**. Note that a central core of aliasing is less evident in this jet. Note also that a small jet of aortic insufficiency is readily separated from the stenotic mitral valve flow.

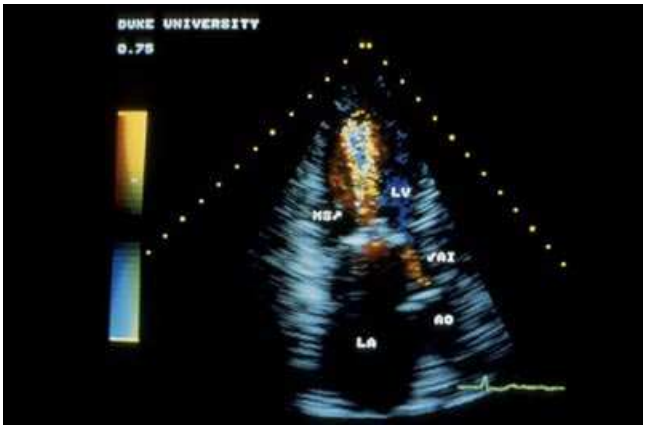

Figure 4. 37 Apical two-chamber view of a small degree of aortic insufficiency readily distinguished from that of mitral stenosis. A variance map was used.

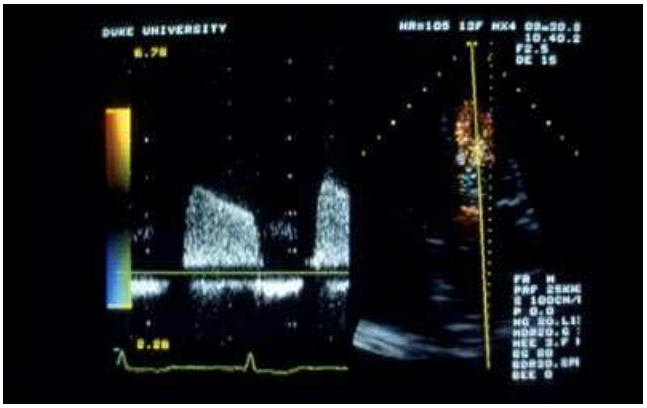

Figure 4. 38 More severe mitral stenosis is depicted on the spectral recording on the left. A variance map was used. For details, see text.

Figure 4. 39 Parasternal short-axis view of flow through a fully open aortic valve as it fills the aortic orifice. A variance map was used.

When a color imaging system contains CW Doppler capabilities, identification of the direction of the stenotic jet is very helpful and allows for reasonably precise parallel orientation of a CW beam with the stenotic jet. This provides a means for operator interaction between the beam and the jet to assure proper recording of peak velocities for gradient quantification.

There is a demonstration in **Figure 4.38** of the combined use of color flow and CW Doppler for detection of severe stenosis where the peak transmitral valve gradient approaches 3 m/s. The pressure half-time is also markedly delayed in this patient. When using systems equipped with CW capabilities, the color flow image is automatically frozen when switching into the conventional mode.

Aortic Stenosis

In normal individuals, flow is usually seen to fill the entirety of the left ventricular outflow tract. In the short-axis view of the aorta, normal flow can be seen filling the aortic valve orifice in some patients. **Figure 4.39** demonstrates the appearance of normal aortic outflow in a variance map. Little aliasing is seen in this view since the maximum scan depth is rather shallow. In addition, the dull hues of red indicate that relatively low mean velocities were calculated in this situation due to the rather perpendicular orientation of the interrogating beam with the aorta.

Unlike mitral stenosis, the forward jet of aortic stenosis into the aortic root is rarely well delineated using color flow methods. In this disorder, turbulence is seen to fill almost the whole of the aortic root and to possess little directional information. When imaged, these jets frequently have marked variance in

Figure 4. 40 Parasternal long-axis jet of aortic stenosis. Marked turbulence is seen where these jets can be detected that originate at the aortic valve level (arrow), and fills almost the entirety of the aortic root. A variance map was used.

Figure 4. 41 Short-axis view at the level of the aortic root, demonstrating turbulent flow in the main pulmonary artery due to pulmonic stenosis. A variance map was used.

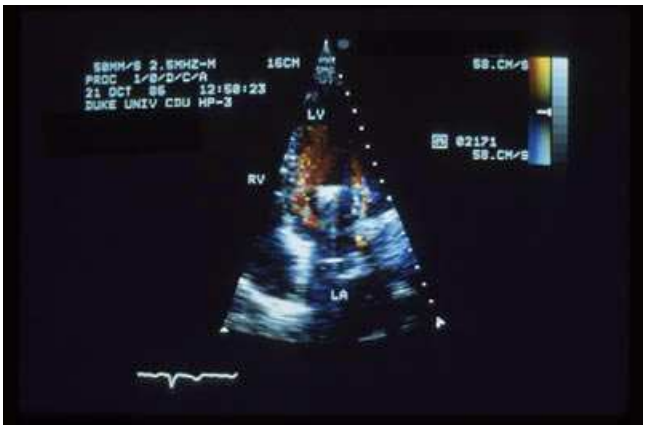

Figure 4. 42 Apical four-chamber view of normal diastolic flow through a Starr-Edwards mitral prosthesis. Note that the flow on either side of the ball is symmetric. A variance map was used; spatial filters are off.

the final display, as is seen in **Figure 4.40**. The turbulence begins at the orifice *(arrow)* and generally fills the entire root. Note that a discrete jet is not visualized.

Tricuspid and Pulmonic Stenosis

Tricuspid stenosis results in a color flow imaging study very similar to that of mitral stenosis except that the abnormal flow is seen to emerge from the tethered tricuspid valve leaflets. Stenosis of the pulmonary valves usually results in a very diffuse jet like that of aortic stenosis. It is, however, more readily detected than that of aortic stenosis. Most degrees of pulmonary stenosis fill the proximal pulmonary artery with a large mosaic, resulting from both aliasing and turbulence.

The pulmonary artery is best investigated using the short-axis approach. **Figure 4.41** shows marked turbulence and aliasing within the pulmonary artery from pulmonic stenosis. Here, abnormal flow is seen up to the bifurcation of the main pulmonary artery.

FLOW IMAGE STUDIES OF PROSTHETIC VALVES

Imaging of flow through prosthetic valve is possible and may be of great help in assessing the proper working status.

Since color flow imaging is so successful in detecting insufficiency from native valves, it might be simply assumed that it is as useful for assessment of prosthetic valve dysfunction. The masking effect described in *Unit 2* is also seen with color flow imaging, and the same cautions should be exercised when performing color flow interpretations as with the conventional approaches.

Color Flow Examination of Prosthetic Valves

Color flow imaging provides a means for

Figure 4. 43 Apical four-chamber view of normal diastolic flow from a Bjork-Shiley mitral prosthesis. Note that these two jets are not symmetric. The smaller one comes from the lesser orifice, while the larger of the jets (arrow) emerges through the greater orifice. A variance map was used.

Figure 4. 44 Left parasternal long-axis view in systole showing abnormal flow posterior to the valve ring into the left atrium,. This is compatible with a periprosthetic leak. Arrows indicate the location of the prosthetic valve ring. A variance map was used.

easy spatial identification of flows through prosthetic valves if the proper transducer orientations and limitations are kept in mind. **Figure 4.42** demonstrates an apical four-chamber view of forward diastolic flow through a Starr-Edwards valve in the mitral position. Jets are seen to emerge on both sides of the ball and enter the left ventricle. The jets are symmetric in size and shape when there is orientation of the interrogating beam directly through the center of the flow plane.

An image of normal diastolic flow through a Bjork-Shiley prosthetic valve as imaged from the apical four-chamber view is shown in **Figure 4.43**. Note carefully that forward flow can be seen through both the major and minor orifices of the valve when the prosthesis is functioning normally. As seen in this example, the area of flow through the major orifice is two or more times larger than the area of flow through the minor orifice. Since the Bjork-Shiley valve is a tilting disc, forward flow should always be imaged through both. When it is not, thrombus or other material may be occluding either orifice. Note that this valve has a lesser orifice and a greater orifice so that normal forward flow will never be symmetric.

Forward flow through a bioprosthesis usually fills the whole of the valve orifice under normal conditions. Occasionally, a perivalvular leak may be visualized, as is seen in the patient in **Figure 4.44**. A small mitral regurgitant jet is visible posterior to the ring of a porcine prosthesis (*arrows*) in systole.

COLOR FLOW IMAGING OF COMMON CONGENITAL DISORDERS

Color flow Doppler echocardiography also has an extremely useful role in the assessment of congenital abnormalities. By superimposing flow data on the two-dimensional echocardiogram, recognition of abnormal flows is easy in many disorders. When examining small infants, there is frequently little time to perform a complete conventional PW Doppler examination. When complex anatomy is encountered, use of blind conventional CW Doppler is often complicated by the absence of usual flow landmarks that assure the user of beam location.

Figure 4. 45 Subcostal view of interatrial shunting. Flow is seen to emerge from a pulmonary vein and cross the interatrial septum into the right atrium. An enhanced map was used, spatial filters are on.

Figure 4. 46 Subcostal view of the large interatrial septal defect in a child. The central core of aliasing is seen through the atrial septal defect. A turbulence map was used.

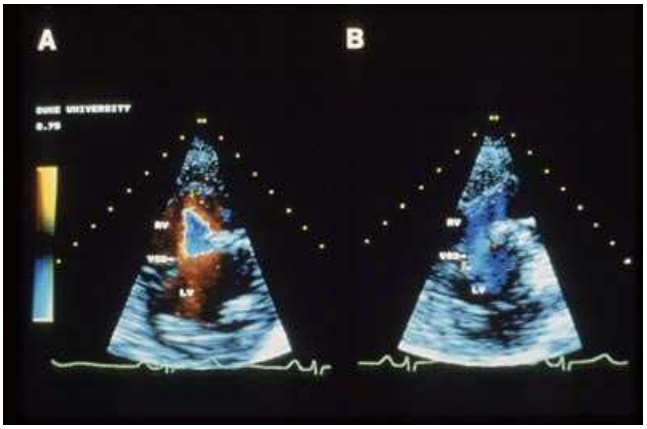

Figure 4. 47 Left parasternal short-axis view of the left ventricle is seen in panel A where the left-to-right component of flow is shown through a very large ventricular septal defect. In panel B, right-to-left component of flow is visualized. A turbulence map was used.

Atrial Septal Defect

In infants and small children, atrial septal defects are often directly visualized using two-dimensional echocardiography. In adults, the situation is somewhat different, as difficulties with image quality and other factors limit detection of the actual defect. **Figure 4.45** demonstrates flow from a pulmonary vein directly across an atrial septal defect from the subcostal view in a 32 year-old woman in whom there was little indication of the presence of such a defect on the two-dimensional image alone.

Color flow imaging helps greatly in identifying patients with interatrial shunting. The subcostal views are clearly the best for this purpose as the interatrial septum is oriented perpendicular to the sound beam and readily visualized, while any abnormal flow through the septum is parallel to the beam and toward the transducer.

In **Figure 4.46**, flow can be seen from the left atrium to the right atrium through a large atrial septal defect in a child. In fact, the anatomic limits of the defect may be more clearly defined by the image of the flow in relationship to the anatomic target information.

Ventricular Septal Defect

Most clinically significant ventricular septal defects in infants are readily imaged with two-dimensional echocardiography. In adults, it is rare to find a totally unsuspected ventricular septal defect that is large. In **Figure 4.47**, there is a very large ventricular septal defect in a 30 year-old woman with Eisenmenger physiology (marked elevation of pulmonary pressures in excess of systemic) from the left parasternal short-axis view of the left ventricle. Systolic flow from left to right is seen as a bright burst of red with a central core of aliasing **(Fig. 4.47, panel A)**. The diastolic image from the same patient shows the right-to-left component in blue **(panel B)**.

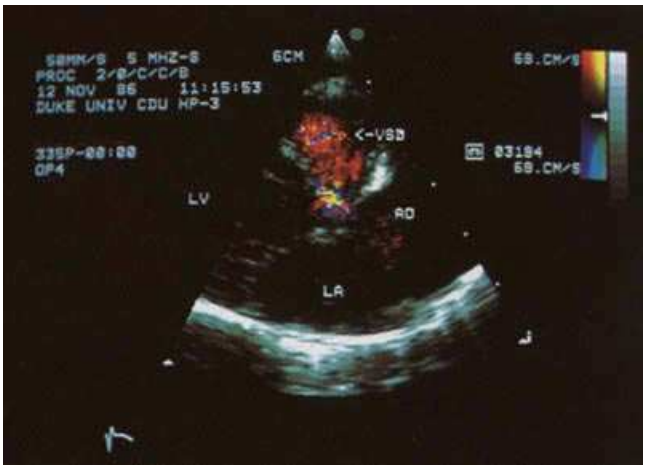

Figure 4. 48 Parasternal long-axis view of the left ventricle demonstrating left-to-right shunting from a subaortic ventricular septal defect. A variance map was used.

Of course, most such defects are small and difficult to image directly. Despite the ready detection of larger defects in children, these smaller defects are nearly impossible to image using two-dimensional echocardiography in adults. Conventional PW Doppler is very reliable for detection of these abnormal flows, but the process is long and arduous as it involves complex mapping of all portions of the interventricular septum.

With color flow imaging, however, these defects are easily seen. **Figure 4.48** shows the typical appearance of an abnormal jet in a patient with a small ventricular septal defect in the subaortic area.

ROLE OF THE VARIOUS DOPPLER METHODS

The Role of Conventional Pulsed Doppler

Conventional PW Doppler is able to locate abnormal flows in space precisely, but suffers because true velocity recordings are not possible due to aliasing. Using spectral displays, the timing of onset of a jet may be accurately recorded but accurate recording of peak velocities is impossible in most abnormal jets since these velocities are invariably high and aliasing results. As a consequence, PW Doppler is commonly used to detect the location of turbulent jets but the examination is laborious and excessively long as it requires tedious mapping to identify the location and size of an abnormal jet.

Conventional PW Doppler does have a unique role for the location of abnormal flow or the timing of flow events. The spectral velocity tracing is mandatory for calculation of flow velocity integrals if cardiac output or other measurements are made.

The Role of Conventional Continuous Wave Doppler

Conventional CW Doppler is able to record very high velocities, but suffers because it is not possible to exactly locate the jet in space. This method is ideal for precisely quantifying transvalvular gradients or other quantitative manipulations based on peak velocity determinations. Along with high PRF, it is the only Doppler method where such high peak velocities can be readily detected. Most users would indicate that mastery of the technique is difficult and time-consuming.

The Role of Color Flow Imaging

Color flow imaging is based on PW Doppler principles and, like conventional PW Doppler methods, cannot accurately record high velocity information. Its unique advantage over conventional PW Doppler is that it displays the flow, normal and abnormal, directly onto the echocardiographic image. For those familiar with two-dimensional echo approaches, the PW Doppler examination may be quickly conducted using color flow. When compared with the

conventional PW Doppler approach, the tedious mapping techniques necessary with the earlier technique are avoided.

Because there is no special display, however, precise timing of events is not possible. Timing information is further complicated by the fact that it takes so long to create the two-dimensional color flow display. In addition, aliasing occurs at least as frequently as with conventional PW Doppler, and peak velocities cannot be detected or identified in disease states.

The Combined Roles of Doppler Methods

Given these facts, it appears that Doppler color imaging has an important role with the conventional approaches. Color flow methods are approximately quantitative concerning the size and direction of the abnormal jets. More precise quantitative work, such as derivations of measurements form peak velocity information, remains within the province of CW Doppler.

There is no question that the basics of color flow mapping may be learned reasonable quickly by experienced users of two-dimensional echocardiography. PW Doppler requires a longer learning time. CW Doppler requires the longest time in order to gain the experience to perform a proper examination.

The examination time required for a color flow study is relatively short in comparison with the other methods. Simply switching color on and off as the two-dimensional examination is performed can reveal useful information in a short period of time. In routine clinical practice, color flow replaces conventional PW Doppler echocardiography in most, but not all, cases. Despite its increased cost, its ease of use and relatively rapid technical mastery has resulted in considerable savings of time and patient cost. While we feel that a complete Doppler examination of the heart requires all Doppler methods, the introduction of color flow has placed the conventional approaches into specific perspectives, now much more readily understood even by beginners in the use of Doppler techniques.

Further Reading
Those interested in learning further about Doppler echocardiography are recommended to read *Basic Doppler Echocardiography* edited by Joseph Kisslo, David Adams and Daniel B. Mark and *Doppler Color Flow Imaging* edited by Joseph Kisslo, David Adams, and Robert N. Belkin (both are published worldwide by Churchill Livingstone). These books have been the inspiration for this teaching program.

Figure Legends

Figure 4. 1 Systolic parasternal long-axis color flow image of mitral regurgitation. The mitral regurgitation jet comprises a mosaic of varying colors. A variance map is used. Note the direction of flow indicated by the color bar on the right (Abbreviations, page 39).

Figure 4. 2 Three color bars from a color flow system. When there is no flow, black is displayed (center) in the standard bar (left), flow toward the transducer at the top is in red, flow away in blue. Progressively faster velocities are displayed in brighter shades of red or blue. The center bar is in an enhanced map, and the right bar in a variance map (explained later in the text).

Figure 4. 3 In a color flow-imaging device, the returning echo data are processed through two channels that ultimately combine the image with the color flow data in the final display.

Figure 4. 4 Color flow Doppler systems use PW Doppler principles in a multigate, rather than range-gate format. For details, see text.

Figure 4. 5 Color flow imaging systems collect the phase shift information at each of the multiple gates and then process the information with color presented in the final display.

Figure 4. 6 Hundreds of gates are present along each line throughout the color flow image. In gates where there is target information, no color is displayed (open gate at lower left),

Figure 4. 7 If color was mapped on a conventional spectral recording, only one color could be placed in each bin. Progressively increasing velocities towards the transducer would be displayed in brighter hues of red while flow away would be displayed in blue.

Figure 4. 8 Schematic representation of spectral recording showing the differences between peak and mean velocities. In the case of normal laminar flow, peak and mean velocities may be very close. For turbulent flow, there may be a significant difference between peak and mean velocity.

Figure 4. 9 Pulse nomenclature used in the development of color flow images. The number of pulse trains determines the size of the pulse packet. The larger the packet, the better the estimation of mean low velocity.

Figure 4. 10 Parasternal long-axis views of an aortic regurgitant jet showing the effect of packet size changes. Panel A was acquired with large packet size, panel B with medium packet size, and panel C with small packet size. Large packet sizes have the best estimates of mean flow but come at the expense of frame rate. Spatial filtering is used with variance maps.

Figure 4. 11 A simple diagram showing the operation of a color flow processor where data from three pulse trains are used to estimate velocity, and one mean estimate is finally displayed in the gate.

Figure 4. 12 At the far ranges gates are separated due to divergence of the radial scan lines. Data from adjacent gates are averaged to smooth the image.

Figure 4. 13 If the color flow data were displayed in a spectral format, aliased flow towards the transducer would be cut off at the top and the aliased flow into the opposite channel would be reversed in color.

Figure 4. 14 Using a color wheel, baseline, or zero, flow is displayed in black. High mean velocity data are aliased between brighter hues of red and blue and may be easily recognized in the final display.

Figure 4. 15 Modified apical four-chamber view of flow through an atrial septal defect and into the tricuspid orifice in diastole. The bright yellow flow aliases into bright blue within the central core of the flow jet (arrow). This is an enhanced map.

Figure 4. 16 In laminar flow there is little variation (variance) of velocities on either side of the mean velocity. In turbulent flow, when many different velocities are present, there is great variance.

Figure 4. 17 Apical four-chamber diastolic view of aortic insufficiency demonstrating two different maps. The image is identical except for the map changes. Panel A shows a conventional red/blue map. Panel B shows a velocity/variance map where the regurgitant jet is readily identified.

Figure 4. 18 When variance is detected, hues of green may be added to the red and blue flows, resulting in shades of yellow, white, and blue-green (cyan).

Figure 4. 19 Parasternal long-axis view of two-dimensional echocardiogram (panel A). The color is switched on (panel B) revealing the mitral regurgitant jet. A variance map is used.

Figure 4. 20 Parasternal long-axis images of mitral insufficiency demonstrating the effect of color gain on the area of a regurgitant jet.

Figure 4. 21 Parasternal short-axis view showing the left anterior descending coronary artery. The flow within the vessel is obscured by the surround tissue artifact in the panel A. The panel B shows good separation between flow and vessel wall.

Figure 4. 22 Left parasternal long-axis view of blood emerging from a pulmonary vein (arrow) and filling the mitral valve orifice. An enhanced map was used.

Figure 4. 23 Parasternal long-axis view of mitral regurgitation directed toward the posterior left atrial wall. A turbulence map was used.

Figure 4. 24 Left parasternal long-axis view showing a more severe degree of mitral regurgitation than seen in the previous figure. A variance map was used.

Figure 4. 25 Subcostal view of severe mitral regurgitation. A variance map was used; spatial filters are off.

Figure 4. 26 Parasternal long-axis views of a mitral regurgitant jet in a patient with a diffuse cardiomyopathy. A variance map was used.

Figure 4. 27 Panel A shows a left parasternal long-axis view of a patient with a very narrow jet of aortic insufficiency. Panel B shows the limits of the jet in short axis.

Figure 4. 28 Left parasternal long-axis view of aortic insufficiency filling the entirety of the left ventricular outflow tract in diastole. A variance map was used.

Figure 4. 29 Parasternal long-axis view of a narrow aortic regurgitant jet directed at the anterior mitral valve leaflet. This jet seems to bounce off the leaflet toward the left.

Figure 4. 30 Parasternal long-axis view of severe aortic insufficiency following the posterior portion of the interventricular septum. A variance map was used. This is the same patient as shown in the next figure.

Figure 4. 31 The severe aortic regurgitation is seen on the right. The simultaneous M-mode color recording (left) shows premature closure of the mitral valve apparatus and the onset of mitral regurgitation in mid-to-late diastole. A variance map was used.

Figure 4. 32 Left parasternal short-axis view of the aortic root and right atrium. Low velocity flow can be seen to emerge from the inferior vena cava and move through the right atrium and tricuspid valve into the right ventricle. An enhanced map was used.

Figure 4. 33 Apical four-chamber view of both tricuspid and mitral regurgitations. The tricuspid regurgitant jet is directed toward the interatrial septum. A variance map was used; spatial filters are off.

Figure 4. 34 Long-axis view of the inferior vena cava during systole where tricuspid regurgitant flow is shown in red. Note the regurgitant flow into the hepatic vein. A variance map was used; spatial filters are on.

Figure 4. 35 Parasternal short-axis views of the aortic root showing the pulmonary outflow tract. Panel A shows flow in very early systole as it fills the proximal pulmonary artery to the bifurcation. Panel B shows flow an instant later when marked aliasing normally occurs. Variance maps were used.

Figure 4. 36 A flame-like appearance of pulmonic insufficiency is seen in the left parasternal short-axis view. A turbulence map was used.

Figure 4. 37 Apical two-chamber view of a small degree of aortic insufficiency readily distinguished from that of mitral stenosis. A variance map was used.

Figure 4. 38 More severe mitral stenosis is depicted on the spectral recording on the left. A variance map was used. For details, see text.

Figure 4. 39 Parasternal short-axis view of flow through a fully open aortic valve as it fills the aortic orifice. A variance map was used.

Figure 4. 40 Parasternal long-axis jet of aortic stenosis. Marked turbulence is seen where these jets can be detected that originate at the aortic valve level (arrow), and fills almost the entirety of the aortic root. A variance map was used.

Figure 4. 41 Short-axis view at the level of the aortic root, demonstrating turbulent flow in the main pulmonary artery due to pulmonic stenosis. A variance map was used.

Figure 4. 42 Apical four-chamber view of normal diastolic flow through a Starr-Edwards mitral prosthesis. Note that the flow on either side of the ball is symmetric. A variance map was used; spatial filters are off.

Figure 4. 43 Apical four-chamber view of normal diastolic flow from a Bjork-Shiley mitral prosthesis. Note that these two jets are not symmetric. The smaller one comes from the lesser orifice, while the larger of the jets (arrow) emerges through the greater orifice. A variance map was used.

Figure 4. 44 Left parasternal long-axis view in systole showing abnormal flow posterior to the valve ring into the left atrium,. This is compatible with a periprosthetic leak. Arrows indicate the location of the prosthetic valve ring. A variance map was used.

Figure 4. 45 Subcostal view of interatrial shunting. Flow is seen to emerge from a pulmonary vein and cross the interatrial septum into the right atrium. An enhanced map was used, spatial filters are on.

Figure 4. 46 Subcostal view of the large interatrial septal defect in a child. The central core of aliasing is seen through the atrial septal defect. A turbulence map was used.

Figure 4. 47 Left parasternal short-axis view of the left ventricle is seen in panel A where the left-to-right component of flow is shown through a very large ventricular septal defect. In panel B, right-to-left component of flow is visualized. A turbulence map was used.

Figure 4. 48 Parasternal long-axis view of the left ventricle demonstrating left-to-right shunting from a subaortic ventricular septal defect. A variance map was used.